



**Synthesis of Pyrrolo-Modified
Nucleotides and their Incorporation into
DNA via Enzymatic Extension**

Jennifer Hannant

Doctor of Philosophy

School of Chemistry

September 2011

Abstract

A series of pyrrole-containing derivatives of the 2-deoxy-pyrimidines, thymidine and cytidine have been prepared by Pd-catalysed cross-coupling between *N*-alkyl-alkynyl functionalized pyrrole (**py**), 2-(2-thienyl)pyrrole (**tp**) and 2,5-bis(2-thienyl)pyrrole (**tpt**) with 5-iodo-2'-deoxyuridine and 5-iodo-2'-deoxycytidine. The length of the alkyl chain linking the nucleoside and pyrrolyl-containing unit was varied from three to five carbon units. The series of nucleosides were characterized by ¹H NMR spectroscopy, ¹³C NMR spectroscopy, ES-MS, UV-vis spectroscopy, cyclic voltammetry and in some cases single-crystal X-ray diffraction. Cyclic voltammetry revealed that all the **py**-, **tp**- and **tpt**-alkynyl derivatives can be electrochemically polymerized to form conductive materials.

Conversion of the **tp**-modified nucleosides into their corresponding nucleotides was performed by phosphorylation at the 5'-hydroxyl site via phosphorus (V) and phosphorus (III) chemistry to yield dTTP-5-**tp** (dTTP*) and dCTP-5-**tp** (dCTP*), respectively. The purified nucleotides were fully characterized by ¹H NMR, ³¹P NMR, ES-MS, MPLC and HPLC. The incorporation of dTTP* and dCTP* into DNA via enzymatic extension was explored.

Polyacrylamide gel electrophoresis indicated that DNA polymerases, Pfu Pol B exo- and Klenow Fragment exo-, can tolerate dTTP* and dCTP* respectively. Gel electrophoresis revealed the successful incorporation of the modified bases into a primer template duplex of up to 37 base pairs. In comparison to standard nucleotides, dTTP* and dCTP* were incorporated at a slower rate. In order to produce functionalized DNA duplexes of microns in length, attempts were made to incorporate the nucleotides into an extending primer sequence via a slippage mechanism. Analysis via agarose gel electrophoresis demonstrated that the polymerases employed in this study could not read the modified DNA as a template as efficient as standard nucleotides but limited extension was observed.

Acknowledgements

First and foremost, I would like to express gratitude to my supervisor Dr. Andrew Pike. Encouraging me to apply for a PhD has given me the great opportunities I am experiencing today. What I thank him for most is the encouragement to expand my horizons, through attending supplementary courses, competitions and conferences. In these I have gained invaluable skills that have allowed me to get where I am today.

I would never have been able to get through my PhD and writing my thesis without the help of two very important people; Dr. Miguel Galindo and Joe Hedley. They have both given me guidance, a vast amount of invaluable help and more importantly, great friendship during this process. I hope I can return the favour one day.

To my fellow students in the CNL, in particular Scott and Jonny, your ‘wit’ and ‘sense of humour’ will not be forgotten. Also, to the other postgraduate students that have come and gone during my time as a PhD student, you have all had an influence on my time in Newcastle, which has made it so memorable.

Tommy, to you I show gratitude for your patience in some testing times. Your kind words, sentiment and fantastic sense of humour always get me through. Thank you!

Finally to my family. Your invaluable support and encouragement has always given me the motivation to achieve and I hope that I can repay you for everything. I know I have made you proud.

“The major reason for setting a goal is for what it makes of you to accomplish it. What it makes of you will always be the far greater value than what you get.”

Jim Rohn

Table of Contents

Chapter 1 - Introduction	1
1.1 Nanomaterials.....	2
1.2 Inorganic 1-dimensional materials.....	3
1.3 Organic 1-dimensional materials.....	5
1.4 DNA as a tool	7
1.4.1 DNA nanostructures	9
1.4.2 DNA as a template.....	10
1.4.3 Metallic-DNA	11
1.4.4 Organic-DNA.....	14
1.4.5 DNA as a scaffold.....	16
1.5 Aims of project.....	19
References.....	21
Chapter 2 - Synthesis of pyrrole-based monomers, functionalization and applications	24
2.1 Pyrrole	26
2.1.1 Pyrrole-thiophene copolymers.....	28
2.2 Results and discussion.....	30
2.2.1 Synthesis of tp and tpt	30
2.2.2 Electrochemical polymerization of py , tp and tpt	32
2.2.3 N-alkylation of py , tp and tpt	35
2.2.4 FT-IR spectroscopy	37
2.2.5 Electrochemical polymerization of N-alkylated monomers	38
2.3 Alkynyl monomers for functionalizing nanowires.....	43
2.3.1 Poly-pentynyl- tp /DNA/Ag nanowires.....	43
2.3.2 Poly-pentynyl- tp /DNA/hybrid “clicked” nanowires	45
2.4 Conclusions	47
2.5 Experimental.....	49
References.....	53
Chapter 3 - Synthesis of modified pyrimidines using N-alkylated monomers	56
3.1 Modified nucleosides.....	57
3.2 Results and discussion.....	62

3.2.1	Synthesis and characterization of C5-modified nucleosides.....	63
3.2.2	FT-IR spectroscopy.....	64
3.2.3	Electrochemistry studies of the modified nucleosides.....	65
3.2.4	UV-Vis spectroscopy studies.....	70
3.2.5	Furanopyrimidone crystal structure.....	71
3.3	Synthesis of 5-pentynyl- tp 2'-deoxycytidine.....	76
3.3.1	FT-IR and UV-vis studies for the direct comparison between dT-5- tp and dC-5- tp	77
3.4	Conclusions.....	79
3.5	Experimental.....	81
3.6	References.....	84
Chapter 4 – Triphosphate synthesis of modified nucleosides.....		86
4.1	Phosphoramidite chemistry.....	87
4.2	Triphosphate chemistry.....	90
4.2.1	Functionalized nucleotide triphosphates.....	91
4.2.2	Acceptance of modified triphosphates by DNA polymerases.....	94
4.3	Results and discussion.....	96
4.3.1	Design and synthesis of modified nucleotide dTTP-5- tp (dTTP*).....	96
4.4	Design and synthesis of modified nucleotide dCTP-5- tp (dCTP*).....	103
4.5	Conclusions.....	112
4.6	Experimental.....	114
	References.....	118
Chapter 5 – Enzymatic incorporation of tp modified nucleotides into DNA.....		120
5.1	Suitability of DNA polymerases for dTTP* by primer extension.....	120
5.1.1	The role of DNA polymerases in DNA polymerization.....	122
5.1.2	qPCR amplification of DNA employing dTTP*.....	129
5.1.3	Enzymatic slippage extension employing dTTP*.....	131
5.2	Suitability of DNA polymerases for dCTP* by primer extension.....	137
5.2.1	Primer extension at every and alternate bases.....	139
5.2.2	Enzymatic slippage extension employing dTTP*.....	141
5.3	Conclusions.....	144
5.4	Experimental.....	146
	References.....	148

Chapter 6 – Conclusions and further work	150
References	153

Appendix

Publications

Chapter 1 - *Introduction*

Chapter 1 – *Introduction*

There is a rapidly growing awareness that the self-recognizing and self-organizing properties of biomolecules can be exploited for the creation of new nanoscale materials with unique properties and capabilities.¹⁻⁴ Building structures on the nanoscale yields new materials that have exhibited novel properties in comparison to their respective macroscopic materials.^{5,6} The new properties are due to the limited motion of electrons on the now confined nanoscale dimensions and are known as quantum effects.⁷ These quantum properties of nanomaterials can be tailored in order to produce novel devices; and have become a key area of research in nanoscience and nanotechnology.⁸⁻¹⁰

Bionanotechnology is the interface between nanotechnology and biology and has applications in a vast number of fields. The interest of this project lies in the use of biological methods in order to fabricate conductive 1D nanostructures, entitled nanowires.

A construction tool that has nanoscale dimensions and has been employed to build these 1D structures is DNA, most often acting as a template. The highly selective recognition properties of the nucleobases make DNA an attractive choice for transformation into a 1-dimensional conductive wire, as they are envisaged to be able to self-assemble multi-components and so subsequently be used in molecular electronics. Here, a novel approach will be employed to enzymatically grow a duplex of DNA that is nanometers in width (1-100 nm) but microns in length and has conductive material directly integrated into it. This biological method will enable control of where conductive units are positioned in order to produce a single molecule conducting nanowire by employing the DNA duplex as a scaffold.

This introductory chapter discusses the importance and fabrication of nanomaterials with a particular emphasis on 1D nanowires. In particular, the attraction of utilizing DNA as a tool for bionanotechnology is reviewed and its role as a template and

scaffold in nanomaterial fabrication is highlighted. Finally, in light of the following discussion, the project goals and the contents of the proceeding chapters are outlined.

1.1 Nanomaterials

Nanomaterials are defined as materials having at least one dimension between 1 and 100 nm. The bottom-up approach towards nanomaterial fabrication allows single molecules to assemble in a supramolecular fashion to produce structures of a higher order. Nanomaterials that possess zero dimensions are at the lowest end of the scale and these materials exist in the form of quantum dots and nanoparticles.^{3,11} The advantageous properties of nanoparticles clearly arise from their size and high surface area to volume ratio. The dimensions are ideal as they can be utilized in applications such as drug delivery systems or for imaging purposes as their size enables them to diffuse in and out of cells.¹¹ However, fabrication of nanoparticles that have a uniform size distribution, i.e. similar morphology and highly monodisperse, although difficult is relatively easy compared to 1D growth.¹² Control of growth along a single dimension is a feature that is essential to this project in order to produce a uniform wire-like structure.

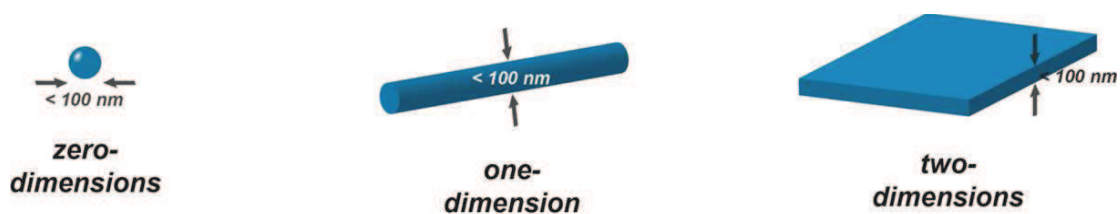


Figure 1. Illustration of 0D, 1D and 2D nanomaterials.

On the other hand, there have been extensive studies performed on bulk conductive materials. 2D nanostructures such as coatings and films offer high conductivity and have been reported widely.¹³ However, like nanoparticles, they also lack the important element of control of growth in addition to the loss of directionality of electron flow. Recent reports have conversely shown that 1D organic structures produce conductivities higher than their respective 2D material due to the channelling of this electron flow down a wire.¹⁴

This exemplifies that on moving to lower dimensions, the properties of nanomaterials, like electrical and thermal behaviour, is expected to change. Experimental challenges are now being overcome to find out how these properties change when synthesizing one-dimensional materials.¹² In particular, semiconductor materials, such as π -conjugated organic polymers, have been used as nanowires and are thought to be practical due to the ability of tuning and controlling their conductivity via doping.¹⁵

Since the 1990's there has been an evolution of semiconductor nanowires.^{16,17} The field has expanded significantly and is now one of the core research areas in nanoscience. Semiconductor nanowires are rod-like semiconductor material structures with a diameter less than 100-200 nm. Recently nanowires have been prepared with diameters of ~ 5 nm.¹⁸ One-dimensional nanowires can be grown in various ways, for example, by epitaxial crystal growth, where a metal can be used to seed the growth of the wire.¹⁹ The diameter of the wire will depend on the type of metal ion used.²⁰ In addition, there are a number of other techniques that can be employed to perform this growth, i.e. CVD which each have their own key advantages.²¹

One important application of 1D nanowires is in the miniaturisation of electronics. Preparing materials, in particular nanowires requires control of size, length, position and direction of the wire. A 2D film does not afford this level of regulation. Being able to align a large amount of wires in one direction will allow for a denser packing of wires onto a chip, hence increasing the transistor density and becoming a more powerful computational resource.

The fabrication of nanowires can be broken down into two general sections, namely the synthesis of inorganic and organic based systems. These two research areas are discussed in the following sections.

1.2 Inorganic 1-dimensional materials

The foundation of semiconductor inorganic 1D nanomaterials was initiated in 1992 with the production of WS₂ nanotubes by Tenne *et al.*²² Transition metal oxide

crystals such as WO_x and MoO_x have natural needle-like structures and they served as a template to assist the longitudinal growth of the nanotubes upon sulfurization with H_2S . The nanotubes produced demonstrate a layered structure which can lead to amorphous and polycrystalline tubes.

As a result, numerous chalcogenide nanotubes have been synthesized in a similar manner, such as CdS, CdSe, ZnS.^{23,24} GaN was synthesized by epitaxial growth on ZnO nanowires by Goldberger *et al.* in order to produce monocrystalline nanotubes.¹⁹ ZnO was employed as a template, possessing dimensions of 2-5 μm in length and 30-200 nm in diameter (Fig. 2a). Trimethylgallium and ammonia were then applied to the system via chemical vapour deposition techniques at 600-700 $^\circ\text{C}$ to deposit the GaN. Once deposited, the samples were treated with 10% H_2 in argon at 600 $^\circ\text{C}$ in order to remove the ZnO template and reveal the single crystal GaN nanotubes as a high-density, ordered and uniform array, with inner dimensions of 30-200 nm and a thickness of 5-50 nm (Fig 2b). Continuation of this technique was performed by Hu *et al.* in the fabrication of single crystal Si nanotubes.²⁵ Although producing nanotubes that have semiconductor properties and are mechanically robust, the techniques employed in the production of inorganic semiconductors generally require extremely high temperatures which can prove costly.

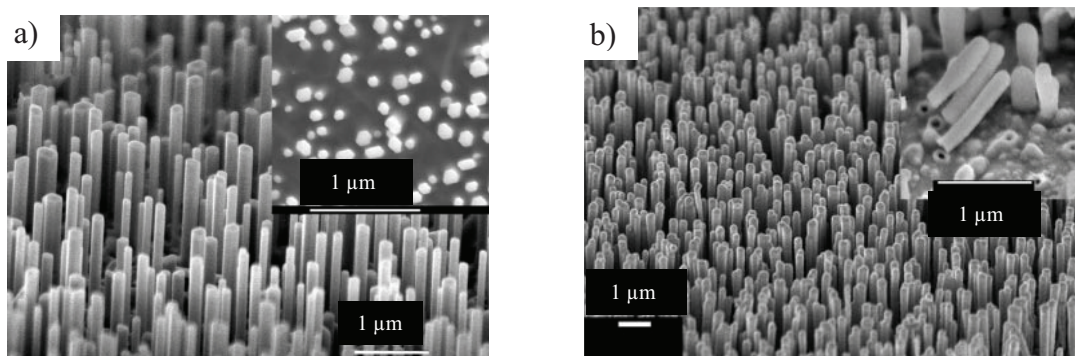


Figure 2 a) SEM of ZnO precursor template and b) SEM of GaN nanotubes array with the ZnO template removed.¹⁹

Inorganic nanotubes are similar to carbon nanotubes in the fact that it is difficult to control their dimensions, structural morphology and in addition, purification

procedures prove challenging.^{26,27} Since reproducibility is a key factor, this is a disadvantage when trying to apply these materials to electronics.

1.3 Organic 1-dimensional materials

Organic semiconductor materials can be functionalized making them versatile materials and what's more, solution processability makes them easy to work with in comparison to many inorganic materials. More importantly, their semiconductor nature can be tuned to produce higher conductivity values via doping and chemical modification.²⁸ Perhaps the best known example of a 1D organic conductor is the carbon nanotube.

Carbon nanotubes were discovered in 1991 by Iijima *et al.* when performing analysis on the formerly discovered fullerenes.²⁹ In these needle-like structures, the carbon atoms form hexagons (like that in fullerenes) and subsequently form a helical structure. While demonstrating excellent conductivity measurements, they also demonstrate difficulty in the control of growth and structure. Due to the 1D structure, electrons move through the tube without scattering, which means they can carry high currents with essentially no heating.³⁰ Carbon nanotubes can form single-walled nanotubes (SWNT) or multi-walled nanotubes (MWNT). SWNT consist of a one-atom thick layer of graphite rolled into a cylinder/tube and they exhibit conductivities typical of semiconductor and metallic behaviour. Existing as only one layer thick, chemical modification can be detrimental to the nanotube properties and cause breakages to C=C bonds, consequently demonstrating a drop in conductivity. Further limitations are that they can only be produced on relatively small scales and the synthesis can be expensive. This is due to the contamination of large amounts of impurities that are formed during production. MWNT consist of multi layers of graphite rolled up into a cylinder. In contrast to SWNT they are more robust to chemical modification. However, carbon nanotubes are now recognized as toxic materials.³¹ Furthermore, whilst semiconductor materials can be tuned to control the band gap via doping, carbon nanotubes do not possess this luxury. For these reasons, semiconducting nanowires have often taken preference over carbon nanotubes in electronic applications.

Organic nanowires have been synthesized in the form of single crystalline nanostructures. Hexabenzocoronene (HBC) is a planar aromatic molecule that can self-organize into nanofibers from the overlapping of π - π interactions (Fig. 3).³²

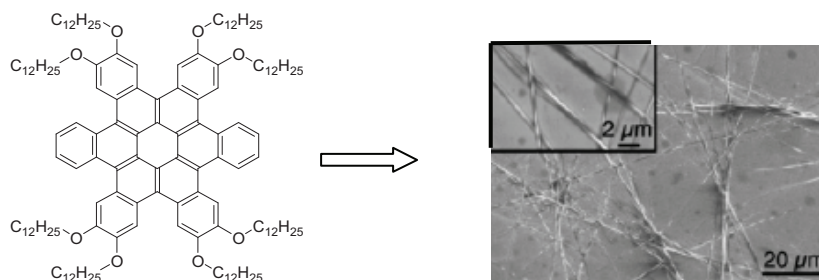


Figure 3. Octa-substituted HBC and SEM image of the nanofibers grown.

The fibers self-assemble along the direction of the π - π stacking to produce a one-dimensional structure. However, as illustrated from the above image, organic crystalline wires are challenging to align in one direction. This is important when targeting electronic applications as the optimal charge transport occurs when the wires are aligned in the same direction. A device was constructed containing a single fibre exhibiting a length of 6.1 μm and 250 nm diameter, illustrating a thick fibre. Carrier mobility tests were attempted but the range between different fibres was too large due to the varied morphologies of the fibres, hereby reiterating the fact that attaining reproducibility is a challenge when fabricating single crystalline nanostructures.

Organic π -conducting polymers have been studied intensely as films and coatings and are attractive due to their flexibility in comparison with inorganic materials. However, the low aspect ratio of bulk conducting polymers makes the production of single wires difficult. Hence, if the growth and direction of the polymer can be controlled in order to produce an ordered, one-dimensional wire, it will then permit the alignment of the wires onto surfaces.³³ A biopolymer that can direct the shape of a 1D wire is DNA. Its natural wire-like structure allows for templating or the covalent integration of groups into DNA to convert native DNA into a polymer with a new function.

1.4 DNA as a tool

DNA is one of the most important molecular building blocks known to mankind and is imperative to life. In 1962, the Nobel Prize was awarded to Watson and Crick for reporting the structure of DNA.³⁴ Thanks to this achievement, an immense amount of research has delved into the nature, the structure and the uniqueness of this biomolecule. Watson and Crick discovered that DNA is made up of four bases, connected to a sugar moiety which provides the linkage to the adjacent nucleotides via phosphate linkers. The spacing between nucleotides is approximately 0.34 nm with a duplex diameter of ~2 nm.³⁵

DNA consists of four bases, the purines and pyrimidines (Fig. 4); adenine (A) and guanine (G) belong to the purine family whilst cytosine (C) and thymine (T) belong to the pyrimidine family. The bases possess functionality that allows complementary hydrogen bonding to their corresponding base, i.e. A with T and G with C. Each nucleobase is covalently bound to a ribose sugar which unites adjacent bases together through a phosphodiester linkage from the 5'-OH to the 3'-OH of the next base. The connection through the phosphate backbone produces a biopolymer existing as a polyanion in nature.

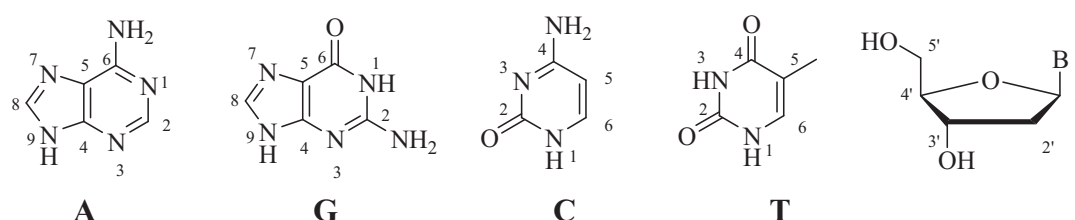


Figure 4. Numbered labelling of the purines; adenine (A) and guanine (G), the pyrimidines; cytosine (C) and thymine (T) and the ribose sugar.

The general consensus is that DNA behaves as an insulator rather than a conductor despite a rigorous literary debate of over 20 years.^{36,37} Therefore, in its native form it is not possible to use DNA in the field of nanoelectronics. However, DNA has a lot of attributes that allow for its conversion to materials that can be used in fields such as electronics or in a wider range of applications such as medical sensing. Structurally it offers an advantage due to the range of lengths it can offer through its polymeric

nature. DNA can be fabricated on scales between the nanoscale and microscale. Automated synthesis can be employed to build relatively short lengths of DNA (up to ~50 base pairs before efficiency drops) but enzymatic extensions can build more elongated duplexes that are microns in length. Extended lengths are also commercially available such as Calf Thymus and Lambda (λ) DNA, which are ~3 μm ³⁸ and ~17 μm respectively. Additionally, it is a relatively stable biomolecule that can withstand temperatures up to 90 °C before denaturing, dependent on the length and base content of the duplex. The stabilization is owed to the π -stacking between the planar bases and the hydrogen bonding holding the single strands together.

Furthermore, the chemical functionality of DNA is an attractive feature. At physiological pH, the phosphate backbone carries one negative charge per bridging unit and hence forms a polyanionic backbone. This ionic functionality allows binding of positively charged molecules through electrostatic interactions. For example, metal cations can be bound in this way as can conducting polymers that generate a polycation when oxidized.³⁹

One other important aspect of DNA is in the coding of DNA that is required for gene expression. This coding facilitates the assembly of two strands of DNA by finding the complementary bases on a second single strand through hydrogen bonds, thus providing the stable duplex. This coding enables sequence control when fabricating DNA-based materials. With knowledge of the self-assembly and coding properties of DNA, it can be exploited to create novel structures for new applications. Its properties of self-assembly are also invaluable, stemming from the structure of the nucleosides. The hydrogen bonding between specific base pairs produces the ordered, regular and uniform structure. In recent years, it was discovered that DNA can be adaptable to nanoscience. It can be of use both structurally and chemically and it is the complementary base pairs that offer structural building capabilities that allow it to be built into higher-order supramolecular structures.

1.4.1 DNA nanostructures

In 1982 Seeman *et al.* proposed that DNA could not only be used as the building blocks to life, but by utilizing its inherent self-recognition properties, complex structures can be built up by self-assembly.⁴⁰ Initially, 2D structures were designed by employing the 1D structure of DNA and effectively gluing sticky ends together via supramolecular chemistry to form junctions. Since then, other methods have been constructed to build higher ordered, 3D structures (Fig. 5). More recently Rothemund *et al.* demonstrated how a long single strand of DNA, after hybridizing with multiple short staple strands at specific sites, can be folded to form 2D and 3D DNA structures. This has led to a whole range of DNA origami shapes being reported.^{1,41,42} Cubes and prisms have been fabricated with the intent of using such hollow shapes as drug delivery systems.⁴³

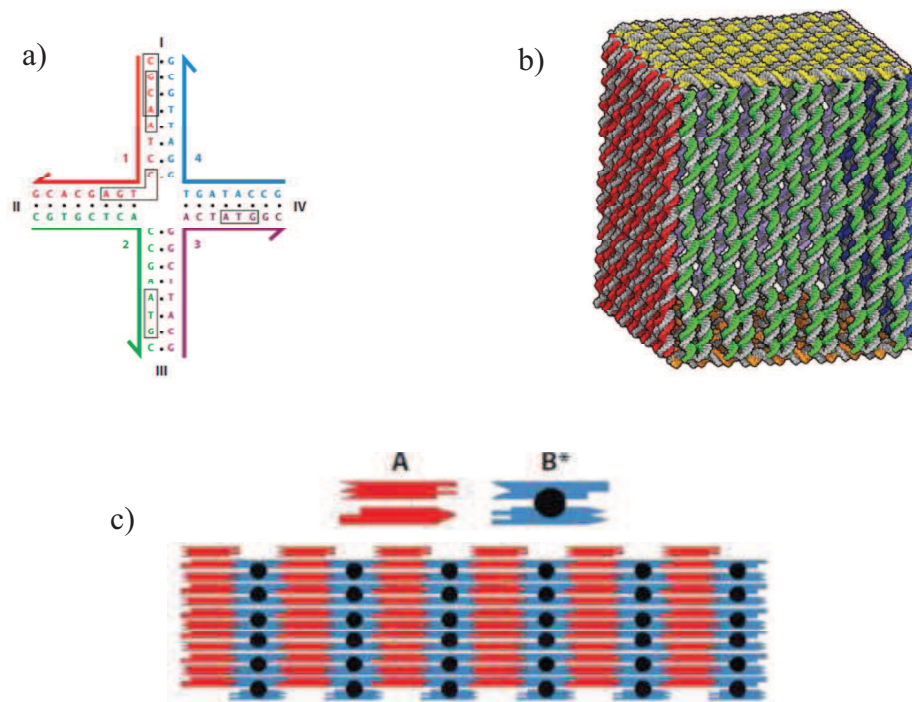


Figure 5. Schematic representations of DNA-based nanostructures. a) Holliday junction; a sequence design of a four-arm junction, b) DNA origami; six DNA sheets folded into a 3D cube⁴³ and c) DNA tiles; 2D tiles assembled together via sticky ends.

Employing these self-assembly methods can produce aesthetic and complex structures but in the majority of cases they do not possess a function beyond that inherent to DNA. However, DNA cannot only be used to assemble 1D, 2D and 3D structures but

its own molecular structure can be manipulated. A range of materials can be harnessed onto the DNA duplex through interactions with the phosphodiester backbone and also the nucleobases, to add additional chemical, electronic and optical properties.^{1,44-46} Methodologies that have been used to assemble material along the DNA duplex to afford electronic properties, i.e. 1D nanowires formation will be discussed in 1.4.1.

1.4.2 DNA as a template

One approach to incorporate functionalized materials along the DNA is to use the duplex as a template for seeding and directing material growth so that it follows the topology of DNA (Fig.6).

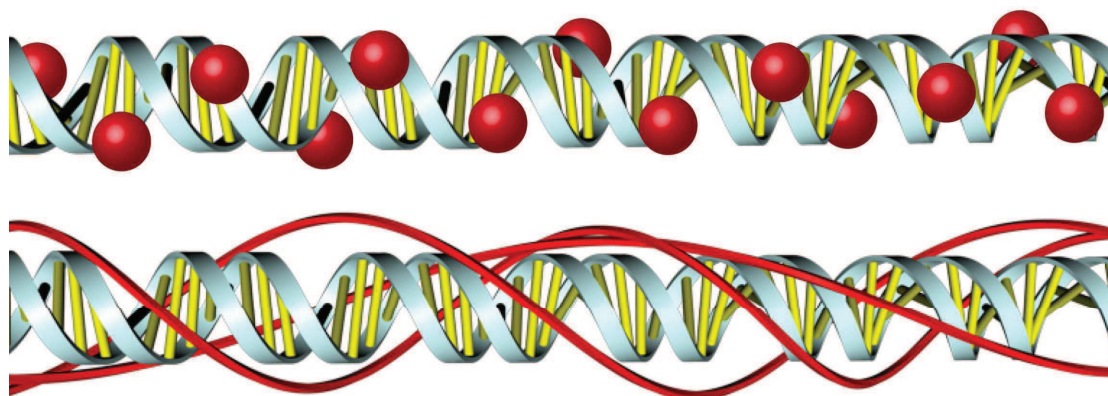


Figure 6. Schematic representation of DNA-hybrid material utilizing the DNA duplex as a template of a) metal ions and b) organic polymers

The majority of research in the area of templating material along DNA has utilized the inherent binding sites of the biomolecule to associate metal ions, although conducting polymers have also been templated in recent years. The most widely used method takes advantage of the negative backbone of DNA to drive templating via electrostatics with positive metal ions or π -conjugated polymers. Here, the length of the templated material is dictated by the length of the DNA.

1.4.3 Metallic-DNA

One of the first conductive DNA-metal hybrid nanowires were constructed by Braun *et al.*, where silver ions were templated onto DNA and reduced to silver metal (Fig 7a).⁴⁷ This seminal paper started a whole generation of templating metals onto DNA. Despite the simplicity of this method, it lacks control over growth and as demonstrated in Fig. 7a, the non-uniformity of the wire denotes a low conductivity in comparison to crystalline silver.⁴⁷ Nanowires containing metals such as gold, silver, palladium, platinum and copper have been fabricated in order to improve the quality and conductance of nanowires.^{35,48,49}

Richter *et al.* studied the templated metallization of palladium onto DNA (Fig. 7b) by activation of DNA with Pd acetate, followed by reduction to Pd nanoclusters and finally absorption of the Pd-DNA onto a carbon-coated grid surface for analysis.³⁵ In solution they discovered that although long wires up to 5 μm were found, the DNA would form loops, thus affecting the linear geometry of the helix and becoming less wire-like. In addition, when metallization of Pd onto the DNA reached diameters of 20-40 nm, it induced bending of the natural structure of the biomolecule which eventually caused the strand to break. As a consequence, they found they could deposit and immobilize the DNA to grow metal clusters of similar diameter to DNA, 3-5 nm. However, longer times revealed aggregation of the Pd clusters up to 40 nm in size.

Since then, uniform Pt nanowires have been produced with a smaller diameter of only a few nanometres by Mertig *et al.* (Fig. 7c).⁴⁸ This was achieved by primarily forming Pt(II)-DNA adducts that secure nucleation sites on the DNA strand. Upon addition and subsequent reduction of Pt^{2+} , formation of nanoclusters occurs at the nucleation sites. The most favourable binding site of the Pt^{2+} is to the N7 position of guanine and the metal coordinates within a few minutes. This work offers a more precise method to selectively bind Pt to specific sites on DNA whilst also allows fine tuning of the size of the Pt nanoclusters formed by controlling the activation times.

Copper templated onto DNA was first reported by Woolley *et al.* (Fig. 7d).⁴⁹ The procedure was performed on a silicon wafer that had been treated with poly-L-lysine to generate a polycationic surface to which polyanionic DNA could bind. The bound DNA was then treated with $\text{Cu}(\text{NO}_3)_2$, to electrostatically bind the $\text{Cu}(\text{II})$, with subsequent reduction to metallic Cu^0 using ascorbic acid. The findings demonstrated that copper did bind to DNA but the coverage was intermittent and some segments revealed no deposition at all. In addition, there was a lack of control over how much $\text{Cu}(\text{II})$ was reduced to the metallic copper and no indication of the conductivity of the metalized DNA was reported.

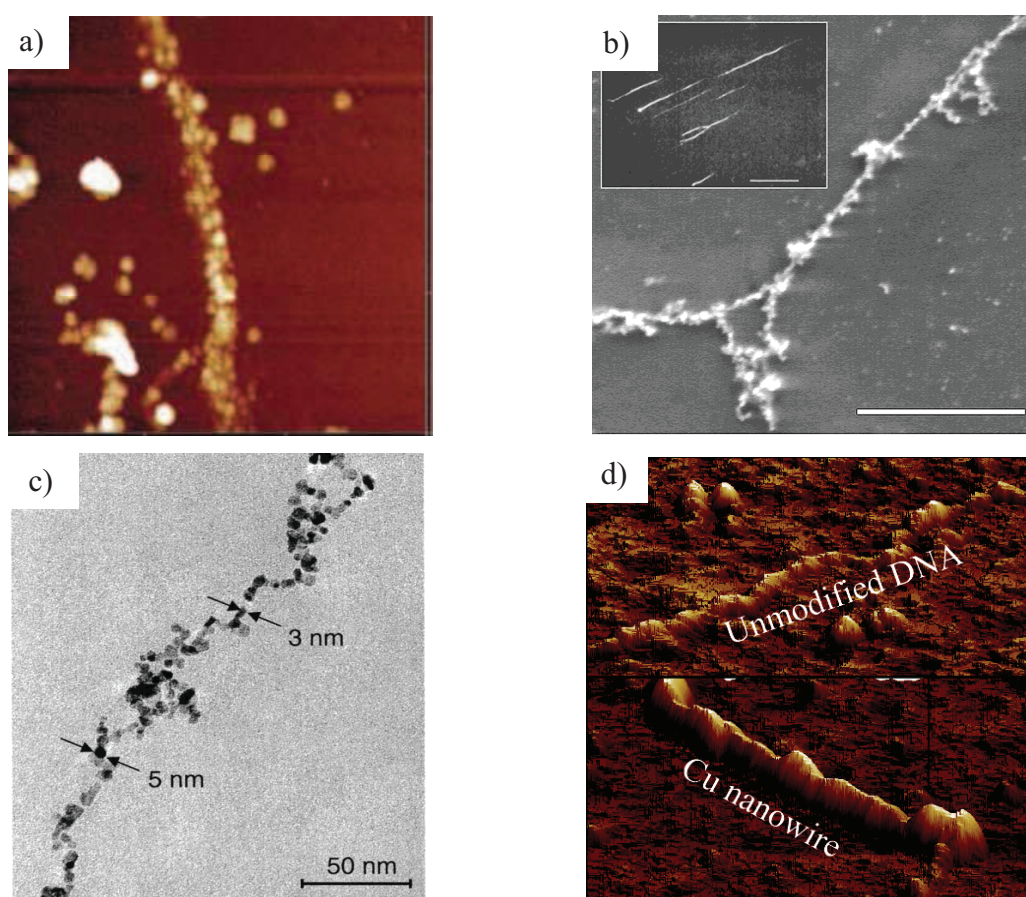


Figure 7. a) AFM image of silver templated DNA produced by Braun *et al.* exhibiting a diameter of 100 nm and length of $15\ \mu\text{m}$ ⁴⁷ b) SEM image of Pd-metalized-DNA, scale bar = $1\ \mu\text{m}$ 40 nm thick on a glass surface (with fluorescence inset)³⁵ c) TEM image of Pt nanoparticles grown on a single molecule of DNA⁵⁰ d) 3D AFM image of DNA deposited on silicon (top) and DNA treated twice with Cu^{2+} and ascorbic acid (bottom).⁴⁹

One of the key problems associated with the metallization of DNA, and templating in general, highlighted using the examples shown in Figure 7, is the difficulty to maintain uniform nanowires through purely electrostatic interactions.⁵¹ In order to fabricate wires for applications such as electronics, simple but highly reproducible methods are required, in addition the wires must be robust to the conditions they are exposed to during fabrication. From this brief literature review on metal templated DNA it becomes apparent that the method of templating cannot always reproduce defined diameters of templated material and so the production of 1D nanowires in this manner is not immediately attractive for device fabrication

One attempt to improve interactions between metals and DNA was via coordination chemistry. Divalent metal ions (Zn^{2+} , Co^{2+} , Ni^{2+}) have been complexed with DNA to form metallic DNA, M-DNA, reported by Lee *et al.*⁵² Employing these transition metals did indeed improve the conductivity of the DNA, but it also induced problems with its structure and stability to pH, most probably by interfering with the hydrogen bonding between the base pairs.

In order to introduce metal ions at precise locations, Shinonoya *et al.* prepared oligonucleotides with metal-mediated base pairs, where the hydrogen bonds have been replaced with metal-coordination sites.⁵³ This method was carried out by the synthesis of an amine ligand covalently bound to the ribose of DNA and then coordinating Pd^{2+} between the two artificial base pairs (Fig. 8).

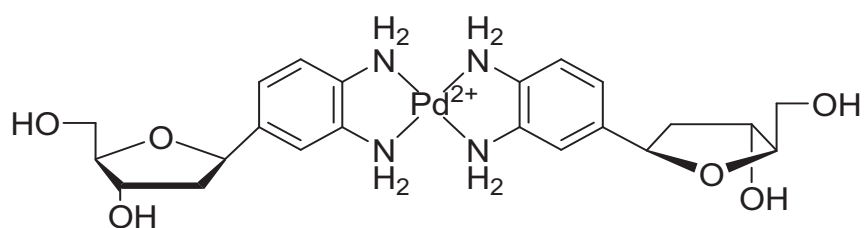


Figure 8. An example of an artificial metal-mediated base pair produced by Shinonoya *et al.* where the bases have been replaced by more stable coordination bonds.⁵³

Metallic-DNA, although offering high conductivities, can often lead to disruptions of the structure of native DNA and hence deviate from its natural wire-like

configuration. Another drawback of modification with metals is that further functionalization may prove difficult. Conversely, if a conductive organic material was employed, i.e. a polymer, organic modification of the polymer could be performed to give the wire supplementary functionality.

1.4.4 Organic-DNA

Just as metals can be templated onto DNA via electrostatic interactions, π -conjugated organic polymers can also follow this method of binding. When monomers such as pyrrole, thiophene and aniline are polymerized and oxidized a polycation is formed. A straightforward electrostatic mode of binding between the polyanionic DNA and polycationic polymer can then be assumed. A benefit of using polymers such as polypyrrole, polythiophene and polyaniline is their respective conductivities can be chemically tuned via doping.⁴⁴ Moreover, unlike metals, conducting polymers can be readily functionalized.⁵⁴ Another advantage of using organic polymers is that they are flexible and so increased uniformity is observed in the nanowires formed. Metal templated DNA often has an appearance of beads on a string indicating lack of contact between adjacent metal particles, whereas polymer coated DNA observes a smoother morphology (Fig 9).^{14,47}

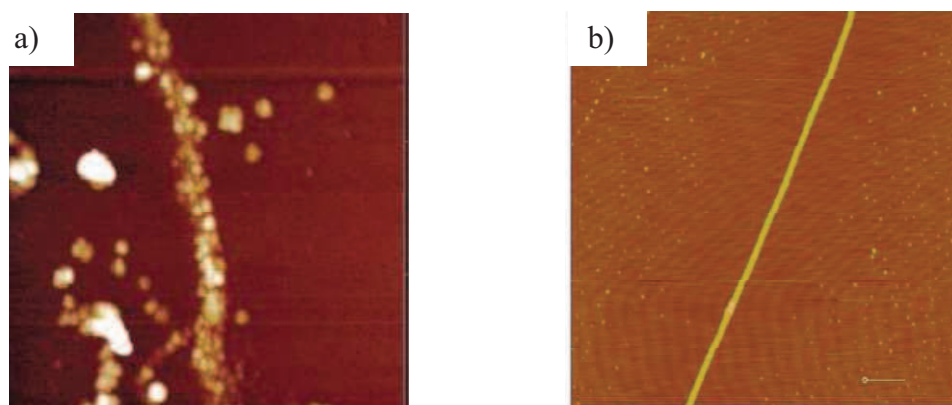


Figure 9. Comparison of a) silver-DNA hybrid nanowire with the appearance of “beads-on-a-string” and b) conductive polyindole nanowire templated on DNA (scale bar 1 μm).

λ -DNA has recently been employed to template polyindole via oxidation using FeCl_3 , and conductivities between 2.5 - 40 S cm^{-1} were observed.¹⁴ These values were higher

than the bulk conductivities which have been reported, 10^{-2} and 10^{-1} S cm⁻¹, and may be attributed to the controlled direction of flow of electrons in a 1D structure in comparison to bulk films.¹⁴ Also observed was a good thermal stability of the wires, up to 100 °C, which is an important requirement of nanowires for electronic applications.

Investigations into the templating of polyaniline onto DNA via non-covalent electrostatic interactions have been performed by several groups.^{55,56} In comparison to polyindole, polyaniline exhibits lower conductivity values of 40×10^{-7} S cm⁻¹. This is thought to be due to the lack of continuity of the polyaniline wire. Improvements in the uniformity of the wire were achieved via controlling pH. At the optimum pH of 4.0, the wire was relatively continuous. However, acidic pH of this level can be detrimental to the structure of DNA and initiate denaturing of the DNA duplex⁵⁷ and consequently polyaniline was not considered in this work.

Polypyrrole has also been a focal polymer in the fabrication of conducting nanowires, particularly in the group of Houlton *et al.*^{45,46} Like the aforementioned polymers, it forms a polycation on oxidative polymerisation which allows for electrostatic binding to polyanionic DNA. Conductivities of up to 4 S cm⁻¹ have been reported for polypyrrole based nanowires and like polyindole they exhibit conductivities above the bulk material.

As discussed above, conducting polymers can be introduced into conductive DNA hybrid nanowires which may have applications in electronic systems. In the case of polyindole and polypyrrole, the wire conductivities are higher in comparison to the bulk materials. One major drawback of templating is that the individual nucleobases of DNA cannot be used for self-assembly as they are buried under the templated material, hence lacking the element of control and reproducibility. However, an important feature relating to all of the previously mentioned polymers is the possibility to undergo chemical modification. In order to stoichiometrically and site-specifically target the individual bases of DNA, the biomolecule can be employed as a scaffold in an alternative approach to functionalize the nucleobases of DNA with monomer units for assembly into highly ordered wires.

1.4.5 DNA as a scaffold

Whereas templating is reliant on interactions between the templating material and binding sites on DNA, scaffolding is the direct integration of a material, covalently bound to the structure of DNA (Fig. 10). Using DNA as a scaffold is not a novel approach. DNA can be employed as a scaffold to organize nanoscale structures on one dimension i.e. nanowires, and also to 2D and 3D structures like ones that have been observed in DNA origami. The purines and pyrimidines have been covalently modified with functional groups varying from fluorescent to redox active moieties and have subsequently been incorporated into oligonucleotides via chemical or enzymatic synthesis with great success.⁵⁸⁻⁶⁰ By modifying the nucleoside building blocks, the self-coding of DNA can still be accessed and so additional functionality can be incorporated into a more complex structure. Incorporating modified nucleobases into DNA can be performed chemically via phosphoramidites in automated synthesis or enzymatically via triphosphates and polymerases in order to produce scaffolds of DNA that can be self-assembled into nanostructures.

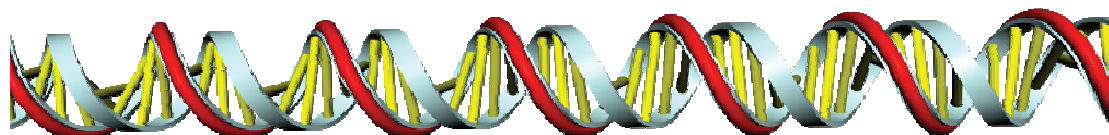


Figure 10. Illustration of DNA-based hybrid material formed by utilizing the DNA duplex as a scaffold to direct material assembly.

The scaffold of DNA can be modified at various sites, for example the nucleobases, the sugar or the phosphate backbone. When building up DNA to longer lengths, either short oligomers or duplexes up to several microns in length, the scaffolding approach signifies the precise placement of modified groups and hence control of the final structure (Fig. 10).

Automated DNA synthesis has the advantage of building ssDNA base by base using a chemical method which is compatible with a range of modifications to the nucleosides.⁶¹ However the over-riding disadvantage of solid-phase synthesis is that the maximum length that can be readily synthesized is approximately 50 bp. After this

point, the overall synthesis degrades and the integrity of incorporation suffers. As the aim of this project is produce wires that are micrometres in length for integrating into circuits, the lengths produced by automated synthesis will not suffice. Furthermore, the conditions used in the synthesizer are reasonably harsh and can have adverse effects on sensitive modifications and this factor has to be taken into consideration when designing functionalized nucleobases. This point is elaborated on further in Chapter 4.

Carell *et al.* have overcome the problems associated with templating by covalently incorporating nucleation sites for metals directly into the nucleobases of DNA.⁶²⁻⁶⁶ By the C5 modification of 5-iodo-2'-deoxythymidine with an alkyne linker via Sonogashira-type chemistry, they were able to subsequently synthesize an aldehyde moiety at the terminal end of the linker on the pyrimidine. The modified nucleoside was then converted into its triphosphate and by utilizing the self-recognition properties of DNA, they built an aldehyde-modified 300mer duplex of DNA via PCR.

Via post-modification, silver was selectively deposited onto the aldehyde modified DNA template by the well recognized Tollens reaction and the appearance of silver nanoparticles and even nanoclusters were observed by TEM studies. Whilst the method of nucleation of nanoclusters onto modified DNA offers a vast number of sites for silver nanoparticle formation, all the sites did not react with the Tollens solution and so a bead-on-a-string appearance develops instead of one continuous wire (Fig. 11). This technique involves utilizing DNA as a scaffold to incorporate the aldehyde containing moiety via PCR, followed by templating of silver nanoparticles.

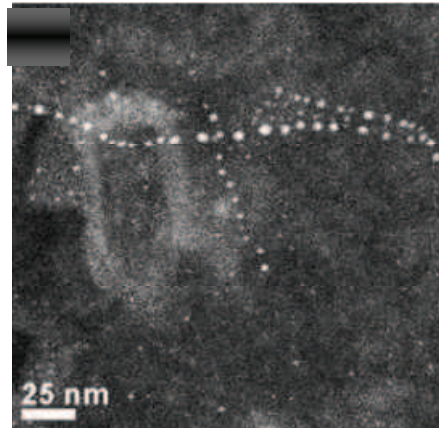


Figure 11. Tollens solution incubated with a 900mer aldehyde-modified DNA duplex.⁶⁷

To counteract the problems of producing long modified dsDNA, DNA polymerases can be employed to catalyze the formation of the phosphodiester linkage between nucleotides. By a range of methods, short strands of DNA can be extended and amplified to form duplexes of DNA that are microns in length. These enzymes rely on primers and templates as a basis for extension. Incorporating one base at a time, the enzyme builds up the dsDNA to a length dictated by either the template or the time of reaction. Primer extension can be employed as a method to test how polymerases accommodate modified nucleotides, as polymerases are very sensitive to changes in the shape of nucleotides.^{60,68} Once the ideal polymerase has been found, modified triphosphates can be integrated into DNA via methods such as PCR (polymerase chain reaction) in order to produce lengths reaching several microns.

PCR primarily requires a template and a primer. A suitable polymerase will fill in the complementary nucleotides opposite a template until it has reached the end of the template. Once this extension is completed, the temperature is raised to denature the dsDNA and on cooling, the primers in solution bind to the single stranded template in an annealing step. Once again, as the primer template is set up, the polymerase incorporates the corresponding nucleotides opposite the template. This cycle is repeated until a defined amount of dsDNA has been amplified. Clearly, the polymerase employed must be thermostable since the temperatures required to denature the dsDNA reach 90 °C.

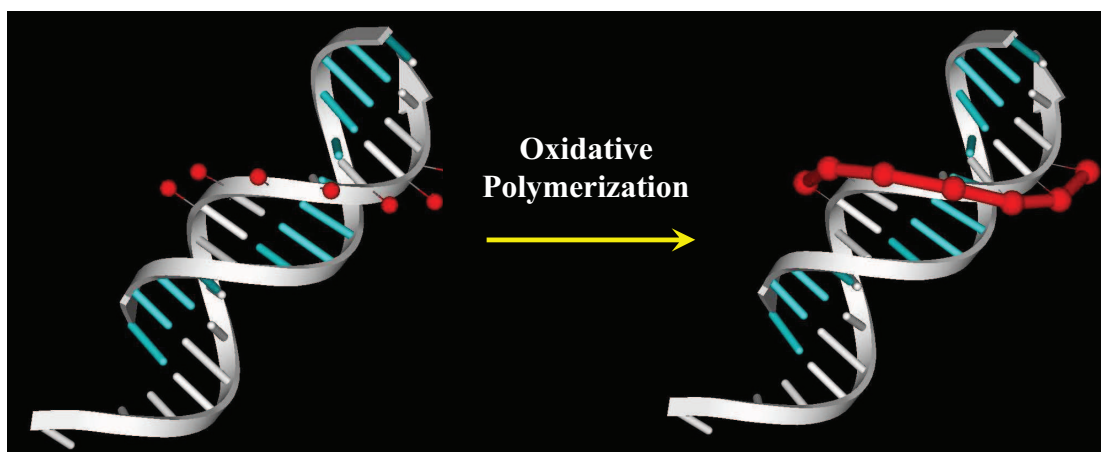
A whole range of modified nucleotides have been incorporated in this manner and have produced functional DNA.⁶⁹⁻⁷¹ However, one drawback of this procedure is in

regard to the template employed. The single stranded template is often extracted from the DNA of a bacterium, known as wild-type DNA. This is the natural form of DNA in that organism and hence its sequence cannot easily be controlled. The base sequence although known is not regular and therefore is a hindrance when intending to incorporate a functionalized nucleotide at specified positions. Sequence specificity can of course be achieved via automated synthesis but again without the desired length. However, an enzymatic methodology established by Kotlyar *et al.* has generated a way of extending a template of DNA, to give a pre-designed sequence of over 10,000 bp in length.

The procedure for extension is initiated using a template such as poly(dA)₁₀-poly(dT)₁₀ or poly(dC)₁₀-poly(dG)₁₀. In a one-pot reaction, a one-to-one helical structure of up to 30,000 base pairs in length (~9 μm) can be fabricated. The method utilizes the Klenow fragment polymerase that is deficient of its exonuclease; the proof-reading function of the polymerase. The extension length is time dependent and hence the dsDNA extends until the reaction quenched by, for example, a chelating compound such as EDTA. This method is very effective when wanting to grow homologous DNA duplexes.^{72,73} Using the methodology of Kotlyar *et al.*, Ijiro *et al.* have developed this strategy to enzymatically grow a copolymer of DNA to selectively bind platinum to specific regions of the duplex, hence functionalizing the DNA.^{74,75} These methods provide an approach to functionalized DNA based systems.

1.5 Aims of project

In light of the previous research reviewed in this chapter, a novel mode is required to extend DNA so that it is fully functionalized with conductive material. Ease of synthesis and reproducible methods are necessary in order to be considered for applications within the electronics industry. It is clear to see that being able to control the synthesis of a wire of precise length and arrangement could lead to an enhancement of the knowledge in how single molecule conductivity can be generated. In summary, by using the scaffold approach to enzymatically and selectively grow DNA in a controlled manner; a duplex of a regular diameter containing functional units at a known location could be afforded. (Scheme 1)



Scheme 1. The general approach of the project illustrating the incorporation of monomer units into specific locations of DNA followed by the oxidation these units to form a conductive wire that follows the shape of DNA.

Furthermore, this approach can overcome common challenges faced in nanowire construction, such as providing a greater uniform dispersion of conductive units and hence a more homogeneous wire. Overcoming these challenges should lead to wires with controlled parameters and higher levels of conductivity than current methods, which is critical for the application of such materials in electronic devices.

In consideration of the above reasoning, this project looks at the integration of the conducting polymers of pyrrole-based derivatives with DNA in an enzymatic scaffold approach. Pyrrole is the polymer of choice due to its high conductivity values, neutral oxidation conditions, ability to be tuned and ease of functionalization. Initially the synthesis and characterisation of the polymers and their subsequent functionalization are described in Chapter 2. Chapter 3 discusses the coupling of the functionalized monomers with the nucleosides deoxythymidine and deoxycytidine via Sonogashira-type chemistry. Chapter 4 extends this synthesis to the conversion of the modified nucleosides into their corresponding triphosphates which leads into a discussion of their incorporation into DNA via DNA polymerases in Chapter 5. Finally, Chapter 6 draws conclusions and identifies future possibilities of this research topic.

References

- (1) Voigt, N. V.; Topping, T.; Rotaru, A.; Jacobsen, M. F.; Ravnsbaek, J. B.; Subramani, R.; Mamdouh, W.; Kjems, J.; Mokhir, A.; Besenbacher, F.; Gothelf, K. V. *Nat. Nanotechnol.* **2010**, *5*, 200.
- (2) Knez, M.; Bittner, A. M.; Boes, F.; Wege, C.; Jeske, H.; Maiss, E.; Kern, K. *Nano Lett.* **2003**, *3*, 1079.
- (3) Willner, I.; Willner, B. *Nano Lett.* **2010**, *10*, 3805.
- (4) Tomczak, M. M.; Slocik, J. M.; Stone, M. D.; Naik, R. R. *Biochem. Soc. Trans.* **2007**, *35*, 512.
- (5) Weber, J.; Singhal, R.; Zekri, S.; Kumar, A. *Int. Mater. Rev.* **2008**, *53*, 235.
- (6) Mas-Balleste, R.; Gomez-Herrero, J.; Zamora, F. *Chem. Soc. Rev.* **2010**, *39*, 4220.
- (7) Barth, S.; Hernandez-Ramirez, F.; Holmes, J. D.; Romano-Rodriguez, A. *Prog. Mater. Sci.* **2010**, *55*, 563.
- (8) Reiss, P.; Couderc, E.; De Girolamo, J.; Pron, A. *Nanoscale* **2011**, *3*, 446.
- (9) Lahiff, E.; Lynam, C.; Gilmartin, N.; O'Kennedy, R.; Diamond, D. *Anal. Bioanal. Chem.* **2010**, *398*, 1575.
- (10) Cui, D. X.; Gao, H. J. *Biotechnol. Prog.* **2003**, *19*, 683.
- (11) Obonyo, O.; Fisher, E.; Edwards, M.; Douroumis, D. *Crit. Rev. Biotechnol.* **2010**, *30*, 283.
- (12) Xia, Y.; Yang, P.; Sun, Y.; Wu, Y.; Mayers, B.; Gates, B.; Yin, Y.; Kim, F.; Yan, H. *Adv. Mater.* **2003**, *15*, 353.
- (13) Tkachev, S. V.; Buslaeva, E. Y.; Gubin, S. P. *Inorg. Mater.* **2011**, *47*, 1.
- (14) Hassanien, R.; Al-Hinai, M.; Farha Al-Said, S. A.; Little, R.; Siller, L.; Wright, N. G.; Houlton, A.; Horrocks, B. R. *ACS Nano* **2010**, *4*, 2149.
- (15) Kim, F. S.; Ren, G. Q.; Jenekhe, S. A. *Chem. Mater.* **2011**, *23*, 682.
- (16) Almawlawi, D.; Liu, C. Z.; Moskovits, M. *J. Mater. Res.* **1994**, *9*, 1014.
- (17) Yan, P.; Xie, Y.; Qian, Y. T.; Liu, X. M. *Chem. Commun.* **1999**, 1293.
- (18) Trivedi, K.; Yuk, H.; Floresca, H. C.; Kim, M. J.; Hu, W. *Nano Lett.* **2011**, *11*, 1412.
- (19) Goldberger, J.; He, R.; Zhang, Y.; Lee, S.; Yan, H.; Choi, H.-J.; Yang, P. *Nature* **2003**, *422*, 599.
- (20) Thelander, C.; Agarwal, P.; Brongersma, S.; Eymery, J.; Feiner, L. F.; Forchel, A.; Scheffler, M.; Riess, W.; Ohlsson, B. J.; Gösele, U.; Samuelson, L. *Mater. Today* **2006**, *9*, 28.
- (21) Wu, Y.; Yang, P. *J. Am. Chem. Soc.* **2001**, *123*, 3165.
- (22) Tenne, R.; Margulis, L.; Genut, M.; Hodes, G. *Nature* **1992**, *360*, 444.
- (23) Rao, C. N. R.; Govindaraj, A.; Deepak, F. L.; Gunari, N. A.; Manashi, N. *Appl. Phys. Lett.* **2001**, *78*, 1853.
- (24) Dloczik, L.; Engelhardt, R.; Ernst, K.; Fiechter, S.; Sieber, I.; Konenkamp, R. *Appl. Phys. Lett.* **2001**, *78*, 3687.
- (25) Hu, J. Q.; Bando, Y.; Liu, Z. W.; Zhan, J. H.; Golberg, D.; Sekiguchi, T. *Angew. Chem. Int. Ed.* **2004**, *43*, 63.
- (26) Remškar, M. *Adv. Mater.* **2004**, *16*, 1497.
- (27) Liang, H. W.; Liu, S.; Yu, S. H. *Adv. Mater.* **2010**, *22*, 3925.
- (28) Briseno, A. L.; Mannsfeld, S. C. B.; Jenekhe, S. A.; Bao, Z.; Xia, Y. *Mater. Today* **2008**, *11*, 38.
- (29) Iijima, S. *Nature* **1991**, *354*, 56.

- (30) Baughman, R. H.; Zakhidov, A. A.; de Heer, W. A. *Science* **2002**, *297*, 787.
- (31) Nel, A.; Xia, T.; MÅrdler, L.; Li, N. *Science* **2006**, *311*, 622.
- (32) Xiao, S.; Tang, J.; Beetz, T.; Guo, X.; Tremblay, N.; Siegrist, T.; Zhu, Y.; Steigerwald, M.; Nuckolls, C. *J. Am. Chem. Soc.* **2006**, *128*, 10700.
- (33) Wang, Y.; Tran, H. D.; Liao, L.; Duan, X.; Kaner, R. B. *J. Am. Chem. Soc.* **2010**, *132*, 10365.
- (34) Watson, J. D.; Crick, F. H. *Nature* **1953**, *171*, 737.
- (35) Richter, J.; Seidel, R.; Kirsch, R.; Mertig, M.; Pompe, W.; Plaschke, J.; Schackert, H. K. *Adv. Mater.* **2000**, *12*, 507.
- (36) Clever, G. H.; Shionoya, M. *Coord. Chem. Rev.* **2010**, *254*, 2391.
- (37) Porath, D.; Bezryadin, A.; de Vries, S.; Dekker, C. *Nature* **2000**, *403*, 635.
- (38) Georgakilas, A. G.; Sakelliou, L.; Sideris, E. G.; Margaritis, L. H.; Sophianopoulou, V. *Radiat. Res.* **1998**, *150*, 488.
- (39) Houlton, A.; Pike, A. R.; Galindo, M. A.; Horrocks, B. R. *Chem. Commun.* **2009**, 1797.
- (40) Seeman, N. C. *J. Theor. Biol.* **1982**, *99*, 237.
- (41) Endo, M.; Hidaka, K.; Sugiyama, H. *Org. Biomol. Chem.* **2011**, *9*, 2075.
- (42) Rajendran, A.; Endo, M.; Katsuda, Y.; Hidaka, K.; Sugiyama, H. *ACS Nano* **2011**, *5*, 665.
- (43) Andersen, E. S.; Dong, M.; Nielsen, M. M.; Jahn, K.; Subramani, R.; Mamdouh, W.; Golas, M. M.; Sander, B.; Stark, H.; Oliveira, C. L. P.; Pedersen, J. S.; Birkedal, V.; Besenbacher, F.; Gothelf, K. V.; Kjems, J. *Nature* **2009**, *459*, 73.
- (44) Moliton, A.; Hiorns, R. C. *Polym. Int.* **2004**, *53*, 1397.
- (45) Dong, L. Q.; Hollis, T.; Fishwick, S.; Connolly, B. A.; Wright, N. G.; Horrocks, B. R.; Houlton, A. *Chem.-Eur. J.* **2007**, *13*, 822.
- (46) Pruneanu, S.; Al-Said, S. A. F.; Dong, L. Q.; Hollis, T. A.; Galindo, M. A.; Wright, N. G.; Houlton, A.; Horrocks, B. R. *Adv. Funct. Mater.* **2008**, *18*, 2444.
- (47) Braun, E.; Eichen, Y.; Sivan, U.; Ben-Yoseph, G. *Nature* **1998**, *391*, 775.
- (48) Mertig, M.; Colombi Ciacchi, L.; Seidel, R.; Pompe, W.; De Vita, A. *Nano Lett.* **2002**, *2*, 841.
- (49) Monson, C. F.; Woolley, A. T. *Nano Lett.* **2003**, *3*, 359.
- (50) Becerril, H. A.; Woolley, A. T. *Chem. Soc. Rev.* **2009**, *38*, 329.
- (51) Seidel, R.; Columbi Ciacchi, L.; Weigel, M.; Pompe, W.; Mertig, M. *J. Phys. Chem. B* **2004**, *108*, 10801.
- (52) Aich, P.; Labiuk, S. L.; Tari, L. W.; Delbaere, L. J. T.; Roesler, W. J.; Falk, K. J.; Steer, R. P.; Lee, J. S. *J. Mol. Biol.* **1999**, *294*, 477.
- (53) Tanaka, K.; Shionoya, M. *Coord. Chem. Rev.* **2007**, *251*, 2732.
- (54) Chen, W.; Guler, G.; Kuruvilla, E.; Schuster, G. B.; Chiu, H. C.; Riedo, E. *Macromolecules* **2010**, *43*, 4032.
- (55) Nickels, P.; Dittmer, W. U.; Beyer, S.; Kotthaus, J. P.; Simmel, F. C. *Nanotechnology* **2004**, *15*, 1524.
- (56) Bardavid, Y.; Ghabboun, J.; Porath, D.; Kotylar, A. B.; Yitzchaik, S. *Polymer* **2008**, *49*, 2217.
- (57) Ma, Y.; Zhang, J.; Zhang, G.; He, H. *J. Am. Chem. Soc.* **2004**, *126*, 7097.
- (58) Seela, F.; Feiling, E.; Gross, J.; Hillenkamp, F.; Ramzaeva, N.; Rosemeyer, H.; Zulauf, M. *J. Biotechnol.* **2001**, *86*, 269.
- (59) Pike, A. R.; Ryder, L. C.; Horrocks, B. R.; Clegg, W.; Connolly, B. A.; Houlton, A. *Chem.Eur. J.* **2005**, *11*, 344.

- (60) Obeid, S.; Baccaro, A.; Welte, W.; Diederichs, K.; Marx, A. *Proc. Natl. Acad. Sci. U. S. A.* **2010**, *107*, 21327.
- (61) Wanninger-Weiß, C.; Wagenknecht, H. A. *Eur. J. Org. Chem.* **2008**, *2008*, 64.
- (62) Gierlich, J.; Burley, G. A.; Gramlich, P. M. E.; Hammond, D. M.; Carell, T. *Org. Lett.* **2006**, *8*, 3639.
- (63) Burley, G. A.; Gierlich, J.; Mofid, M. R.; Nir, H.; Tal, S.; Eichen, Y.; Carell, T. *J. Am. Chem. Soc.* **2006**, *128*, 1398.
- (64) Gramlich, P.; Warncke, S.; Gierlich, J.; Carell, T. *Angew. Chem., Int. Ed.* **2008**, *47*, 3442.
- (65) Gierlich, J.; Gutsmedl, K.; Gramlich, P.; Schmidt, A.; Burley, G.; Carell, T. *Chem. Eur. J.* **2007**, *13*, 9486.
- (66) Fischler, M.; Simon, U.; Nir, H.; Eichen, Y.; Burley, G.; Gierlich, J.; Gramlich, P. M.; Carell, T. *Small* **2007**, *3*, 1049.
- (67) Wirges, C. T.; Timper, J.; Fischler, M.; Sologubenko, A. S.; Mayer, J.; Simon, U.; Carell, T. *Angew. Chem., Int. Ed.* **2009**, *48*, 219.
- (68) Gramlich, P. M. E.; Wirges, C. T.; Gierlich, J.; Carell, T. *Org. Lett.* **2007**, *10*, 249.
- (69) Thum, O.; Jager, S.; Famulok, M. *Angew. Chem. Int. Edit.* **2001**, *40*, 3990.
- (70) Jager, S.; Rasched, G.; Kornreich-Leshem, H.; Engeser, M.; Thum, O.; Famulok, M. *J. Am. Chem. Soc.* **2005**, *127*, 15071.
- (71) Jäger, S.; Famulok, M. *Angew. Chem., Int. Ed.* **2004**, *43*, 3337.
- (72) Kotlyar, A. B.; Borovok, N.; Molotsky, T.; Fedeev, L.; Gozin, M. *Nucleic Acids Res.* **2005**, *33*, 525.
- (73) Borovok, N.; Molotsky, T.; Ghabboun, J.; Cohen, H.; Porath, D.; Kotlyar, A. *FEBS Lett.* **2007**, *581*, 5843.
- (74) Tanaka, A.; Matsuo, Y.; Hashimoto, Y.; Ijiro, K. *Chem. Commun.* **2008**, 4270.
- (75) Shionoya, M.; Tanaka, K. *Curr. Opin. Chem. Biol.* **2004**, *8*, 592.

Chapter 2 - *Synthesis of pyrrole-based monomers, functionalization and applications*

Chapter 2 – *Synthesis of pyrrole-based monomers, functionalization and applications*

In the previous chapter, the challenges of 1D material growth were assessed and whilst a great deal is based on inorganic material, a number are based on organic materials. Although biopolymers such as DNA have a defined 1D structure, they have properties of an insulator and are not conductive.¹ Other polymers such as organic conductive polymers can play an important role in electronic applications and will therefore be the core focus of this chapter.

Organic polymers are interesting materials for nanoscale electronic applications because they are conductive, flexible, economical, and most importantly can be readily functionalized.² Semiconducting organic polymers have shown a lot of promise in the field of nanotechnology due to their ease of synthesis and important electrical properties.³ These materials have potential for applications such as electrical components and biosensors owing to unique possessing electrical, optical or mechanical properties.⁴

In the 1970's, more specifically in 1977, the conducting nature of polyacetylene was discovered and led to a new field of research.^{5,6} Polyacetylene (Fig. 1) was realized to be electrically conductive with conductivities of 10^{-9} S cm⁻¹ facilitated by its conjugated system. The alternating single and double bonds generate the conjugated system and it is the π -electron backbone which is responsible for its electronic properties. However, Shirakawa *et al.* revealed that the conductivity of the polymers can be tuned by doping with oxidizing (p-doping) agents such as chlorine, bromine and iodine or reducing (n-doping) agents, for example sodium, to increase the density of charge carriers within the polymer. The electrical conductivity of polyacetylene was increased to 10^5 S cm⁻¹ when doped.

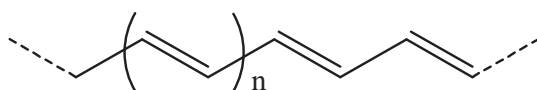


Figure 1. Structure of polyacetylene

As a result, there has been an increased interest in synthesizing conducting organic polymers.⁷ The most familiar conductive polymers are polyacetylene, polyaniline, polyindole, polypyrrole and polythiophene. They are all semiconductive organic polymers due to comprising of a π -conjugated system, alongside possessing low band gaps (Table 1) which allow the transfer of electrons through the material.⁷

Polymer	Band gap (eV)
Polyacetylene ⁸	1.5
Polypyrrole ⁹	2.5
Polythiophene ^{8,9}	2.1-2.2

Table 1. Conducting polymers with their respective band gaps, illustrating semiconductor materials.

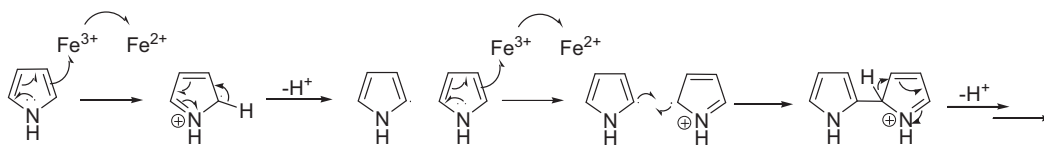
Special interest has been shown in the highly conducting polymers of aniline,^{10,11} indole,¹² pyrrole¹³ and thiophene.¹⁴⁻¹⁶ This attraction is due to the ease of preparation, being relatively cheap starting materials and significantly having the essential property of high conductivity in the range of $\sim 1 \times 10^{-3}$ to $\sim 1 \times 10^3$ S cm⁻¹.⁷ The polymers are also versatile in their processability as they can be used as bulk polymers such as films and powders but can also be produced in a more controlled manner to fabricate wires. However, processing of conducting polymers can be difficult as they are very insoluble. To overcome the difficulty of constructing 1D nanowires, one approach has been to use concepts from supramolecular chemistry, more specifically through templating to direct the wires in one dimension. For example, DNA can be utilized as a template to define the morphology and size of nanowires by assembling and organizing polymers through a combination of the electrostatic binding between the negative phosphate backbone and polycationic polymer charge, and via groove binding.^{10,11,17} Polyaniline templated DNA has been reported,¹¹ although will not be considered due to reasoning met in Chapter 1. A

key feature of organic polymers is the element of functionalization. Polymers such as polypyrrole have the ability to be functionalized with derivatives demonstrated at the *N*-position via alkylation. Modifying here does not disturb the conjugation system upon polymerization. Specific electronic properties can be achieved by manipulation of the structure and one mode of doing so is by synthesizing co-monomers. Hence, polymers consisting of pyrrole and further co-polymers of pyrrole and thiophene will be focussed on in order to assess their electronic properties and also their size, as the objective is to introduce them into DNA without deviating from its natural helical structure. Therefore, the following sections highlight some fundamental aspects of polypyrrole and polythiophene chemistry.

2.1 Pyrrole

As previously mentioned, conducting polymers are very attractive in materials science and this project will concentrate on pyrrole-based polymers. Polypyrrole has a number of attractive features such as its conductivity, stability, ease of preparation and functionalization.^{13,18-20} Potential functionalization is a beneficial attribute of pyrrole, as the polymer can be modified but retain its conductivity in order to generate versatility. Polymers such as polyaniline require an acidic pH as low as 4.0 to initiate the polymerisation.²¹ The acidic conditions required are harsh in comparison to the neutral conditions used for polymers like polypyrrole.

'Pyrrole Black' is the term given to the polymer as it forms a black film when polymerized. It was first reported by Kanazawa *et al.* in 1979 and exhibited conductivities of up to 100 S cm^{-1} .²² More recently, 2D films of polypyrrole have been produced which demonstrate conductivities over 1000 S cm^{-1} when doped.²³ Polymerisation of pyrrole is relatively straightforward and can be achieved chemically and electrochemically. It can be polymerized chemically to form the polycation using oxidants such as FeCl_3 and is also possible to polymerize the pyrrole monomers electrochemically, which will be demonstrated in 2.2.2.



Scheme 1. Mechanism of the chemical oxidation of pyrrole.

When pyrrole polymerizes it does so through the 2- and 5-positions (α positions) of the heterocyclic ring (Scheme 1). Evidence has supported this mechanism by attempting to polymerize an α -substituted (2-position) pyrrole which consequently did not polymerize.²⁴ However, β -substituted (3-, 4-positions) pyrrole proceeded to polymerize but has been shown to have detrimental effects on the electrical conductivity of the polymer due to the out of plane twisting of the ring system caused by sterically demanding β -substituents.²⁴ Functionalization of the heterocyclic structure is an advantageous situation to produce more versatile polymers. Polypyrrole can be functionalized either on the carbon-ring or through *N*-alkylation of its nitrogen which allow it to still function as a semiconductor. Pyrrole has been substituted at the β - and *N*-H position²⁴ and each substitution can considerably affect the structure and conductivity of the pyrrole polymer.²⁵ For example, when pyrrole is substituted at the β -position, the planarity of the ring is reduced and there is a drop in conductivity.²⁵ *N*-methylpolypyrrole can be considered as the simplest case for *N*-alkylation of pyrrole and exhibits conductivities of $\sim 10^{-3}$ S cm⁻¹.²⁴ The *N*-methylation revealed a drop in conductivity in comparison to unmodified polypyrrole and is considered to be due to the disrupted planarity of the ring system which will affect the conjugation and hence the electron flow within the polymer.²⁴

Furthermore, substituting with an electron withdrawing group, such as nitro- and cyano-derivatives, have demonstrated lower HOMO/LUMO energy band gaps and in turn producing a polymer that is capable of exhibiting higher conductivities.³

2.1.1 Pyrrole-thiophene copolymers

The use of co-polymers (polymers made from two or more different monomer units) offers an alternative strategy to obtain novel conducting and structural properties. However, polymerizing monomer units of different nature often afford irregular polymers with a highly unpredictable structure. A more subtle way of preparing regular co-polymers has been shown by polymerizing heterogeneous monomer units made from two or more different monomers, such as 2-(2-thienyl)pyrrole (**tp**), 2,5-bis(2-thienyl)pyrrole (**tpt**) (Fig. 2).²

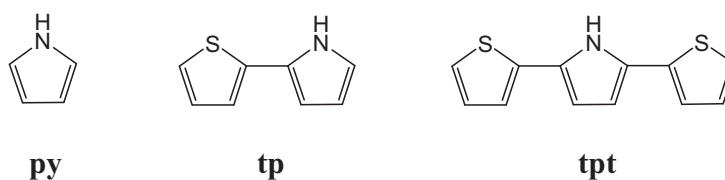


Figure 2. Monomer unit precursors of π -conducting polymers. Pyrrole (**py**), 2-(2-thienyl)pyrrole (**tp**), 2,5-bis(2-thienyl)pyrrole (**tpt**).

This methodology facilitates the control of polymer structure and periodicity upon polymerization of the heterogeneous monomer units, especially when symmetrical monomers units such as **tpt** are employed. The π -conducting polymer obtained from pyrrole (**py**), 2-(2-thienyl)pyrrole (**tp**), 2,5-bis(2-thienyl)pyrrole (**tpt**) monomers have shown low band gap, easy processing, stable and high conductivity.

Combining the high conductivities of polypyrrole with the exceptional chemical stability of thiophene is an attractive approach for tailoring the polymers. Extending the ring length will provide varied spacing when attempting to integrate into DNA, whilst the ease of polymerization of an extended system will improve due to the greater π -electron delocalization in the system.²⁶ **Tp** has been described as a stable polymer with conductivities up to 1 S cm^{-1} ,²⁷ and it has been reported that extension of the ring system raises the HOMO residing on pyrrole and lowers the LUMO on thiophene, hereby

decreasing the band gap.²⁸ Therefore, this chapter describes the synthesis and polymerization of **py**, **tp** and **tpt**, functionalization and application in nanowire formation. The functionalization will be achieved via *N*-alkylation, which aims to equip these monomer units with functional groups that will allow their covalent attachment to nucleosides in the DNA framework, the nucleation of metals or to take part in ‘click’ chemistry.

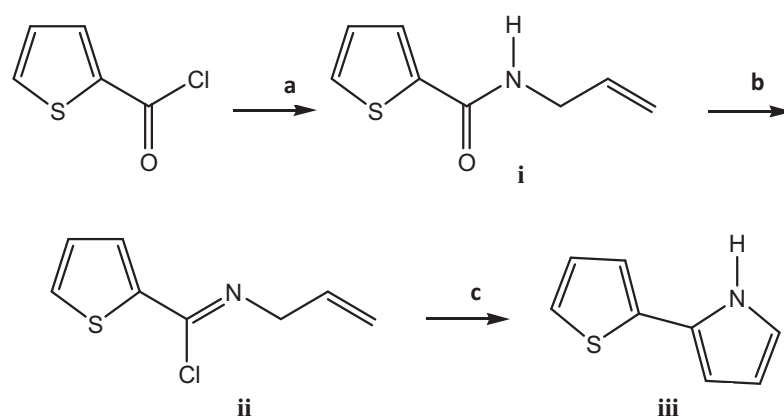
2.2 Results and Discussion

In order to produce 1D conducting polymers that have a potential application in electronics, they must have the ability to be tuned and functionalized for versatility in higher ordered applications. As films of pyrrole exhibit conductivities up to 100 S cm^{-1} , this combined with a low oxidation potential from a monomer such as thiophene, enables a system that can be polymerized easily with high conductivities.²⁶ Furthermore, retaining the nitrogen on the pyrrole ring will allow for further modification. The next section will explore the synthesis into **tp** and **tpt** and demonstrate how using the nitrogen on pyrrole can harness a range of 3- and 5- carbon alkyne linkers which additionally have potential for further functionalization. In addition, the applications of one of the alkylated precursors, **5-tp**, is recognized as potential for electronics and medical sensing.

2.2.1 Synthesis of **tp** and **tpt**

A series of monomers and subsequent *N*-alkylated monomers were prepared. The compounds have been characterized by ¹H NMR spectroscopy, ES-MS, UV-Vis spectroscopy and cyclic voltammetry. Single crystal X-Ray data for *N*-alkylated derivative **3-tpt** illustrates the attachment of the 3-carbon alkyl chain -containing a terminal alkyne group- to the N atom of the pyrrolyl ring. Particular emphasis was made on the electronic structure and redox properties of the compounds in order to assess their ability to grow conducting polymers.

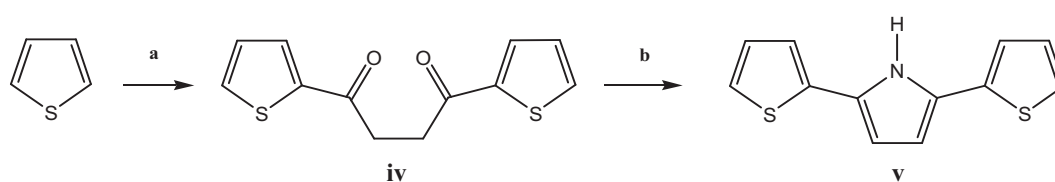
Pyrrole can be purchased commercially and requires distillation before use. However, **tp** and **tpt** were synthesized according to literature. An overview of the synthesis of these units is describe below (Scheme 2, Scheme 3).^{29,30}



Scheme 2. The three step production of **tp** a) allylamine, pyridine, b) thionyl chloride, DMF and toluene, c) potassium tert-butoxide, 1,4-dioxane and DMF.

Thiophene carbonyl chloride is reacted with allylamine in an S_N2 reaction and produces thiophene allylcarboxamide (**i**) in yields of up to 82%. After purification, this is then reacted with thionyl chloride in toluene and a few drops of DMF are added to aid the substitution. Purification was not required, only washing to remove excess thionyl chloride and any traces of DMF and thus producing thiophene imidoyl chloride (**ii**) in yields of up to 85%. The third step requires an elimination step to ring close the imidoyl chloride to generate the formation of 2-(2-thienyl) pyrrole, **tp** (**iii**).

In the addition of two thiophene rings to the 2- and 4- positions of pyrrole, i.e. the formation of **tpt**, the synthesis is shown in Scheme 3^{31,32}.



Scheme 3. The two step production of **tpt** a) succinyl chloride, $AlCl_3$ (anhydrous) and DCM, b) acetic acid, ammonium acetate and acetic anhydride.

In the first step, thiophene undergoes Friedel-Crafts acylation by employing succinyl chloride and aluminium chloride to form the di-ketone; 1,4-bis(2-thienyl)-1,4-butanedione. The Paal-Knorr synthesis³³ was then followed by refluxing the di-ketone in ammonium acetate and hot propionic acid yielded the ring-closed product **tpt** in 72% yield.

2.2.2 Electrochemical polymerisation of py, tp and tpt.

The electrochemical polymerization of pyrrole (**py**), 2-(2-thienyl)pyrrole (**tp**), 2,5-bis(2-thienyl)pyrrole (**tpt**) was investigated through cyclic voltammetry, Figures 3-5. Electrochemical polymerisation was employed as it allows the precise control of polymer growth, as opposed to chemical oxidation. The results are tabulated in Table 2.

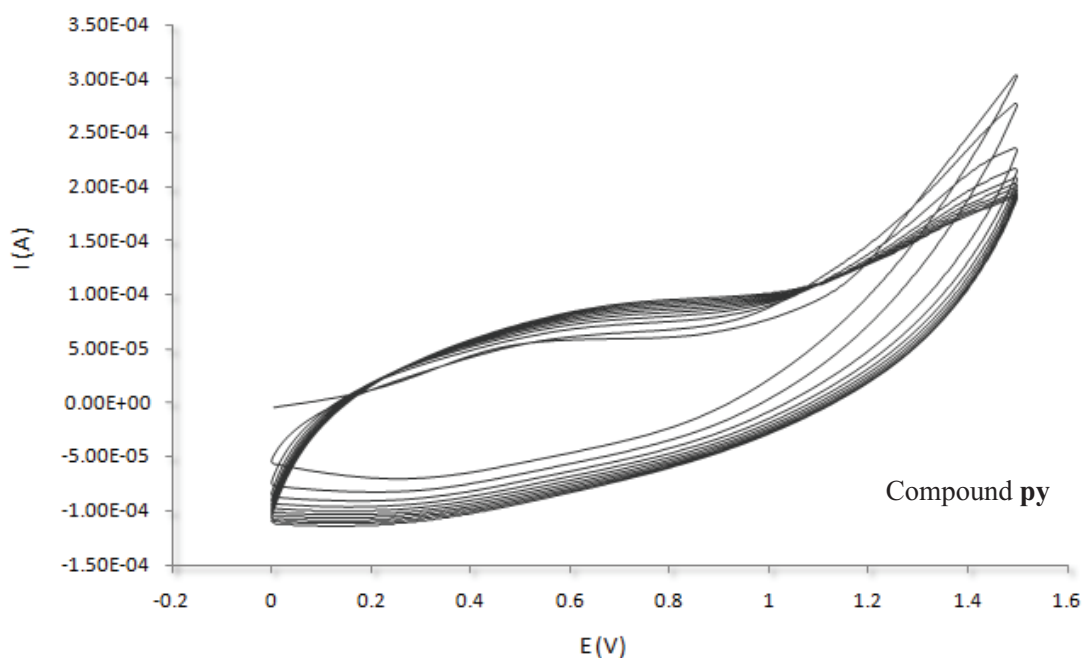


Figure 3. CV for **py**. Conditions: 10 mM of sample, 100 mM LiClO₄, acetonitrile, r.t., working electrode Pt, counter electrode Au and Ag-quasi reference electrode. Scan rate 0.2 V/s.

The cyclic voltammogram shows the expected oxidation of the monomer above 1.05 V. When the pyrrole monomer is oxidized, it exhibits a redox reaction. On the return sweep, there is no evidence of monomer reduction which is as expected as the oxidized monomer will have polymerized. However, oxidation of the polymer starts to increase from ~0.5 V with successive cycles.

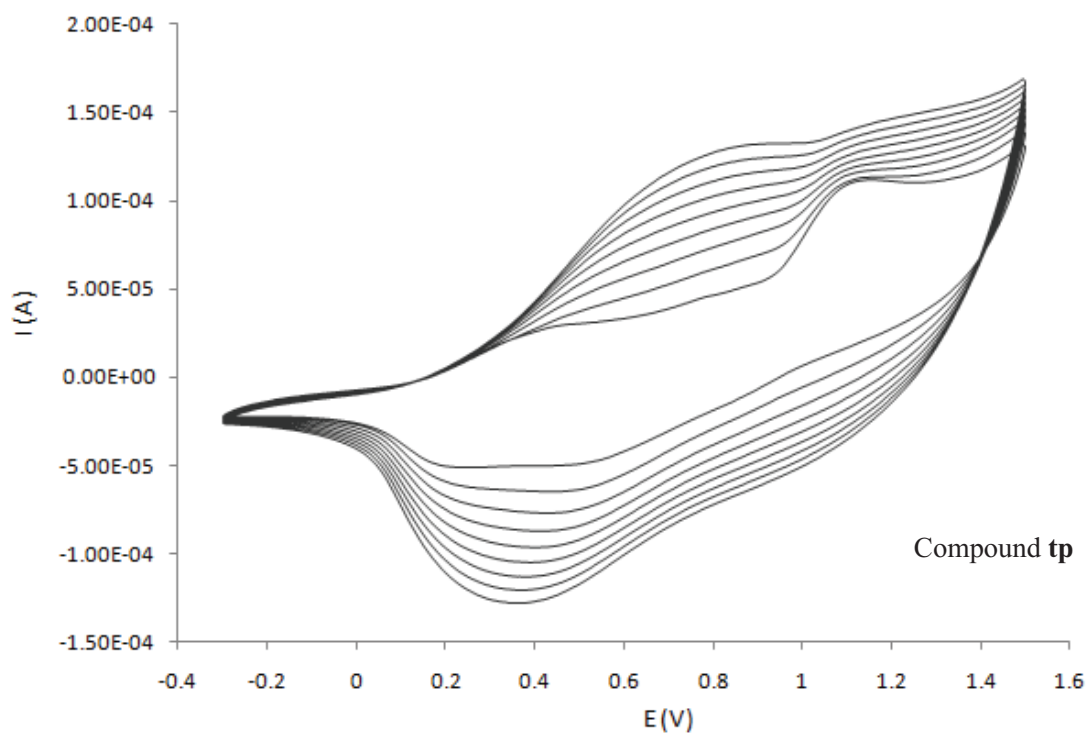


Figure 4. CV for **tp**. Conditions: 10 mM of sample, 100 mM LiClO₄, acetonitrile, r.t., working electrode Pt, counter electrode Au and Ag-quasi reference electrode. Scan rate 0.2 V/s.

The oxidation of the **tp** monomer occurs at 1.15 V. Again, it exhibits the expected irreversible polymerization due to the oxidation and so it cannot revert to its monomer state. In this CV, the oxidation of the polymer arises at ~0.7 V. In addition to this, the reduction of the polymer can be observed at a current of ~0.35 V. The voltammogram illustrates that the oxidation and reduction peaks of the polymer are more pronounced and grow with each cycle.

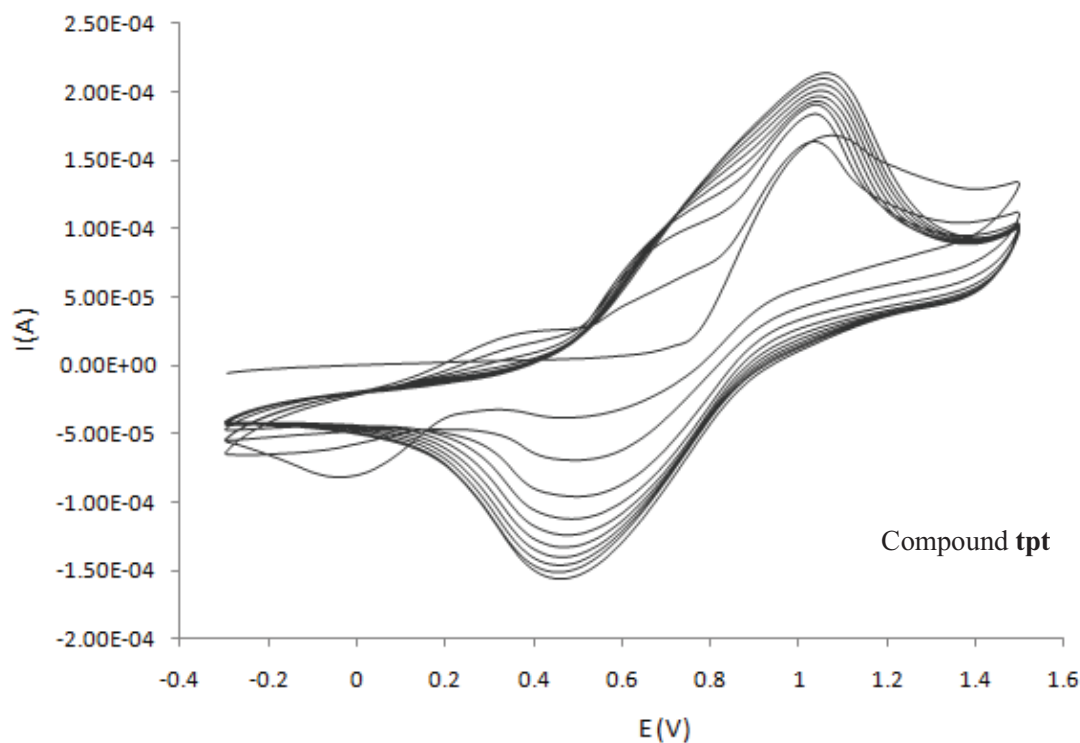


Figure 5. CV for **tpt**. Conditions: 10 mM of sample, 100 mM LiClO₄, acetonitrile, r.t., working electrode Pt, counter electrode Au and Ag-quasi reference electrode. Scan rate 0.2 V/s.

The first oxidation of the **tpt** monomer occurs at 1.07 V. In this CV, the oxidation of the polymer occurs at ~0.35 V. In addition to this, the reduction of the polymer can be observed from the increasing peaks at ~0.45 V. The monomer unit **tpt** exhibits the lowest oxidation potential which is indicative of an extended ring system due to the greater π -electron delocalization.

By analysis of the voltammograms in Figures 3 to 5, the extension of the ring system from **py** to **tp** to **tpt**, demonstrates that the anodic peak becomes less positive. This is an expected result as the oxidation potential of the monomer decreases with the increase in conjugation of the ring systems as the extra conjugation induces extra stability of the radical cation formed.³⁴

The pyrrole containing monomers have demonstrated that they can be polymerized electrochemically, and hence, there is now an opportunity to functionalize the monomers

in order to generate versatility to the system whilst retaining the ability for electropolymerization.

2.2.3 *N*-alkylation of pyrrole (py), 2-(2-thienyl)pyrrole (tp), 2,5-bis(2-thienyl)pyrrole (tpt)

In order to introduce functionality to the ring systems to make the polymers more versatile whilst not affecting the conjugation of the rings, alkylation at the *N*-position of the pyrrole ring was performed. The N-H moiety of pyrrole allows facile deprotonation and subsequent *N*-alkylation using alkylating agents such as alkyl halides. In this instance, *N*-alkylation was performed by initial deprotonation of an appropriated monomer unit followed by reaction with and haloalkyl derivate containing a terminal alkynyl group, for example 5-chloro-1-pentyne.

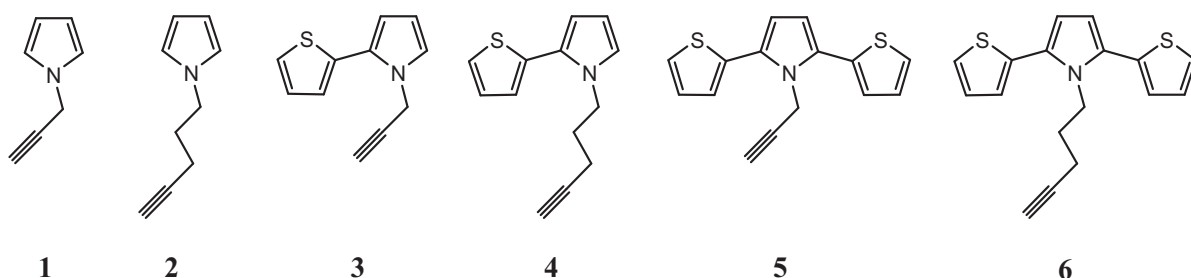
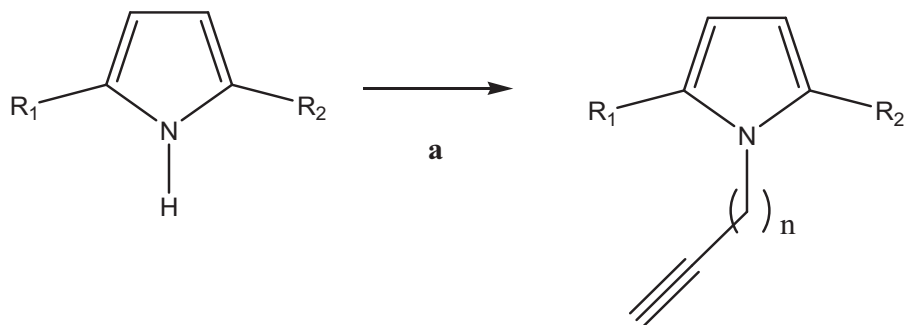


Figure 6. Structures of *N*-alkylated alkyne units 1–6.

N-alkylation is a suitable approach to attach functional alkyl chains into these monomer units through the N atom of the pyrrole ring, as it has been widely used for the attachment of other different functional groups into these and related systems.^{35,36,37} The *N*-alkylated polymer precursors 1-6 (Fig. 6), with 5- and 3-carbons alkyl chain (Scheme 1), were synthesized by initial deprotonation of the **py**, **tp** and **tpt** units with sodium hydride and

subsequent alkylation by the appropriate *n*-5- or *n*-3-alkynyl derivative, 5-chloro-1-pentyne and propargyl bromide respectively (Scheme 4).



Scheme 4. Synthetic route for the *N*-alkylation of pyrrole derivatives. a) NaH, haloalkyne derivative (either propargyl bromide or 5-chloro-1-pentyne), DMF, rt. $R_1 = R_2 = \text{H}$ (**py**), $R_1 = \text{H}$, $R_2 = \text{thiophene}$ (**tp**), $R_1 = R_2 = \text{thiophene}$ (**tp**). $n = 1$ or 3 .

Each of the heterocyclic systems illustrated in section 2.2.1 were *N*-alkylated with 3- and 5- alkyl-alkynyl chain lengths (Fig. 6). All of the *N*-alkylated derivatives were characterized by ^1H NMR spectroscopy, ^{13}C NMR spectroscopy and high-resolution ES-MS, FT-IR spectroscopy and UV-vis spectroscopy. The ^1H NMR spectrum exhibited the expected loss of the *N*-H proton, alongside the up-field shift of the pyrrole protons and a downfield shift of the thiophene protons.

The yield obtained for the synthesis of **1** was lower (10%) when the purification was performed by flash column chromatography on silica. However, adding water to the reaction mixture when it was completed and subsequent extraction in DCM gave rise to compound **1** in yields up to 80%. The reason may be explained by the high reactivity of the α and β position of the pyrrole heterocycle to give rise to undesired side products on silica.

Confirmation of 3-**tpt** was achieved through single crystal X-ray diffraction (Fig. 7). In the figure, the hetero atoms from the thienyl-pyrrole-thiophene have an alternating up-down-up orientation. The thienyl rings are almost coplanar with dihedral angles of 12.7°, but in relation to the pyrrole ring, are twisted to angles of 29.1° and 40.7° individually. These values are consistent with the previously reported *N*-methyl-**tpt** by Ferraris *et al.*,³⁸ where the **tpt** unit demonstrated interplanar angles between 31.3-34.2°. By comparison of 3-**tpt**, the addition of two carbons to the alkyl chain, substituted at the nitrogen on pyrrole, has insignificant effect on the monomer planarity, and hence the ability of polymerization.

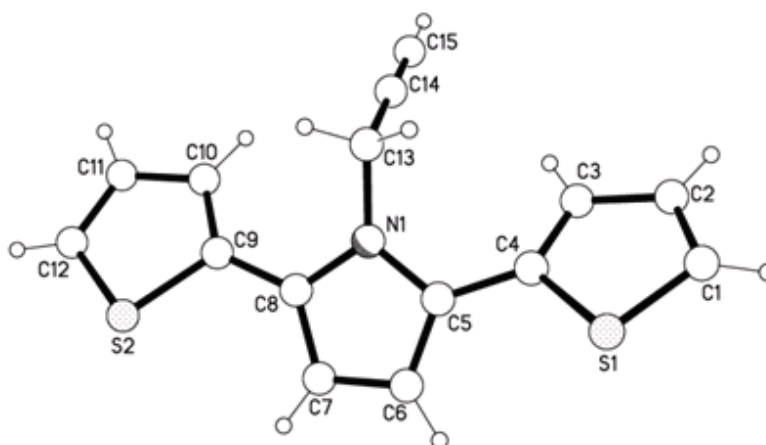


Figure 7. Molecular structure of *N*-alkylated-**tpt**.

2.2.4 FT-IR spectroscopy

Infrared characterization was performed in order to identify and compare the various vibrational groups on the compounds and to further confirm the alkylation of the monomers with the indication of an alkyne peak (Table 2).

Wavenumber (cm ⁻¹)						Assignment
3-py	5-py	3-tp	5-tp	3-tpt	5-tpt	
		695	695	695	696	C-H thiophene
728	721	788	786	772	754	C-H pyrrole
		843	843	844	845	C-S thiophene
1090	1089	1076	1081	1087	1076	ring breathing pyrrole
1281	1282	1291	1297	1299	1304	C-C stretch in-plane
2126	2120	2121	2130	2119	2120	alkyne C≡C
3296	3295	3287	3290	3263	3279	alkyne C-H

Table 2. Vibrational bands of the alkylated monomers and their assignments. The monomers were tested as neat compounds.

Assignment of the vibrational bands was achieved using literature references for **tp**.²⁷. The vibrations at ~2120 cm⁻¹ and ~3280 cm⁻¹ confirm the presence of the alkyne moiety present in the compounds. The peaks at ~695 cm⁻¹ and ~844 cm⁻¹ validate the existence of the thiophene ring as the pyrrole compound lacks these vibrations. The vibrational information is useful if modifications are to be made to the structure as in chapter 3 by employing the alkyne group.

The focus now turns to the electrochemical properties of the alkylated monomers in order to make a direct comparison of **py**, **tp** and **tpt** and study the effect of alkylation on the polymerization of the monomer.

2.2.5 Electrochemistry of the *N*-alkylated monomers

The electrochemical polymerization of the monomers was investigated through cyclic voltammetry, Figures 8-10. The results are tabulated in Table 3. The anodic peak becomes less positive on the increase in unit length of the monomer, from **py** > **tp** > **tpt**. This is due to the stabilisation of the radical produced on oxidation when there is a longer conjugated system.

Compound	E/V (peak)	E/V (I = 0.1 mA)
Py	>1.50	1.05
Tp	1.15	1.03
Tpt	1.07	0.89
5-py	>1.50	1.08
5-tp	1.04	0.89
5-tpt	0.99	0.78

Table 3. CV oxidation peaks of the pyrrole containing monomers, **py**, **tp**, **tpt** and the *N*-alkylated monomer units, **5-py**, **5-tp**, **5-tpt**, obtained from the cyclic voltammograms. Conditions: 10mM of sample, 100mM LiClO₄, acetonitrile, r.t., working electrode Pt, counter electrode Au and Ag quasi-reference electrode. Scan rate 0.2 V/s.

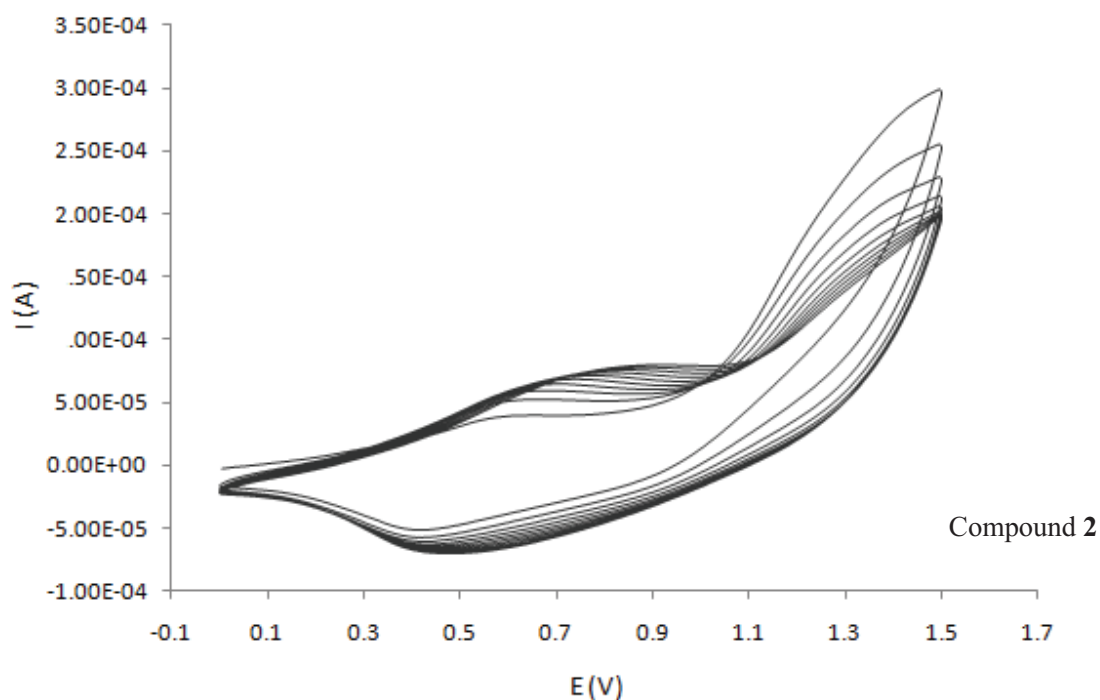


Figure 8. CV of 5-py (**2**). Conditions: 10 mM of sample, 100 mM LiClO₄ in MeCN, r.t., working electrode Pt, counter electrode Au and quasi-reference electrode Ag. Scan rate 0.2 V/s.

In the above cyclic voltammogram (Fig. 8), it can be determined that the polymerization of the monomer is irreversible. The initial oxidative wave occurs at a potential of ~1.46 V which oxidizes the monomer into the polymer. When this wave is reversed towards a negative potential, a reduction peak is observed at ~-0.45 V which is the reduction of the polymer film produced. Subsequent cycles observe the formation of an oxidation peak at a lower potential which steadily increase to a higher current with each cycle due to the formation of polymer film, with a synergistic decrease in the monomer oxidation.

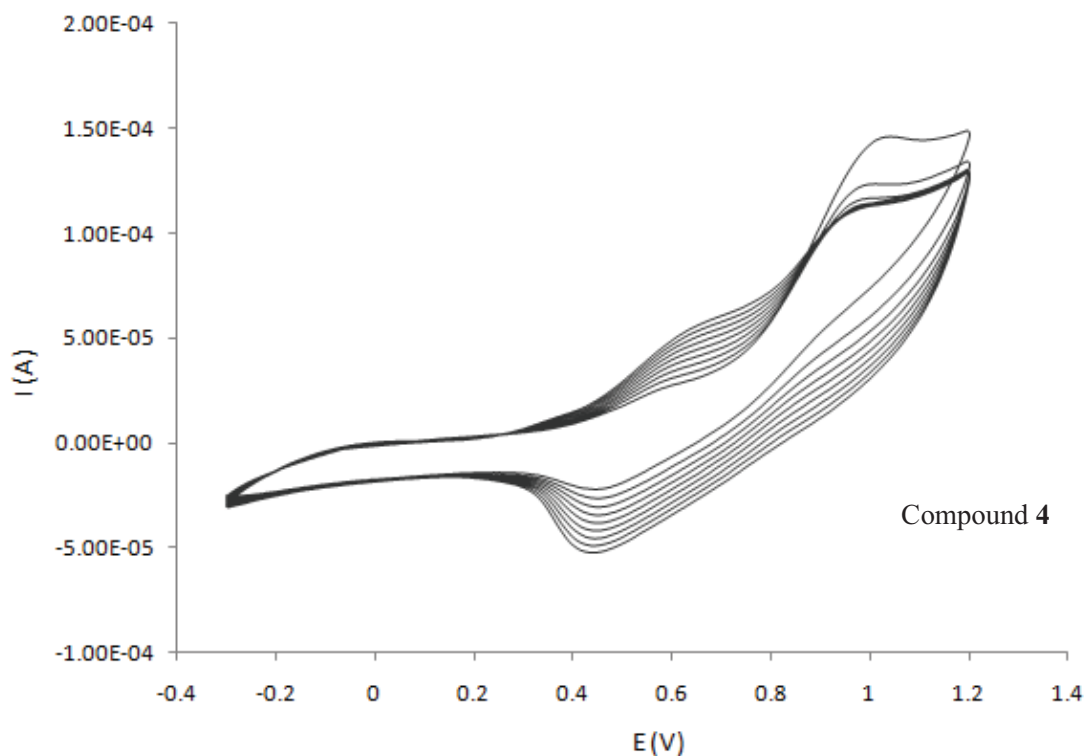


Figure 9. Cyclic voltammogram of 5-tp (4). Conditions: 10 mM of sample, 100 mM LiClO₄ in MeCN, r.t., working electrode Pt, counter electrode Au and quasi-reference electrode Ag. Scan rate 0.2 V/s.

In the above cyclic voltammogram (Fig. 9), the initial oxidative wave occurs at a potential of ~ 1.19 V which oxidizes the monomer into the polymer. When this wave is reversed towards a negative potential, a reduction peak is observed at ~ 0.43 V. As expected, the oxidation potential of the polymer (~ 0.66 V) is drastically lower than the oxidation of the monomer (~ 1.19 V), signifying that the increase in conjugation length stabilizes the radical formation upon oxidation.

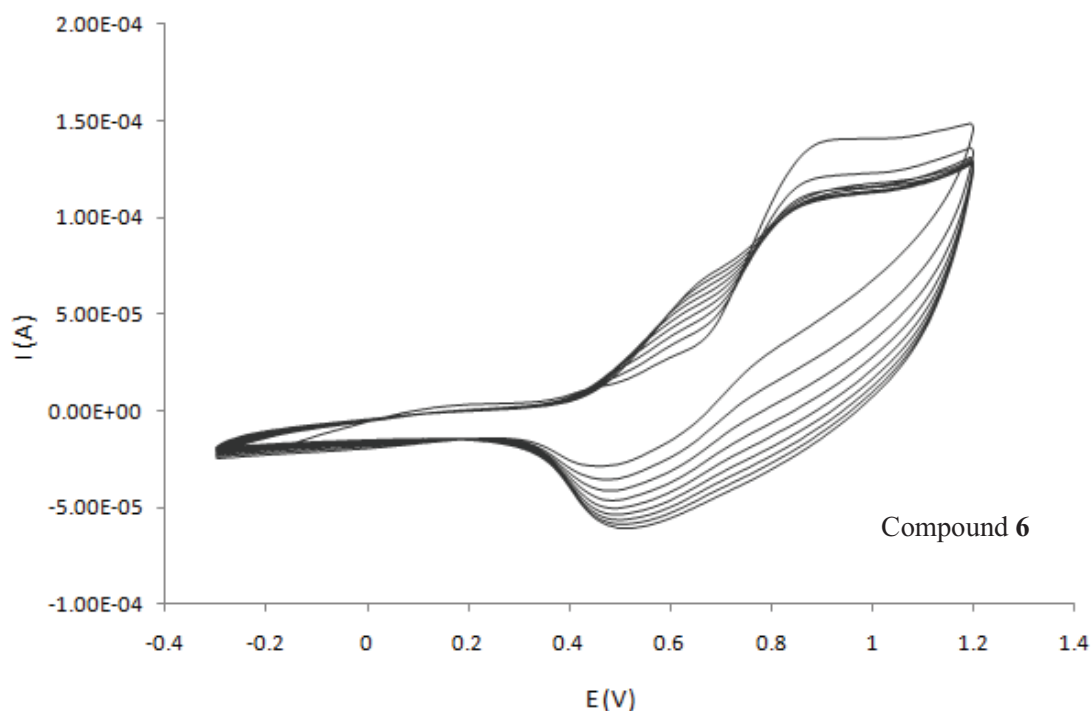


Figure 10. Cyclic voltammogram of 5-tpt (6). Conditions: 10 mM of sample, 100 mM LiClO₄ in MeCN, r.t., working electrode Pt, counter electrode Au and quasi-reference electrode Ag. Scan rate 0.2 V/s.

In the above cyclic voltammogram (Fig. 10), the initial oxidative wave occurs at a potential of ~ 0.87 V. When this wave is reversed towards a negative potential, a reduction peak is observed at ~ 0.50 V. Once more, the oxidation potential of the polymer (~ 0.65 V) is significantly lower than the oxidation of the monomer (~ 0.87 V) denoting that the length of the conjugation has increased and will stabilize the radicals formed on oxidation.

Alkylation at the *N*-position of pyrrole normally increases the oxidation potential due to steric constraints imparted by the alkyl group.³⁷ However, Table 3 illustrates a decrease in the oxidation potential of the alkylated monomers indicating a stabilization effect from the alkyne chain.

The electrochemical studies demonstrate that **py**, **tp**, **tpt** and their alkylated derivatives can all be polymerized to form a range of redox active compounds. The chemical composition of the heteroaromatic compounds can be assessed by FT-IR studies.

2.3 Alkynyl monomers for functionalizing DNA nanowires

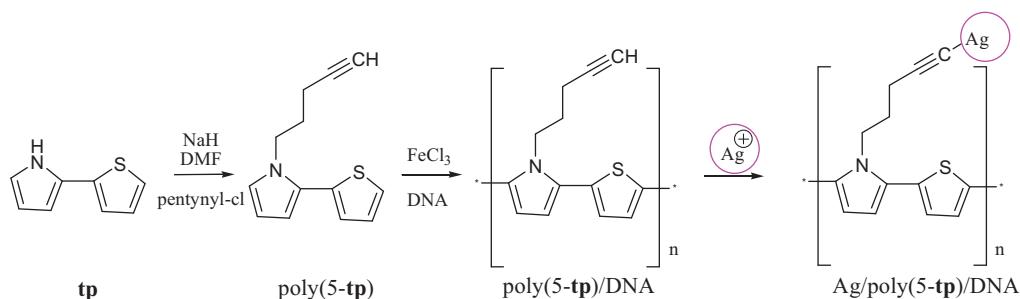
Introducing an alkyne group to the monomers is an attractive approach for further functionalization since it can be included in reactions such as the cross-coupling Sonogashira reaction or ‘click’ chemistry. When the aforementioned monomers are polymerized they form a polycation as shown in Scheme 1. The polycation can be employed to electrostatically bind polyanions, for example, the biomolecule DNA. This process is known as DNA templating and has been frequently found in the literature, showing that this is a common experiment. DNA-templating has been demonstrated with metals and with conducting polymers such as polypyrrole and polyaniline, as discussed in Chapter 1.^{11,13,39} Described next are two approaches that can take advantage of the alkyne group.

2.3.1 Poly-pentynyl-tp/DNA/Ag nanowires

DNA templated nanowires are formed when a polycationic material can bind to DNA’s inherent polyanionic charge via electrostatic interactions, for example, metal-templated DNA such as Pt-DNA^{40,41} or organic templated DNA, such as polyaniline-DNA.¹¹ Having established that the alkylated monomers **py**, **tp** and **tpt** can be polymerized by cyclic voltammetry and retaining the exposed alkyne group, incorporation of 5-**tp** into nanowires via templating was performed and subsequently functionalized using two approaches.

The polymerization of 5-**tp** using FeCl₃ in the presence of DNA, forms a uniform templated DNA-poly(5-**tp**) hybrid nanowire in solution (Scheme 5). Electrostatic Force

Microscopy (EFM) has confirmed that the hybrid nanowire is electrically conducting, however due to its semiconducting nature, the conductance is not as high as with metals.



Scheme 5. DNA-templated synthesis of poly(5-tp) nanowires and deposition of Ag nanocrystals.⁴²

When the poly(5-tp) polymer is wrapped around DNA, its alkyne group is exposed and protruding out of the polymer/DNA hybrid. Tollens reagent was freshly prepared by reaction of aqueous silver nitrate and sodium hydroxide. Silver oxide (Ag_2O) was precipitated out of solution and subsequently dissolved by ammonium hydroxide. Silver ions are then produced and can be activated onto the polymer which is subsequently reduced to nanocrystals. As previously shown in the case of Braun *et al.*,⁴³ silver nanowires have been constructed but they lack the uniformity and linearity which is important for conductance. In this case, the alkyne moiety can be reduced to produce a negative charge on the terminal carbon of the alkyne which can consequently form a sigma bond with the silver crystals. These crystals are then given the direction to be nucleated right along the length of the polymer. Without the alkyne moiety, the nanocrystals appear intermittently along the wire (Fig. 11a) with the bead on a string appearance, however the alkyne addition generates a denser packing of the nanocrystals (Fig. 11c). These interactions of the close-lying nanocrystals allow for enhanced conductance as shown by the EFM image (Fig. 11d). The EFM image confirms that the wire is electrically conducting due to the negative phase shift (black) which is owed to the close electrical contact of the Ag nanoclusters. This demonstrates improved functionality and performance through increased complexity of the system.

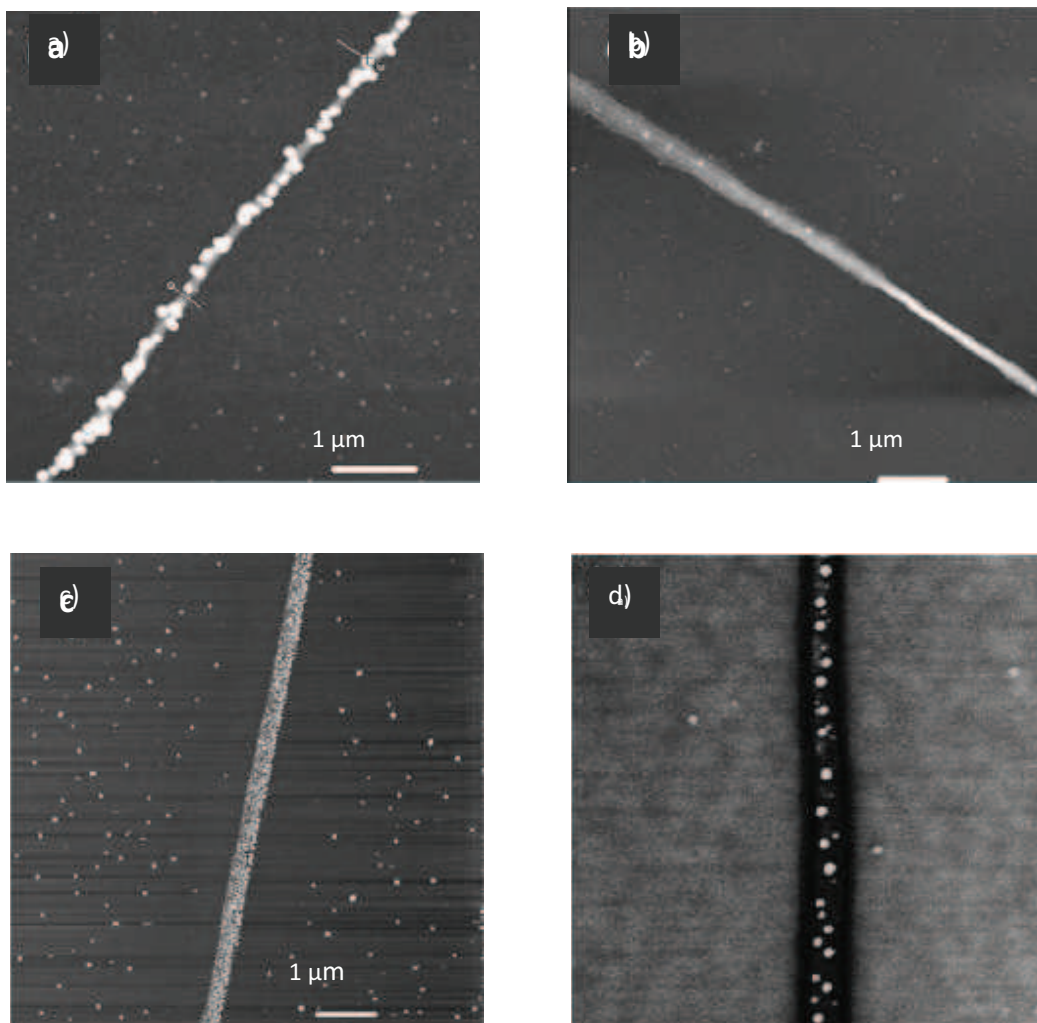
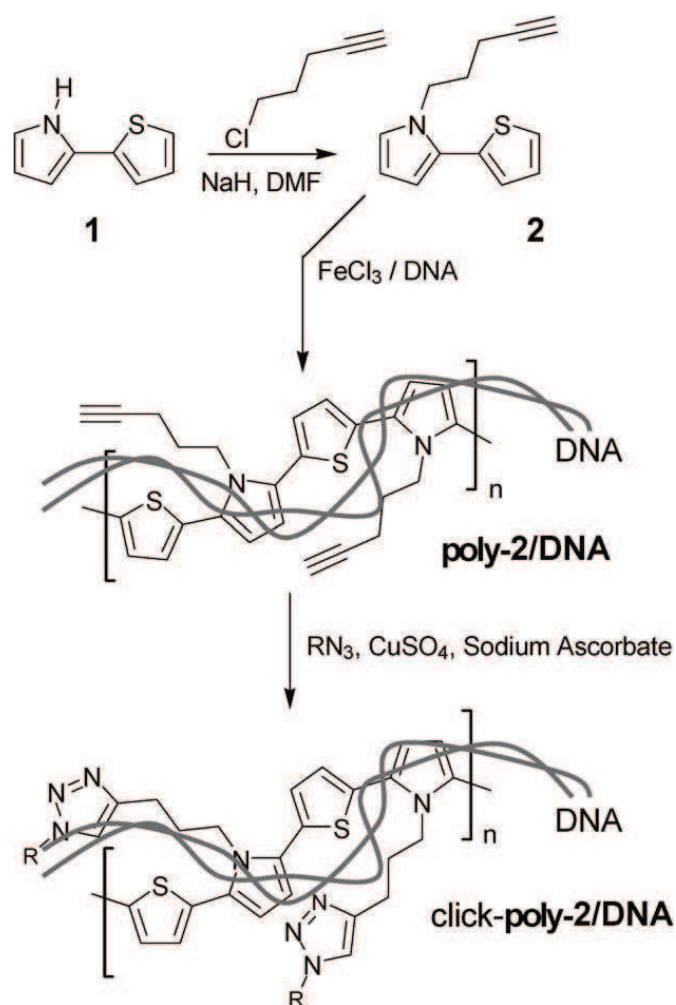


Figure 11. Images of a) AFM of Ag/DNA; b) AFM of Ag/DNA/poly(**tp**); c) AFM of Ag/DNA/poly(**5-tp**); d) EFM of Ag/DNA/poly(**5-tp**).

2.3.2 Poly-pentynyl-**tp**/DNA hybrid “clicked” nanowires

In a second approach to increase functionality of nanowires, ‘click’ chemistry can be employed as it is a versatile method to add a second functionality to a wire. The pentynyl-**tp** can be further exploited via ‘click’ chemistry after using the wire-like structure of DNA as a template to electrostatically bind the polycation polymer to polyanionic DNA and hence produce a hybrid conductive nanowire.⁴⁴ The potential for

this application is in sensing techniques due to the electrical and fluorescence responses that can be generated by ‘clicking’ on an appropriate material. Having the alkyne moiety of poly-pentynyl-**tp** exposed, further functionality can be introduced. In this case, a fluorescent dansyl group was modified with an azide group. Following the facile 1,3-Huigsen cycloaddition, otherwise known as “click” chemistry, the terminal alkyne can react with the azide to form the tetrazole ring that covalently binds the two moieties together, see Scheme 6.



Scheme 6. Synthetic route to the formation of alkyne-bearing DNA-polymer hybrids and the subsequent “click” modification with an azide. R = dansyl group. AFM was employed to measure the topography of the DNA on the SiO₂ surface before and after hybridisation with the polymer and then after “click” modification. EFM was

performed on bare DNA and hybridized poly(5-**tp**)-DNA to illustrate if the conducting polymer/DNA hybrid was conductive. Fluorescence Force Microscopy (FFM) was also performed as a way to detect the click reaction product of the fluorescent dansyl-azide group with the polymer. This work demonstrated that poly-pentynyl-TP/DNA nanowires are conductive and that they can be readily functionalized by employing “click” chemistry.

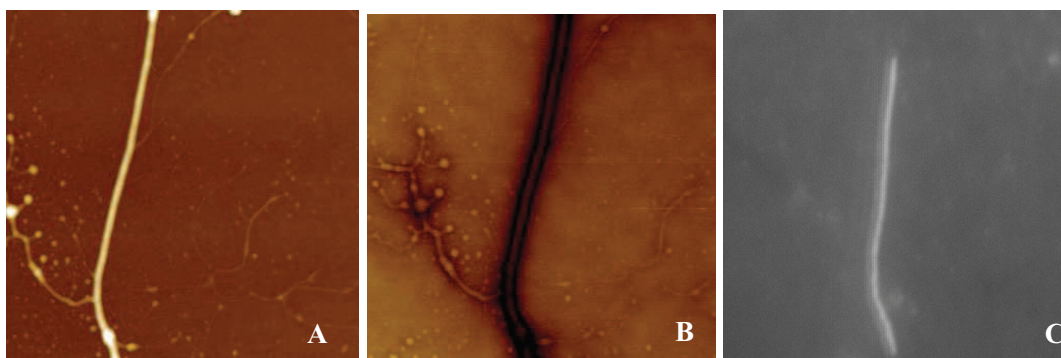


Figure 12. AFM (A) and EFM (B) images of a poly-5-**tp**/DNA hybrid nanowires before and after modification with dansyl azide. AFM image (A), 4 μm scan size, 45 nm height scale; EFM image (B), 4 μm scan size, 10 $^\circ$; fluorescence image (C), 20 \times 20 μm image size.

2.4 Conclusions

Owing to the intense current research into conducting nanowires using conducting polymers that have functionality for a variety of applications, the synthesis of three conducting polymers; **py**, **tp** and **tpt** and their modified alkylated derivatives was demonstrated. The alkylated monomers were synthesized in high yields and characterized by ^1H NMR spectroscopy, ^{13}C NMR spectroscopy, FT-IR, mass spectrometry and UV-vis spectroscopy. A crystal structure of 3-**tpt** was also achieved. The target compounds have proven to be versatile and 5-**tp** in particular has shown to be an ideal contender for hybridization to DNA to form conducting nanowires whilst having the alkyne moiety available for nucleation of silver nanocrystals. In a similar method, the alkylated polymer was able to react with azides in “click” chemistry to form a possible transducing element for potential use in sensing applications. The

alkylated monomers seem to now be suitable contenders for further functionalization. The next approach is to use this alkyne moiety to perform Sonogashira-type carbon-carbon bond formation to covalently bind the alkylated monomers to nucleosides of DNA. This could allow the modified nucleosides to be incorporated into DNA and no longer use DNA as a template but as a scaffold.

2.5 Experimental

Materials: Reagents were purchased from Aldrich and used as received unless otherwise stated. Pyrrole (**py**) was distilled prior to use. Triethylamine was distilled from KOH and then degassed with dry N₂ for 30 min. Anhydrous DMF and 1,4-dioxane were used as received and degassed with dry N₂ for 30 min. All reactions were performed under N₂ using standard Schlenk techniques. NMR experiments were performed on a 300 MHz Bruker Spectrospin WM 300 WB spectrometer, electronic absorption spectra were recorded on a Hitachi U-3010 Spectrophotometer, infrared spectra were recorded on Varian 800 FT-IR (Scimitar Series) spectrometer and high resolution mass spectra with electrospray ionization (HRMS-ESI) were measured on a Waters Micromass LCT Premier mass spectrometer.

Thiophene N-allylcarboxamide^{29,30} (**i**): Thiophene carbonyl chloride (10 g, 68.3 mmol) was added to allylamine (0.51 ml, 68.3 mmol) in pyridine (60 ml). The mixture was stirred at room temperature until completion by TLC. The mixture was then dissolved in toluene and the solvent was removed *in vacuo* until all pyridine was removed via co-evaporation with toluene. The orange oil produced was then dissolved in DCM and washed with water (3 x 50 ml). This organic was dried using magnesium sulfate and solvent removed *in vacuo* to afford an orange solid of yield 11.05 g, 97 %.

¹H NMR (300 MHz, CDCl₃, 25 °C) δ = 4.00 (2H, t; CH₂, J = 6 Hz), 5.15 (2H, m, CH₂), 5.85 (1H, quint; CH, J = 6 Hz), 6.10 (1H, s; NH), 7.01 (1H, dd; CH, J = 4 Hz, 5 Hz), 7.41 (1H, dd; CH, J = 1 Hz, 5 Hz), 7.46 (1H, dd; CH, J = 1 Hz, 4 Hz).

Thiophene Imidoyl chloride^{29,30} (**ii**): Thiophene allylamine (11 g, 66 mmol), thionyl chloride (20 ml) in toluene (80 ml) and DMF (1 ml) was stirred for 18 hr. The solvent was then removed *in vacuo* to afford an orange oil (10.96 g, 89.5 %).

^1H NMR (300 MHz, CDCl_3 , 25 °C) δ = 4.23 (2H, dt; CH_2 , J = 2 Hz), 5.17 (2H, m; CH_2), 5.94 (1H, m; CH), 6.98 (1H, dd; CH , J = 4 Hz, 5 Hz), 7.39 (1H, dd; CH , J = 1 Hz, 5 Hz), 7.72 (1H, dd; CH , J = 1 Hz, 4 Hz).

2-(2-thienyl)-pyrrole^{29,30} (tp) (iii): Imidoyl chloride (11 g, 59 mmol) in anhydrous 1,4-dioxane (50 ml) was added drop wise to a solution of potassium *tert*-butoxide (19.96 g, 178 mmol) in anhydrous DMF (100 ml) at 0 °C and this was allowed to stir for 60 min. The solution was then poured over iced water (400 mL) and extracted with ether. The ethereal layers were combined, dried with magnesium sulfate and evaporated to afford a brown oil which was then purified by column chromatography on silica, in the solvent system hexane: ethyl acetate (80:20). This gave a brown solid with a yield of 6.76 g, 76.9 %.

^1H NMR (300 MHz, CDCl_3 , 25 °C) δ = 6.19 (1H, q; CH_{py}), 6.35 (1H, m; CH_{py}), 6.74 (1H, m; CH_{py}), 6.95 (2H, m; CH_{th}), 7.08 (1H, dd; CH_{th}), 8.33 ppm (1H, s; NH).

1,4-Bis(2-thienyl)-1,4-butanedione^{31,32} (iv): A solution of thiophene (96.1 mL, 1.2 mmol) and succinyl chloride (55.1 mL, 0.5 mol) in anhydrous CH_2Cl_2 (100 mL) was slowly added to a suspension of AlCl_3 (160 g, 1.2 mmol) in DCM (150 mL) with vigorous stirring over 5 h, in an ice water bath. The mixture was then hydrolysed with ice and HCl (50 mL) with vigorous stirring for 30 min. The mixture was then extracted with CH_2Cl_2 (mL) and the combined organic fractions were washed with 2 M HCl, water and sodium hydrogen carbonate. The organic layer was then dried over magnesium sulfate, filtered and the solvent was removed *in vacuo*. The product was then crystallized in cold ethanol to yield the pure product in a yield of 0.21 g, 70.0 %.

^1H NMR (300 MHz, CDCl_3 , 25 °C) δ = 3.38 (s, 4H; CH_2), 7.13 (dd, 2H; CH), 7.63 (dd, 2H; CH), 7.80 (dd, 2H; CH).

2,5-Bis(2-thienyl)pyrrole^{31,32} (*tpt*) (*v*): A mixture of (btbd) (0.25 g, 1.0 mmol) in anhydrous propionic acid (10 mL) was charged with ammonium acetate (0.19 g, 2.5 mmol) and acetic anhydride (0.75 mL, 8.0 mmol). The reaction mixture was cooled in a water bath and sonicated until a fine dispersion was obtained. The dispersion was quickly decanted into a round-bottom flask, fitted with a condenser and was heated to a gently reflux for 10 h. After cooling to room temperature, the majority of propionic acid and acetic anhydride were removed *in vacuo*. Water (50 mL) was added to the solution and neutralized with 2M NaOH. The aqueous solution was then extracted with CH₂Cl₂ (3 x 50 mL) and the combined organic fractions were washed with 10 % sodium bicarbonate (x 2) and brine. The organic layer was then dried over Na₂SO₄ and concentrated *in vacuo*. The solvent was removed *in vacuo* and the crude product was purified on silica using a gradient of 0–5% ethyl acetate in hexane. The appropriate fractions were combined and solvent was removed *in vacuo* to yield the pure product in yield 0.17 g, 72 %.

¹H NMR (300 MHz, CDCl₃, 25 °C) δ = 6.33 (d, 2H; CH_{py}), 6.93 (m, 2H; CH_{th}), 6.99 (dd, 2H; CH_{th}), 7.06 (dd, 2H; CH_{th}), 8.5 (s, 1H; NH).

General procedure for the alkylation of 2-(2-thienyl)pyrrole and 2,5-bis(2-thienyl)pyrrole (1-6).

The appropriate monomer unit (5 mmol) was dissolved in anhydrous DMF (100 mL). To this solution sodium hydride (60% dispersion in mineral oil) (1.5 equiv) was added under nitrogen and the mixture was stirred until H₂ evolution ceased. The appropriate alkynyl derivative (2 equiv) was then added and the mixture was stirred in the dark overnight. The resulting suspension was filtered through Celite and the solvent removed *in vacuo*. Water (100 mL) was added and the resulting mixture was extracted with CH₂Cl₂ (3 × 200 mL) and the solution dried over magnesium sulfate. The solvent was removed *in vacuo* and the crude product was purified on silica using a gradient of 0–5% ethyl acetate in hexane. The appropriate fractions were combined and solvent was removed *in vacuo* to yield the pure product.

***N*-(pent-4-ynyl)pyrrole (2)**: Yield: 80% as an oil. ¹H NMR (CDCl₃): δ = 1.96 (m, 2H, CH₂), 2.03 (t, 1H, CH), 2.16 (m, 2H, CH₂), 4.05 (t, 2H, CH₂), 6.16 (t, 2H, CH_{py}), 6.68 (t, 2H, CH_{py}). ¹³C-NMR (CDCl₃): δ = 120.70, 108.45, 83.10, 69.68, 47.92, 30.38, 15.75. IR (neat, cm⁻¹): 3295, 2120, 1500, 1282, 1089, 722. HRMS (ESI): m/z: calc for C₉H₁₁N [M+H]⁺: 134.0958; found: 134.0970.

***N*-(prop-2-ynyl)-2-(2-thienyl)pyrrole (3)**: Yield: 8% as an oil. ¹H NMR (CDCl₃): δ = 2.42 (t, 1H; CH), 4.75 (d, 2H; CH₂), 6.24 (t, 1H; CH_{py}), 6.33 (q, 1H; CH_{py}), 6.94 (q, 1H, CH_{py}), 7.08 (m, 1H, CH_{th}), 7.13 (dd, 1H, CH_{th}), 7.32 (dd, 1H, CH_{th}). ¹³C-NMR (CDCl₃): δ = 134.60, 127.68, 126.93, 126.20, 125.57, 122.86, 111.24, 109.23, 79.09, 73.72, 37.17. IR (neat, cm⁻¹): 3287, 2121, 1291, 843, 788, 695. HRMS (ESI): m/z: calc for C₁₁H₉NS [M+H]⁺: 188.0531; found: 180.0534. UV (MeOH): λ_{max} 290 nm.

***N*-(pent-4-ynyl)-2-(2-thienyl)pyrrole (4)**: Yield: 70% as an oil. ¹H NMR (CDCl₃): δ = 1.92 (m, 2H, CH₂), 2.03 (t, 1H, CH), 2.19 (m, 2H, CH₂), 4.19 (t, 2H, CH₂), 6.23 (m, 1H, CH_{py}), 6.36 (m, 1H, CH_{py}), 6.84 (s, 1H, CH_{py}), 7.08 (m, 2H, CH_{th}), 7.31 (m, 1H, CH_{th}). ¹³C-NMR (CDCl₃): δ = 135.33, 127.51, 126.73, 125.93, 125.21, 123.37, 111.19, 108.49, 83.26, 69.62, 46.43, 30.36, 16.08. IR (neat, cm⁻¹): 3290, 2130, 1429, 1298, 843, 787, 695. HRMS (ESI): m/z: calc for C₁₃H₁₃NS [M+H]⁺: 216.0843; found: 216.0847. UV (MeOH): λ_{max} 284 nm.

***N*-(prop-2-ynyl)-2,5-bis(2-thienyl)pyrrole (5)**: Yield: 69% as a solid, mp 121-122 °C. ¹H NMR (CDCl₃): δ = 2.52 (t, 1H, CH), 4.77 (d, 2H, CH₂), 6.40 (s, 2H, CH_{py}), 7.13 (m, 2H, CH_{th}), 7.32 (dd, 2H, CH_{th}), 7.40 (m, 2H, CH_{th}). ¹³C-NMR (CDCl₃): δ = 134.82, 129.26, 127.87, 126.12, 125.70, 111.23, 80.74, 73.71, 35.90. IR (neat, cm⁻¹): 3263, 2119, 1494, 1422, 1333, 1200, 844, 772, 695. HRMS (ESI): m/z: calc for C₁₅H₁₁NS₂ [M+H]⁺: 270.0394; found: 270.0411. UV (MeOH): λ_{max} 318 nm. Single crystals of **5** suitable for X-ray diffraction were obtained by concentration of a solution in ethyl acetate.

N-(*pent-4-ynyl*)-2,5-bis(2-thienyl)pyrrole (**6**): Yield: 46% as a solid, mp 36-40 °C. ¹H NMR (CDCl₃): δ = 1.78 (m, 2H, CH₂), 1.86 (t, 1H, CH), 2.03 (m, 2H, CH₂), 4.28 (m, 2H, CH₂), 6.36 (s, 2H, CH_{py}), 7.11 (m, 4H, CH_{th}), 7.33 (m, 2H, CH_{th}). ¹³C-NMR (CDCl₃): δ = 135.30, 128.84, 127.58, 126.51, 125.65, 111.53, 83.05, 69.22, 44.61, 30.12, 16.12. IR (neat, cm⁻¹): 3279, 2120, 1470, 1410, 1305, 1198, 837, 754, 696. HRMS (ESI): m/z: calc for C₁₇H₁₅NS₂ [M+H]⁺: 298.0724; found: 298.0718. UV (MeOH): λ_{max} 309 nm.

References

- (1) Porath, D.; Bezryadin, A.; de Vries, S.; Dekker, C. *Nature* **2000**, *403*, 635.
- (2) Nalwa, H. S. *Conducting polymers (Handbook of advanced electronic and photonic materials and devices)* Academic, 2001.
- (3) Fomina, L.; Zaragoza Galán, G.; Bizarro, M.; Godínez Sánchez, J.; Zaragoza, I. P.; Salcedo, R. *Mater. Chem. Phys.* **2010**, *124*, 257.
- (4) Gerard, M.; Chaubey, A.; Malhotra, B. D. *Biosens. Bioelectron.* **2002**, *17*, 345.
- (5) Shirakawa, H.; Louis, E. J.; MacDiarmid, A. G.; Chiang, C. K.; Heeger, A. J. *J. Chem. Soc., Chem. Commun.* **1977**, 578.
- (6) Chiang, C. K.; Druy, M. A.; Gau, S. C.; Heeger, A. J.; Louis, E. J.; MacDiarmid, A. G.; Park, Y. W.; Shirakawa, H. *J. Am. Chem. Soc.* **1978**, *100*, 1013.
- (7) Kim, F. S.; Ren, G.; Jenekhe, S. A. *Chem. Mater.* **2010**, *23*, 682.
- (8) Jenekhe, S. A. *Nature* **1986**, 322, 345.
- (9) Parakka, J. P.; Chacko, A. P.; Nikles, D. E.; Wang, P.; Hasegawa, S.; Maruyama, Y.; Metzger, R. M.; Cava, M. P. **1996**.
- (10) Datta, B.; Schuster, G. B. *J. Am. Chem. Soc.* **2008**, *130*, 2965.
- (11) Nickels, P.; Dittmer, W. U.; Beyer, S.; Kotthaus, J. P.; Simmel, F. C. *Nanotechnology* **2004**, *15*, 1524.
- (12) Hassanien, R.; Al-Hinai, M.; Farha Al-Said, S. A.; Little, R.; Siller, L.; Wright, N. G.; Houlton, A.; Horrocks, B. R. *ACS Nano*, *4*, 2149.
- (13) Dong, L.; Hollis, T.; Fishwick, S.; Connolly, B. A.; Wright, N. G.; Horrocks, B. R.; Houlton, A. *Chem.-Eur. J.* **2007**, *13*, 822.
- (14) Roncali, J. *Chem. Rev.* **1992**, *92*, 711.
- (15) Roncali, J. *Chem. Rev.* **1997**, *97*, 173.
- (16) Saxena, V.; Malhotra, B. D. *Curr. Appl. Phys.* **2003**, *3*, 293.
- (17) Ma, Y.; Zhang, J.; Zhang, G.; He, H. *J. Am. Chem. Soc.* **2004**, *126*, 7097.
- (18) Pruneanu, S.; Al-Said, S. A. F.; Dong, L. Q.; Hollis, T. A.; Galindo, M. A.; Wright, N. G.; Houlton, A.; Horrocks, B. R. *Adv. Funct. Mater.* **2008**, *18*, 2444.
- (19) Pike, A. R.; Patole, S. N.; Murray, N. C.; Ilyas, T.; Connolly, B. A.; Horrocks, B. R.; Houlton, A. *Adv. Mater.* **2003**, *15*, 254.
- (20) Ansari, R. *E-Journal of Chemistry* **2006**, *3*, 186.
- (21) Ma, Y. F.; Zhang, J. M.; Zhang, G. J.; He, H. X. *J. Am. Chem. Soc.* **2004**, *126*, 7097.
- (22) Kanazawa, K. K.; Diaz, A. F.; Geiss, R. H.; Gill, W. D.; Kwak, J. F.; Logan, J. A.; Rabolt, J. F.; Street, G. B. *J. Chem. Soc., Chem. Commun.* **1979**, 854.
- (23) Bufon, C. C. B.; Heinzl, T.; Espindola, P.; Heinze, J. *J. Phys. Chem. B* **2010**, *114*, 714.
- (24) Kanazawa, K. K.; Diaz, A. F.; Krounbi, M. T.; Street, G. B. *Synth. Met.* **1981**, *4*, 119.
- (25) Hegewald, R.; Jakisch, L.; Pionteck, J. *Synth. Met.* **2009**, *159*, 103.
- (26) Srinivasan, S.; Schuster, G. B. *Org. Lett.* **2008**, *10*, 3657.
- (27) Ping, Z.; Federspiel, P.; Grunberger, A.; Nauer, G. E. *Synth. Met.* **1997**, *84*, 837.
- (28) Aleman, C.; Domingo, V. M.; Fajari, L.; Julia, L.; Karpfen, A. *J. Org. Chem.* **1998**, *63*, 1041.

- (29) Engel, N.; Steglich, W. *Angew. Chem., Int. Ed. Engl.* **1978**, *17*, 676.
- (30) Niziurski-Mann, R. E.; Cava, M. P. *Adv. Mater.* **1993**, *5*, 547.
- (31) Merz, A.; Ellinger, F. *Synthesis* **1991**, 462.
- (32) Merrill, B. A.; LeGoff, E. *J. Org. Chem.* **1990**, *55*, 2904.
- (33) Parakka, J. P.; Jeevarajan, J. A.; Jeevarajan, A. S.; Kispert, L. D.; Cava, M. P. *Adv. Mater.* **1996**, *8*, 54.
- (34) Vautrin, M.; Leriche, P.; Gorgues, A.; Cava, M. P. *Electrochem. Commun.* **1991**, *1*, 233.
- (35) Yim, E. S.; Park, M. K.; Han, B. H. *Ultrason. Sonochem.* **1997**, *4*, 95.
- (36) Belen'kii, L.; Gromova, G.; Smirnov, V. *Chem. Heterocycl. Compd.* **2008**, *44*, 1092.
- (37) Vautrin, M.; Leriche, P.; Gorgues, A.; Cava, M. P. *Electrochem. Commun.* **1999**, *1*, 233.
- (38) Ferraris, J. P.; Andrus, R. G.; Hrcncir, D. C. *J. Chem. Soc., Chem. Commun.* **1989**, 1318.
- (39) Coffey, J. L.; Bigham, S. R.; Pinizzotto, R. F.; Yang, H. *Nanotechnology* **1992**, *3*, 69.
- (40) Seidel, R.; Columbi Ciacchi, L.; Weigel, M.; Pompe, W.; Mertig, M. *J. Phys. Chem. B* **2004**, *108*, 10801.
- (41) Mertig, M.; Colombi Ciacchi, L.; Seidel, R.; Pompe, W.; De Vita, A. *Nano Lett.* **2002**, *2*, 841.
- (42) Farha Al-Said, S. A.; Hassanien, R.; Hannant, J.; Galindo, M. A.; Pruneanu, S.; Pike, A. R.; Houlton, A.; Horrocks, B. R. *Electrochem. Commun.* **2009**, *11*, 550.
- (43) Braun, E.; Eichen, Y.; Sivan, U.; Ben-Yoseph, G. *Nature* **1998**, *391*, 775.
- (44) Hannant, J.; Hedley, J. H.; Pate, J.; Walli, A.; Farha Al-Said, S. A.; Galindo, M. A.; Connolly, B. A.; Horrocks, B. R.; Houlton, A.; Pike, A. R. *Chem. Commun.* **2010**, *46*, 5870.

**Chapter 3 - *Synthesis of modified
pyrimidines using N-alkylated
monomers***

Chapter 3 – *Synthesis of modified pyrimidines using N-alkylated monomers*

The syntheses of three conducting polymers; **py**, **tp** and **tpt** and their modified alkylated derivatives were discussed in Chapter 2. The polymer of 5-**tp** has shown to be an ideal contender for hybridization to DNA to form templated conducting nanowires whilst, in one method, having the alkyne moiety available for nucleation of silver nanocrystals. In a similar method, the alkylated polymer was able to react with a fluorescent azide in “click” chemistry. These findings demonstrate two possible ways to exploit conducting polymers in electronic devices. Using polymer templated DNA is an ideal way of utilizing the electrostatics between the two molecules.^{1,2} However, a key aim of this project was to develop methods to control the growth of the conducting nanowire and unfortunately, current templating approaches lack this attribute.

A major disadvantage with templating is the difficulty in defining the maximum size of the nanowire and is currently challenging to get single strand interactions. One way to circumvent the templating difficulty is to covalently link the alkynyl monomers to the nucleosides of DNA, in order to create the opportunity to build and incorporate into precise lengths of oligomers of DNA. In this way, the monomers are positioned in such a way that they can be linked together to form a single molecule of conductive polymer (See Scheme 1, Chapter 1). This is a smart approach which employs a purely organic strategy to fix DNA and organic conductive polymers together. Schuster *et al.* have demonstrated a similar approach in order to incorporate the modified bases into short oligomers of DNA.³

A key reason for modifying DNA in this way is to exploit the self-assembly property of the base-pairs in order to build up complex molecular architectures. As elegantly demonstrated in the work of Seeman *et al.*,⁴ the sequence information encoded in the biopolymer of DNA provides a means to introduce multifunctional groups into juxtaposition. Even the rather straightforward ability to synthesize precise lengths of

oligomers is a highly attractive attribute for the integration into synthetic systems, a feature which is lost in templated materials.

3.1 Modified nucleosides

The four nucleosides, A, C, G, T, are the fundamental building blocks of DNA. Modifications to the nucleosides can have importance in fields such as medicine and drug discovery⁵ by employing them as antiviral (AZT)⁶ and anti-tumour agents,⁷ imaging agents in PET (positron emission tomography) scanning (Fig. 1a)⁸ and optical probes.⁹ More recently efforts to apply the unique properties of DNA to address challenges in the field of nanoscale material science and technology have led to a wide range of new derivatives emerging. Examples have been demonstrated by the replacement of natural base pairs with metal-chelating variants,¹⁰⁻¹³ with the resulting materials exhibiting cooperative magnetic behaviour, for instance.¹⁴ Other examples include the introduction of multiple adjacent porphyrin groups into short oligonucleotides forming discrete photoactive regions of defined length.¹⁵⁻¹⁷

Most importantly, nucleoside modifications can be synthesized at various sites^{9,18-20} and several structural modifications have been fabricated in the advancement of modifying nucleosides, for example modification of the ribose moiety for anti-HIV treatments with vinyl sulphone derivatives.²¹ However, the most advantageous site is to modify the C5 position of pyrimidines as it does not disturb the supramolecular bonding between the nucleobases or interfere with the phosphodiester backbone. Various research groups have performed modifications at the C5 position with a range of functional groups in an effort to produce a library of antiviral and anti-cancer drugs. Dembinski *et al.* reported the modification at the C5 position of uridine (Fig. 1b) with alkynyl derivatives via Sonogashira-type chemistry that have given rise to antiproliferation agents that are toxic to cancer cells.²²

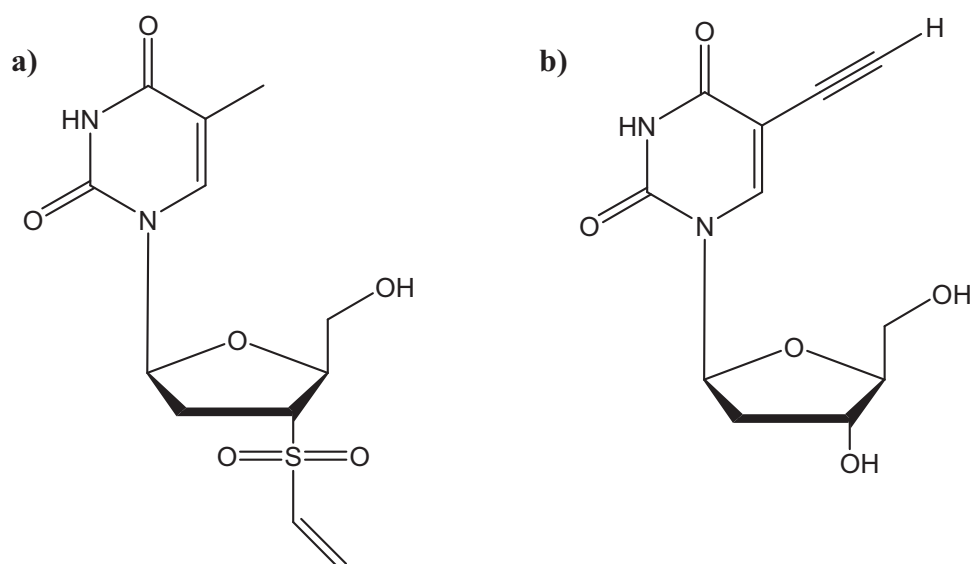


Figure 1. Two examples of different site modification of thymidines nucleosides a) 3'-OH modified thymidine used for PET scanning and (b) C5-modified uridine with antiproliferation properties

One of the intrinsic properties of nucleoside chemistry is that the functional groups i.e. hydrogen bonding sites, the 5'-OH employed for triphosphate chemistry or the 3'-OH used in phosphoramidite chemistry (Fig. 2), often require protection if further chemistry is to be attempted to introduce additional functionality. For this reason, the pyrimidine of choice for modification in this project is deoxythymidine as its hydrogen bonding sites do not need protecting. Furthermore, 2'-deoxythymidine is commercially available as the C5-iodo derivative and modifications at this position enable the functionalized moiety to be situated in the major groove of DNA and hence cause no disruption to the DNA duplex or its intrinsic hydrogen-bonding between base pairs. Moreover, the halonucleoside version allows for Sonogashira type reactions at the C5 position. In particular, Sonogashira-type chemistry allows the 5-iodo form of the nucleoside to be united with an alkyne, a functional group already incorporated into the conductive polymer monomer units described in Chapter 2.

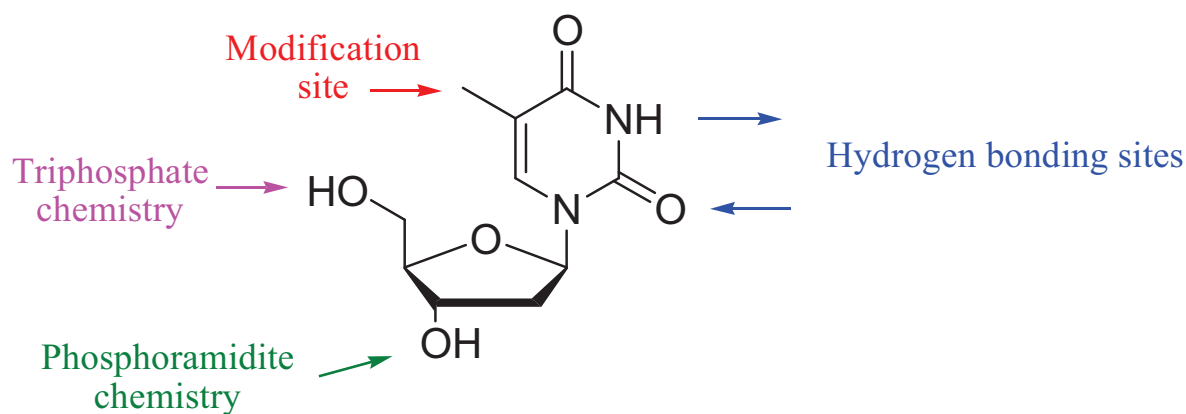


Figure 2. Possible modification sites at C-5, 3'-OH and 5'-OH prevents disruption of possible hydrogen bonding.

Numerous research groups have reported the C5 modification of thymidine with the subsequent incorporation into DNA.^{23,24} Houlton *et al.* have reported on redox-active pyrimidine nucleosides based on a ferrocenyl group and demonstrated their incorporation into oligonucleotide strands at both standard CPG supports and at silicon electrodes.²⁵ Insertion of conjugated ferrocenes has no structural implication to the double helix of DNA and the modified oligonucleotide is most likely to be used in applications such as sensing by employing it as an 'electronic tag', however, the focal point of this project is to create a material for electronic integration into devices, requiring wire-like materials, i.e. conducting polymer nanowires.

There are a number of examples of organic polymers coupled to nucleosides and included into short oligomers of DNA in the literature. Integrating the modified nucleosides into DNA allows the base to be positioned site-specifically.³ Schuster *et al.* modified cytidine with aniline-containing monomers via a triazole displacement from the deoxycytidine precursor with N-(2-aminoethyl)aniline (Fig. 3).²⁶ The aniline-containing monomers were then incorporated into a defined length of DNA, a 22mer containing six adjacent modified deoxycytidines, via phosphoramidite chemistry and subsequently converted into conducting polymers by oxidative polymerisation utilising horseradish peroxidase and H₂O₂. In order to enhance the conductivity of the polymer, aniline had to be doped with HCl and the optimum pH for this process is pH 4.0. Whilst this produces the necessary conducting polymer, the

pH can initiate denaturing of the DNA double strand. Evidence from the melting temperatures (T_m) demonstrated that the temperature decreased with every addition of monomer incorporated into the helix giving rise to an unstable DNA duplex. In addition, when Ma *et al.* performed templating of polyaniline onto DNA, conductivity measurements were obtained by bridging the nanowire across two gold electrodes. Low conductivities were detected (nS) by comparison to polypyrrole nanowires at 4 S cm^{-1} ²⁷ and also observed was that the formation of continuous wires was difficult due to agglomerates of DNA developing in solution thus preventing complete coverage by the polymer. This suggests that it is problematical to grow single conducting wires across an electrode due to gaps in the continuity.²⁸ A single break (Fig. 3b) is detrimental to the nanowire due to the discontinuous electron flow. For the above reasons polyaniline is a less favourable polymer to use due to the necessity of harsh conditions and the disruption to the important structure of DNA, in comparison to the polymers in Chapter 2 where the reaction conditions required are neutral.

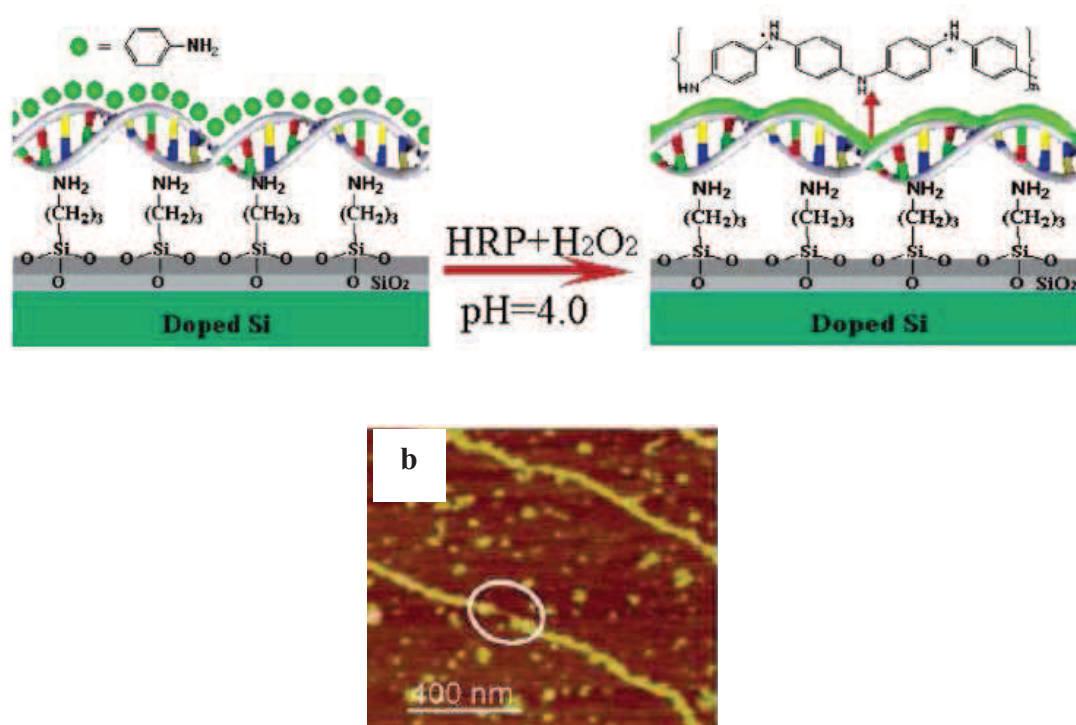
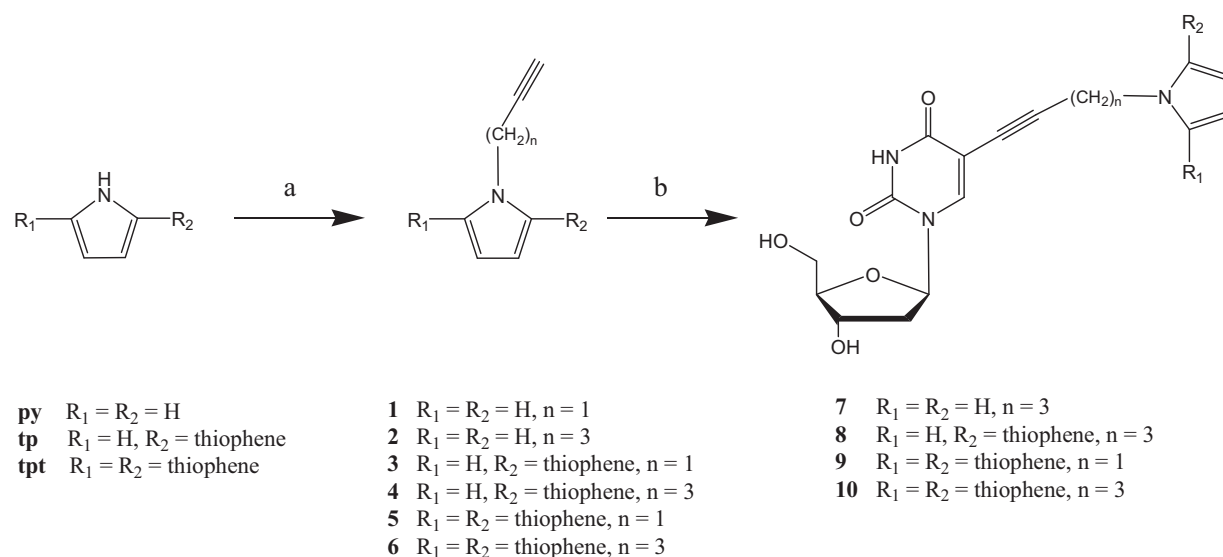


Figure 3. a) Schematic to illustrate how an aniline modified nucleoside is incorporated into DNA via automated synthesis and subsequently modified and b) discontinuous polyaniline/DNA nanowires²⁹

The alkynyl **py**, **tp** and **tpt** units reported in Chapter 2 have shown to be stable at neutral pH. In addition they can be readily polymerized either chemically by FeCl_3 ^{1,2} or via electrochemical methods whilst retaining the terminal alkyne group. Therefore, this chapter describes the investigations into the synthesis of a range of alkynyl modified **py**, **tp** and **tpt** units that have been coupled to halonucleosides using Sonogashira-type chemistry with the intention of encompassing the nucleosides into oligomers of DNA in Chapter 4.

3.2 Results and discussion

A series of pyrrolyl-thienyl-thymidine, **7-10**, (Fig. 4) and pyrrolyl-thienyl-cytidine, **11** nucleosides, were prepared by Pd-catalyzed cross-coupling between *N*-alkynyl modified polymer precursors and 5-iodo-2'-deoxyuridine (Scheme 1) or 5-iodo-2'-deoxycytidine. The compounds have been characterized by ¹H NMR spectroscopy, ¹³C NMR spectroscopy, cyclic voltammetry, ES-MS, FT-IR spectroscopy and UV-Vis spectroscopy. The modified nucleoside isomer **8b** was also studied by X-Ray diffraction confirming the attachment of *N*-alkylated unit **4** to position C5 of the nucleobase. Particular emphasis was made on the electronic structure and redox properties of the compounds in order to assess their ability to grow conducting polymers. CV showed that using polymer precursor **tp** or **tpt** attached to the nucleobases give rise to more conducting polymer than using nucleobases holding the **py** unit, due to the enhanced current observed with **tp** and **tpt** and the well-defined surface wave in comparison to **py**. It was found that when increasing the carbon-bridge length minor changes in the oxidation potential of the polymer precursors occurs.



Scheme 1. Synthetic route for *N*-alkylated polymer precursors **1-6** and pyrrolyl-thienyl modified nucleosides **7-10**. (a) NaH, alkynyl derivate (propargyl bromide or 5-chloro-1-pentyne), DMF, rt; (b) 5-iodo-deoxyuridine, Pd(PPh₃)Cl₂, CuI, Et₃N, DMF, 12 h.

3.2.1 Synthesis and characterization of C5-modified nucleosides (7-10).

The polymer precursor units pyrrole (**py**), 2-(2-thienyl)pyrrole (**tp**) and 2,5-bis(2-thienyl)pyrrole (**tpt**) were initially functionalized with suitable chains containing a terminal alkyne group capable to take part in Pd-catalysed cross-coupling reactions (Sonogashira), and therefore to react with the appropriate halonucleoside (Scheme 1). A series of 3- and 5-carbon alkyl chains were employed as the bridging unit linking the nucleoside and the monomer unit **py**, **tp** and **tpt** to investigate how this change in linker length would affect the flexibility and polymerisation of the polymer. Therefore, four units were chosen as targets for synthesis, in order to compare the affect of **py**, **tp** and **tpt** and their respective linkages. These units are shown in Fig. 4.

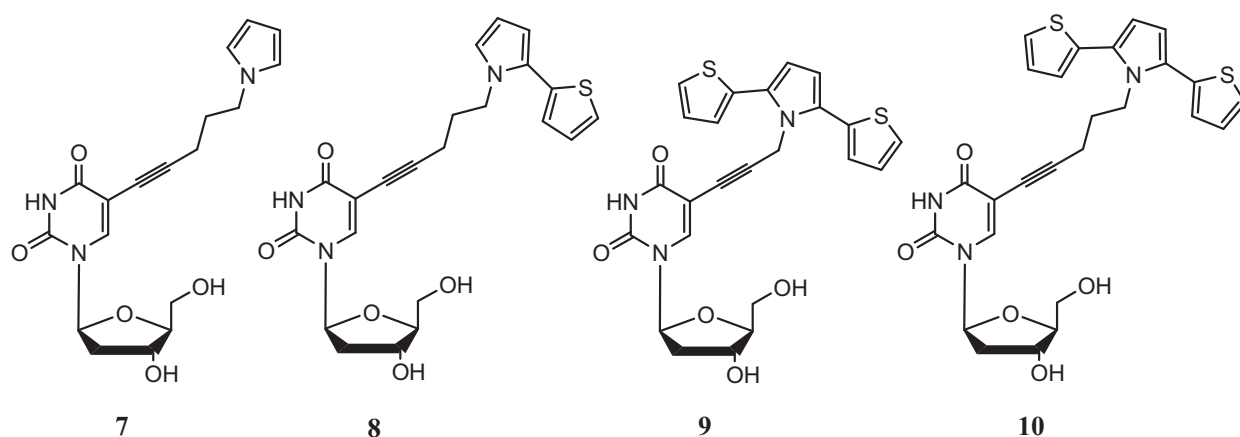


Figure 4. Structures of modified thymidine derivatives 7-10.

Synthesis of the modified thymidine nucleosides **7-10** was carried out using the conditions of Ghilagaber *et al.* for Sonogashira cross-coupling.³⁰ 5-Iodo-2'-deoxyuridine and the alkylated substrates were employed using bis(triphenylphosphine)dichloropalladium(II) as precatalyst and copper iodide(I) as co-catalyst. Typical yields ranged from 30-78 % and were characterized by ¹H NMR spectroscopy, ¹³C NMR spectroscopy, FT-IR spectroscopy, UV-vis spectroscopy and high resolution ES-MS.

The Sonogashira cross-coupling reactions were extensively studied to acquire the optimal conditions. This included using solvents such as acetonitrile and DMF, different temperatures and times. However, when searching the literature, Ghilagaber *et al.* suggested it was the concentration of the nucleoside at 0.13 M that determined the most favourable yield.³⁰ The optimum conditions also included running the reaction overnight at room temperature which provided the ideal reaction conditions for the coupling reaction.

3.2.2 FT-IR spectroscopy

Infrared characterization was performed in order to identify and compare the various functional groups on the compounds (Table 1).

Wavenumber (cm ⁻¹)				Assignment
7	8	9	10	
-	696	697	692	C-H thiophene
727	772	770	766	C-H pyrrole
-	843	843	841	C-S thiophene
1050	1053	1051	1052	N1-C1'-H thymidine
1277	1277	1281	1275	C-N thymidine
1459	1460	1462	1469	N-H thymidine
1675	1674	1681	1644	C=O and C=C thymidine

Table 1. Vibrational bands of the modified thymidine units coupled to the *N*-alkylated monomers. The samples were tested as neat compounds.

Assignment of the vibrational bands of the thymidine ring was achieved using literature references for deoxythymidine.^{31,32} The vibrations between 692 cm⁻¹ and 843 cm⁻¹ confirm the presence of the heterocyclic pyrrole and thiophene units bound to the nucleoside. The C-H peak at ~ 3280 cm⁻¹ in the alkylated species in Chapter 2 has clearly disappeared from the spectrum which confirms the loss of this proton during the reaction. This vibrational information is valuable in determining completion of the coupling reaction.

3.2.3 Electrochemistry studies of the modified nucleosides

The electrochemical properties of the modified thymidines units were investigated through cyclic voltammetry, Figures 5-8. In some cases, the oxidation peak was not clear, therefore, a potential at a fixed current of 0.1 mA is also tabulated and the results are tabulated in Table 2.

Compound	E/V (peak)	E/V (I = 0.1 mA)
7	1.37	-
8	>1.50	1.26
9	1.33	0.95
10	1.42	1.14

Table 2. CV oxidation peaks of the *N*-alkylated monomer units obtained from the cyclic voltammograms. Conditions: 10 mM of sample, 100 mM LiClO₄, acetonitrile, r.t., working electrode Pt, counter electrode Au and Ag quasi-reference electrode. Scan rate 0.2 V/s.

The CVs for modified nucleosides bearing the **tpt** show small changes in the oxidation potential between compounds **9** and **10** with the 3- and 5-carbon bridge length, 1.33 and 1.42 V respectively. When comparing the different substituent units, **py (7)**, **tp (8)** and **tpt (10)**, linked to the nucleoside by the same 5-carbon bridge, significant changes appear in the cyclic voltammograms, 1.37, >1.50 and 1.42 V respectively. Compounds **8** and **10** show clear evidence of polymer formation (Figures 6 and 8 respectively) illustrated by broad reduction peak centred near 0.2V which is common for conducting polymers.³³

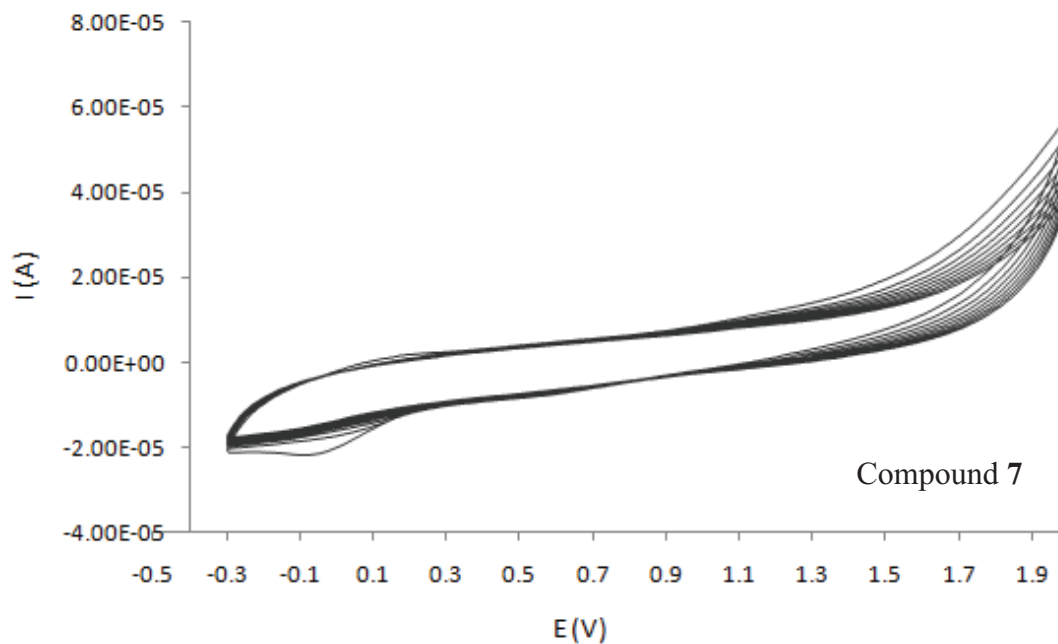


Figure 5. CV of dT-5-py (7). Conditions: 10 mM of sample, 100 mM LiClO₄ in MeCN, r.t., working electrode Pt, counter electrode Au and quasi-reference electrode Ag. Scan rate 0.2 V/s

However, the **py**-based compound **7** produces a poorly conductive film as evident in the low currents observed and the lack of well-defined surface waves (Fig.5). This is typical for a poorly conductive polymer that insulates the electrode.

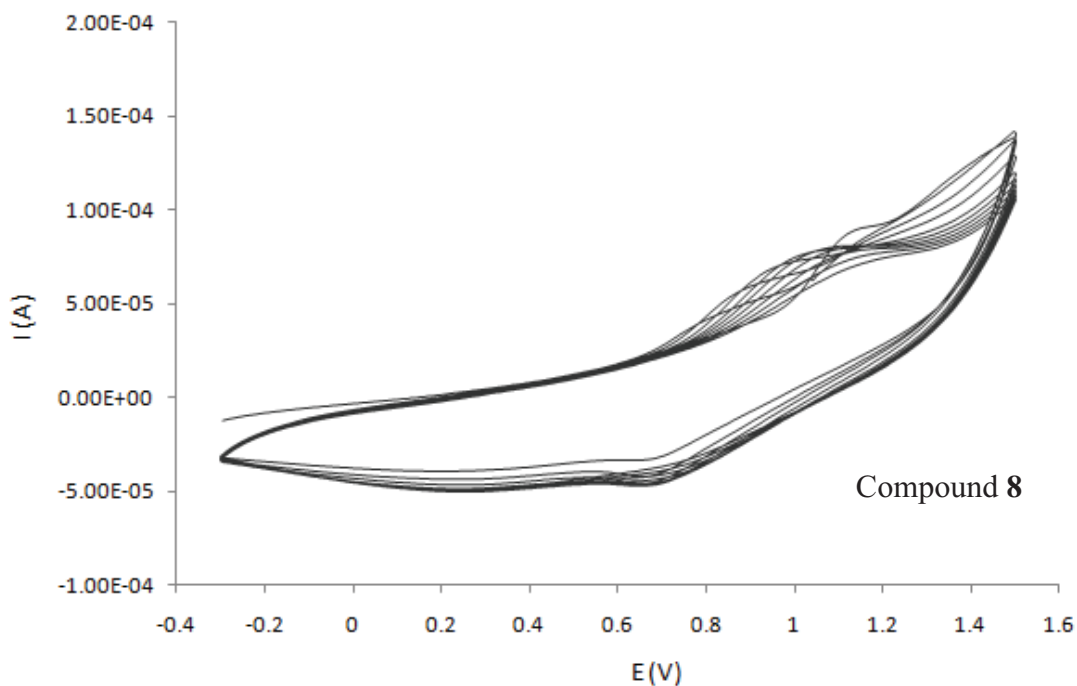


Figure 6. Cyclic voltammogram of dT-5-tp (8). Conditions: 10 mM of sample, 100 mM LiClO₄ in MeCN, r.t., working electrode Pt, counter electrode Au and quasi-reference electrode Ag. Scan rate 0.2 V/s

In the above cyclic voltammogram (Fig. 6), the initial oxidative wave occurs at a potential above ~ 1.46 V which oxidizes the monomer into the polymer. When the wave is reversed towards a negative potential, a reduction peak is observed at ~ 0.70 V which signifies the reduction of the polymer. Upon successive repeated waves, the reduction peaks increases in size as the polymer gets longer in length. As expected, the oxidation potential of the polymer (~ 0.96 V) is considerably lower than the oxidation of the monomer, signifying that the increase in conjugation length of the polymer stabilizes the radical formation on oxidation.³⁴

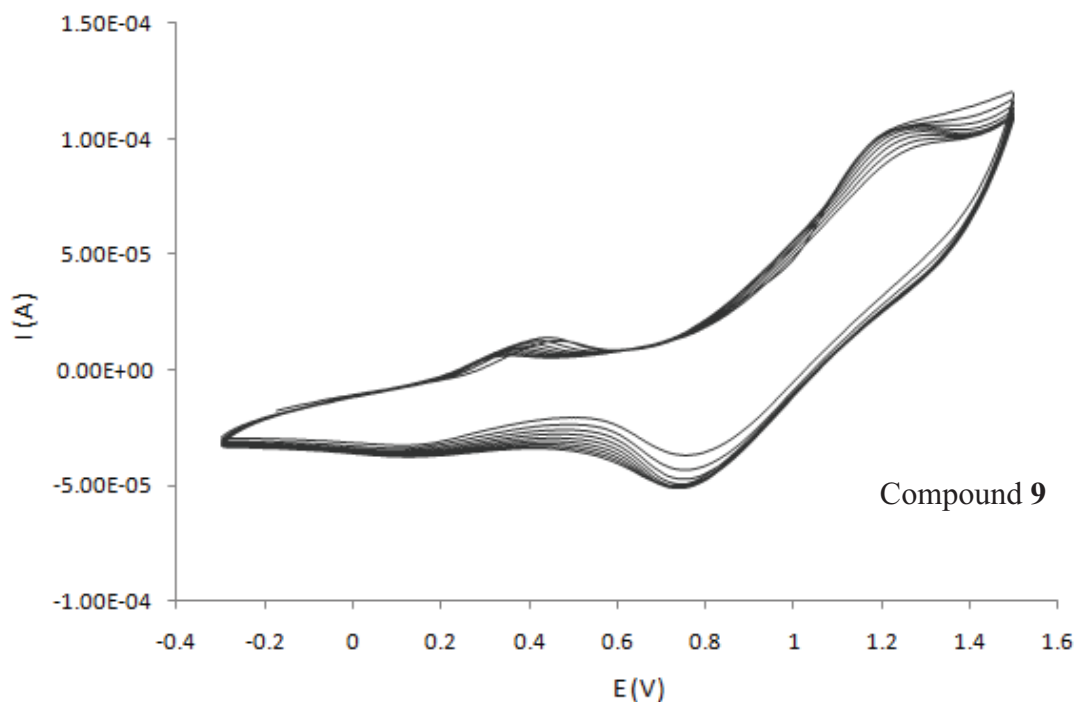


Figure 7. Cyclic voltammogram of dT-3-tpt (9). Conditions: 10 mM of sample, 100 mM LiClO₄ in MeCN, r.t., working electrode Pt, counter electrode Au and quasi-reference electrode Ag. Scan rate 0.2 V/s

In Fig. 7, the initial oxidative wave occurs at a potential of ~ 1.21 V indicating the oxidation of the monomer into the polymer. When the wave is reversed, a reduction peak is observed at ~ 0.75 V. Once more, the oxidation potential of the polymer (~ 0.39 V) is less positive than the oxidation of the monomer (~ 1.33 V) denoting that the length of the conjugation has increased and hence will stabilize the radicals formed on oxidation.

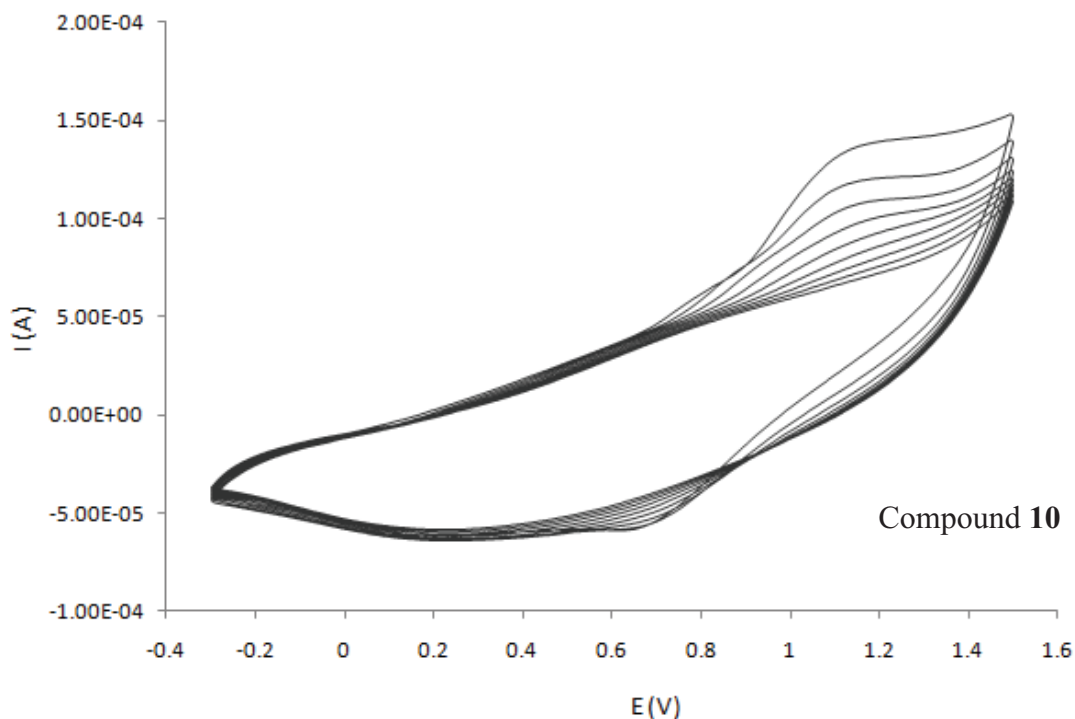


Figure 8. Cyclic voltammogram of dT-5-tpt (10). Conditions: 10 mM of sample, 100 mM LiClO₄ in MeCN, r.t., working electrode Pt, counter electrode Au and quasi-reference electrode Ag. Scan rate 0.2 V/s

In the above cyclic voltammogram (Fig. 8), the initial oxidative wave occurs at a potential of ~1.13 V denoting the oxidation of the modified nucleoside monomer dT-5-tpt into the polymer. When this wave is reversed towards a negative potential, a reduction peak is observed at ~0.65 V. The decrease in oxidation potential of the monomer (~1.13 V) versus the polymer (~0.50 V) further demonstrates the stability of the radical upon conjugation of an extended ring system.

By comparison of the redox potentials of dT-3-tpt and dT-5-tpt, the oxidation potentials are comparable indicating that the carbon bridge length does not affect the polymerization of the polymer and acts strictly as a linker between the nucleoside and the monomer. In contrast to the data of 5-py in Chapter 2, the coupled nucleoside, dT-5-py, shows a surface wave with a drop in current. A plausible reason for the decrease in current is that the electron density of the pyrrole ring may spread onto the linker and further onto the nucleoside, thus decreasing the affinity for polymerization. As dT-5-tp and dT-5-tpt possess extra conjugation from the extended ring system, the possibility of the electron density spreading onto the linker and nucleoside is reduced,

demonstrated by their surface-waves showing typical trends of conducting polymers.³⁴

To gain further insight into the electronic structure of the modified nucleosides, UV-vis spectroscopy (UV-vis) was employed.

3.2.4 UV-vis spectroscopy studies

Table 3 presents the wavelengths of maximum absorption (λ_{\max}) and the molar extinction coefficients (ϵ) of **7-10**.

Compound	λ_{\max} (nm)	ϵ ($\text{M}^{-1}\text{cm}^{-1}$)
7	289	8.12×10^3
8	291	1.22×10^4
9	297	2.11×10^4
10	306	1.31×10^4

Table 3. Wavelengths of maximum absorption λ_{\max} (nm) and molar extinction coefficient ϵ for modified nucleosides **7-10**.

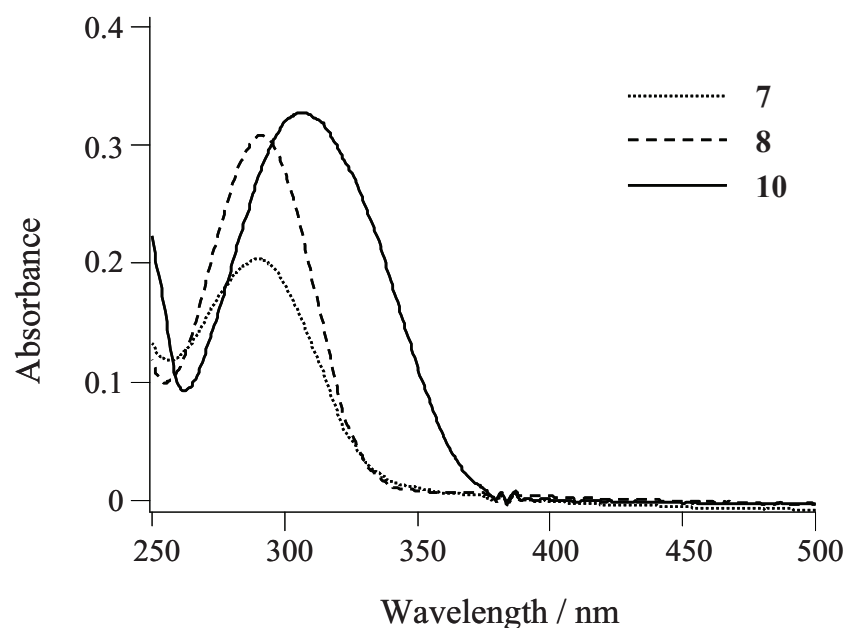
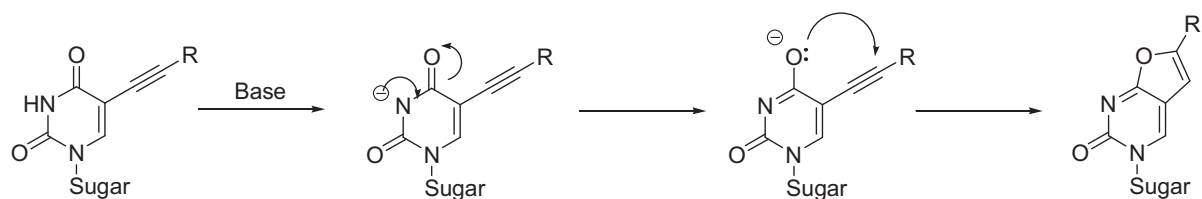


Figure 9. UV-vis spectra for compounds **7**, **8** and **10**. All spectra were recorded at 0.025mM of the title compounds in MeOH.

For the series of compounds containing a pentynyl bridge, **7**, **8** and **10**, the expected red-shift is observed as the aromatic group increases in size in the order **py** < **tp** < **tpt**, although this is small in the case of **7** > **8**. The effect of increasing alkyl-chain length for the **tpt** derivatives, **9-10**, does not show any notable trend.

3.2.5 Furanopyrimidone crystal structure

In the preparation of **8**, evidence of a second product was indicated by ^1H NMR spectroscopy. It had the same number of protons as **8** but there were shifts in two peaks. This was evident by a new peak at $\delta = 6.37$ ppm indicating a structure with an uncoupled aromatic proton, in this range typically a vinyl proton. Another feature that supports this is the downfield shift of the H6 resonance to $\delta = 8.67$. In addition to this, the resonance observed in **8** from the amino proton had disappeared suggesting a rearrangement had taken place (Scheme 2). Clear confirmation of this product was determined by single-crystal structure analysis (Fig. 11) and revealed it to be the furanopyrimidone isomer which has been reported previously.²⁵



Scheme 2. Proposed mechanism for the formation of the furanopyrimidone ring³⁵

The mechanism for production of the ring-closed product is shown in Scheme 2 and accords with the ¹H NMR and crystal structure analysis; the proton on N-4 has been transferred to the carbon of the triple bond to become an alkene in the five membered ring and accounts for the new singlet at $\delta = 8.67$ ppm.

Although the furanopyrimidone formed was an unwanted side-product from this reaction, they do have remarkable biological properties. For example, Balzarini *et al.* have shown that the furanopyrimidone in Fig. 10 inhibits the replication of the varicella-zoster virus (VZV) with no cytotoxicity.³⁶

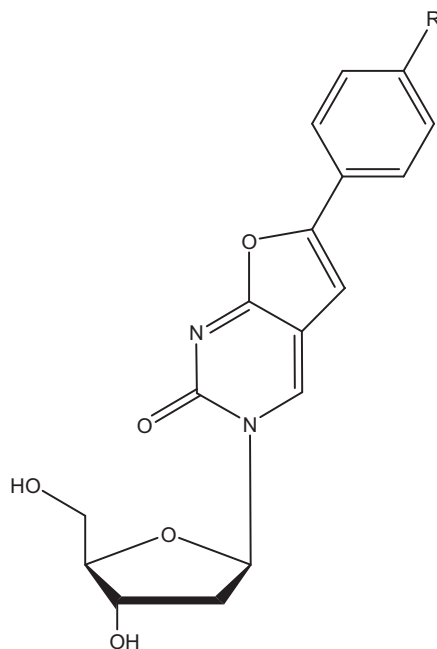


Figure 10. Structure of the ring-closed anti-VZV drug, BCNA.

Fig. 11 presents the molecular structure and numbering scheme used for **8i**. All bond lengths and angles lie within the expected ranges by comparison to analogous compounds and selected parameters are summarized in Table 4.

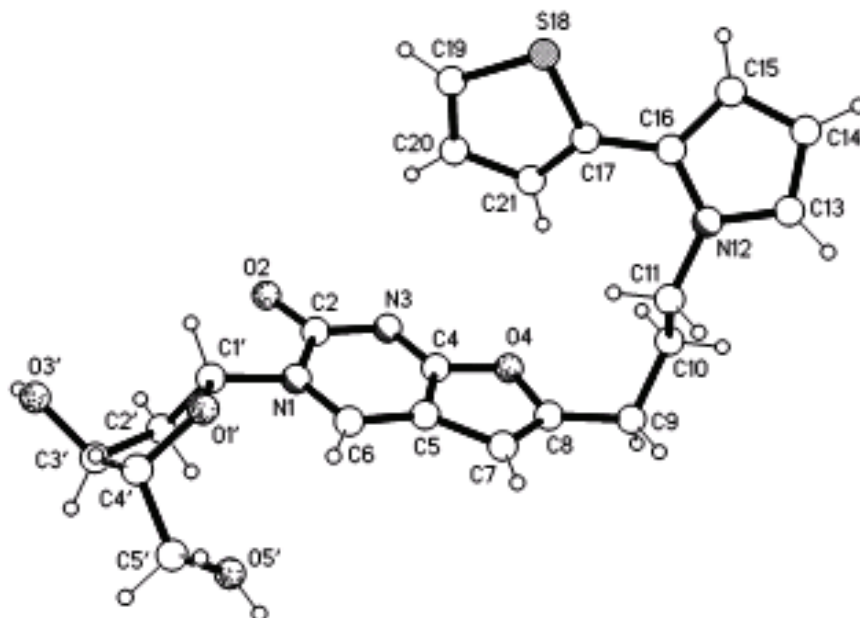


Figure 11. Molecular structure of the furanopyrimidone derivative **8i**

The analysis shows that the **tp** subunit lays over the furanopyrimidone ring with a shortest distance H21...O4 of 2.68 Å. The interplanar angle between the thiophene ring and pyrrole ring is 34.1° with the two rings exhibiting an up-down arrangement although the thienyl ring is disordered over two positions, comparable to the crystal structure of the 3-**tp**t unit in Chapter 2. The disorder of thienyl-pyrrole based systems has been previously reported.³⁷ The nucleoside exhibits an anti arrangement with the deoxyribose unit adopting a C2'-endo conformation. Hydrogen bonding is observed between the O2 of the nucleoside and H3' of the sugar (O2...H3' = 1.92 Å).

Selected bond lengths	Thienyl-pyrrole-furano-thymidone (Å)
O2–C2	1.231(5),
C2–N3	1.368(6)
C2–N1	1.407(6)
N1–C6	1.343(6)
C6–C5	1.364(6)
C5–C4	1.393(6)
N3–C4	1.306(6)
C4–O4	1.370(5)
O4–C8	1.418(5)
C8–C9	1.481(6)
C8–C7	1.320(7)
C7–C5	1.456(6)
C13–C19 (size of unit)	6.065

Table 4. Selected bond lengths (Å) for thienyl-pyrrole-furano-thymidone

In order to assess the suitability of the monomer coupled nucleosides for building nanowires via incorporation into DNA, the size of the monomer unit versus the distance between adjacent bases in DNA was taken into consideration. According to the crystal structure of **8i**, the distance between the α -thiophene and α -pyrrole position, is 6.065 Å. The distance between two adjacent base pairs in B-DNA is 3.4 Å according to Watson and Crick.³⁸ These values reveal that this monomer would fit comfortably into a sequence at every other position, perhaps at adjacent positions, without deformation of the DNA helix. Conversely, if dT-5-**tpt** is incorporated at adjacent or alternate positions, polymerisation may be sterically hindered, as the distance of the length of the **tpt** monomer is 9.98 Å, according to the crystal structure in Chapter 2, thus will not fit the natural spacing.

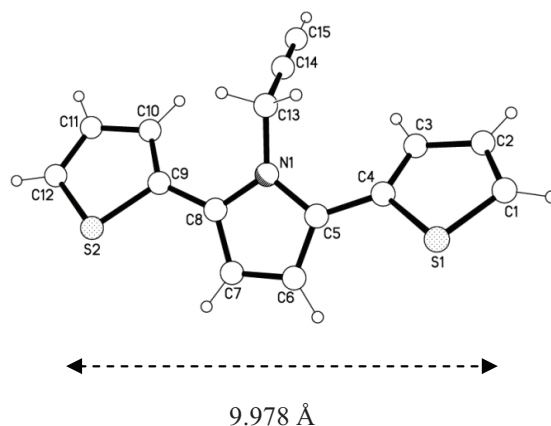
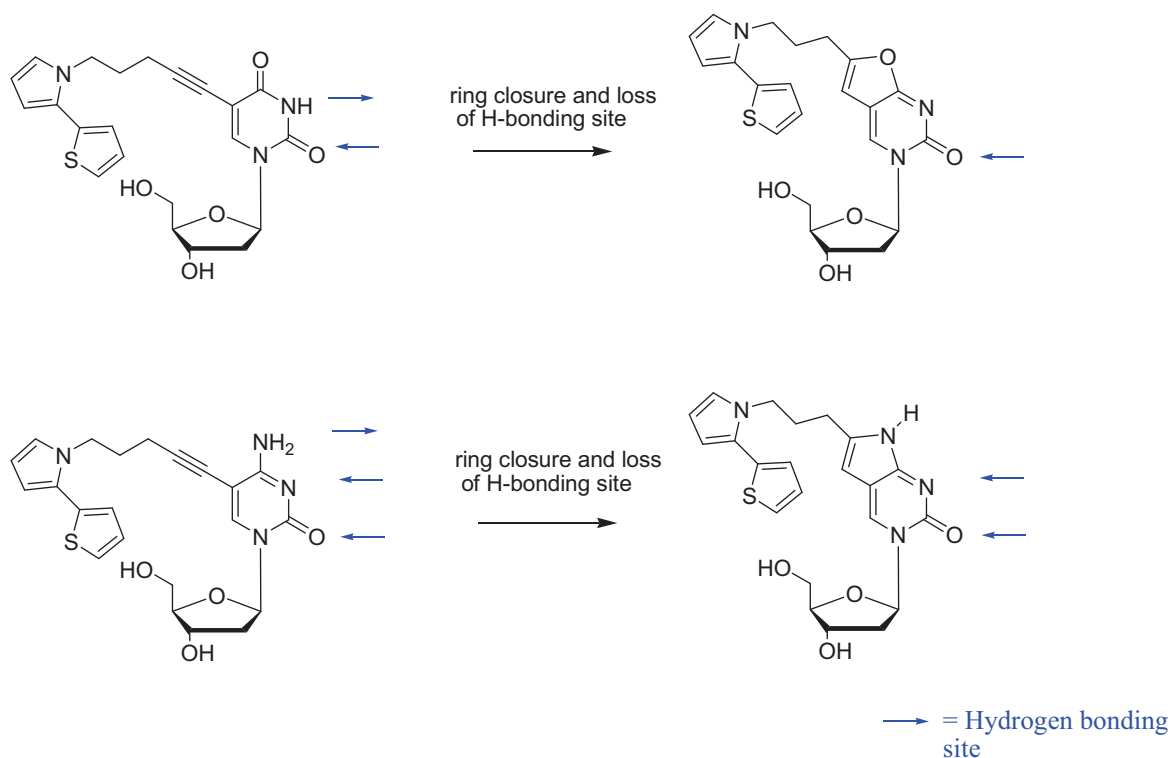


Figure 12. View of the molecular structure of one of the independent molecules in 5 with the distance from C1-C12

All of the modified thymidine derivatives have the pyrrole containing moiety held away from the phosphate backbone region of DNA and lies in the major groove. However, the furanopyrimidone product has now lost the N3 proton that can be used in the Watson-Crick hydrogen bonding. This signifies that this cyclized product cannot be used to bond with a complementary base in DNA as one of its two potential hydrogen binding sites has been lost (Scheme 3). However, it is still possible to obtain the pure pyrimidine products that can subsequently be used to hydrogen bond with complementary bases.

As a result of forming the unwanted ring closed side product **8i** and signifying the loss of the hydrogen bond donor on N3, it was decided that the modification of deoxycytidine should be attempted. As deoxycytidine lacks the proton at the N3 position, the initiation of the ring-closing synthesis by abstraction of this proton in thymidine can be avoided. Although a hydrogen can be abstracted from the N4 position to form a possible ring-closed side-product, two hydrogen bonding sites are still available in the modified deoxycytidine, in comparison to deoxythymidine which would have only one remaining hydrogen bond intact (Scheme 3). Therefore, the modified deoxycytidine would be stable to exist in a duplex and hence, 5-iodo-2'-deoxycytidine will be modified following the previous Sonogashira protocol.

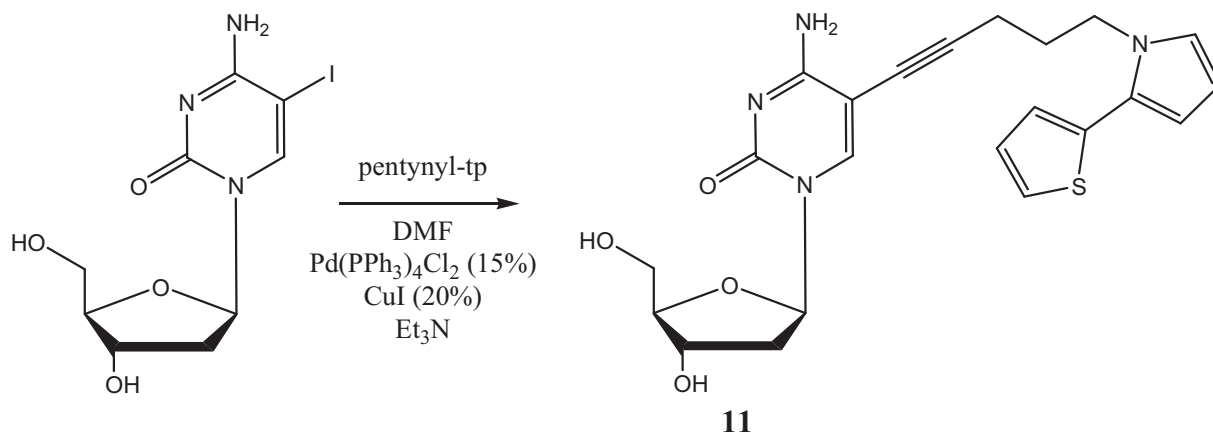


Scheme 3. Schematic showing the loss of hydrogen bonding at N3 of **8i** and N4 of dC-5-**tp** upon ring-closure.

3.3 Synthesis of 5-pentynyl-**tp** 2'-deoxycytidine

2'-Deoxycytidine is the other member of the pyrimidine family. It is structurally similar to 2'-deoxythymidine but can offer three Watson-Crick hydrogen bonds to the complementary guanine. Like 5-iodo-2'-deoxyuridine, the 5-iodo derivative of deoxycytidine is also commercially available hence, can also be modified at the C5 position for Sonogashira-type chemistry (Scheme 4). Therefore, the C5 position was modified with pentynyl-**tp** in the palladium-catalysed cross-coupling reaction. The decision to modify with pentynyl-**tp** was due to the electrochemical properties shown in 3.2.3 in addition to the size of the monomer unit. The length of the monomer indicates that it would fit comfortably into a sequence at every other position, although possibly at every position, without deformation of the DNA. In the case of deoxycytidine, there is no N3 proton available and therefore, the cyclized furanopyrimidone product can be avoided in utilising this pyrimidine. ¹H NMR spectroscopy and high-resolution ES-MS confirmed the structure. Identical conditions

were employed in the cross-coupling reaction however; a lower yield (35%) was obtained in comparison to deoxythymidine and 5-**tp**.



Scheme 4. Sonogashira cross-coupling of 5-iodo-2'-deoxycytidine and pentynyl-**tp**.

In order to further characterize the modified deoxycytidine and construct a comparison between its respective modified pyrimidine, dT-5-**tp**, FT-IR spectroscopy and UV-vis spectroscopy were employed.

3.3.1 FT-IR and UV-vis studies for the direct comparison between dT-5-**tp** and dC-5-**tp**

Infrared characterization was performed in order to identify and compare the various functional groups on the compounds. Assignment of the vibrational bands of the cytosine ring was achieved using literature references for deoxycytidine (Table 5).³⁹ The vibrations of the thienyl-pyrrole unit appear at similar frequencies. The strong peak at 1642 cm⁻¹ is quite broad and is likely to be covering peaks from other similar frequency vibrations.

Wavenumber (cm ⁻¹)		Assignment
dT-5-tp	dC-5-tp	
696	700	C-H thiophene
772	780	C-H pyrrole
843	843	C-S thiophene
1053	1053	N1-C1'-H cytidine/thymidine
1277		C-N thymidine
1460		N-H thymidine
	1502	C4=N3 cytidine
	1642	C=C and C2=O cytidine
1674		C=C, C2=O and C4=O thymidine
	3324	NH ₂ cytidine

Table 5. Vibrational bands of the modified thymidine units coupled to the *N*-alkylated monomers. The samples were tested as neat compounds.

According to literature, this is a common feature around this frequency and is likely to be masking a peak denoting NH₂ bending from the base of deoxycytidine that typically appears at ~1705 cm⁻¹. In adenine the NH₂ peak features at 1675 cm⁻¹ according to Mathlouthi *et al.*³⁹ The peak at 1642 cm⁻¹ also signifies the C=C in addition to the C2=O. As a rule, the carbonyl peak is normally assigned between 1720 cm⁻¹ and 1700 cm⁻¹, however in this case and confirmed in the literature, it appears at a lower frequency. The C-H peak at ~3280 cm⁻¹ in the alkylated species in Chapter 2 has evidently disappeared from the spectrum which confirms the loss of this proton during the reaction.

UV-visible spectroscopy was used to study the electronic structure of dC-5-tp and form a comparison between dT-5-tp and dC-5-tp. Table 6 represents the comparison of maximum wavelength absorptions and the molar extinction coefficients of the two modified pyrimidines.

Compound	λ_{\max} (nm)	ϵ ($M^{-1}cm^{-1}$)
dT-5- tp	291	1.22×10^4
dC-5- tp	294	9.44×10^3

Table 6. Wavelengths of the maximum absorption λ_{\max} (nm) and molar extinction coefficient ϵ for modified nucleosides **8** and **11**. All spectra were recorded at a concentration of 0.025 mM in MeOH

There is a slight red shift of dC-5-**tp** in comparison to dT-5-**tp**. This observed shift is expected as the chromophore in the pyrimidine ring of cytidine; $[-C=C-C=N-]$ provides extra conjugation through the ring system.⁴⁰

The investigation into the structural comparisons between dT-5-**tp** and dC-5-**tp** indicates that although the nucleosides are somewhat structurally dissimilar, bearing the 5-**tp** unit has little effect on the vibrational and electronic properties of the monomer. Therefore, employing either nucleoside for incorporation into DNA will offer an insight into the behaviour of the nucleosides whilst maintaining the comparable behaviour of the **tp** monomers.

3.4 Conclusion

Due to the current interest in conductive organic polymers and DNA, the synthesis of modifying both thymidine and cytidine pyrimidines was accomplished. Thymidine has been modified with a range of linkers and monomers to decipher which candidate would be suitable for incorporation into DNA whilst providing the highest conductivity of the conducting polymer that would also be generated. Once the Sonogashira synthesis had been optimized, for **7-10** high yields of the modified nucleosides was achieved and characterized by 1H NMR spectroscopy, ^{13}C NMR spectroscopy, FT-IR spectroscopy, high-resolution ES-MS and UV-vis spectroscopy. The isolation and X-ray diffraction analysis of the ring closed isomer dT-5-**tp** was

also achieved. The modified nucleosides having their functionalized moiety at the C5 position make them ideal candidates to be incorporated into DNA without disrupting the structure of DNA. Modifying cytidine was carried out in order to avoid the ring-closing step that was observed with thymidine. Besides, modifying both pyrimidines thymidine and cytidine will generate more diversity in the upcoming triphosphate synthesis. Therefore, the synthesis into triphosphates will be introduced and discussed in the following chapter as this will be the method by which the modified bases can be integrated into DNA.

Studies using phosphoramidite chemistry have been attempted and currently, work by Schuster *et al.* has shown promise. However, due to limitations in yield and length of the automated method, the enzymatic incorporation of modified nucleotides has several advantages. Therefore conversion into the triphosphate substrate which is necessary for enzymatic extension will be discussed in Chapter 4.

3.5 Experimental

Reagents were purchased from Sigma-Aldrich and used as received unless otherwise stated. Triethylamine was distilled from KOH and then degassed with N₂ for 30 min before use. DMF was degassed with N₂ for 30 min before use. All reactions were performed under N₂ under standard Schlenk conditions. ¹H NMR spectra were performed on a 300 MHz Bruker Spectrospin WM 300 WB spectrometer. Electronic absorption spectra were recorded on a Hitachi U-3010 Spectrophotometer. Mass spectra were measured on a Waters Micromass LCT Premier mass spectrometer.

General Procedure for Sonogashira Coupling (7-11):

A Schlenk flask was charged with 0.13M solution of 5-iodo-2'-deoxyuridine (1 mmol, 1 equiv) in anhydrous degassed DMF. To this solution was added bis(triphenylphosphine) dichloropalladium(II) (0.15 mmol, 0.15 equiv), copper(I) iodide (0.2 mmol, 0.2 equiv), anhydrous degassed triethylamine (2 mmol, 2 equiv) and the corresponding alkyl derivate (1.5 mmol, 1.2 equiv). The mixture was stirred at room temperature until completion by TLC (c.a. 15 h). Disodium EDTA 5% (v/w) (5mL) was added to the resulting mixture before evaporation to dryness. The crude product was redissolved in dichloromethane (150 mL) and washed twice with disodium EDTA 5% (v/w) (50 mL) and once with water (50 mL) before being dried over sodium sulphate. After filtration and concentration by rotary evaporation the reaction mixture was loaded onto a silica gel column packed with dichloromethane, and eluded by using dichloromethane and methanol (95:5). Fractions containing the product were combined and solvent removed to yield the following compounds;

7: Yield: 10% as an off white solid, mp 65-70 °C. ¹H NMR (dms^o-d₆); δ = 1.89 (quin, 2H; CH₂), 2.12 (dd, 2H; C₂H), 2.25 (t, 2H; CH₂), 3.59 (m, 2H; C₅H), 3.79 (q, 1H; C₄H), 4.00 (t, 2H; CH₂), 4.23 (quin, 1H; C₃H), 5.13 (t, 1H; OH), 5.25 (d, 1H; OH), 5.98(t, 2H; CH_{py}), 6.11 (t, 1H; C₁H), 6.77 (t, 2H; CH_{py}), 8.18 (s, 1H; C₆H), 11.60 (s, 1H; NH). ¹³C-NMR (dms^o-d₆); δ = 162.07, 149.82, 143.00, 120.91, 107.92, 99.29, 92.40, 88.06, 85.16, 74.11, 70.56, 61.47, 47.68, 30.40, 16.47. IR (neat, cm⁻¹): 1675, 1277, 1089, 1050, 727. HRMS (ESI): m/z: calc for C₁₈H₂₁N₃O₅ [M+Na]⁺: 382.1379; found: 382.1371. UV (MeOH): λ_{max} 289 nm.

8: Yield: 78% as a pale yellow solid, mp 67-70 °C. ¹H NMR (dms_o-d₆); δ = 1.80 (m, 2H; CH₂), 2.12 (dd, 2H; C₂H), 2.28 (t, 2H; CH₂), 3.58 (m, 2H; C₅H), 3.79 (q, 1H; C₄H), 4.16 (t, 2H; CH₂), 4.24 (quin, 1H; C₃H), 5.11 (t, 1H; OH), 5.25 (d, 1H; OH), 6.07 (t, 1H; CH_{tp}), 6.12 (t, 1H; C₁H), 6.21 (dd, 1H; CH_{tp}), 6.95 (t, 1H; CH_{tp}), 7.06 (dd, 1H; CH_{tp}), 7.13 (dd, 1H; CH_{tp}), 7.45 (dd, 1H; CH_{tp}), 8.01 (s, 1H; C₆H), 11.60 (s, 1H; NH). ¹³C-NMR (dms_o-d₆): δ = 162.03, 149.82, 143.02, 134.75, 128.05, 125.98, 125.26, 125.24, 124.10, 110.44, 108.10, 99.25, 92.29, 88.06, 85.18, 74.14, 70.61, 61.50, 46.14, 30.12, 16.49. IR (neat, cm⁻¹): 1674, 1277, 1053, 843, 696. HRMS (ESI): m/z: calc for C₂₂H₂₃N₃O₅S [M+Na]⁺ : 464.1256; found: 464.1254. UV (MeOH): λ_{max} 291 nm.

8i: During the purification of **8**, chromatography with (9:1) CH₂Cl₂/MeOH showed a second product with a greater R_f. This fraction was collected and slow evaporation of the solvent gave single crystals which were analyzed by X-ray diffraction and found to be of **8i**. Yield: 11%. ¹H NMR (dms_o-d₆); δ = 1.80 (m, 2H; CH₂), 2.12 (dd, 2H; C₂H), 2.28 (t, 2H; CH₂), 3.58 (m, 2H; C₅H), 3.79 (q, 1H; C₄H), 4.16 (t, 2H; CH₂), 4.24 (quin, 1H; C₃H), 5.11 (t, 1H; OH), 5.25 (d, 1H; OH), 6.07 (t, 1H; CH_{tp}), 6.12 (t, 1H; C₁H), 6.21 (dd, 1H; CH_{tp}), 6.37 (s, 1H; C₇H), 6.95 (t, 1H; CH_{tp}), 7.06 (dd, 1H; CH_{tp}), 7.13 (dd, 1H; CH_{tp}), 7.45 (dd, 1H; CH_{tp}), 8.67 (s, 1H; C₆H).

9: Yield: 60% as a pale yellow solid, mp 98-101 °C. ¹H NMR (dms_o-d₆); δ = 2.15 (m, 2H; C₂H), 3.60 (m, 2H; C₅H), 3.81 (q, 1H; C₄H), 4.25 (quin, 1H; C₃H), 4.92 (s, 2H; CH₂), 5.14 (t, 2H; OH), 5.28 (d, 2H; OH), 6.01 (t, 1H; C₁H), 6.34 (s, 2H; CH_{tpt}), 7.18 (dd, 2H; CH_{tpt}), 7.48 (dd, 2H; CH_{tpt}), 7.57 (dd, 2H; CH_{tpt}), 8.27 (s, 1H; C₆H), 11.69 (s, 1H; NH). ¹³C-NMR (dms_o-d₆): δ = 161.78, 149.74, 144.40, 134.02, 128.88, 128.38, 126.26, 126.01, 110.60, 97.87, 89.28, 88.23, 85.54, 78.15, 70.56, 61.54, 48.95, 36.71. IR (neat, cm⁻¹): 1682, 1281, 1089, 1051, 843, 770, 697. HRMS (ESI): m/z: calc for C₂₄H₂₁N₃O₅S₂ [M+Na]⁺: 518.0820; found: 518.0807. UV (MeOH): λ_{max} 297 nm.

10: Yield: 30% as a pale yellow solid, mp 139-141 °C. ¹H NMR (dms_o-d₆); δ = 1.66 (m, 2H; CH₂), 2.12 (dd, 2H; C₂H), 2.21 (t, 2H; CH₂), 3.58 (m, 2H; C₅H), 3.81 (q, 1H; C₄H), 4.23 (m, 1H; C₃H), 4.30 (t, 2H; CH₂), 5.10 (t, 1H; OH), 5.27 (d, 1H; OH), 6.31 (t, 1H; C₁H), 6.30 (s, 2H; CH_{tpt}), 7.10 (dd, 2H; CH_{tpt}), 7.23 (dd, 2H; CH_{tpt}), 7.53

(dd, 2H; CH_{tp}), 8.09 (s, 1H; C_6H), 11.59 (s, 1H; NH). ^{13}C -NMR (dms o - d_6): δ = 161.88, 149.80, 143.03, 134.35, 128.46, 128.15, 126.22, 126.06, 111.01, 99.23, 91.87, 88.05, 85.15, 73.92, 70.68, 61.55, 44.22, 29.87, 16.52. IR (neat, cm^{-1}): 1645, 1275, 1099, 1052, 841, 766, 692. HRMS (ESI): m/z : calc for $\text{C}_{26}\text{H}_{25}\text{N}_3\text{O}_5\text{S}_2$ $[\text{M}+\text{Na}]^+$: 546.1133; found: 546.1136. UV (MeOH): λ_{max} 306 nm.

11: Yield: 35% as a pale brown solid. ^1H NMR (dms o - d_6): δ = 1.88 (m, 2H; CH_2), 1.99 (dd, 2H; $C_2\cdot H$), 2.35 (t, 2H; CH_2), 3.57 (m, 2H; $C_5\cdot H$), 3.78 (q, 1H; $C_4\cdot H$), 4.14 (t, 2H; CH_2), 4.20 (quin, 1H; $C_3\cdot H$), 5.06 (t, 1H; OH), 5.21 (d, 1H; OH), 6.08 (t, 1H; CH_{tp}), 6.12 (t, 1H; $C_1\cdot H$), 6.20 (dd, 1H; CH_{tp}), 6.79 (s, 1H; NH'), 6.94 (t, 1H; CH_{tp}), 7.06 (dd, 1H; CH_{tp}), 7.12 (dd, 1H; CH_{tp}), 7.48 (dd, 1H; CH_{tp}), 7.68 (s, 1H; NH'), (8.01 (s, 1H; C_6H). IR (neat, cm^{-1}): 3324, 1642, 1502, 1237, 1053, 843, 780, 700. (ESI): m/z : calc for: $\text{C}_{22}\text{H}_{24}\text{N}_4\text{O}_4\text{S}$ $[\text{M}]^+$: 441.1575; found: 441.1596. UV (MeOH): λ_{max} 294 nm.

References

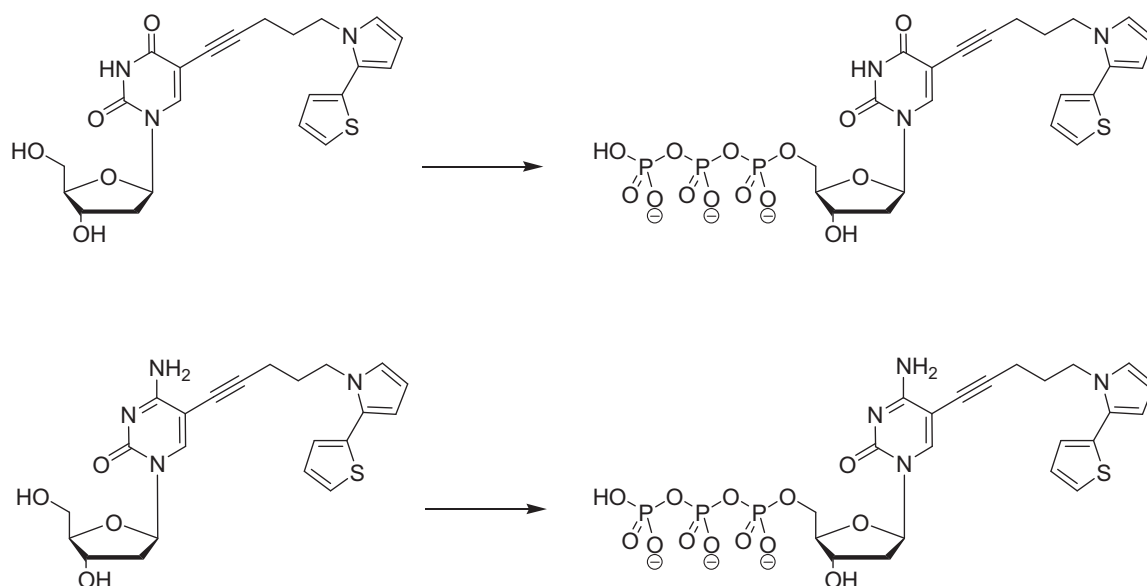
- (1) Farha Al-Said, S. A.; Hassanien, R.; Hannant, J.; Galindo, M. A.; Pruneanu, S.; Pike, A. R.; Houlton, A.; Horrocks, B. R. *Electrochem. Commun.* **2009**, *11*, 550.
- (2) Hannant, J.; Hedley, J. H.; Pate, J.; Walli, A.; Farha Al-Said, S. A.; Galindo, M. A.; Connolly, B. A.; Horrocks, B. R.; Houlton, A.; Pike, A. R. *Chem. Commun.* **2010**, *46*, 5870.
- (3) Chen, W.; Guler, G. z.; Kuruvilla, E.; Schuster, G. B.; Chiu, H.-C.; Riedo, E. *Macromolecules* **2010**, *43*, 4032.
- (4) Seeman, N. C. *Nature* **2003**, *421*, 427.
- (5) Kumar, V.; Parmar, V. S.; Malhotra, S. V. *Biochimie*, *92*, 1260.
- (6) Mitsuya, H.; Weinhold, K. J.; Furman, P. A.; St Clair, M. H.; Lehrman, S. N.; Gallo, R. C.; Bolognesi, D.; Barry, D. W.; Broder, S. *Proc. Natl. Acad. Sci. U. S. A.* **1985**, *82*, 7096.
- (7) Lee, Y.-S.; Park, S. M.; Kim, H. M.; Park, S.-K.; Lee, K.; Lee, C. W.; Kim, B. H. *Bioorg. Med. Chem. Lett.* **2009**, *19*, 4688.
- (8) James, D.; Escudier, J.-M.; Amigues, E.; Schulz, J.; Vitry, C.; Bordenave, T.; Szlosek-Pinaud, M.; Fouquet, E. *Tetrahedron Lett.* **2010**, *51*, 1230.
- (9) Wanninger-Weiß, C.; Wagenknecht, H. A. *Eur. J. Org. Chem.* **2008**, *2008*, 64.
- (10) Meggers, E.; Holland, P. L.; Tolman, W. B.; Romesberg, F. E.; Schultz, P. G. *J. Am. Chem. Soc.* **2000**, *122*, 10714.
- (11) Clever, G. H.; Kaul, K.; Carell, T. *Angew. Chem. Int. Ed.* **2007**, *46*, 6226.
- (12) Tanaka, K.; Clever, G. H.; Takezawa, Y.; Yamada, Y.; Kaul, C.; Shionoya, M.; Carell, T. *Nature Nanotech.* **2006**, *1*, 190.
- (13) Wirges, C. T.; Timper, J.; Fischler, M.; Sologubenko, A. S.; Mayer, J.; Simon, U.; Carell, T. *Angew. Chem. Int. Ed.* **2009**, *48*, 219.
- (14) Tanaka, K.; Tengeiji, A.; Kato, T.; Toyama, N.; Shionoya, M. *Science* **2003**, *299*, 1212
- (15) Bouamaied, I.; Nguyen, T.; Ruhl, T.; Stulz, E. *Org. Biomol. Chem.* **2008**, *6*, 3888.
- (16) Nguyen, T.; Brewer, A.; Stulz, E. *Angew. Chem. Int. Ed.* **2009**, *48*, 1974.
- (17) Wagenknecht, H.-A. *Angew. Chem. Int. Ed.* **2009**, *48*, 2838.
- (18) Seley, K. L.; Zhang, L.; Hagos, A.; Quirk, S. *J. Org. Chem.* **2002**, *67*, 3365.
- (19) Liu, P.; Sharon, A.; Chu, C. K. *J. Fluorine Chem.* **2008**, *129*, 743.
- (20) Mathé, C.; Périgaud, C. *Eur. J. Org. Chem.* **2008**, *2008*, 1489.
- (21) Bera, S.; Sakthivel, K.; Pathak, T.; Langley, G. J. *Tetrahedron* **1995**, *51*, 7857.
- (22) Meneni, S.; Ott, I.; Sergeant, C. D.; Sniady, A.; Gust, R.; Dembinski, R. *Bioorg. Med. Chem.* **2007**, *15*, 3082.
- (23) Brazier, J. A.; Shibata, T.; Townsley, J.; Taylor, B. F.; Frary, E.; Williams, N. H.; Williams, D. M. *Nucleic Acids Res.* **2005**, *33*, 1362.
- (24) Ozaki, H.; Mine, M.; Shinozuka, K.; Sawai, H. *Nucleos. Nucleot. Nucl.* **2004**, *23*, 339.
- (25) Pike, A. R.; Ryder, L. C.; Horrocks, B. R.; Clegg, W.; Connolly, B. A.; Houlton, A. *Chem.--Eur. J.* **2005**, *11*, 344.
- (26) Datta, B.; Schuster, G. B. *J. Am. Chem. Soc.* **2008**, *130*, 2965.
- (27) Pruneanu, S.; Al-Said, S. A. F.; Dong, L. Q.; Hollis, T. A.; Galindo, M. A.; Wright, N. G.; Houlton, A.; Horrocks, B. R. *Adv. Funct. Mater.* **2008**, *18*, 2444.
- (28) Ma, Y.; Zhang, J.; Zhang, G.; He, H. *J. Am. Chem. Soc.* **2004**, *126*, 7097.

- (29) Ma, Y. F.; Zhang, J. M.; Zhang, G. J.; He, H. X. *J. Am. Chem. Soc.* **2004**, *126*, 7097.
- (30) Ghilagaber, S.; Hunter, W. S.; Marquez, R. *Tetrahedron Lett.* **2007**, *48*, 483.
- (31) Mathlouthi, M.; Seuvre, A.-M. *Carbohydr. Chem.* **1984**, *134*, 23.
- (32) Tsuboi, M.; Komatsu, M.; Hoshi, J.; Kawashima, E.; Sekine, T.; Ishido, Y.; Russell, M. P.; Benevides, J. M.; Thomas Jr, G. J. *J. Am. Chem. Soc.* **1997**, *119*, 2025.
- (33) Galindo, M. A.; Hannant, J.; Harrington, R. W.; Clegg, W.; Horrocks, B. R.; Pike, A. R.; Houlton, A. *Org. Biomol. Chem.* **2011**, *9*, 1555.
- (34) Nalwa, H. S. *Conducting polymers (Handbook of advanced electronic and photonic materials and devices)* Academic, 2001.
- (35) Yu, C. J.; Yowanto, H.; Wan, Y.; Meade, T. J.; Chong, Y.; Strong, M.; Donilon, L. H.; Kayyem, J. F.; Gozin, M.; Blackburn, G. F. *J. Am. Chem. Soc.* **2000**, *122*, 6767.
- (36) Balzarini, J.; McGuigan, C. *Biochim. Biophys. Acta* **2002**, *1587*, 287.
- (37) Ferraris, J. P.; Andrus, R. G.; Hrcir, D. C. *J. Chem. Soc., Chem. Commun.* **1989**, 1318.
- (38) Watson, J. D.; Crick, F. H. *Nature* **1953**, *171*, 737.
- (39) Mathlouthi, M.; Seuvre, A. M.; Koenig, J. L. *Carbohydr. Res.* **1986**, *146*, 1.
- (40) Cavalieri, L. F.; Bendich, A.; Tinker, J. F.; Brown, G. B. *J. Am. Chem. Soc.* **1948**, *70*, 3875.

**Chapter 4 – *Triphosphate
synthesis of modified nucleosides***

Chapter 4 – *Triphosphate synthesis of modified nucleosides*

The preceding chapter reported investigations into the synthesis and characterization of modified nucleosides. The target compounds **7-11** were synthesized by coupling the monomers described in Chapter 2 to the nucleosides deoxythymidine and deoxycytidine via alkyne linkers. The findings from Chapter 3 show that **tp** modified nucleosides dT-5-**tp** and dC-5-**tp** should be exploited in DNA. To realize this goal, the conversion of **8** and **11** to triphosphate derivatives is detailed and their enzymatic incorporation into DNA in this following chapter (Scheme 1).



Scheme 1. Schematic to illustrate the triphosphate formation of dTTP* and dCTP* from their respective nucleoside precursors.

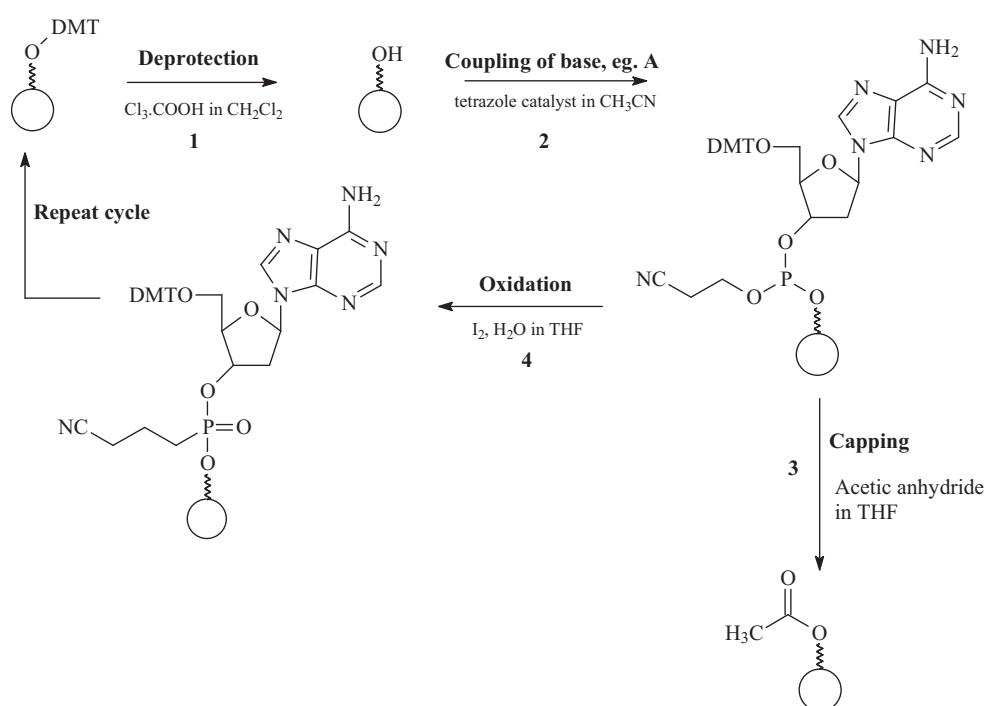
As highlighted in Chapter 1, employing DNA as a template allows the simple hybridization of the polyanionic DNA to a polycationic conducting polymer. However, this method lacks control and could potentially hinder the formation of a 1-dimensional nanowire. Furthermore, it does not use the sequence-specific code inherent to DNA to its advantage. Therefore, in employing the “DNA as a scaffold”

approach, the coding that is intrinsic to DNA can be exploited and in turn be used to build up a 1-dimensional structure by specifically inserting modified bases in predetermined positions. This is a sophisticated technique that offers direct organization of the nanowire.

The vast amount of literature on DNA synthesis highlights that there are two leading ways in completing this task; phosphoramidite and triphosphate chemistry.^{1,2 3-7} The former employs automated solid-support chemistry and the latter works by making use of enzymes, more specifically DNA polymerases.

4.1 Phosphoramidite chemistry

DNA oligonucleotides can be synthesized through automated solid-phase DNA-synthesis utilizing phosphoramidite chemistry. In this process, oligomers of DNA are constructed base by base from a solid-support in the form of CPG columns or silicon wafers.^{8,9} These supports possess a DMT-protected hydroxyl group that acts as an anchor to initiate the synthesis (Scheme 2).



Scheme 2. Schematic illustrating the steps of automated solid-phase DNA synthesis.

Deprotection of the DMT group of the solid support reveals the hydroxyl group that can be coupled to a nucleoside bearing a phosphoramidite at its 3'-OH position. To avoid potential side reactions, a capping step is obligatory to protect any unreacted hydroxyl groups. The final step in the cycle is the oxidation of the phosphite triester to the stable phosphate triester. The cycle is then repeated until the desired number of nucleosides is built onto the support.

DNA synthesis is simple to perform and can produce short oligomers in high yields at 99.89 % per cycle.¹⁰ However, modifications to the nucleosides must be inert to prevent unwanted reactions during a range of conditions in the automated synthesis. For example, the acidic detritylation of DMT-cleavage, acyl protecting groups in the capping step, iodine oxidation and base-catalyzed cleavage from the solid-support could induce side reactions.¹¹

Many research groups have employed this approach to test the suitability of modified bases in short oligomers and their effect on the DNA duplex. Carrell *et al.* have recently chemically synthesized and incorporated 5-hydroxymethylcytosine, a naturally occurring base in mammalian cells, into an oligomer of DNA successfully without disrupting the stability of the duplex.¹ In Chapter 3 it was noted that Schuster *et al.* modified deoxycytidine with an aniline monomer (Fig. 1a) and incorporated this non-canonical base into a short oligomer of DNA via phosphoramidite chemistry, although this modification enforced a disruption to the duplex structure.¹² To improve the conductivity of the polyaniline, doping was required in the form of HCl, although the harsh acidic conditions had a detrimental affect on the DNA helix stability. For this reason, Schuster's group then proceeded to use a different unit to modify the deoxycytidine base with, a fused thienyl-pyrrole unit (Fig. 1b).¹³ The modified nucleoside was converted to its phosphoramidite form and six units were incorporated into a 33-mer oligomer of DNA. Melting temperatures of the native duplex versus the modified duplex were compared and it was found to be 23 °C lower in the modified duplex. Although circular dichroism (CD) proved that the DNA helix retained its B-form indicating that the modified fused-**tp** unit did not disrupt the geometry of the structure to a great extent. Upon polymerization of the fused-**tp** units using the same conditions for polyaniline, the melting temperature decreased by a further 3 °C to 46 °C, demonstrating that the duplex was more distorted. The decrease in stability could

be due to the size of the monomer. Having a shorter unit length in comparison to the **tp** unit in Chapter 2, it may force the duplex out of position upon polymerization.

In 2010, Schuster chose a similar path as discussed in Chapter 2 and 3 by increasing the length of the monomer unit and so deoxycytidine was modified with a **tpt** unit (Fig 1c).¹⁴

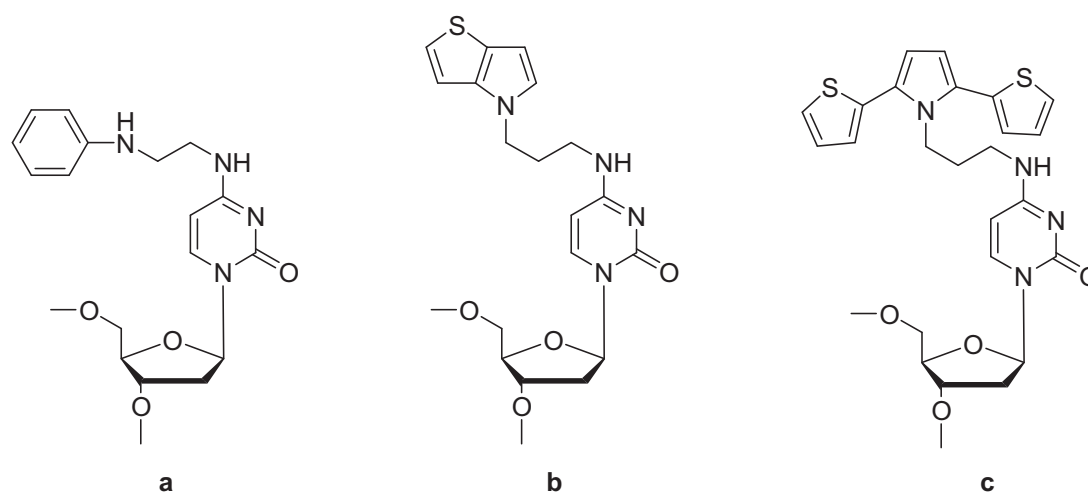


Figure 1. Modified cytidine analogues, increasing in monomer size have been transformed to the phosphoramidite and incorporated into oligomers of DNA.

Once again, the modified phosphoramidite was incorporated into an oligomer of DNA and the polymerization of the **tpt** units was accomplished (Fig. 2). Unlike aniline and the fused thienyl-pyrrole unit, incorporating the **tpt** unit into oligomers did not disrupt the duplex of DNA and increasing the number of **tpt** units further increased its stability. Upon oxidation it was discovered that interstrand polymerization may occur which could prohibit the formation of single molecular wires.

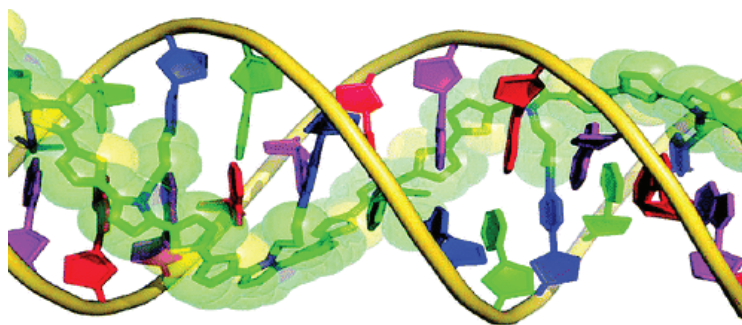


Figure 2. A graphical model of polymerized **tpt** that has been covalently bound to cytidine and incorporated into a short oligomer of DNA.

Schuster's work demonstrated that modified pyrimidines could be incorporated into short oligomers of DNA, be polymerized and more importantly, produce short conducting polymers whilst retaining the duplex of DNA. Given that the melting temperatures were reduced is to be expected with modified bases. Whilst employing stylish chemistry that exhibits DNA acting as a scaffold to produce conducting polymers, the lengths of the wires achieved are too short. Phosphoramidite chemistry will not allow for this as limitations arise when trying to synthetically produce longer lengths as the overall yield of the coupling steps drops to ~70 % after approximately 50 bases (each coupling step at 99.8%, and multiplied by 50 cycles). Incorporating functionalized bases also makes their modifications susceptible to side reactions due to the harsh conditions in the synthesis. Hence, additional protecting groups must be introduced to prevent any unwanted side reactions. These issues associated with automated synthesis could prove problematic in meeting the scope of this project. As a result, a different approach has been employed. Employing enzymes to extend DNA over microns in length will allow the goal to be reached. To facilitate the enzymatic method, the nucleosides must not be converted into phosphoramidites, but triphosphates. It is the triphosphate moiety that DNA polymerases will accept in order to extend a duplex of DNA.

4.2 Triphosphate chemistry

An alternative method for the controlled introduction of a modified nucleoside into DNA is to convert the modified nucleoside into its nucleotide which can then be utilized by DNA polymerases for enzymatic extension. This approach enables the

placement of site-specific modifications into the DNA strand by employing a predetermined template. However, this methodology depends on the ability of the enzyme to recognize the modified substrate to allow its incorporation into DNA.

Interest into triphosphates, their synthesis and isolation, was initiated with the attraction to ATP due to its importance in transporting energy from cells to metabolic processes whilst also aiding the processes used by enzymes and cells to function. In 1949, ATP was synthesized, isolated and analyzed by Michelson and Todd using arduous methods.¹⁵ Since then, efforts have been made to improve the purification techniques. HPLC has been employed for the separation from starting materials using volatile triethylammonium bicarbonate buffers to leave the protonated stable triphosphate. Currently, a choice of column media can be used to initially separate the crude products according to anionic charge and then using a reversed-phase media to separate the compounds according to polarity, to yield pure triphosphates. Since the isolation of ATP, the production of modified triphosphates has shown a great deal of interest in order to functionalize duplexes of DNA to subsequently use the DNA in applications such as electronics or sensing in medicine to use a few examples.^{5,7}

4.2.1 Functionalized nucleotide triphosphates

The functionalization of dNTP's has been widely reported as the behaviour of non-standard nucleotides has been recognized in various therapeutic and diagnostic applications.¹⁶⁻¹⁹ Chapter 3 demonstrated how the nucleosides deoxythymidine and deoxycytidine were modified at the C5 position with pyrrole containing moieties. The modification was performed at the C5 position in order to maintain the projection of the modification into the major groove which not only retains the helical structure of DNA, but also implies that the nucleotide derivatives can be tolerated by polymerase enzymes.^{20,21} The pyrimidines are commonly modified at the C5 position for this reason. Likewise, the purines bases have also been functionalized to minimize disruption to the hydrogen bonding sites.²²

Modification, however, is not restricted to sites on the nucleobases, as the sugar and backbone moieties of the triphosphate have also been modified.²³⁻²⁵ Various groups

have mimicked the ribose component while retaining the phosphodiester linker, for example, glycol nucleic acid (GNA) (Fig. 3).²⁶ This simple molecule contains a two carbon bridge between the phosphodiesters, in comparison with the three carbon bridge between standard phosphodiesters. When incorporated into a duplex GNA generates a stable double helix structure.

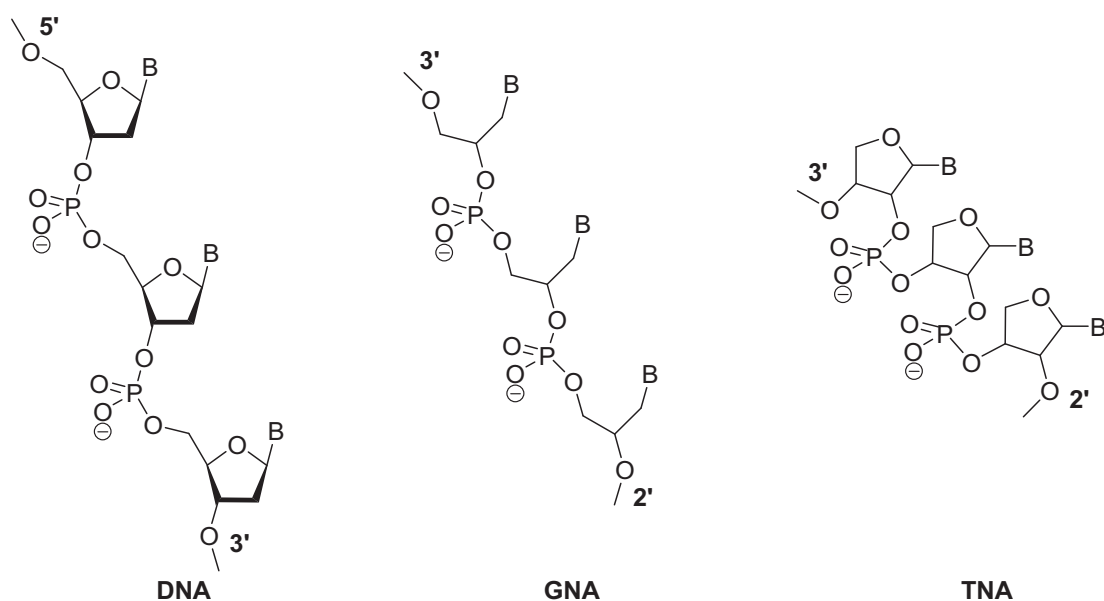


Figure 3. Molecular structures of DNA, GNA and TNA.

α -Threofuranosyl nucleic acid (TNA) is another imitation of the phosphodiester linkage except in this scenario, the link is between the 3' and 2' carbons as opposed to the 5' and 3' carbons in natural DNA (Fig 3). In addition, several groups have also replaced the phosphodiester with alternative linkages such as phosphorothioates which can be found naturally.^{25,27} For instance, the formation of adenosine 5'-O-(1-thiotriphosphates) by using PSCl_3 instead of POCl_3 in the monophosphate formation,^{24,25} and thymidine β,γ -imidotriphosphates where the pyrophosphate has been replaced by imidotriphosphate to act as an HIV inhibitor²³ (Figure 4) are just two further examples.

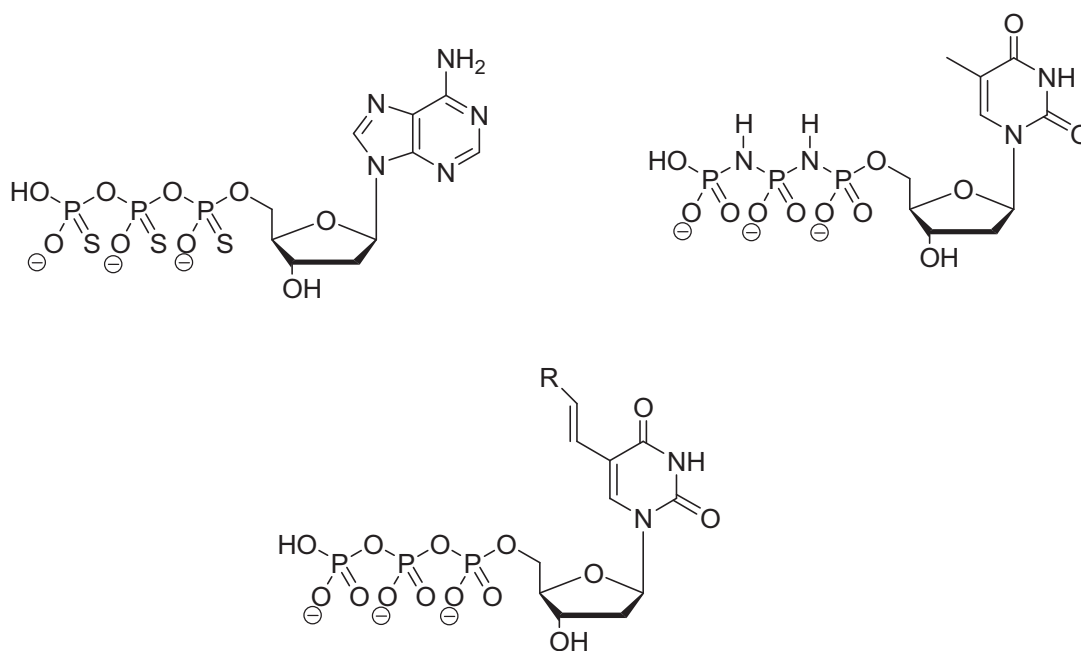


Figure 4. Chemical structures of synthesized modified nucleoside-5'-O-triphosphates.

The methods of synthesizing triphosphate analogues can be difficult due to the relative instability of triphosphates. For example, triphosphates are hydrophilic and favour aqueous reaction media, whereas the modifications observed in Chapter 3 generally prefer organic reaction conditions due to their hydrophobic moieties. These differences make it difficult to perform modifications on nucleosides followed by conversion into a nucleotide and the mixture of hydrophilic/hydrophobic components, make the isolation and purification challenging. A further difficulty lies in the fact that post-synthetic triphosphates lack stability and can decompose at room temperature within several days. In particular, kept in their protic form is thought to accelerate their decomposition due the acidity of their environment.⁵ This can be circumvented by storing in a neutral buffer at cold temperatures of less than 4 °C. Despite these obstacles, the following section discusses the ability of polymerases to accept modified nucleotides in the enzymatic production of dsDNA.

4.2.2 Acceptance of modified triphosphates by DNA polymerases

The first triphosphate to be modified and used as a substrate in DNA synthesis was a biotin-labeled dUTP by Langer *et al.* in 1981.²⁸ Since that time a range of modified triphosphates have been prepared and shown to be accepted by DNA polymerases without experimental rationale.²⁹ In the majority of cases, modification is performed prior to DNA synthesis. However, several groups use a two-step approach whereby incorporation of a modified nucleoside precursor into DNA is performed and then subsequently functionalized in post-modification. Carell *et al.* have ably demonstrated the method of post-modification by employing ‘click’ chemistry to add substituent’s after the DNA has been amplified by PCR.³⁰⁻³⁴ Initially, alkynyl triphosphates are synthesized and subsequently incorporated into DNA via PCR amplification. A variety of functionalized azides may be used, for example, an azide-modified galactose,³⁰ providing nucleation sites for metals, e.g. silver.^{32,35,36} The alkyne and azide can then be ‘clicked’ together via the 1,3-Huisgen cycloaddition to create a bridge between the DNA and a functional unit.

The dNTP of choice is pre-modified with a generic linker that will protrude into the major groove and that has been known to be accepted by a DNA polymerase. The nature of the chemistry ensures the process is versatile, facile and reproducible, a requirement that is necessary when up-scaling. In previous work, Carrell *et al.* have acknowledged that the synthesis of modified triphosphates and their acceptance by DNA polymerases is a difficult task and using the same protocol does not work for every substrate. Therefore, all four nucleosides were modified to assess which base could be most easily incorporated enzymatically. Using post-modification is an excellent method to guarantee reproducibility and further avoids factors such as incompatibility of reaction conditions for modification. Clearly this is a very attractive method, although one drawback of employing PCR to incorporate and amplify DNA is the need for primers and templates of DNA. Templates, typically wild-type DNA can be purchased commercially. However, using wild-type DNA means that there is no way of controlling the precise placements of the bases that are to be modified as the sequence is preset. Hence it is impossible to determine the positions of the modified nucleotides. Carell *et al.* strived to circumvent this problem by modifying all

four nucleotides to synthesize a fully functional DNA duplex, but unfortunately the polymerases would not accept all four modifications in succession.³⁷

In contrast, Famulok *et al.* also attempted modifying every nucleotide and incorporating via PCR which was executed successfully, producing a fully functional DNA duplex.³⁸ Not only was every modified nucleotide incorporated, but each base was functionalized with a different group, producing a versatile, fully functional DNA duplex. Significantly, it was also shown that modified ssDNA could serve as a template to incorporate modified bases during primer extension.³⁹⁻⁴¹ The key requirement in this enzymatic extension methodology is a polymerase that will incorporate a broad spectrum of modified bases. Initially Famulok *et al.* amplified only relatively short strands, i.e. 79 mer duplexes. Progress was then directed to using the fully functional DNA as a template for PCR. However, the modified DNA did not amplify to the same level in comparison to a system of natural DNA and natural dNTP's (30 % amplification). Although incorporation was achieved, it resulted in structural changes to the conformation of dsDNA when every base was replaced with non-canonical ones and the characteristic right-handed B-form shifted to the left-handed Z-form.³⁸

With the purpose of retaining the control of nanowire formation via the site-specific placement of modified nucleotides, the conversion of the nucleosides prepared in Chapter 3 into their triphosphate derivatives is introduced in the following sections. More specifically, the **tp** containing nucleosides, dT-5-**tp** and dC-5-**tp** were prepared for incorporation into DNA via triphosphate synthesis.

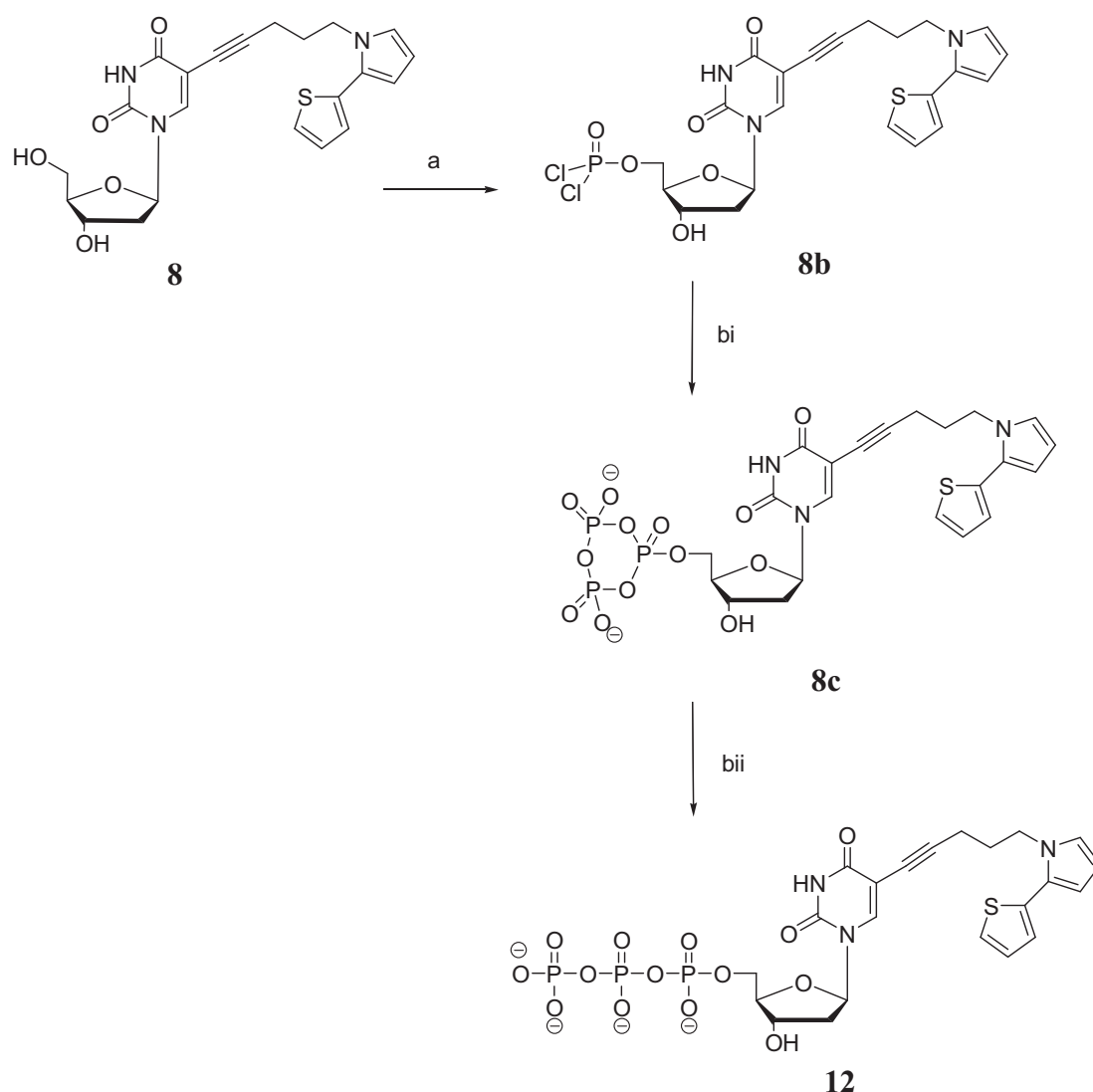
Section 4.3 describes the phosphorylation of the modified nucleoside dT-5-**tp**, its purification and analysis by anionic exchange MPLC and reversed-phase HPLC and section 4.4 discusses the phosphorylation, purification and isolation of dC-5-**tp**.

4.3 Results and Discussion

4.3.1 Design and synthesis of modified nucleotide dTTP-5-tp (dTTP*)

Conversion of dT-5-**tp** and dC-5-**tp** to their corresponding triphosphates was performed by employing the methods according to Ludwig⁴² and Yoshikawa.⁴³ The synthesis of dTTP-5-**tp** (dTTP*) was carried out using phosphorus(V) chemistry and dCTP-5-**tp** (dCTP*) using phosphorus(III) chemistry. The compounds have been characterized by ¹H NMR spectroscopy, ³¹P NMR spectroscopy, ES-MS and UV-vis spectroscopy.

The nucleoside precursor dT-**tp** was converted to its triphosphate (dTTP*) in a phosphorylation reaction using phosphorus(V) in three steps, see Scheme 3.



Scheme 3. Synthesis of dTTP*; a) dT-**tp**, P(OMe)₃, 1,8-bis(dimethylamino)naphthalene, POCl₃, bi) bis(tr-n-butylammonium)pyrophosphate, DMF, tributylamine, ii) TEAB.

In the phosphorylation reaction, the nucleoside is dissolved in trimethylphosphate PO(OMe)₃ with slight heating. Yoshikawa *et al.* discovered that trialkylphosphates accelerated the rate at which phosphorylation occurs whilst acting as a solvent.⁴³ When a component of the modified nucleoside is potentially susceptible to acid treatment from POCl₃, i.e. the alkyne linker, 1,8-bis(dimethylamino)naphthalene (proton sponge) should be used (Fig. 5). This also helps in accelerating the rate of reaction and also protects the alkyne linkage from any side reactions when using the strong acid, phosphoryl oxychloride. Protection is required as the reaction liberates

HCl. The alkyne group could undergo reduction to its alkene and produce unwanted side-products. Kovacs *et al.* made an attempt to neutralize the liberated HCl by adding a base but all the bases they tried, failed.⁴⁴ Therefore, due to its large size and high basicity, 1,8-bis(dimethylamino)naphthalene (Proton Sponge®) (pKa of 12.1 for its conjugate acid in aqueous solution), is the current preferred addition to the reaction as it will absorb protons from the solution, but is also sterically hindered so will not act as a nucleophile.⁴⁵

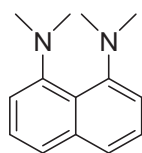


Figure 5. Chemical structure of Proton Sponge®.

Yoshikawa *et al.* initially hypothesized that adding H₂O to the reaction induced further HCl formation which increased selectivity for the phosphorylation of the primary hydroxyl group.⁴³ However, since that time it has been discovered that using a dry phosphoryl oxychloride in addition to employing the proton sponge to absorb any acid bi-products, maximized the selectivity. Therefore, the phosphoryl oxychloride must be freshly distilled before adding to the reaction to ensure it is free from water which could hinder the phosphorylation. It is added at 0 °C as the reaction is exothermic. After approximately 2 h 30 min, maximal formation of the intermediate, **8b**, was observed (Fig. 6 dTMP-**tp** at 31.3 min). The tri-n-butylammonium pyrophosphate buffer is then prepared in a separate flask and added immediately.

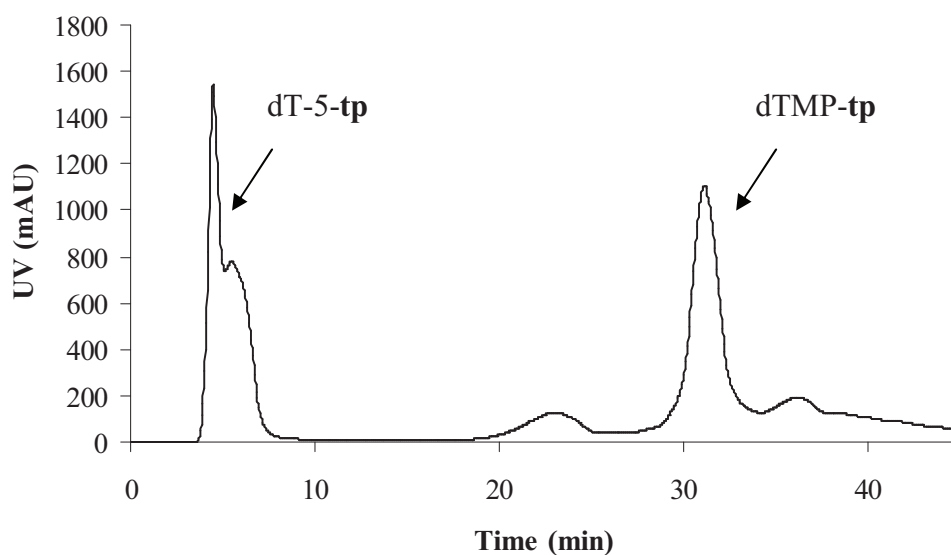


Figure 6. Chromatogram to illustrate MPLC analysis of the formation of dTMP-**tp** at 31.3 min.

This reaction is monitored for completion using anionic exchange MPLC. When the chromatogram shows that the ratio of triphosphate (**8c**) to monophosphate (**8b**) reaches approximately 3:1 (Fig. 6), the reaction is quenched with TEAB buffer which breaks the cyclic triphosphate into the linear triphosphate. This is a quick reaction and is usually complete within 1 h. The reaction mixture is then purified using anionic exchange MPLC (sepharose media) to remove the starting nucleoside and monophosphate on a basis of a difference in charge.

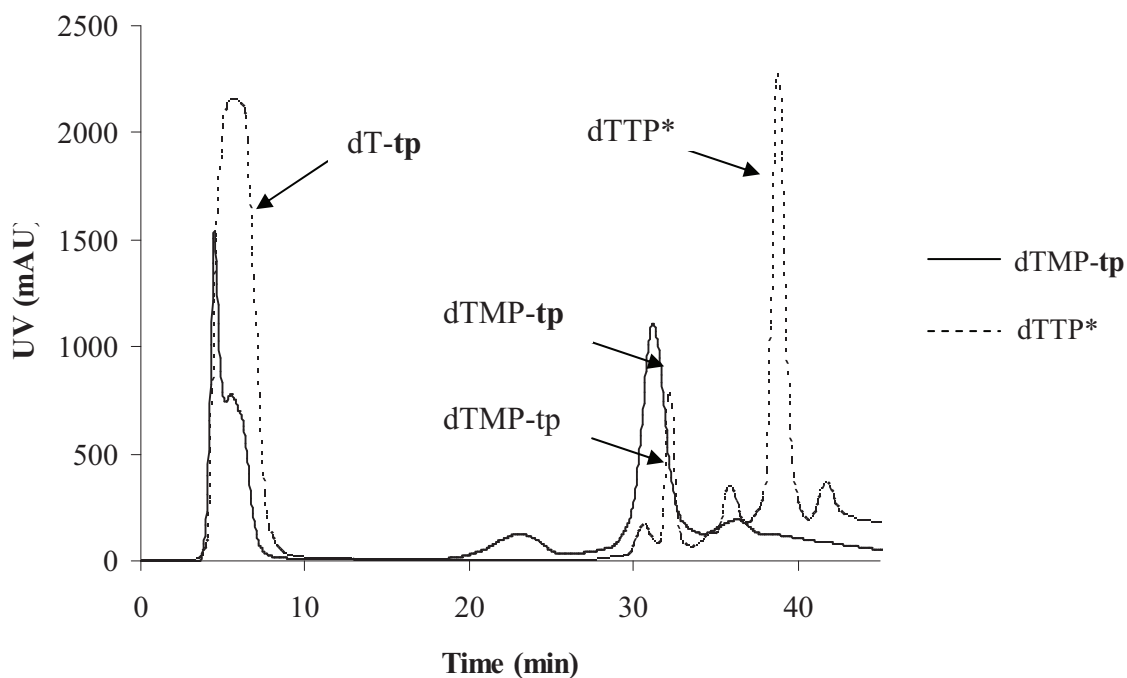


Figure 7. Chromatograph showing the comparison of dTMP-**tp** formation vs dTTP* formation.

The crude sample of the dTTP* synthesis contained a mixture of three components as seen by analysis via MPLC. The unreacted starting material, dT-**tp**, was eluted first since it carries no charge, between 4 and 9 min. The second product to be eluted is dTMP-**tp** at 31 min. Finally, dTTP* is the last to be eluted, at 39 min, since it carries three negative charges and so binds to the column more strongly. After separating the fractions, the solvent was removed by freeze-drying.

In comparison to the natural nucleotide, dTTP (Fig. 8), dTTP* is eluted after a longer retention time. The coupled 5-alkynyl-**tp** linker adds steric bulk to the nucleotide and so it migrates at a slower rate through the sepharose media.

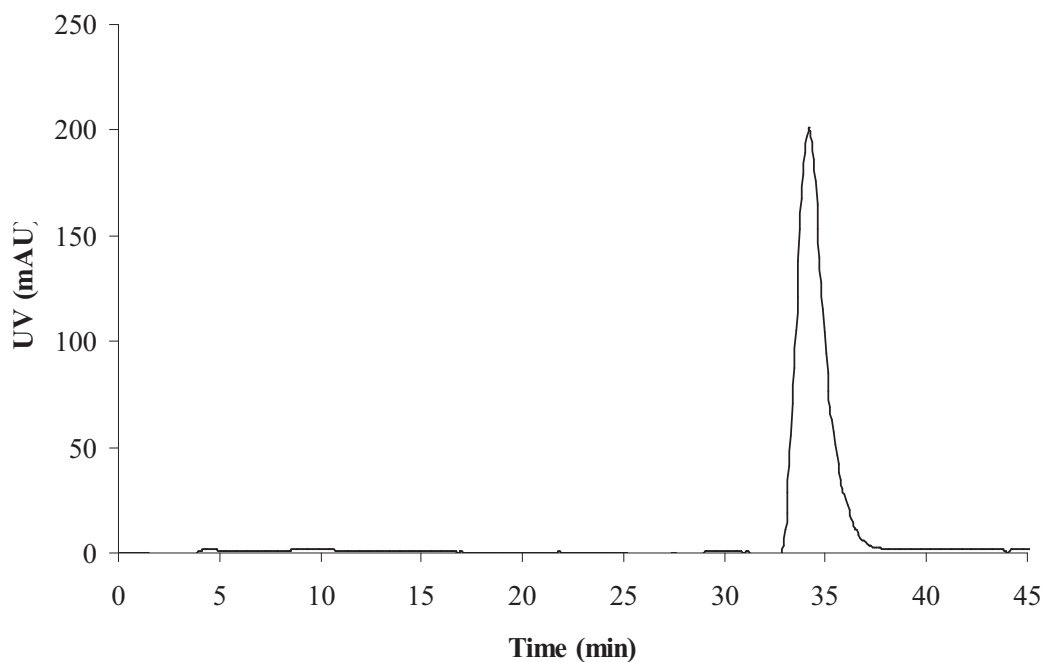


Figure 8. Chromatogram to illustrate MPLC analysis of standard dTTP at 34 min.

After isolating dTTP* via MPLC, ^{31}P NMR spectra revealed three peaks; $\delta = -5.57$ (d, 1P, γ -P), -10.27 (d, 1P, α -P), -19.62 (t, 1P, β -P) illustrating triphosphate formation. In addition to the three peaks, a singlet at -20.71 ppm was also observed. From the literature, it has been deduced that this peak signifies pyrophosphate formation (Fig. 9).⁴⁶ It has a similar charge to the triphosphate and so can overlap with dTTP* during the separation via MPLC, becoming indistinguishable.

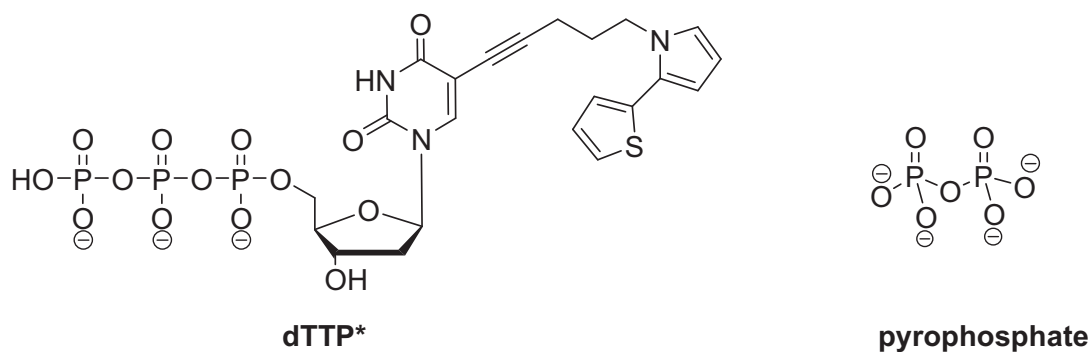


Figure 9. Chemical structures of dTTP* and the unwanted side-product, pyrophosphate to illustrate the similar charge on the compounds.

It was therefore necessary to remove the pyrophosphate and this was achieved by employing HPLC. Reversed-phase HPLC was performed using 0.1 M TEAA buffer (Solvent A) and acetonitrile (Solvent B) with a gradient of solvent B: 0 - 40 % over 50 min. dTTP* was eluted with a retention time of 31mins. As the column was reversed-phase, the pyrophosphate eluted first due to it being more polar in comparison to the dTTP (Fig. 10).

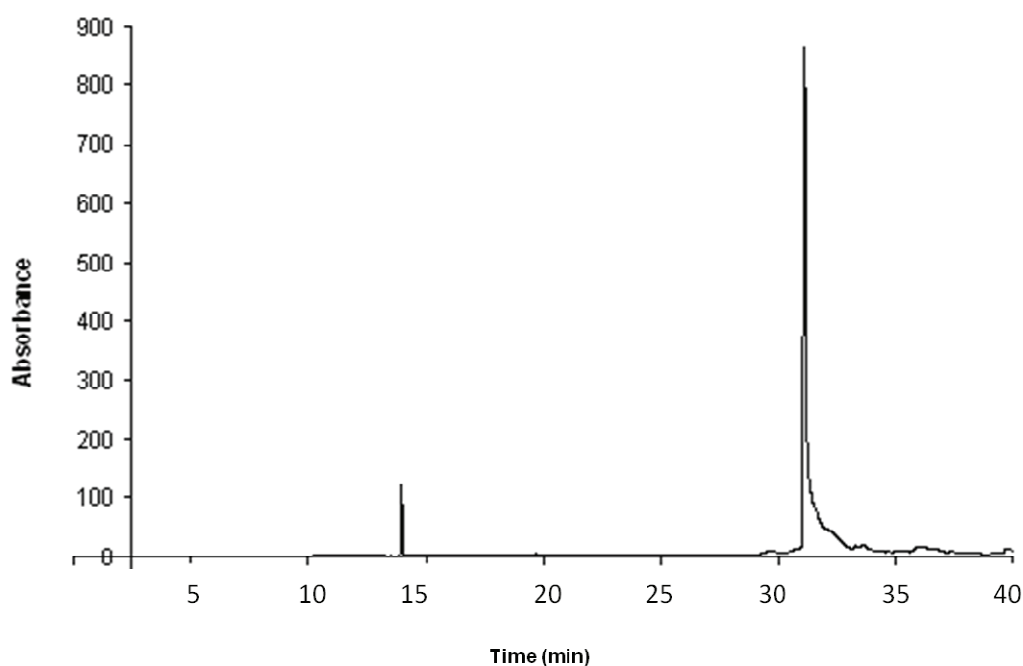


Figure 10. Chromatogram showing the purification of dTTP*, eluted at 31 min.

The ^{31}P NMR spectra now only showed the three desired peaks at; $\delta = -5.57$ (d, 1P, γ -P), -10.27 (d, 1P, α -P), -19.62 (t, 1P, β -P) confirming isolation of the pure triphosphate had been accomplished. Further confirmation was obtained by high resolution ES-MS which showed a molecular ion of mass $[\text{M-H}]^-$ 680.00 formed, calculated 680.02, UV-vis spectroscopy was used to study the electronic structure of the modified nucleoside **8** and nucleotide **12** (Fig. 11). Addition of the triphosphate moiety does not have any notable effect on the maximum absorption wavelength in comparison to its nucleoside other than further confirmation that isolation of the nucleotide was correct, the λ_{max} was 291 nm for dT-5-**tp** and 292 nm for dTTP*

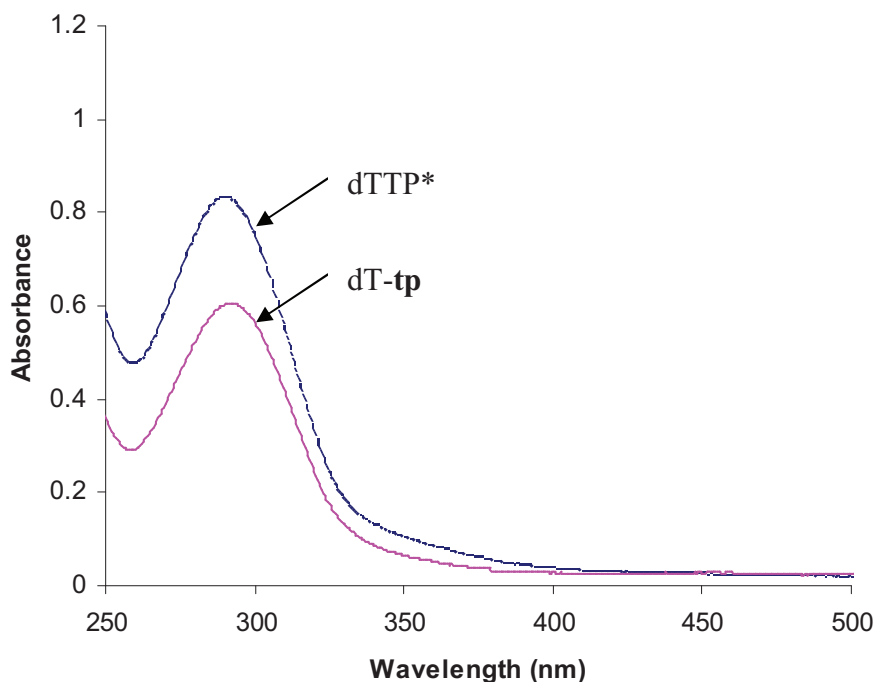


Figure 11. Comparison of the UV-vis spectra for compounds dT-tp and dTTP*.

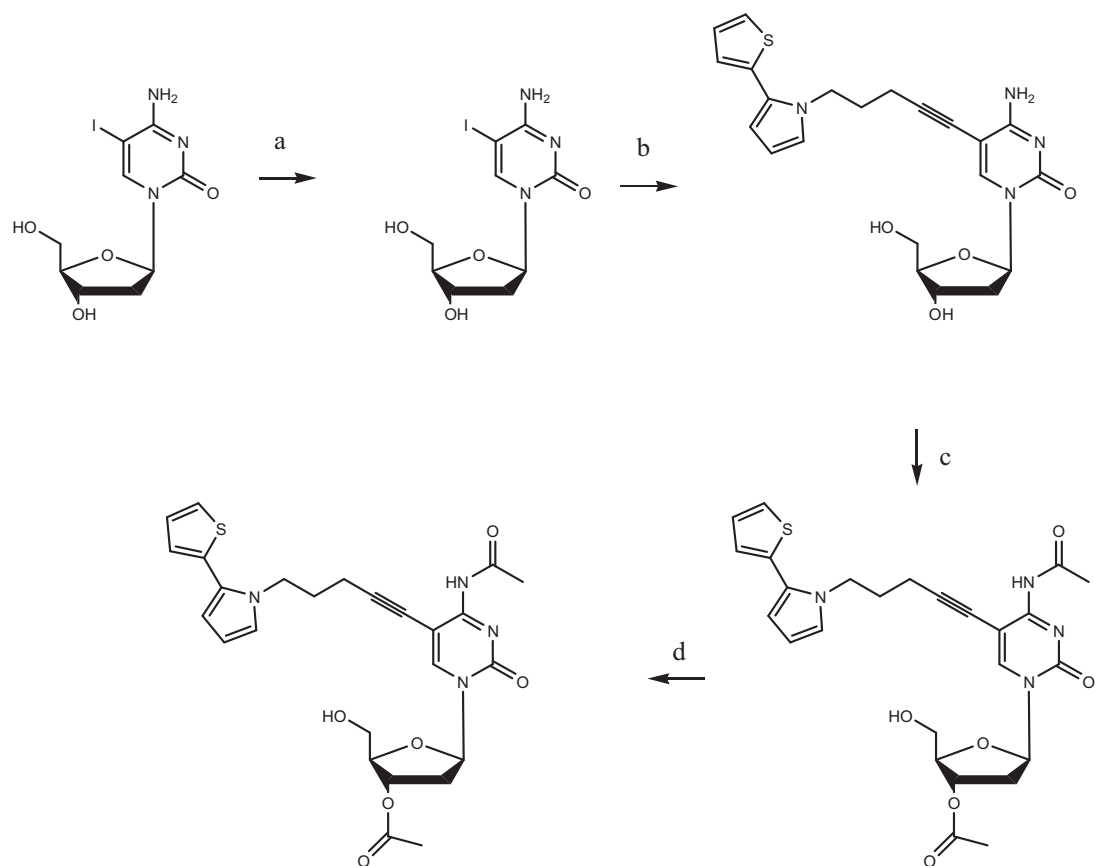
The above results clearly show that the modified triphosphate has been synthesized and isolated and so attention was then turned to whether dTTP* will be accepted by DNA polymerases to produce oligomers in Chapter 5.

4.3.2 Design and synthesis of modified nucleotide dCTP-5-tp (dCTP*)

In order to test more than a single modified nucleotide, dCTP* was also synthesized as dTTP* may prove problematic in enzymatic extension reactions due to the difference in the number of hydrogen bonds formed between complementary bases. The A-T base pair contains only two hydrogen bonds and could be deemed less stable, perhaps even more so in the case of a modified deoxythymidine. As a result, forming the DNA double strand to such desired lengths is less likely. However, if deoxycytidine was modified and subsequently accepted by the polymerases, when incorporating into a long strand of DNA through enzymatic extension, three hydrogen bonds are formed generating a stronger binding and more stable structure.

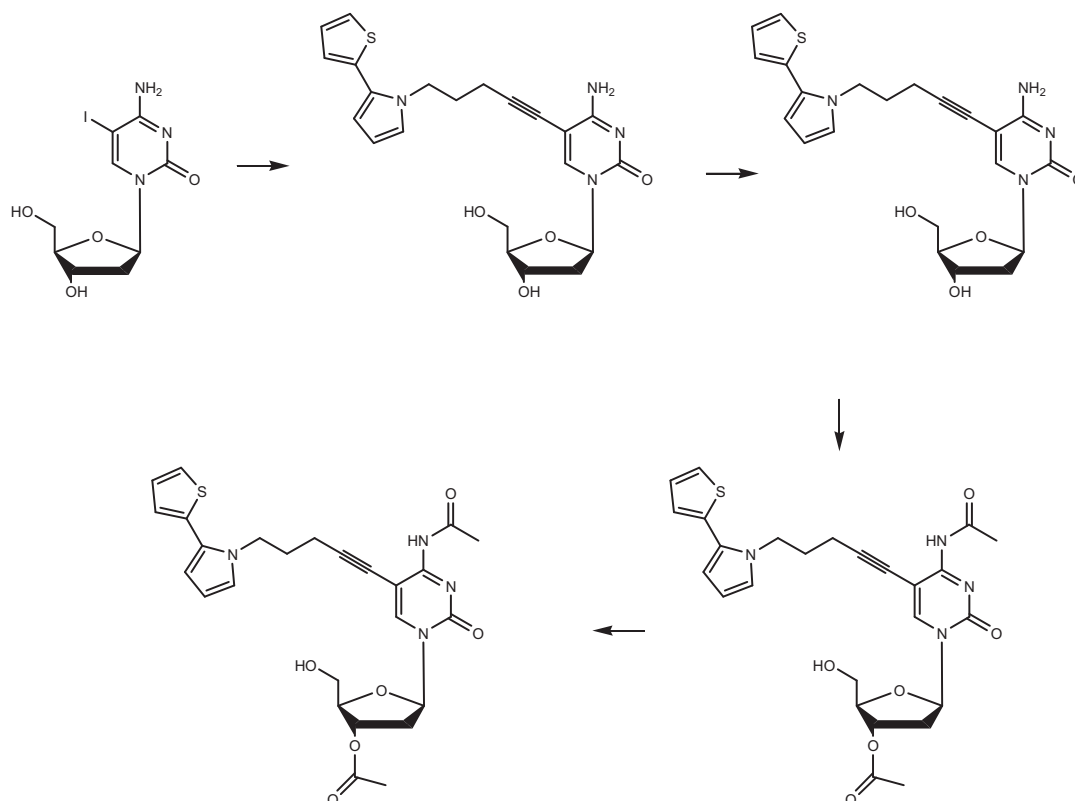
Although the conversion of the modified nucleoside (dT) into the triphosphate (dTTP*) was successful, the same synthetic method failed when attempting to convert dC-5-**tp** into dCTP*. Modifications to nucleosides can have a detrimental effect on the conversion to the triphosphate when employing phosphorus(V) chemistry. The reactions can be slow, inefficient or not react at all.⁴⁶ Nevertheless, another method can be exploited that is more forgiving. Employing salicyl chlorophosphate (phosphorus(III)) as a more potent phosphorylating agent is attractive; however it lacks the regioselectivity observed with phosphorus(V) leaving the 3'-OH and the exocyclic amine susceptible to attack, highlighting the earlier preference of thymidine due to ease of synthesis. Therefore, in the phosphorylation of deoxycytidine, both the exocyclic amino group and the 3'-OH require protection.

In order to simultaneously protect the NH₂ and the 3'-OH, the 5'-OH should be protected first. The 5'-OH is a primary hydroxyl group, hence a protecting group would regioselectively favour this hydroxyl due to the lack of steric hindrance. Therefore Scheme 4 and Scheme 6 below show two possible routes towards the synthesis of 3'-OH and amino protected deoxycytidine, prepared for the formation of the triphosphate.



Scheme 4. Scheme to illustrate a) the regioselective protection of 5'-OH with TBDMS-Cl (tert-butyldimethylsilyl chloride) followed by b) Sonogashira reaction at the C5 position, c) subsequent protection of exocyclic amine and 3'-OH and finally d) the deprotection of 5'-OH to leave the available site for triphosphate chemistry.

The above scheme is theoretically the ideal way to obtain the regioselective protection of the 3'-OH and the amino group, as the initial silyl ether can be removed using, for example, tetra-n-butylammonium fluoride, to ensure that the acetyl protecting groups remain intact. However, the regioselectivity proved to be problematic as both the 3'-OH and 5'-OH were protected simultaneously. Several attempts to optimize the reaction did not achieve the desired regioselectivity as ^1H NMR spectra indicated the disappearance of both OH peaks. On the other hand, in the second approach, the 5'-OH is protected by the acid labile DMT group before acylation of 3'-OH and exocyclic amine. During deprotection, usually by 2% TCA in DCM, it was noticed that the acyl groups were also susceptible to removal.



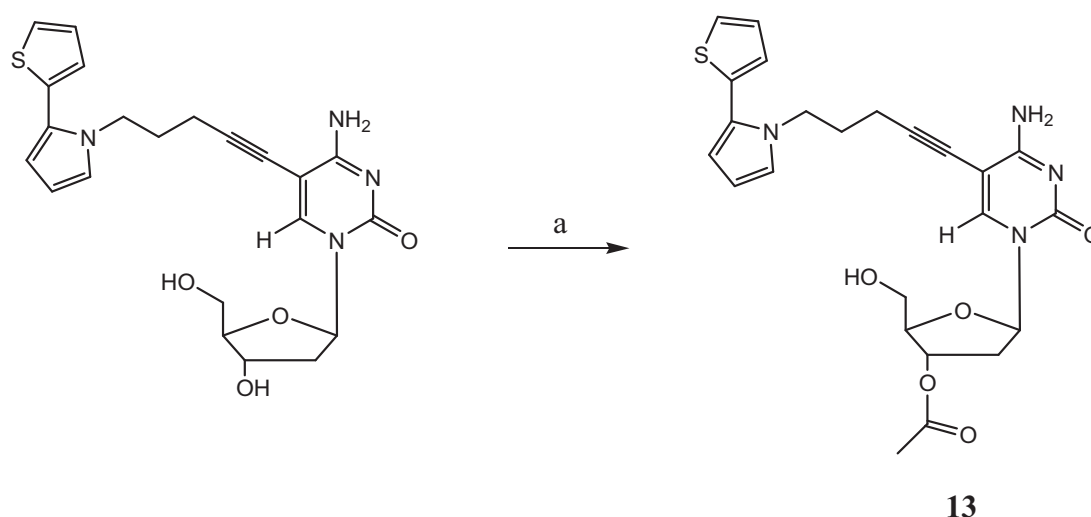
Scheme 5. The alternative initial protection of 5'-OH using DMT-Cl and the subsequent acyl protecting groups. The scheme illustrates a) Sonogashira reaction at the C5 position followed by b) the regioselective protection of 5'-OH with DMT-Cl (dimethyltrityl chloride), c) subsequent protection of exocyclic amine and 3'-OH and finally d) the deprotection of 5'-OH to leave the available site for triphosphate chemistry.

Both of the above routes produced very low yields. Therefore in order to avoid repeated protection/deprotection steps, enzymes were employed to regioselectively protect the 3'-OH group in one step.

Moris *et al.* have reported that the hydroxyl groups on nucleosides can be regioselectively monoacylated utilising a range of biocatalysts, namely lipase enzymes.⁴⁷⁻⁴⁹ Lipase enzymes can selectively modify primary or secondary hydroxyl groups due to variations in the structure of the enzyme. The regioselectivity and yields of the reactions are very dependent on the reaction conditions, for example solvent, time, temperature and even the molar ratio of reagents.

According to the literature, the most common biocatalyst of choice for selectively protecting the 3'-OH group is *Pseudomonas cepacia* lipase (PSL-C).⁵⁰ Employing low-polarity solvents such as 1,4-dioxane and THF are reported to give the optimum

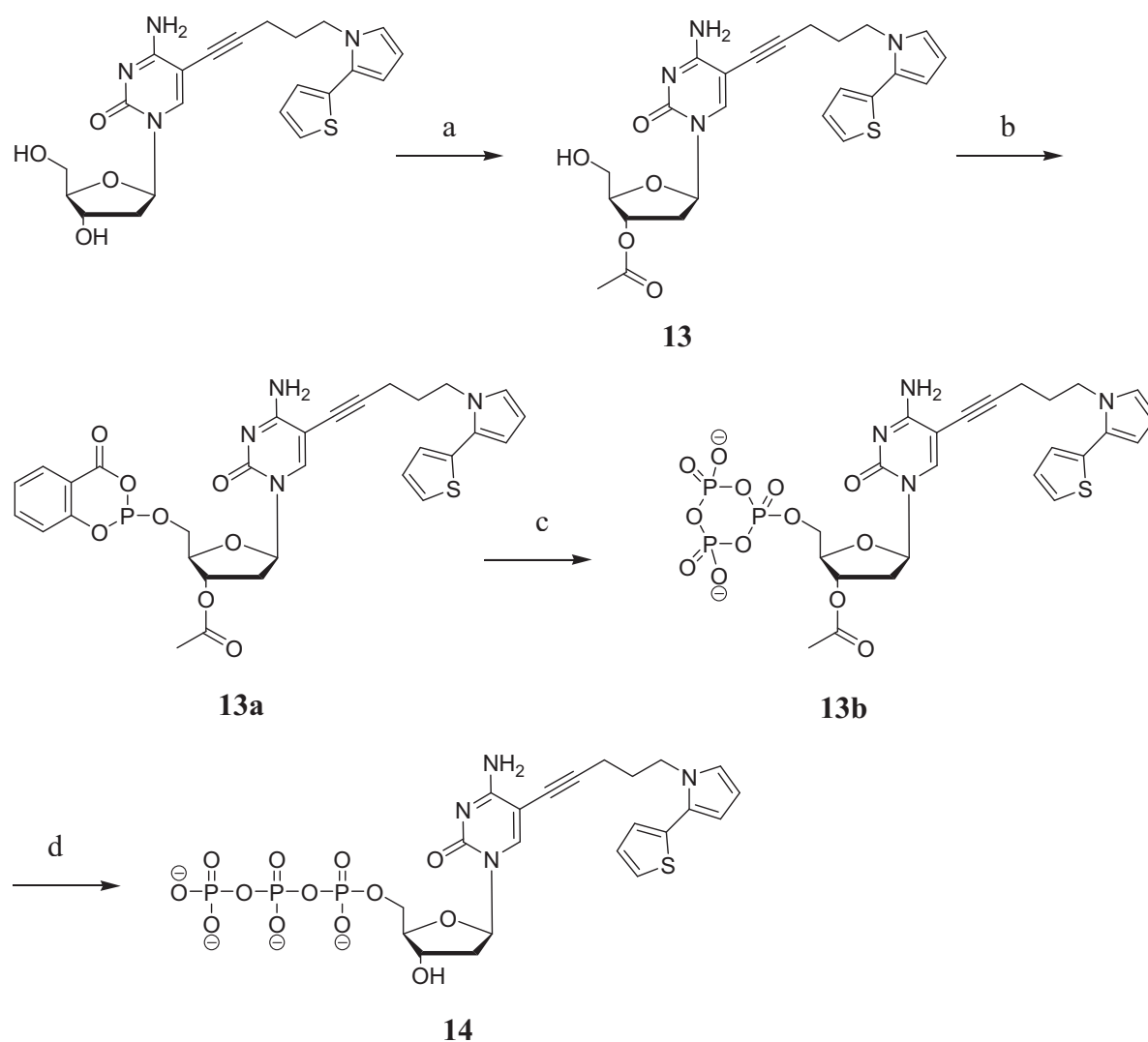
yields and regioselectivity. However, when using 1,4-dioxane as the reaction media for dC-**tp**, the reaction failed to start. When THF was utilized, the reaction yielded the 3'-OH protected dC-**tp** in approximately 28% yield (Scheme 6). Anhydrous solvents were necessary as water can often compete with the acyl donors to produce the hydrolysed product. On the contrary, reports have shown that water can generate conformational mobility of the enzyme, allowing for the optimal conformation by acting as a lubricant for the enzyme to reposition and hence improving its activity.⁵¹ However, in this case, an organic solvent is required due to the increased hydrophobicity of the modification 5-**tp** upon the pyrimidine.



Scheme 6. Regioselective 3'-OH protection of dC-**tp**. a) THF, vinyl acetate, PCL Amano.

Two enzymes were employed for the acylation reaction, Porcine pancreas lipase and *Pseudomonas cepacia* Amano lipase (PCL Amano). However, only the latter drove the reaction forward which could be due to the structure of the enzyme and how it binds modified deoxycytidine in its active site. From the literature PSC-L Amano is known to protect the more sterically hindered 3'-OH position of any nucleoside.⁵⁰ The crystal structure shows that there are three binding sites within the active site known as 'pockets'. These pockets consist of amino acids that can selectively hydrogen bond to various substituents of the nucleoside if they have the correct orientation. The large hydrophobic pocket is the site where the acyl chain can be orientated in the correct position for nucleophilic attack by the nucleoside. The medium sized pocket is where

the nucleophilic 3'-OH group is placed. The alternate hydrophobic pocket binds parts of the nucleophile.⁵² Altogether, these pockets hold the nucleoside in a specific orientation so only certain conformations are fully hydrogen bonded in the enzymes active site.



Scheme 7. Scheme to illustrate the reaction of a 3'-O-Ac protected nucleoside utilising phosphorus(III) chemistry followed by triphosphate formation; a) acylation of 3'-OH using vinyl acetate, followed by triphosphate synthesis b) salicyl chlorophosphate, 1,4-dioxane, pyridine, c) bis(tri-n-butylammonium)pyrophosphate, DMF, tributylamine, d) 1 % iodine solution in pyridine/water, 5 % NaHSO₃, NH₄OH.

Once the 3'-OH had been protected, the triphosphate conversion could be performed via the phosphorus(III) route (Scheme 7). The resulting acetyl protected 3'-OH is stable to the reaction conditions and is only removed with the treatment of ammonia. The conversion was monitored by MPLC in order to analyse and purify dCTP* from

its monophosphate and starting precursor **dC-tp**. The setup for MPLC was the identical to the **dTTP*** synthesis.

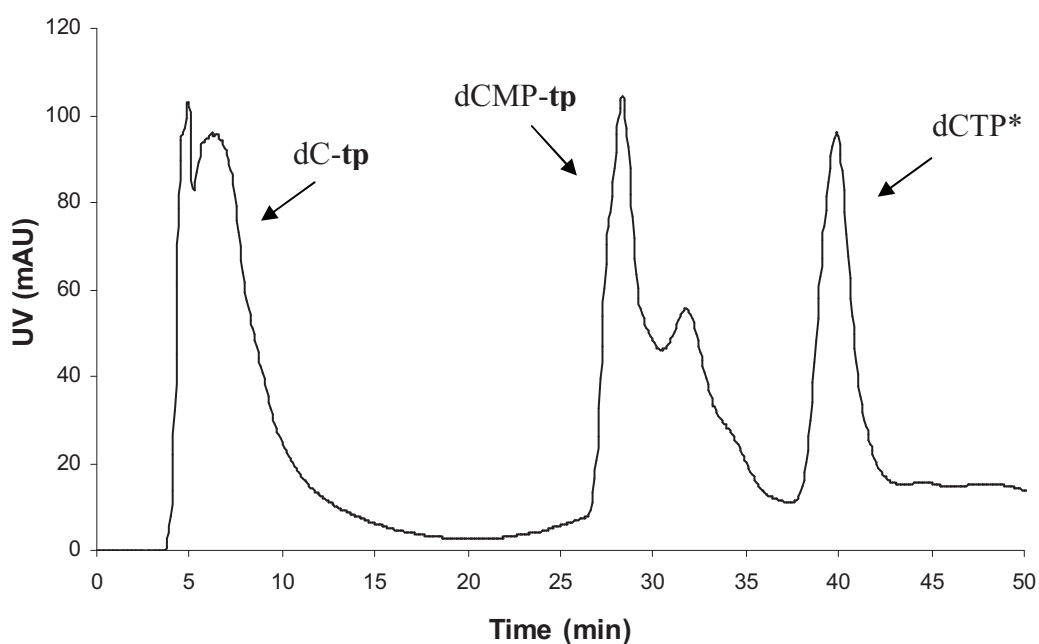


Figure 12. Chromatogram to illustrate the formation of **dCTP*** at 40 min.

MPLC analysis illustrated that the starting material **dC-tp** was the first product to be eluted between 4 and 10 min since there is minimal binding to the charged column (Fig. 12) and the monophosphate (**dCMP-tp**) was eluted at 28 min. The monophosphate binds more strongly to the charged column so a more salt concentrated basic buffer is required to compete with the charge to elute it. **dCTP*** had a retention time of 40 min as the triphosphate has three negative charges associated. It will bind to the column tightly and therefore a highly salt concentrated basic solvent will enforce the elution.

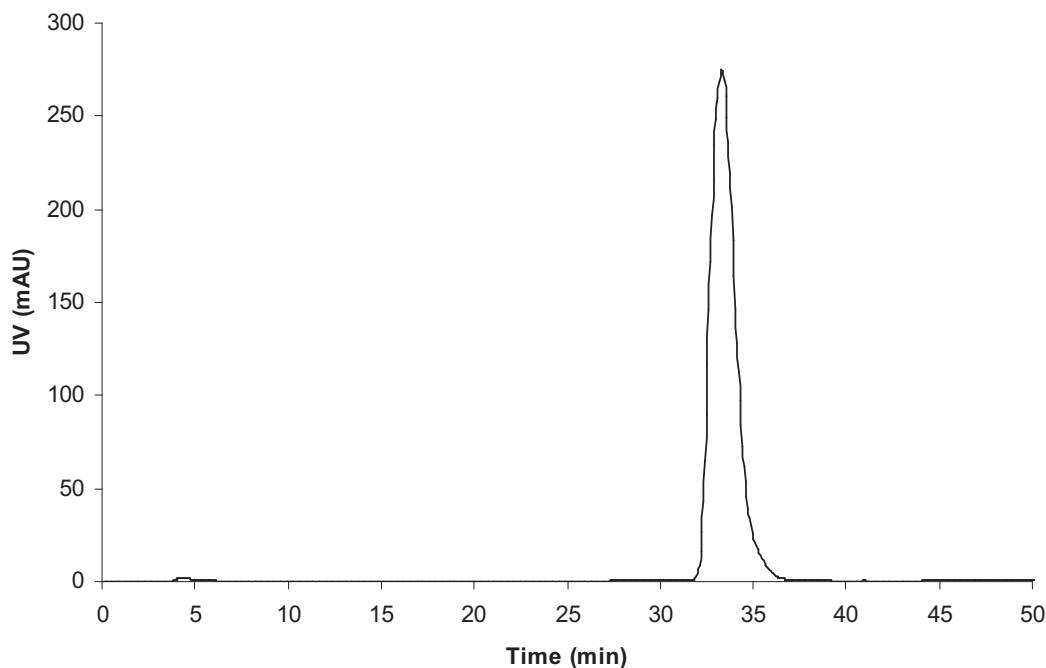


Figure 13. Chromatogram to illustrate the retention time of standard dCTP at 33 min.

In comparison with a commercially available dCTP (Fig 13), dCTP* is eluted at a similar retention time. dCTP is eluted at 33 min in comparison to dCTP* which is eluted at a slightly later retention time due to the increased size of the molecule. The linkage of the 5-**tp** on dCTP* increases the steric bulk of the molecule. The purification is performed using Sepharose© as the column media, a cross linked polysaccharide that implements slower migration for bigger molecules.

In order to purify dCTP* from any similarly charged compounds, for example excess pyrophosphate as in the case for dTTP*, reversed-phase HPLC was employed using TEAA buffer, 0.1 M (Solvent A) and acetonitrile (Solvent B). dCTP* was eluted at a retention time of 38 min in a gradient of solvent B 0-40% over 50 min.

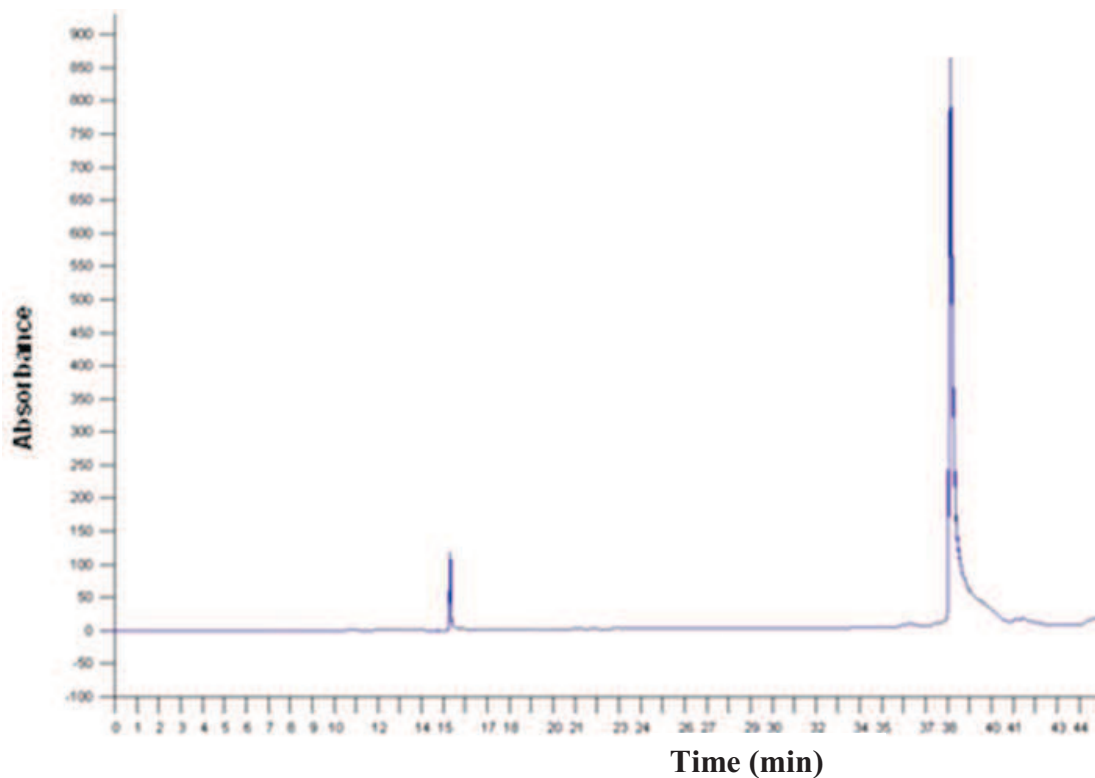


Figure 14. Chromatogram showing the purification of dCTP*, eluted at 38 min.

The ^{31}P NMR spectra revealed two broad peaks at $\delta = -10.11$ ppm and -22.34 ppm. Due to the low overall yield obtained from this chemistry, the NMR signal-to-noise ratio was considerably lower than desired and the resonances were not as clear. However, it can be concluded from the peak integration that the α - and γ - phosphorus resonances are coincident on each other due to their similar environments.

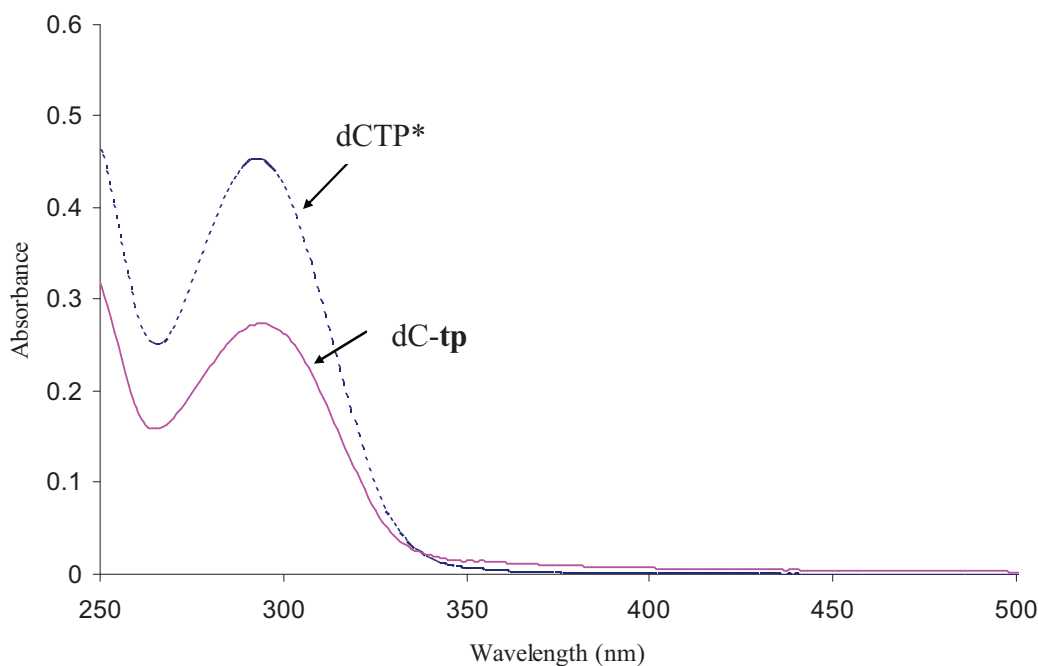


Figure 14. Graph to compare the absorbance of dC-**tp** versus dCTP* to subsequently determine the concentration of dCTP*.

UV-Vis spectroscopy was performed to study the electronic structure of the modified nucleotide dCTP* (Fig. 14). Addition of the triphosphate moiety does not have any notable effect on the maximum absorption wavelength in comparison to its nucleoside other than further confirmation that isolation of the nucleotide was correct, the λ_{max} was 294 nm for dC-5-**tp** and 292 nm for dCTP*

4.4 Conclusions

In summary, dTTP* and dCTP* were synthesized according to phosphorus(V) and phosphorus(III) chemistry respectively. dT-5-**tp** reacted with phosphorus(V) in standard Yoshikawa phosphorylation. dC-5-**tp** was less reactive towards phosphorus(V) and so the less regioselective phosphorus(III) was employed. This synthesis required protection of the 3'-OH of the sugar with an acetyl group which was facilitated by employing PCL Amano lipase. Once the triphosphate synthesis had been optimized, the modified triphosphates were purified and characterized by

MPLC, HPLC, ^1H NMR spectroscopy, ^{31}P NMR spectroscopy, high-resolution ES-MS and UV-vis spectroscopy. The next logical step was to investigate how dTTP* and dCTP* are accepted by DNA polymerases and with what fidelity.

4.5 Experimental

Reagents were purchased from Sigma-Aldrich and used as received unless otherwise stated. POCl₃ was freshly distilled prior to use. DMF was degassed with N₂ for 30 min before use. All reactions were performed under argon. MPLC was performed on a GE Healthcare AKTA Primer Plus. Analysis and purification runs were performed on a HiTrap Q Sepharose column. HPLC was performed on a Varian Pro Star system. Analytical runs were performed on a HiChrom ODS 5 μ column with an injection loop of 100 μL. The column was incubated at 25 °C. ¹H NMR spectra were performed on a 300 MHz Bruker Spectrospin WM 300 WB spectrometer, ³¹P NMR spectra were performed on a JEOL 400 MHz spectrometer. Electronic absorption spectra were recorded on a Hitachi U-3010 Spectrophotometer. Mass spectra were measured on a Waters Micromass LCT Premier mass spectrometer. For band-density analysis of gel images, 'Image Quant' software (GE Healthcare) was employed.

Preparation of dTTP* (12)

dT-5-**tp** (0.2 mmol, 80 mg) and proton sponge (55 mg) was dried overnight in the presence of phosphorus pentoxide in a vacuum oven. The oven was opened to a balloon filled with argon to keep the nucleoside under an argon atmosphere. A gas tight syringe was washed with anhydrous DMF and trimethylphosphate before drawing with trimethylphosphate (0.5 mL) and ejecting into the dT-5-**tp** containing flask. The proton sponge was immediately added and the mixture required a little heating to dissolve. The flask was then inserted into an ice bath and stirred for 10 min. Freshly distilled, dry phosphoryl chloride (0.24 mmol, 23 μL) was then injected via a gas tight syringe and allowed to stir for 3 h. After 30 min then every subsequent hour, an aliquot (10 μL) was taken, quenched with TEAB (0.1M) (100 μL) followed by a few drops of DMF to aid solubility, and then analysed by MPLC for phosphorylation completion. Upon maximal monophosphate formation, a dry 10 mL pear-shaped flask was filled with argon and stoppered. To this, bis(tri-n-butylammonium pyrophosphate) (0.5 M, 1.2 mL), DMF (2 mL) and tri-n-butylamine (1.2 mmol, 290 μL) were added. This was mixed for approximately 30 s and then added in one portion to the monophosphate mixture. MPLC analysis was again performed on

aliquots from the reaction. After 1 h the reaction was complete. The reaction was then quenched with TEAB (0.1 M, 20 mL) and left to stir for 1 h. This solution was then extracted with diethyl ether (3 x 15 ml), diluted with water and then purified by MPLC and subsequently HPLC to leave a yellow oil/solid. ^{31}P NMR (D_2O): $\delta = -5.20$ (d, 1P, $\gamma\text{-P}$), -10.01 (d, 1P, $\alpha\text{-P}$), -19.10 (t, 1P, $\beta\text{-P}$). (ESI): m/z: calculated for: $\text{C}_{22}\text{H}_{26}\text{N}_3\text{O}_{14}\text{SP}_3$ $[\text{M-H}]^-$: 680.0200 found: 680.0000.

5'-OH protection of dC-tp with TBDMS-Cl

A flask was charged with DMF (15 mL) and dC-5-**tp** (0.6 mmol, 1 equiv) was added. To this solution was added imidazole (0.8 mmol, 1.3 equiv) and anhydrous TBDMS-Cl (0.8 mmol, 1.3 equiv). The mixture was stirred at room temperature for 16h. A solution of ethanol: water (1:1) (50 mL) was added to the mixture and a precipitate formed. This was filtered and washed again with the ethanol: water solution (1:1) (20 mL). This was filtered again and washed with diethyl ether (2 x 10 mL). The residue was dried under vacuum.

^1H NMR ($\text{dms}\text{-d}_6$): $\delta = 0.08$ (d, 6H; CH_3), 0.11 (d, 6H, CH_3), 0.87 (d, 9H; CH_3), 0.90 (d, 9H; CH_3), 2.10 (m, 2H, C_2H), 3.73 (d, 1H; C_5H), 3.77 (d, 1H; C_5H), 3.84 (dd, 1H; C_4H), 4.33 (q, 1H, C_3H) 6.08 (t, 1H; C_1H) 6.67 (s, 1H; NH), 7.88 (s, 1H; NH'), 7.90 (s, 1H; C_6H). Yield: 26%. (ESI): m/z: calculated for: $\text{C}_{21}\text{H}_{40}\text{N}_3\text{O}_4\text{Si}_2\text{I}$ $[\text{M}+\text{Na}]^+$: 604.1500 found: 604.1526.

5'-OH protection of dC-tp with DMT-Cl

A flask was charged with pyridine (10 mL) and dC-5-**tp** (0.23 mmol, 1 equiv) was added. To this solution was added DMAP (0.07 mmol, 0.3 equiv), DMT-Cl (0.53 mmol, 2.3 equiv) and anhydrous degassed triethylamine (0.53 mmol, 2.3 equiv). The mixture was stirred at room temperature for 16h. Sodium bicarbonate 5% (v/w) (5mL) was added to the resulting mixture before evaporation to dryness. The crude product was redissolved in dichloromethane (150 mL) and washed twice with sodium bicarbonate 5% (v/w) (50 mL) and once with water (50 mL) before being dried over magnesium sulfate. After filtration and concentration by rotary evaporation the

reaction mixture was loaded onto a silica gel column packed with dichloromethane and triethylamine (99:1) and eluted by using dichloromethane, methanol and triethylamine (95:4:1). Fractions containing the product were combined and solvent removed to yield the following compounds;

^1H NMR (dms o - d_6): δ = 1.68 (m, 2H; CH_2), 2.13 (m, 2H; C_2H), 2.14 (t, 2H; CH_2), 2.84 (m, 1H; C_3H), 2.85 (m, 2H; C_5H), 3.70 (s, 6H; CH_3), 3.95 (t, 3H; CH_2), 4.26 (m, 1H; CH), 5.32 (d, 1H; C_3OH), 6.06 (t, 1H; C_1H), 6.13 (t, 1H; CH_{ip}), 6.21 (dd, 1H; CH_{ip}), 6.83 (s, 1H; NH'), 6.84 (q, 8H; CH), 7.02 (d, 1H; CH_{ip}), 7.03 (dd, 1H; CH_{ip}), 7.14 (t, 1H; CH_{ip}), 7.25 (dd, 5H; CH), 7.45 (d, 2H; CH_{ip}), 7.71 (s, 1H; NH''), 7.88 (s, 1H; C_6H). Yield: 32%. (ESI): m/z: calc for: $\text{C}_{43}\text{H}_{42}\text{N}_4\text{O}_6\text{S}$ $[\text{M}+\text{Na}]^+$: 765.2921 found: 765.2723.

3-OH protection of dC-tp using Amano lipase (13)

To a flask containing dC-5-tp (307 mg, 0.70 mmol) was added anhydrous THF (10 mL) and vinyl acetate (0.26 mL, 2.80 mmol) under N_2 . This was allowed to stir for 1h. To this solution was added lipase Amano (440 mg) and this solution was stirred for 48 h under N_2 at 55 °C. The mixture was then filtered to remove the enzyme and washed with MeOH. After concentration *in vacuo*, the product was loaded onto a silica gel column chromatography packed with DCM and eluted using an increasing gradient of MeOH (0-20 %). Yield = 25.7 %. (ESI): m/z: calc for: $\text{C}_{24}\text{H}_{27}\text{N}_4\text{O}_5\text{S}$ $[\text{M}+\text{H}]^+$: 483.1702 found: 483.1704.

^1H NMR (dms o - d_6): δ = 1.85 (m, 2H, CH_2), 2.06 (s, 3H, CH_3), 2.1-2.3 (m, 2H, C_2H), 2.35 (t, 2H, CH_2 , J=7.0 Hz), 3.62 (dd, 2H, C_5H , J = 3.7, 4.4 Hz), 4.01 (m, 1H, C_3H), 5.19(m, 1H, C_4H) 5.23 (t, 1H, $\text{C}_5\text{-OH}$), 6.08 (dd, 1H, CH_{ip} , J=2.8, 3.5 Hz), 6.16 (dd, 1H, C_1H , J=5.7, 8.4 Hz), 6.21 (dd, 1H, CH_{ip} , J = 1.8, 3.6 Hz), 6.86 (s, 1H, NH), 6.94 (dd, 1H, CH_{ip} , J = 1.9, 2.6 Hz), 7.06 (dd, 1H, CH_{ip} , J = 3.6, 5.1 Hz), 7.13 (dd, 1H, CH_{ip} , J = 1.1, 3.6), 7.47 (dd, 1H, CH_{ip} , J = 1.1, 5.1 Hz), 7.75 (s, 1H, NH), 8.07 (s, 1H, C_6H). Yield: 26 % (ESI): m/z: calc for: $\text{C}_{24}\text{H}_{26}\text{N}_4\text{O}_5\text{S}$ $[\text{M}]^+$: 483.1702 found: 483.1707.

Preparation of dCTP* (14)

dC-5-**tp**-3'-OAc (89 mg, 0.18 mmol) was co-evaporated with anhydrous pyridine (3 x 5 ml) and left in the vacuum oven overnight in the presence of phosphorus pentoxide. A 1 M solution of 2-chloro-4H-1,2,3-dioxaphosphorin-4-one in anhydrous 1,4-dioxane was prepared and left standing overnight over molecular sieves. The next day dC-tp-3'-O-Ac was dissolved in anhydrous pyridine (600 μ L) and anhydrous 1,4-dioxane (200 μ L). 2-Chloro-4H-1,2,3-dioxaphosphorin-4-one (220 μ L) was added to the vigorously stirring reaction flask. After 45 min, a flask containing 0.5 M bis(tri-n-butylammonium)pyrophosphate in DMF (0.6 mL, 0.3 mmol) and dry tributylamine (145 μ L, 0.6 mmol) was vortexed for approximately 30 s and added immediately to the reaction mixture. After 30 min, a 1 % iodine solution (w/v) in pyridine and water (1:1 v/v) (2 mL) was added. After stirring for 20 min, three drops of 5 % NaHSO₃ (w/v) was added and subsequently evaporated to dryness. Water (10 mL) was then added and left stirring for approximately 30 min. NH₄OH (20 mL) was then added and left to stir for 2 h before evaporating to dryness. Yield = 10.5 mg, 8.6 %. ³¹P NMR (D₂O): δ = -10.11 ppm (broad peak, 2P, γ -P, α -P), -22.34 ppm (broad peak, 1P, β -P). (ESI): m/z: calcd for: C₂₂H₂₆N₄O₁₃SP₃ [M-H]⁻ : 679.0430 found: 679.0425.

References

- (1) Munzel, M.; Globisch, D.; Trindler, C.; Carell, T. *Org. Lett.* **2010**, *12*, 5671.
- (2) Wanninger-Weiß, C.; Wagenknecht, H. A. *Eur. J. Org. Chem.* **2008**, *2008*, 64.
- (3) Zhang, S.; Chaput, J. C. *Curr. Protoc. Nucleic Acid Chem.* **2010**, *Chapter 4*, Unit4.40.
- (4) Seela, F.; Feiling, E.; Gross, J.; Hillenkamp, F.; Ramzaeva, N.; Rosemeyer, H.; Zulauf, M. *J. Biotechnol.* **2001**, *86*, 269.
- (5) Burgess, K.; Cook, D. *Chem. Rev.* **2000**, *100*, 2047.
- (6) Gierlich, J.; Gutmiedl, K.; Gramlich, P.; Schmidt, A.; Burley, G.; Carell, T. *Chem.Eur. J.* **2007**, *13*, 9486.
- (7) Borsenberger, V.; Kukwikila, M.; Howorka, S. *Org. Biomol. Chem.* **2009**, *7*, 3826.
- (8) Pike, A. R.; Patole, S. N.; Murray, N. C.; Ilyas, T.; Connolly, B. A.; Horrocks, B. R.; Houlton, A. *Adv. Mater.* **2003**, *15*, 254.
- (9) Pike, A. R.; Ryder, L. C.; Horrocks, B. R.; Clegg, W.; Connolly, B. A.; Houlton, A. *Chem. Eur. J.* **2005**, *11*, 344.
- (10) Blackburn, G. M.; Gait, M. J.; Loakes, D.; Williams, D. M. *Nucleic acids in chemistry and biology*; 3rd Revised edition ed.; Royal Society of Chemistry, 2005.
- (11) Bandy, T. J.; Brewer, A.; Burns, J. R.; Marth, G.; Nguyen, T.; Stulz, E. *Chem. Soc. Rev.* **2011**, *40*, 138.
- (12) Datta, B.; Schuster, G. B. *J. Am. Chem. Soc.* **2008**, *130*, 2965.
- (13) Srinivasan, S.; Schuster, G. B. *Org. Lett.* **2008**, *10*, 3657.
- (14) Chen, W.; Guler, G. z.; Kuruvilla, E.; Schuster, G. B.; Chiu, H.-C.; Riedo, E. *Macromolecules* **2010**, *43*, 4032.
- (15) Michelson, A. M.; Todd, A. R. *J. Chem. Soc.* **1949**, 2487.
- (16) Borsenberger, V.; Howorka, S. *Nucl. Acids Res.* **2009**, *37*, 1477.
- (17) Hocek, M.; Vrabel, M.; Cahova, H.; Riedl, J.; Kalachova, L.; Pivonkova, H.; Horakova, P.; Havran, L.; Fojta, M. *Nucl. Acids Symp. Ser.* **2008**, *52*, 53.
- (18) Holzberger, B.; Marx, A. *Bioorgan. Med. Chem.* **2009**, *17*, 3653.
- (19) Jan, R.; Petra, H.; Peter, S.; Radek, P.; Lud; ecaron; k, H.; Miroslav, F.; Michal, H. *Eur. J. Org. Chem.* **2009**, *2009*, 3519.
- (20) Obeid, S.; Baccaro, A.; Welte, W.; Diederichs, K.; Marx, A. *Proc. Natl. Acad. Sci. U. S. A.* **2010**, *107*, 21327.
- (21) Weisbrod, S. H.; Marx, A. *Chem. Commun.* **2008**, 5675.
- (22) Pujari, S. S.; Xiong, H.; Seela, F. *J. Org. Chem.* *75*, 8693.
- (23) Ma, Q. F.; Bathurst, I. C.; Barr, P. J.; Kenyon, G. L. *J. Med. Chem.* **1992**, *35*, 1938.
- (24) Goody, R. S.; Isakov, M. *Tetrahedron Lett.* **1986**, *27*, 3599.
- (25) Eckstein, F. *Annu. Rev. Biochem.* **1985**, *54*, 367.
- (26) Meggers, E.; Zhang, L. *Acc. Chem. Res.* **2010**, *43*, 1092.
- (27) Eckstein, F. *Biochimie* **2002**, *84*, 841.
- (28) Langer, P. R.; Waldrop, A. A.; Ward, D. C. *Proc. Natl. Acad. Sci. U. S. A. - Biol. Sci.* **1981**, *78*, 6633.
- (29) Zhao, G.; Guan, Y. *Acta Biochim. Pol.* **2010**, *42*, 722.
- (30) Gramlich, P. M. E.; Wirges, C. T.; Gierlich, J.; Carell, T. *Org. Lett.* **2007**, *10*, 249.
- (31) Gierlich, J.; Burley, G. A.; Gramlich, P. M. E.; Hammond, D. M.; Carell, T. *Org. Lett.* **2006**, *8*, 3639.

- (32) Burley, G. A.; Gierlich, J.; Mofid, M. R.; Nir, H.; Tal, S.; Eichen, Y.; Carell, T. *J. Am. Chem. Soc.* **2006**, *128*, 1398.
- (33) Gutmiedl, K.; Wirges, C. T.; Ehmke, V.; Carell, T. *Org. Lett.* **2009**, *11*, 2405.
- (34) Gramlich, P.; Warncke, S.; Gierlich, J.; Carell, T. *Angew. Chem., Int. Ed.* **2008**, *47*, 3442.
- (35) Wirges, C. T.; Timper, J.; Fischler, M.; Sologubenko, A. S.; Mayer, J.; Simon, U.; Carell, T. *Angew. Chem., Int. Ed.* **2009**, *48*, 219.
- (36) Fischler, M.; Simon, U.; Nir, H.; Eichen, Y.; Burley, G.; Gierlich, J.; Gramlich, P. M.; Carell, T. *Small* **2007**, *3*, 1049.
- (37) Gramlich, P. M. E.; Wirges, C. T.; Manetto, A.; Carell, T. *Angew. Chem., Int. Ed.* **2008**, *47*, 8350.
- (38) Jager, S.; Rasched, G.; Kornreich-Leshem, H.; Engeser, M.; Thum, O.; Famulok, M. *J. Am. Chem. Soc.* **2005**, *127*, 15071.
- (39) Thum, O.; Jäger, S.; Famulok, M. *Angew. Chem. Int. Ed.* **2001**, *40*, 3990.
- (40) Jager, S.; Rasched, G.; Kornreich-Leshem, H.; Engeser, M.; Thum, O.; Famulok, M. *J. Am. Chem. Soc.* **2005**, *127*, 15071.
- (41) Jäger, S.; Famulok, M. *Angew. Chem., Int. Ed.* **2004**, *43*, 3337.
- (42) Ludwig, J.; Eckstein, F. *J. Org. Chem* **1989**, *54*, 631.
- (43) Yoshikawa, M.; Kato, T.; Takenishi, T. *Tetrahedron Lett.* **1967**, *8*, 5065.
- (44) Kovács, T.; Ötvös, L. *Tetrahedron Lett.* **1988**, *29*, 4525.
- (45) Cohen, S. D.; Mijovic, M. V.; Newman, G. A. *Chem. Commun.* **1968**, 722.
- (46) Murphy, P. J.; Williams, D. M.; Harris, V. H. *Organophosphorus reagents: A practical approach in chemistry*; Oxford University Press Inc., 2004.
- (47) Gotor, V.; Moris, F.; Garciaalles, L. F. *Biocatalysis* **1994**, *10*, 295.
- (48) Moris, F.; Gotor, V. *Tetrahedron* **1993**, *49*, 10089.
- (49) Moris, F.; Gotor, V. *J. Org. Chem.* **1993**, *58*, 653.
- (50) Díaz-Rodríguez, A.; Fernández, S.; Lavandera, I.; Ferrero, M.; Gotor, V. *Tetrahedron Lett.* **2005**, *46*, 5835.
- (51) Klibanov, A. M. *Trends Biotechnol.* **1997**, *15*, 97.
- (52) Lavandera, I.; Fernández, S.; Magdalena, J.; Ferrero, M.; Grewal, H.; Savile, C. K.; Kazlauskas, R. J.; Gotor, V. *ChemBioChem* **2006**, *7*, 693.

**Chapter 5 – *Enzymatic
incorporation of tp modified
nucleotides into DNA***

Chapter 5 – *Enzymatic incorporation of tp modified nucleotides into DNA*

The previous chapter investigated the synthesis of **tp** modified nucleotides; dTTP* and dCTP*, via phosphorylation at the 5'-OH of the modified nucleoside. The forthcoming chapter will attempt to develop a method to incorporate modified nucleotides into a duplex of DNA and extend the duplex up to micrometers in length by a relatively novel approach of extension, namely the enzymatic slippage extension.^{1,2} Enzymatically synthesizing functional DNA from a natural template and modified nucleotides will in turn produce a single molecular conducting nanowire, applicable for electronics.

Described here is the first enzymatic synthesis of oligodeoxynucleotides up to microns in length, in which dTTP or dCTP was replaced with dTTP* or dCTP* respectively. A range of DNA polymerases were tested initially to examine the polymerases suitability for the modified nucleotide when incorporating into a short duplex of DNA via primer extension reactions. Following the primer extension reaction is an investigation into how modified nucleotides can act as a template in DNA with the intention of incorporating canonical nucleotides opposite to the modified nucleotide in a complementary fashion, a factor necessary for the enzymatic slippage extension.

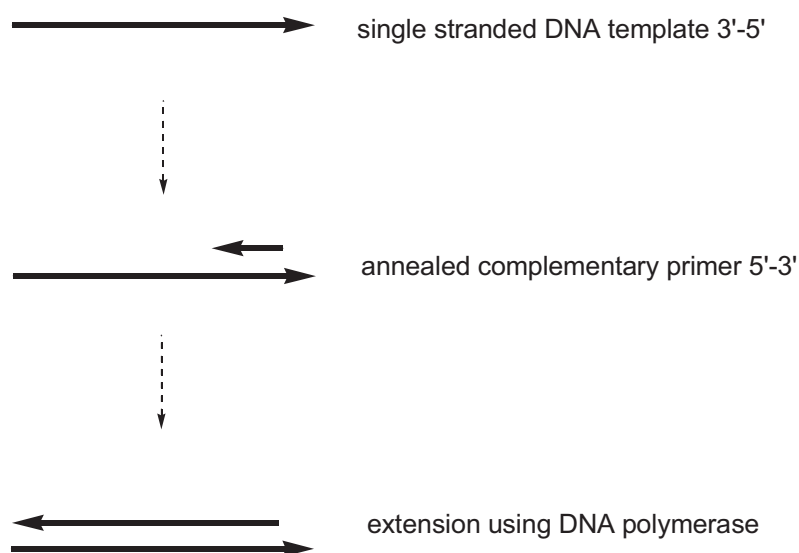
5.1 Suitability of DNA polymerases for dTTP* by primer extension

In order to explore the suitability of a DNA polymerase for a modified nucleotide, i.e. dTTP*, the initial test was to perform a primer extension reaction with a range of DNA polymerases. It is the most basic trial to test a polymerases affinity for nucleotides. In this type of reaction, incorporation of the modified nucleotide into a short duplex, for example, a 45 bp oligomer is attempted and subsequently analysed to determine which polymerases will accept the nucleotide as a substrate for incorporation and with what fidelity. The polymerases investigated included Klenow

Fragment *exo-* (Kf⁻), *Pyrococcus furiosus* *exo-* (Pfu-pol B *exo-*) and *Thermus Aquaticus* (*Taq*).

Primer extension is a method that requires a template in order to extend its primer by incorporating complementary nucleotides from a solution opposite the template. The primer is the initial segment of an oligomer that is to be extended, on which elongation depends. The template is a sequence of DNA that directs the synthesis of a complementary sequence. The role of the DNA polymerase is to incorporate the correct dNTP opposite its complementary base in the template from the 3'-terminus of the primer strand. The enzyme reliably catalyzes the formation of the phosphodiester linker between nucleotides.

As illustrated by Scheme 1, a template is obtained with a predetermined sequence of, for example, 45 bases long in the 3' to 5' direction. A shorter primer of, for example, 31 bases is annealed complementary to the template in the 5' to 3' direction generating the initial primer-template setup. Complementary dNTP's are successively incorporated opposite the template by the appropriate DNA polymerase which extends the primer to the full length of the template.



Scheme 1. Schematic to illustrate the process of primer extension.

Initiation of the extension requires the polymerase to hold and secure the primer-template in the correct orientation in its active site. The active sites of polymerases possess comparable structures to one another; however the functionalities of the structure differ greatly. All polymerases possess domains that are analogous to the shape of the human right hand; a thumb, palm and fingers as illustrated in Figure 1.

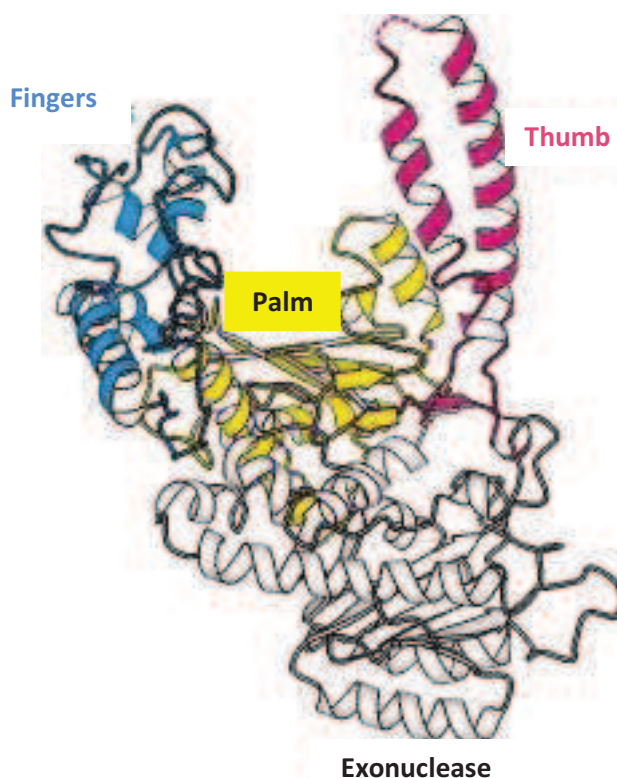
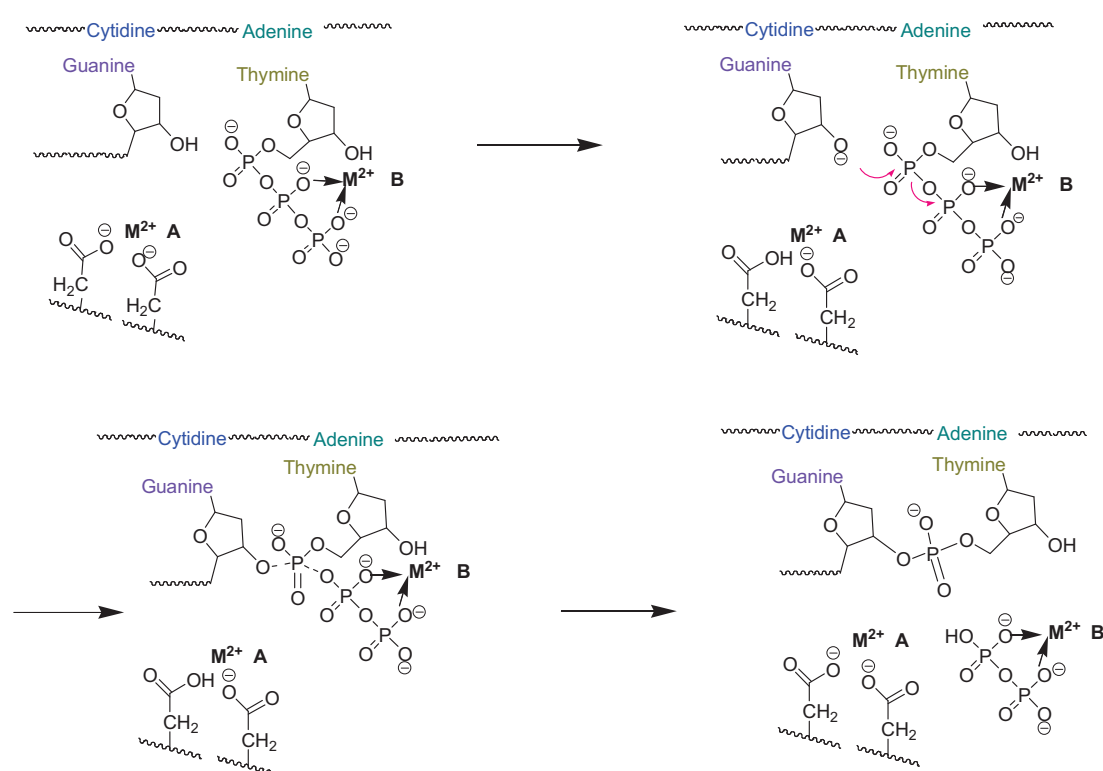


Figure 1. DNA polymerase structure.³

5.1.1 The role of DNA polymerases in DNA polymerization

When the polymerase binds to the DNA primer-template, the DNA is held between the polymerases fingers and thumb. The thumb positions the DNA duplex near the 3'-end of the primer. The fingers help to recognize the appropriate dNTP's and transport them to the 3'-end of the primer. The active site is contained in the palm moiety and it is here where the amino acid residues hydrogen bond to the incoming base and facilitate the phosphoryl transfer of the nucleotides.⁴ If the incoming base is recognized as one of the Watson-Crick base pairs, it will bind to the template and trigger a conformational change in the polymerase. The conformational change re-

assembles the active site into the correct orientation which then initiates polymerization.⁵ To facilitate the nucleophilic attack, aspartate residues within the active site are bound to two metal ions, most likely Mg^{2+} . The positive ions help stabilize the negative charges on the incoming triphosphate whilst at the same time activate the 3'-hydroxy group at the end of the nucleoside primer by allowing the aspartate residue to abstract the proton from the hydroxyl group (Scheme 2). The two metal ions are used with all polymerases from different families to facilitate the polymerization of the DNA duplex.⁶



Scheme 2. Scheme to illustrate the chemical mechanism for phosphoryl transfer catalysed by DNA polymerases.^{7,8}

When all entities are held in the correct orientation, the activated 3'-O⁻ group attacks the α -phosphate of the incoming nucleotide forming a pentacoordinate transition state between the two nucleotides. The transition state is stabilized via the divalent metal ions. The bond between the α - and β -phosphate is then broken and subsequently forms the pyrophosphate leaving group. On doing so, the pyrophosphate abstracts the proton from the aspartate residue and this process continues until; a) all of the primer

has been filled in or b) if the enzyme's action is halted, by for example, quenching with a chelating agent.

The fidelity of incorporation differs between polymerases and is determined by how well substrates can bind to the active site of the polymerase. If the geometry of the substrate in the active site is in the correct orientation, the active site of the polymerase can form hydrogen bonds to the substrate which can facilitate the phosphodiester linkage more rapidly than if in the wrong orientation. Another factor affecting this formation is π -stacking between the incoming substrate and the neighboring bases. If the polymerase does not hold a substrate in the correct orientation and there are no stabilizing interactions (either hydrogen bonds or π - π stacking) then the substrate will dissociate from the polymerase complex and will not be incorporated. This can occur when modified bases are employed as the modification interferes with the expected enzyme conformation. Therefore, a range of active site geometries belonging to a series of DNA polymerases should be investigated to determine which polymerase will hold a dNTP in place without dissociation before the phosphodiester linkage is complete. However, the exact catalytic mechanism of polymerase extension still requires further exploration and is often an exercise in trial and error to explore the most efficient polymerase.

A number of DNA polymerases exist and they have been divided into six sub-groups called families. The families are separated according to their amino acid sequence homology and crystal structure analyses.⁶ The most studied are the polymerases from Family A, including Klenow Fragment (KF) and *Taq*.⁴

Klenow fragment is a polymerase belonging to the *E. coli* polymerase I family. Its structure was the first to be established in the polymerase family, illustrated in Figure 1. The grey region of the protein in Figure 1 is the exonuclease moiety. The role of the exonuclease is to proofread the incoming nucleotides and remove any misincorporated nucleotides to ensure that only Watson-crick base pairs are incorporated, thus ensuring the fidelity of the polymerase.⁹ The editing process is performed by assessing the conformation of the active site. If only Watson-Crick base pairs are incorporated then the residues of the enzyme will form hydrogen bonds to

the incoming nucleotide, as will the incoming nucleotide to the complementary template strand. However, if an incorrect nucleotide enters the active site, the hydrogen-bonding will be weaker as the optimal geometry will be affected. Hence the orientation of the active site will be disrupted which causes the enzyme to stall in its action. If this disruption occurs, the exonuclease moiety senses the stalling and binds the partially melted 3'-single stranded primer into its domain to excise the abnormal base and allow the polymerization process to continue.

As the focal point of this project is to incorporate modified bases into the DNA duplex, it would not be feasible if the exonuclease functionality is intact. In order to accept modified bases and avoid excision, an enzyme devoid of its 3'-5' proofreading exonuclease activity, so-called Klenow fragment exo- (KF⁻) is required. In lacking the exonuclease function, the polymerase retains its activity and is therefore an ideal candidate for the incorporation of modified bases into DNA.

Taq and KF are structurally very similar. However, *Taq* is a thermostable polymerase and can operate at high temperatures whereas KF⁻ denatures at such temperatures. Therefore, their efficiency at base incorporation differs depending on the temperature of the reaction media. At room temperature KF is very efficient, whereas *Taq* displays more than a 10-fold decrease in activity at room temperature. *Taq* belongs to the thermostable bacteria, *Thermus Aquaticus* and is also part of the family A polymerases. It demonstrates the highest activity at its optimal temperature of 75-80 °C.⁴ In comparison to another thermostable polymerase, Pfu polymerase, *Taq* is less accurate by approximately 10-fold as it does not possess the 3'-5' proofreading activity.⁵

Pfu polymerase belongs to the archaeal family-B of enzymes and is isolated from *Pyrrococcus furiosus*. It has excellent fidelity with its 3'-5' exonuclease proofreading moiety intact; it makes a misincorporation mistake approximately one in 10⁶ bases incorporated.¹⁰ The Pfu-Pol exo⁻ which is disabled in its 3'-5' proofreading ability, is approximately 60-fold less accurate.⁵ Famulok *et al.* found that Pfu-Pol and family B polymerases in general were able to incorporate modified nucleotides to a higher fidelity than the family A polymerases.¹¹

The aforementioned enzymes have exhibited excellent fidelity with modified bases^{8,12} thus each was tested to discover which polymerase was the most efficient at accepting dTTP*. A 31/45 primer/template setup was trialled. This system contained four adenine sites against which the modified nucleotide, dTTP* could be incorporated. The length and hence extension of the primer strand was analysed using denaturing polyacrylamide gel electrophoresis (PAGE) (Fig. 2). The primer extension reaction incorporating dTTP* was performed and compared against a positive control extension whereby the primer-template was extended using all four natural dNTP's and also against a null control whereby no enzyme was added to the reaction. The lack of primer extension in the null control acts as a marker for where the unextended primer appears.

Primer sequence:

5' - cy5 - GGGGATCCTCTAGAGTCGACCTGCAGGGCAA - 3'

Template sequence:

3' - CCCCTAGGAGATCTCAGCTGGACGTCCCGTTTCGTTTCGAAACAGAGG - 5'

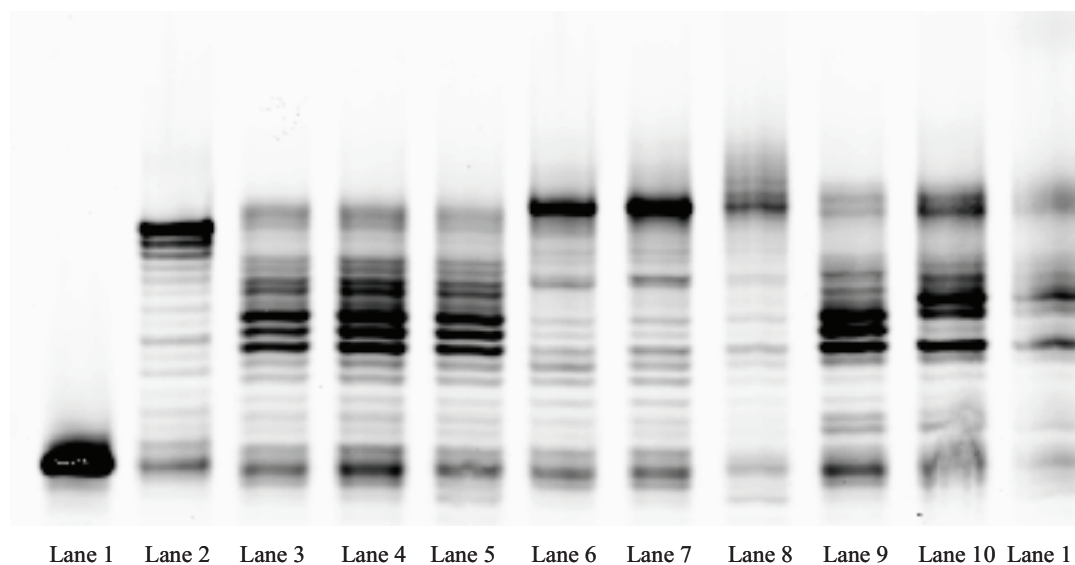


Figure 2. KF⁻, Pfu Pol B exo- & Taq polymerases extension of 31p-45t. Lane 1 = unextended cy5-labelled 31 base primer. Lane 2 = products of cy5-31p/45t extension by Taq (with natural dNTP mix). Lanes 3-5 = products of cy5-31p/45t extension by KF⁻ at 30 min, 3 h and 21 h time points, respectively (with “special” dNTP mix). Lanes 6-8 = products of cy5-31p/45t extension by Pfu Pol B exo- (family B) at 30 min, 3 h and 21 h time points, respectively (with “special” dNTP mix). Lanes 9-11 = products of cy5-31p/45t extension by Taq at 30 min, 3 h and 21 h time points, respectively (with “special” dNTP mix).

The results of a preliminary set of enzymatic extension experiments are shown in Figure 2. Lane 1 shows the unextended cy5-labeled primer due to the absence of enzyme in the reaction. As there is no extension, the short primer will migrate furthest on the gel. Lane 2 is a control, employing *Taq* (compare lanes 1 and 2) and using natural dNTP's and indicates the approximate position on the gel for a fully extended ssDNA 45mer. Lanes 3, 4 and 5 show the results of extension with KF^- polymerase and the modified thymidine triphosphate (dTTP*) at different time intervals. Clearly, the ssDNA has not been fully extended and stalls at the first addition of the modified thymidine. Lanes 6, 7 and 8 show the results of the extension utilizing Pfu Pol B exo-polymerase. The gel indicates that full extension is observed with Pfu-Pol exo- and hence this is proof that the modified base has been incorporated four times into a duplex of DNA. After 30 min, the ssDNA has been fully extended proving that this is a suitable polymerase for the incorporation of the modified dTTP*. Lanes 9, 10 and 11 show the results when employing *Taq*. In lane 9 (after 30 min) the results are similar to the KF^- in that the bulk extension pauses at the introduction of the first dTTP*. However, after 3 h, there is some evidence of full extension due to the dark band at the top of the gel. By comparison of Pfu Pol B exo-, the rate of extension is much slower and so may complicate future reactions.

The trial experiment revealed that KF^- and *Taq* did not recognize dTTP* as a substrate for primer extension as the primer did not extend fully. The rationalization for the low fidelity exhibited by KF^- and *Taq* could be due to the conformational changes that are observed when the modified base enters the active site. On entering the active site, the modified base must form strong hydrogen bonds to the complementary base on the template and also to the active site of the polymerase. Only this will trigger the conformational change in the polymerase that allows polymerization to proceed.

As Pfu Pol B exo- was able to generate a fully extended product, the next task was to investigate the acceptance of dTTP* in a time-dependent manner by employing primer-extension again in order to assess the efficiency of the enzyme in contrast to its acceptance of natural dNTP's.

A direct comparison of the rate of reaction between natural dNTP's versus a mix including dTTP* was performed. This was prepared by setting up a reaction pot of the

primer template, reaction buffer (10x), dNTP's and Pfu Pol B exo- polymerase. The reactions were started with the addition of the enzyme and aliquots were taken at the given time intervals. Lane 1 shows the unextended cy5-labeled 31 base primer. The absence of enzyme in the reaction means that no extension is observed. Therefore the short ssDNA travels the furthest in the gel. Lane 2 is again a control and signifies the position on the gel for a fully extended ssDNA 45mer employing Pfu-Pol exo polymerase (compare lanes 1 and 2) and using natural dNTP's. Lanes 3 to 11 show the reaction products of the extension at varied time intervals. Figure 3a illustrates that the primer is fully extended after 3 min. In comparison to Figure 3b, the primer is not fully extended until 10 min, showing that the enzyme works approximately 7 min slower when trying to incorporate dTTP*. The polyacrylamide gel in Figure 3b illustrates that the rate of incorporation of dTTP* was achieved at a slower rate than natural nucleotides (Fig. 3a) which is commonly observed with modified nucleotides.^{11,12}

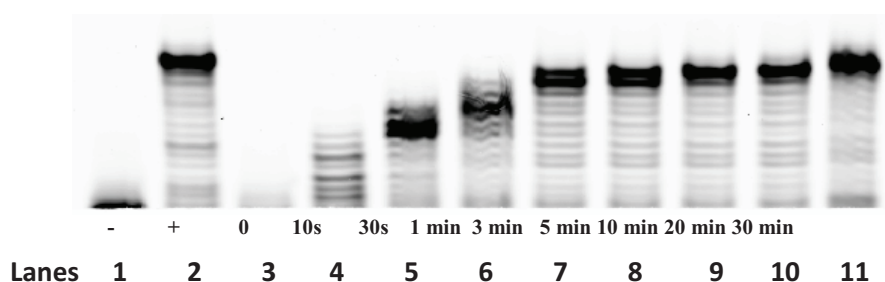


Figure 3a. PAGE of the control extension using “normal” dNTP mix. Lane 1 = unextended cy5-labelled 31 base primer. Lane 2 = fully-extended 45 base product. Lanes 3-11 = products of cy5-31p/45t extension by Pfu exo- pol B at 0 s, 30 s, 1 min, 3 min, 5 min, 10 min, 20 min and 30 min time points respectively.

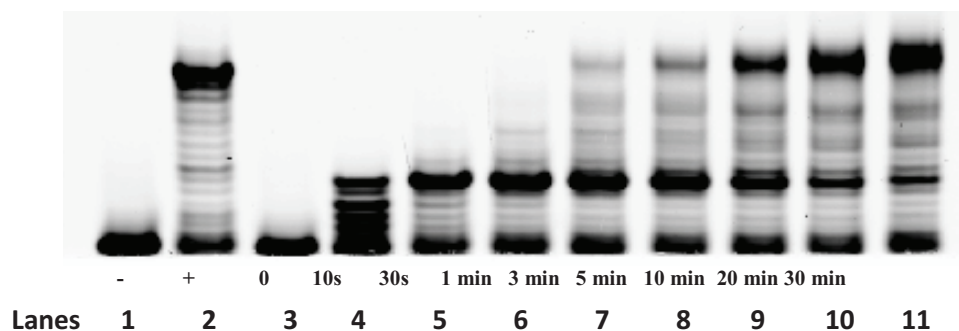


Figure 3b. PAGE of the modified extension using modified dNTP mix. Lane 1 = unextended cy5-labelled 31 base primer. Lane 2 = fully-extended 45 base product. Lanes 3-11 = products of cy5-31p/45t extension by Pfu exo- pol B at 0 s, 30 s, 1 min, 3 min, 5 min, 10 min, 20 min and 30 min time points respectively.

The decreased rate of incorporation of the modified nucleotide may be accounted for by a detrimental change in conformation of the enzyme. According to Marx *et al.*, modified nucleotides can reduce the interactions of the amino acid residues of the enzyme with the primer due to increased sterics forcing them apart.¹³ The stabilization of the closed conformation of the enzyme is therefore reduced on insertion of the next nucleotide. As there is a reduction in hydrogen bonding, the enzyme conformation becomes more flexible and is unable to clamp the primer/template duplex to the finger domain and so fidelity is lost. The polymerase has to now endeavor to reform its active conformation, hence reducing the efficiency of the process.

5.1.2 qPCR amplification of DNA employing dTTP*

With the promising results from the primer extension, the modified base was then tested for its ability to be incorporated using quantitative PCR (qPCR). qPCR or real time PCR uses fluorescence to detect and quantify how many DNA duplexes can be amplified. In standard PCR, a primer template is extended in the 5' to 3' direction, incorporating dNTP's from solution using a DNA polymerase to build a strand that is complementary to the template. Once it has extended, the DNA duplex is denatured at 95 °C. This yields two single stranded oligomers of DNA. The temperature is then

cooled to between 50-60 °C and the annealing step ensues. In this step the primer template formation is set up once more on each denatured single strand. Yet again, the dNTP's are incorporated and the primer is elongated at temperatures dependent on the polymerase employed. This cycle of steps is repeated until a) the reaction is quenched by a chelating agent, b) the dNTP's have been used up or c) the enzymatic activity has exhausted. In every step, the amount of DNA doubles and hence an exponential increase in DNA is observed. In qPCR, a fluorescent dye is incorporated into the reaction to quantify the amount of amplified DNA. The dye used in the experiment was SYBR green I and binds to the dsDNA formed via intercalation. If there is more DNA available, more SYBR green I can bind to the DNA and so an increase in fluorescence is observed indicating DNA amplification. SYBR green I was used as the dye as it gives a strong fluorescence when bound to dsDNA. Other dyes like ethidium bromide were not chosen as they bind dsDNA with a lower intensity.

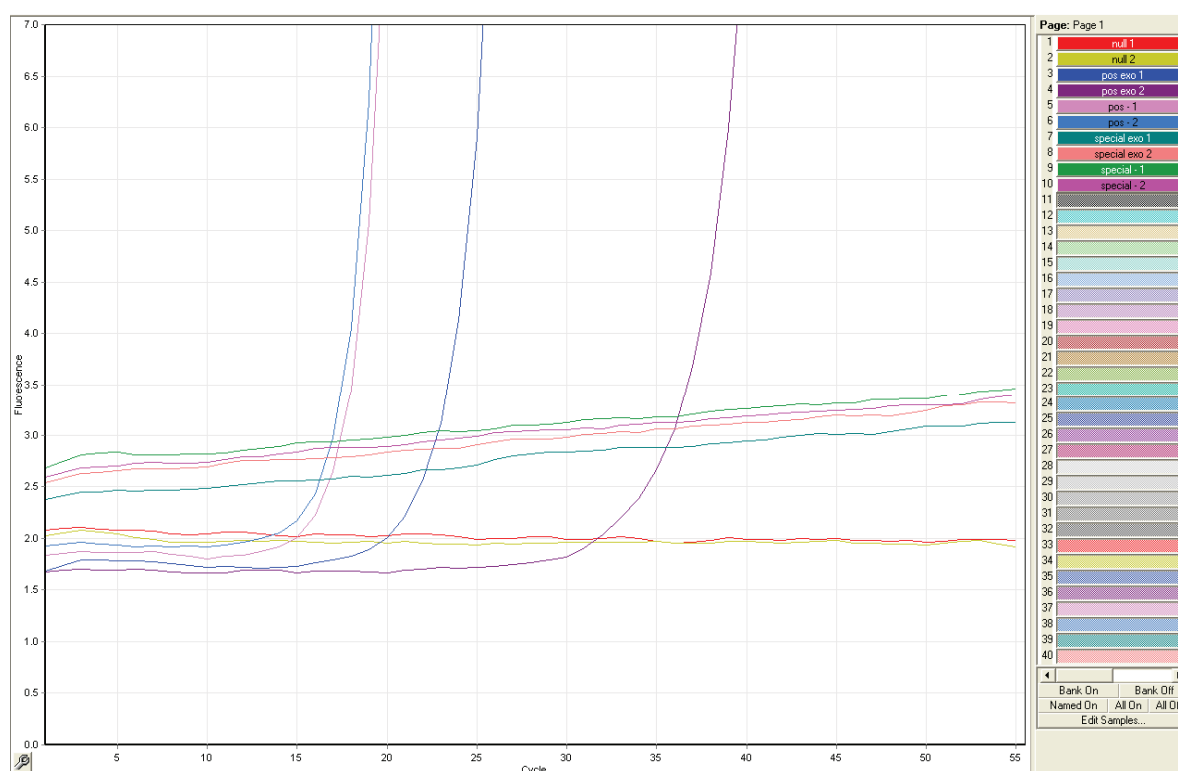


Figure 4. qPCR to observe if dTTP* can be incorporated into dsDNA and be amplified. Sample 1 + 2 = Null (without enzyme). Sample 3 + 4 = Positive control using natural dNTP's and Pfu-Pol exo⁺. Sample 5 + 6 = Positive control using natural dNTP's and Pfu-Pol exo⁻. Sample 7 + 8 = Modified dNTP mix and Pfu-Pol exo⁺. Sample 9+10 = Modified dNTP mix and Pfu-Pol exo⁻.

In Figure 4 the X-axis indicates the cycle number and the Y-axis shows the fluorescence in arbitrary units. The qPCR experiment was performed using wild-type DNA as a template, forward and reverse primers, the natural nucleotides; dATP, dCTP and dGTP, the modified dTTP* and the polymerases Pfu Pol B (retaining its exonuclease, Pfu Pol exo^+) and Pfu Pol B exo^- . A positive control was set up under the same conditions using all four natural dNTP's. The reactions were stopped after 55 cycles.

Unfortunately, the data in Figure 4 demonstrates only a slight linear increase in the fluorescence in the test reaction when employing dTTP*. By comparison of the control reaction when the natural dNTP's were employed, an exponential increase is observed in the fluorescence. Attempts were made to change the conditions of the PCR, such as increasing the elongation time as it was reasoned that the polymerase may not be acting as efficiently as with the natural nucleotides. However, there was no improvement to the amplification of DNA. It therefore appears that the modified base may not be functioning efficiently as a template. The polymerase has to incorporate a natural nucleotide, i.e. dATP opposite the complementary dTTP* in the template in order to build and amplify the DNA duplex. A further possible reason for the lack of amplification could be due to the high temperatures of the experimental procedure, in order to denature the dsDNA, This could have a detrimental effect on the **tp**-modification of the deoxythymidine. High temperatures can induce polymerization of the thienyl-pyrrole units which could cause aggregation and further precipitate out of solution and hence not be incorporated by the polymerase.

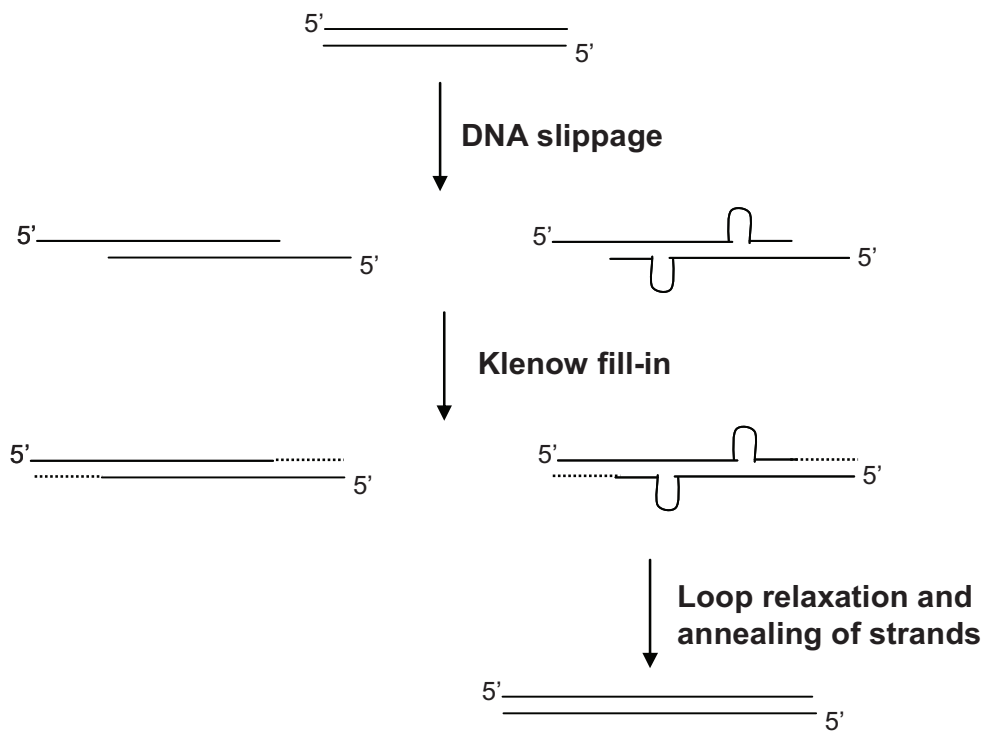
Although dTTP* could not be incorporated into lengths of DNA by qPCR to induce amplification of the DNA, an alternate approach, the enzymatic slippage extension of DNA was investigated.

5.1.3 Enzymatic slippage extension

There are a several ways to extend double stranded lengths of DNA. A method met earlier in the chapter was primer extension. This is a useful method to extend primers to reach the length of the template producing relatively short lengths of dsDNA

consisting of ~50 base pairs. In order to extend to microns in length, a method denoted as DNA slippage can be employed to extend a duplex of DNA by means of DNA replication mechanisms, which is initiated by a DNA polymerase. Studies have shown that Klenow fragment and *Taq* polymerase have been capable to facilitate this mechanism using short repeat units of heterogeneous polymers.¹⁴ Studies into the field began in the early 1960's with expanding short repeats of homo- and heteropolymers using polymerase I from *Escherichia coli*.¹⁵ Following this discovery, investigations into the extension of longer lengths, i.e. 5000-10,000 base pairs have been reported.¹⁶

A molecular mechanism of the strand slippage is not well established. One theory proposed was that the strands slide on each other towards the 5'-direction, breaking and then reforming H-bonding between complementary base pairs (Scheme 3, left). Reports have concluded that slippage is dependent on the 3'-end of the slippage strand.¹⁷ When the strand slips, it reveals a template at the 3'end where the dNTP's in solution can subsequently fill in the strand like that of a standard enzymatic DNA primer extension. This is replicated continuously until the reaction is quenched or until there is exhaustion of the dNTP's.



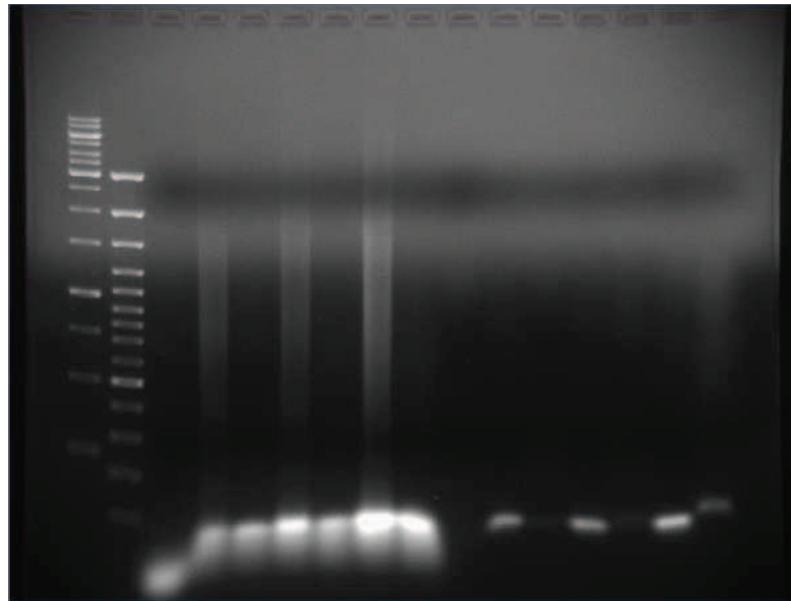
Scheme 3. Model for dT₂₀-dA₂₀ slippage extension.

Yet, due to the ever increasing number of base pair hydrogen bonds that must be broken to break longer and longer duplexes, it would be feasible to assume that this would require increasingly higher temperatures to denature the duplex as the length of the double strand increases. However, a second, more feasible mechanism has been proposed from experimental evidence.¹ Kotlyar *et al.* have demonstrated growth of up to 10 kbp by employing KF⁻. The suggestion is that loop formation (loop *de novo*) is induced at the 3'-end of the DNA strand. Illustrated in Figure 3, right, the enzyme binds to the 3'-end of the DNA. It is hypothesized that a loop *de novo* is produced by the polymerase pulling the ssDNA into its active site.¹ Once more it leaves a primer-template set-up that is utilized in the standard primer extension mechanism to incorporate the dNTP's. The polymerase then dissociates from the DNA strand, the loop then relaxes and the cycle is repeated. The production of loops continuously reveals unpaired ends that can be filled in with dNTP's. The time frame from the loop

formation until relaxation is microseconds signifying that the extension occurs at a fast rate.^{1,18} Furthermore, loop formation in DNA strands is not uncommon and further to this, do not destabilize the duplex structure or produce over-crowding in the grooves.¹⁹ This will be beneficial to bases that have a modification protruding out into the major groove.

Kotlyar *et al.* have synthesized the growth of poly(dA)-poly(dT) and poly(dA)-poly(dT) generating homopolymers, whereas Ijiro *et al* have produced dsDNA with an alternating d(AT) sequence with its complementary d(TA).^{2,20} Schlotterer *et al.* even extended trinucleotide repeats, such as CAG:CTG, via slippage extension.²¹ Each have been extended up to 10kb in length in the presence of KF⁻ and have found that the growth is time dependent. Therefore, this slippage reaction was executed in order to synthesize a defined, functionalized length of **tp** modified DNA by employing Pfu Pol B *exo*-.

The procedure for production of high molecular weight dsDNA comprises of a one-to-one double helical complex. Two templates were employed; poly(dA)₂₀-poly(dT)₂₀ and poly(dAT)₁₀ and the standard reaction mixture consisted of extension buffer, dATP, dTTP* and dTTP (for control reactions). The reaction was initiated by addition of Pfu Pol B *exo*- and was carried out at 45 °C over a range of time intervals before quenching with EDTA. Gel electrophoresis analysis was executed in a 1% non-denaturing agarose gel containing ethidium bromide as shown in Figure 5.



Lanes 1 2 3 4 5 6 7 8 9 10 11 12 13 14 15 16

Figure 5. Agarose gel illustrating the results of attempted enzymatic extension reaction (with two templates and two dNTP mixes) Lane 1 = 0.5 μg of Fermentas 1 kb DNA ladder. Lane 2 = 0.5 μg of Fermentas 100 bp DNA ladder. Lanes 3-9 = products of template 1 extension by Pfu pol B with unextended marker in lane 3, 1 hour time points in lanes 4 & 5, 3 hour time points in lanes 6 & 7 and 18 hour time points in lanes 8 & 9. Lanes 10-16 = products of template 2 extension by Pfu pol B with unextended marker in lane 10, 1 hour time points in lanes 11 & 12, 3 hour time points in lanes 13 & 14 and 18 hour time points in lanes 15 & 16. NB/ Lanes 4, 6, 8, 11, 13 & 15 contained the control dNTP reactions. Lanes 5, 7, 9, 12, 14 & 16 contained the modified dTTP* reactions.

As demonstrated by the gel above, nearly all samples run the length of the gel indicating a lack of extension. In the control extension, commercial dNTP's were employed at different time points (lanes 4, 6 and 8). Streaking was observed in these lanes without the desired monodispersed bands. Streaking often occurs when aggregates form which cannot be resolved by the agarose gel. No extension was observed for the modified triphosphate incorporation, except for a positive result observed in lane 16 which indicates a band at around the 250 bp point, according to the ladder in Lane 1. Although this shows some extension, the required length is between 5000 and 10000 base pairs and Pfu Pol B exo- may be too slow on incorporating the modified triphosphate.

Ijiro *et al.* have extended three templates; $(\text{dG})_{10}\text{-(dC)}_{10}$, d(AT)_{10} and $(\text{dA})_{20}\text{-(dT)}_{20}$, into high molecular weight dsDNA, however the rates of each extension decreased respectively. $(\text{dG})_{10}\text{-(dC)}_{10}$ extended at a rate of 36 bp min^{-1} , whereas the rate of

d(AT)₁₀ was only 7 bp min⁻¹.² Taking into consideration the slower rate of d(AT) in slippage extension, the extensions were repeated with an extended time of 72 hours. Yet again, no extension was observed indicating that in this instance the polymerase that cannot facilitate the slippage extension mechanism.

The findings from the experiment imply that Pfu Pol B exo- cannot function efficiently in this type of mechanism. It also suggests that the capacity for DNA extension is different for individual polymerases¹⁴ because only KF⁻ has been employed in the slippage extension of high molecular weight homopolymers. Pfu Pol B exo- and KF⁻ belong to different families and so the alteration in active site structure may affect the way by which they extend DNA, suggesting that Pfu Pol B exo- may not be applicable to this type of reaction.

KF⁻ is the polymerase of choice to extend dsDNA to microns in length in the literature and so it was trialed for the incorporation of dTTP* under a range of conditions using the two templates poly(dA)₂₀-poly(dT)₂₀ and poly(dAT)₁₀.^{1,2,20,22} Although the primer extensions revealed that KF⁻ was not efficient in extending the primer in comparison to Pfu Pol B exo-, it is recognized for facilitating slippage extensions and so it was tested with dTTP*. As the **tp**-monomer linked to the nucleoside is very hydrophobic, difficulties may potentially arise with dissolving the nucleotide in aqueous buffers. Buffer systems comprised of KPi (10x) and MgCl₂ and tris (10x) and MgCl₂ respectively which may well inhibit the enzymatic process. For that reason DMSO and DMF were also added separately to different reactions in order to improve the solubility. However, the gels revealed that no extension occurred, proving that as in the primer extensions, KF⁻ cannot recognize dTTP* as a substrate, even under various conditions.

Therefore, instead of attempting to modify dTTP* further in order to be accepted by KF⁻, it was hypothesized that dC could be modified, as an alternative; to investigate how this modified base is accepted by polymerases.

5.2 Suitability of DNA polymerases for dCTP* by primer extension

Once again, to explore the polymerase-substrate specificity, a range of DNA polymerases were investigated with pre-designed primer-template DNA sequences (Fig. 6).

5' - Cy5 - GGGGATCCTCTAGAGTCGACCTGC - 3'
3' - CCCCTAGGAGATCTCAGCTGGACGTCCGTACGTTTCAACAGAGG - 5'

The designed primer-template sequence will direct the incorporation of six dCTP* nucleotides. A varied distribution will test how the polymerases accept the nucleotide at different sites in respect to each other, alternate, adjacent and distant.

As in the dTTP* studies, the polymerases chosen lacked the 3'-5' exonuclease activity and included Pfu Pol B exo-, Pfu Pol D exo-, Klenow Fragment exo-, *Taq* polymerase and V93Q. In this experiment, the reaction mixture was made up and initiated with the addition of the enzyme. It was performed at 40 °C and aliquots were taken and quenched at 60 s, 3 min and 10 min time points to further examine the kinetics of each polymerase. The products were analysed by polyacrylamide denaturing gel electrophoresis (PAGE) and are illustrated in Figure 6.

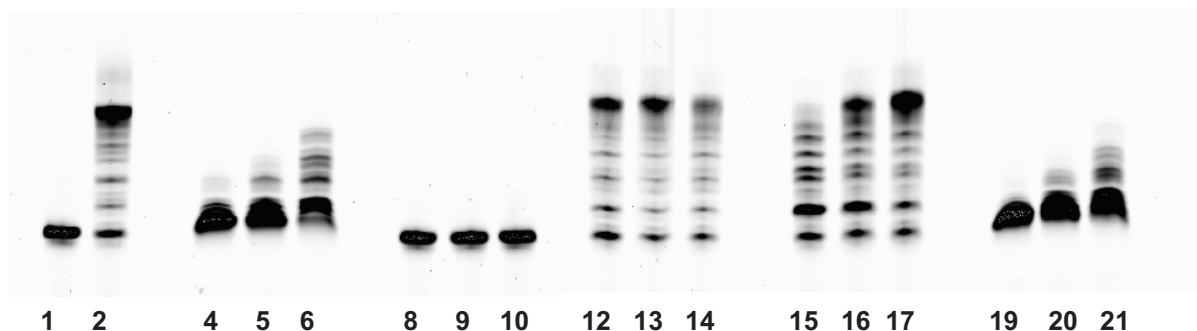


Figure 6: Pfu Pol B *exo-*, Pfu Pol D *exo-*, Klenow fragment *exo-*, *Taq* polymerase and V93Q extension of Cy5-24p-44t. Lane 1 = unextended cy5-labelled 24 base primer. Lane 2 = products of cy5-24p/44t extension by *Taq* DNA polymerase (with normal dNTP mix). Lanes 4-6 = products of cy5-24p/44t extension by Pfu pol B *exo-* at 1 min, 3 min and 10 min time points, respectively (with “special” dNTP mix). Lanes 8-10 = products of cy5-24p/44t extension by Pfu pol D *exo-* at 1 min, 3 min and 10 min time points, respectively (with “special” dNTP mix). Lanes 12-14 = products of cy5-24p/44t extension by Klenow fragment *exo-* at 1min, 3 min and 10 min time points, respectively (with “special” dNTP mix). Lanes 15-17 = products of cy5-24p/44t extension by *Taq* polymerase at 1min, 3 min and 10 min time points, respectively (with “special” dNTP mix). Lanes 19-21 = products of cy5-24p/44t extension by V93Q polymerase at 1min, 3 min and 10 min time points, respectively (with “special” dNTP mix).

The primer extension reaction incorporating dCTP* was performed and compared against a null control with no polymerase added, Lane 1, and a positive control whereby the primer-template was fully extended using all four natural dNTP's and *Taq*, Lane 2. Lanes 4-6 show the results of extension with Pfu Pol B *exo-* polymerase and the modified deoxycytidine triphosphate (dCTP*) at different time intervals. Evidently, the ssDNA has not been fully extended after 1 min and stalls at the first addition of the modified deoxycytidine triphosphate. However, after 3 min, a stronger band is observed and subsequently after 10 min the polymerase has accepted more of the modified triphosphate. Lanes 8, 9 and 10 exhibit the results of the extension when utilizing Pfu Pol D *exo-* polymerase. At each time point, no extension is visible indicating that the polymerase does not accept the modified substrate. Lanes 12-14 illustrates the extension using KF⁻ and undoubtedly shows full extension after 1 min indicating KF⁻ readily incorporates the modified substrate at a fast rate. Lanes 15-17 show the results when employing *Taq* polymerase. In lane 15 (after 1 min) the extension is promising but has not extended fully at this time-point. However, in the lanes 16 and 17, the results are similar to the KF⁻ polymerase in that of 12-14 demonstrating maximum extension. This proves that *Taq* also accepts the modified substrate but performs at a slower rate than KF⁻. Lanes 19-21 demonstrate that the

V93Q polymerase stalls after 1 min and then after 10 min initiates the incorporation of the bases. However the rate is again too slow to progress with this polymerase and at the time-points studies here, does not actually reach full extension.

The results visibly show that KF⁻, *Taq* and to a certain extent, Pfu-Pol B exo-recognized dCTP* as a substrate for primer extension. In comparing the gel data, KF⁻ proceeds most efficiently and at 1 min the primer is fully extended. Pfu Pol B exo- requires longer time. Therefore, the next experiment was to determine how a more sterically demanding primer-template sequence would affect the DNA polymerases.

5.2.1 Primer extensions at every and alternate bases

Since dCTP* could be incorporated into primer-template sequences that were reasonably spaced apart, the next task was to test the polymerases ability for successive incorporations. This factor of spacing had to be tested as the goal of the project is to incorporate the modified nucleotide according to the enzymatic slippage reaction which requires a homopolymer template, or a template containing alternate bases.^{1,2,20} If the modified bases are adjacent to each other, it could be sterically demanding for the polymerase. Two templates were designed to encode up to seven alternate incorporations (A37) and 13 consecutive, adjacent incorporations (B37). The primer extensions were performed using KF⁻ and *Taq*. In the experiment, a control extension was performed using all four natural dNTP's for both templates. Figure 7 shows the results of the primer extension experiments.

Primer-template for the extension of modified base incorporation at alternate bases:

Primer sequence:

5' - cy5 - AAAAGTCCTCTAGAGTCGACCTGA - 3'

Template sequence:

A37 3' - TTTTCAGGAGATCTCAGCTGGACTGAGTGCGTCCGAG - 5'

B37 3' - TTTTCAGGAGATCTCAGCTGGACTGGGGGGGGGGGGG - 5'

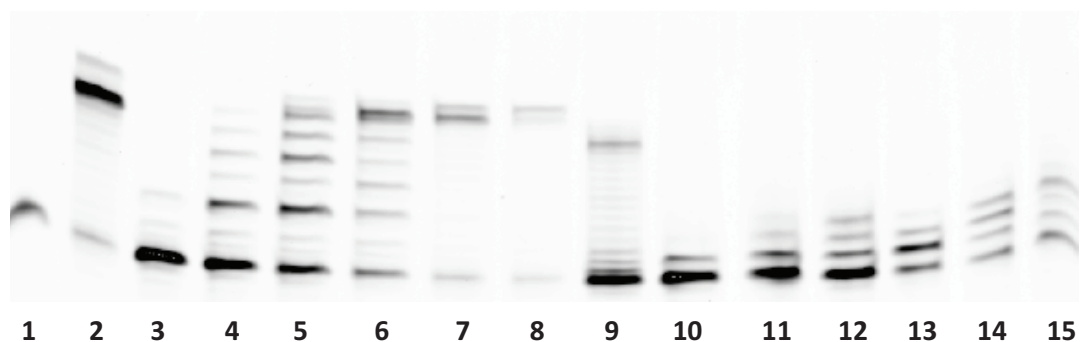


Figure 7. Primer extension of alternate and every base. Lane 1 = unextended cy5-labelled 24 base primer. Lane 2 = fully-extended 37 base product with dCTP* at alternate bases employing *Taq*. Lanes 3-5 = products of cy5-24p/37t extension by *Taq* at 30 s, 3 min and 10 min time points respectively. Lanes 6-8 = products of cy5-24p/37t extension by KF^- at 30 s, 3 min and 10 min time points respectively. Lane 10 = fully-extended 37 base product with dCTP* at every base employing *Taq*. Lanes 11-12 = products of cy5-24p/37t extension by *Taq* at 30 s, 3 min and 10 min time points respectively. Lanes 13-15 = products of cy5-24p/37t extension by KF^- at 30 s, 3 min and 10 min time points respectively.

The results compare primer extensions that will incorporate dCTP* at alternate and adjacent bases using two polymerases, *Taq* and KF^- . Lane 1 shows the unextended cy5-labeled primer and the band runs further down the gel due to the absence of enzyme in the reaction. Lane 2 is a positive control and indicates the approximate position on the gel for a fully extended ssDNA 37mer employing *Taq* (compare lanes 1 and 2) and natural dNTP's. Lanes 3 to 5 show the results of extension with *Taq* polymerase and the modified deoxycytidine triphosphate, dCTP*, at different time intervals and only after 10 min does the extension reach its maximum. Lanes 6 to 8 show the results of the extension utilizing KF^- . It is illustrated in the figure that full extension is observed within 30 s of the addition of enzyme to the mixture and so demonstrating that the modified base has been incorporated seven times into a duplex of DNA and hence is a suitable polymerase for the incorporation of dCTP*.

Lane 9 shows the result of the control extension where thirteen deoxyguanosines are adjacent to each other, in comparison to the alternate template, A37. The control reaction extends the 24 base primer, incorporating only natural dNTP's and employing *Taq*. In lanes 10 to 12, the results demonstrate that *Taq* polymerase stalls after two bases at the 30 s time point and subsequently stalls after incorporating four dCTP* after 3 min and 10 min respectively. The same is also observed with KF^- at the

same time points demonstrating that polymerases cannot function properly when trying to incorporate the modified bases that are next to each other.

The results show that the family A polymerases were able to accept the modified base at alternate positions, however with different rates. In contrast, at every position the polymerases would not accept the base and hence the extension stalled. A reason for this is that the size of the **tp** monomer attached to the bases may be sterically hindering the incorporation of bases at the adjacent position. As the spacing between nucleotides is 3.4 Å and the size of the **tp** unit is 6.16 Å, the most suitable sequence of the monomers would be at alternating positions. These findings have also been observed in the literature, for example, Famulok *et al.* modified all dNTP's and attempted to incorporate the functionalized nucleotides against templates that were rich in one of the nucleotides. The family A polymerases did not accept the modified nucleotides at adjacent positions. However, when employing family B polymerases, for instance, Pfu exo-, full extension was observed showing that these polymerases are not sequence-dependent.¹¹

Earlier in the chapter, qPCR was the next obvious step to discover if the modified nucleotide could be incorporated into a duplex of DNA, followed by amplification. However, KF⁻ was the most processive enzyme in incorporating dCTP* in primer extension reactions, but as it is not a thermostable polymerase, qPCR could not be performed. During PCR, the temperatures reaches 90 °C in order to melt the DNA, this would destroy the polymerase. Therefore, the enzymatic slippage extension was investigated to find out if dCTP* could be integrated and observe extension of a short template of DNA.

5.2.2 Enzymatic slippage extension

For the enzymatic incorporation of dCTP* into DNA via the slippage extension approach, the template poly(dC)₁₀-poly(dG)₁₀ was employed. The standard reaction mixture consisted of extension buffer, dGTP, dCTP* and dCTP (for control reactions). The reaction was initiated by addition of the polymerases; Pfu Pol B exo-, KF⁻ and *Taq* and was carried out at 45 °C for Pfu Pol B exo- and *Taq* and at 37 °C for

KF⁻, over a range of time intervals before quenching with EDTA. Agarose gel electrophoresis analysis was executed in a 1% non-denaturing agarose gel containing ethidium bromide as shown in Figure 8.

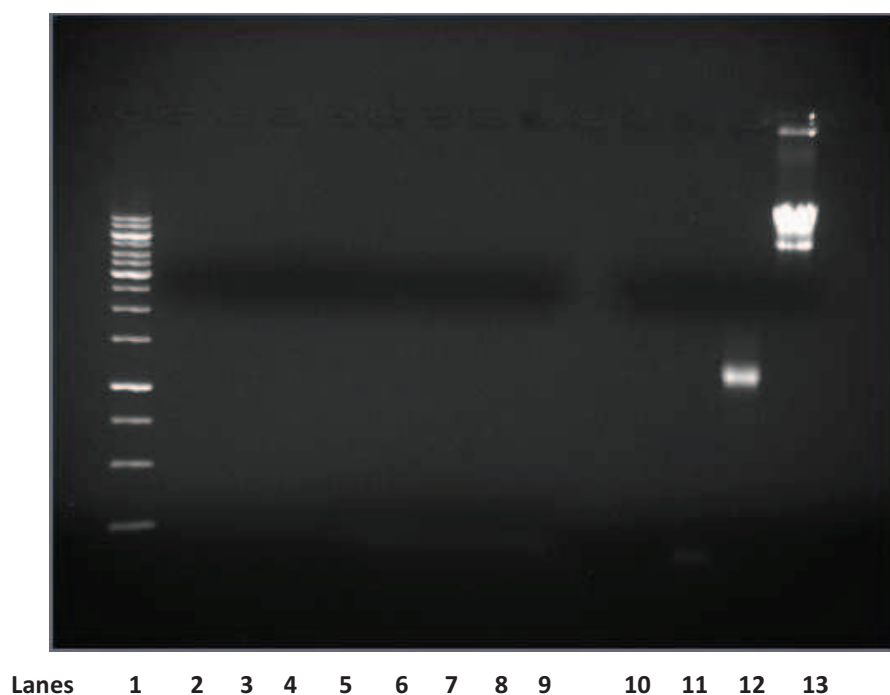


Figure 8. Mobility of poly(dC)₁₀-poly(dG)₁₀ DNA duplexes in a 1% agarose gel. Lane 1 = 1kb ladder. Lane 2-5 = product of poly(dG)-poly(dC) slippage extension of control dNTP's at 0, 1 h, 3h and 18 h time points, using Pfu Pol B exo-. Lanes 6-9 = product of poly(dG)-poly(dC) slippage extension of modified dCTP* and unmodified dGTP, at 0, 1 h, 3h and 18 h time points using Pfu Pol B exo-. Lanes 10-13 = product of poly(dG)-poly(dC) slippage extension of control dNTP's at 0, 1 h, 3h and 18 h time points, using KF⁻.

From the above gel (Fig. 8), it is clear that there is no observable extension when employing the Pfu Pol B exo- (lanes 3-9) with neither canonical nor modified triphosphates. The lack of extensions could be due to the active site of the polymerase, i.e. it does not perform to the same mechanism as the KF⁻. Conversely, in lanes 11-13, it can be observed that there is clear extension using the control, unmodified dNTP's. At 0 h there is no extension which is expected. In lane 11, at 1 h, there is a band just below the 250 base pair marker point the DNA ladder. After 3 h, there is a clear band at approximately 1100 base pairs. The optimal results are observed after 18 h with a thick band of extended product between approximately 8000 and 10,000 base pairs. It is evident from the bands that they grow continuously

at a time-dependent rate, which is illustrated by the monodispersed bands. The gel is also a drastic improvement in comparison to the gels observed earlier in the chapter when employing the poly(dA)₂₀-poly(dT)₂₀ and the poly(dAT)₁₀ templates. Although there has been no observed extension when employing KF⁻ with the **tp** modified dCTP* (lanes 2-5 Fig. 9), it is still a positive result in that the control extension was successful.

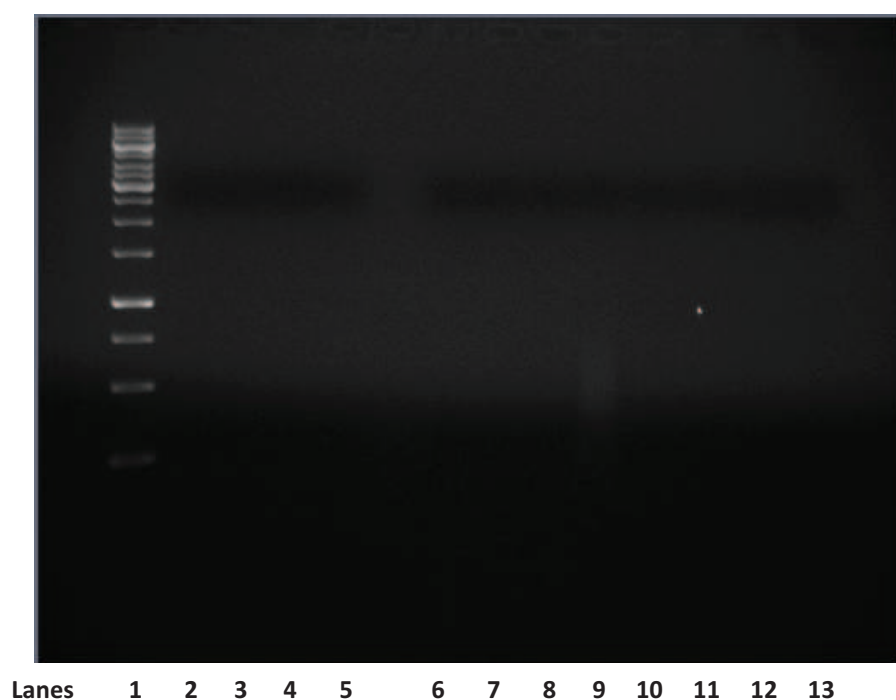


Figure 9. Mobility of poly(dC)-poly(dG) DNA duplexes in a 1% agarose gel. Lane 1 = 1kb ladder. Lanes 2-5 = product of poly(dG)-poly(dC) slippage extension of modified dCTP* and unmodified dGTP, at 0, 1 h, 3 h and 18 h time points using KF⁻. Lanes 6-9 = product of poly(dG)-poly(dC) slippage extension of control dNTP's, at 0, 1 h, 3 h and 18 h time points using *Taq*. Lanes 10-13 = product of poly(dG)-poly(dC) slippage extension of modified dCTP* and unmodified dGTP, at 0, 1 h, 3 h and 18 h time points using *Taq*.

In Figure 9; lanes 2-5, illustrates the results of enzymatic slippage extension when employing KF⁻ and dCTP*. The gel shows no of extension when attempting to employ the modified nucleotide. As the KF⁻ extended the template with standard triphosphates, the problem is quite clearly the modified nucleotide dCTP*. A reason for the lack of extension is quite possibly the polymerase not having the ability to read the modified nucleotide and use it as a template to incorporate a complementary

nucleotide opposite. The modification may cause a distortion to the polymerase active site and prevent the required conformation that facilitates the phosphodiester linkage between two nucleotides. If the polymerase dissociates from the dCTP*, the extension will stall and hence no extension will be observed. Lanes 6-13 illustrate the attempted enzymatic slippage extension employing *Taq* polymerase. Lanes 6-9 exhibits the extension results when using standard dNTP's. Lanes 10-13 show the outcome of the extension using dCTP* and dGTP. The results resemble the lack of extension when employing Pfu Pol B exo-. Once again, *Taq* polymerase may not function in this type of mechanism. Primer extension demonstrated that by binding to a natural template, all of the polymerases could withstand an incoming modified nucleotide. However, in the reverse situation whereby using the modified nucleotide as a template to incorporate standard nucleotides opposite the modification, the polymerases will not accept this action and stall. Therefore, structural modifications to the modified nucleotides dTTP* and dCTP* may be necessary to improve the binding between the polymerase active site and modified nucleotide to facilitate the slippage extension mechanism.

The gel electrophoresis studies performed have illustrated that only KF⁻ will extend the poly(dC)-poly(dG) via the slippage mechanism. However, this only occurs with the natural dNTP's and demonstrated that the enzyme will not incorporate the modified base under conditions employed here. The most reasonable explanation for this is that the enzyme will not read the modified base as a template. To expand on this, as the DNA slips, it leaves an overhang and the enzyme can then incorporate bases opposite this overhang. However, after a subsequent slip the **tp** modified base is revealed as the new overhang. It appears likely that the polymerase cannot incorporate bases opposite this modified overhang as it does not recognize it as a readable template, as was reported earlier in the case for primer extension.

5.3 Conclusions

In summary, both modified nucleotides dTTP* and dCTP* were incorporated successfully into dsDNA by primer extension reactions using polymerases. Pfu Pol B exo- was the polymerase that accepted dTTP* most efficiently and KF⁻ was the best

candidate for utilizing dCTP* as a substrate. The products were observed by denaturing polyacrylamide gel electrophoresis.

Incorporating the modified nucleotides into DNA via the enzymatic slippage extension was unfortunately unsuccessful. dTTP* may not have been incorporated due to the inherent nature of the polymerase Pfu-Pol B exo-. This polymerase has not been reported to function in such a mechanism and literature has shown that only KF⁻ can extend homopolymers in this way.^{1,2,20} However, when employing KF⁻ to incorporate dCTP*, incorporation was unsuccessful. Nevertheless, hypotheses have been made in Chapter 6 in order to try and amend the process to facilitate the incorporation of the modified nucleotide into a long functionalized polymer.

5.4 Experimental

Reagents were purchased from Sigma-Aldrich, MWG and New England Biolabs and used as received unless otherwise stated. For band-density analysis of gel images, 'Image Quant' software (GE Healthcare).

Primer Extension Reactions

5'-Cy5-labeled primer was annealed to the appropriate template in 1x reaction buffer by heating the mixture up to 95 °C for 5 min and then allowing cooling slowly to room temperature for 1 h. The extension reactions were carried out in 20 µL volumes containing 20 mM Tris-HCl, pH 8.5, 10 mM KCl, 20 mM MgSO₄, 10 mM (NH₄)₂SO₄, 200 nM primer-template and 2.5 mM of each of the four dNTP's. The reactions were initiated upon the addition of the enzyme Pfu-Pol exo- (800 nM). The assay temperature was 40 °C and timed 20 ml aliquots were withdrawn and the reaction quenched by addition of 40 ml stop buffer (40% formamide, 0.1M EDTA and orange G) The samples were denatured by heating to 90 °C for 10 min and then rapidly cooled on ice. The quenching buffer used to stop primer-template extension reactions was supplemented with 250 nM of an oligodeoxynucleotide, complementary to the template strand. An excess of such a nucleic acid confiscates the template strand and prevents any re-annealing of the extended fluorescent primer, which interferes with gel electrophoretic analysis, after the denaturation step

Polyacrylamide gel electrophoresis

The ssDNA reaction products was electrophoresed in a 1 x TBE, 17 % denaturing polyacrylamide gel containing 8 M urea, 10 % ammonium persulfate (350 µL) and TEMED (10 µL). The gel was electrophoresed for 4h at 35 W for 1 h and extension products were detected using a Typhoon scanner (GE Healthcare) and quantified using Imagequant software (GE Healthcare)

qPCR

The reactions were carried out in a 20 μL reaction volume containing; 10 x reaction buffer supplied with the polymerase (2.0 μL), H_2O (6.7 μL), 50 % glycerol (3.2 μL), DMSO (0.6 μL), forward and reverse primer mix (1 μL , 15 μM), Sce genomic DNA (0.5 μL) and SYBR Green (1 μL). The dNTP's (4.0 μL , 2.5 mM) and Pfu pol exo- (1.0 μL , 1 μM) were added last to initiate the reaction. Fifteen PCR cycles (30 s at 95 $^\circ\text{C}$, 30 s at 55 $^\circ\text{C}$ and 7 minutes at 70 $^\circ\text{C}$) were used.

General procedure for slippage enzymatic extensions

Synthesis of extended DNA duplexes were performed in a 40 μL reaction pot containing; 10 x extension buffer (supplied with the polymerase), 1.5 mM of relevant natural dNTP and 1.5 mM relevant modified dNTP. The reaction was primed using 100 nM of the relevant template. The reactions were initiated upon the addition of the polymerase (1 μM) and reacted at 3 time points; 30 min, 3 h (at 45 $^\circ\text{C}$) and then 18 h (at 55 $^\circ\text{C}$) (all reactions at 37 $^\circ\text{C}$ for KF⁻). The reaction was quenched with the addition of 0.1 M EDTA (1 μL).

Agarose gel electrophoresis

The DNA samples were electrophoresed and visualized on a 1% agarose gel containing ethidium bromide (0.5 $\mu\text{g}/\text{mL}$) for 1h at 105 V at room temperature using bromphenol loading dye. TBE buffer was used to prepare the gel and as the running buffer. The dimensions of the agarose gel were 10 x 10 cm with 10-wells.

References

- (1) Kotlyar, A. B.; Borovok, N.; Molotsky, T.; Fedeev, L.; Gozin, M. *Nucleic Acids Res.* **2005**, *33*, 525.
- (2) Tanaka, A.; Matsuo, Y.; Hashimoto, Y.; Ijio, K. *Chem. Commun.* **2008**, 4270.
- (3) Berg, J. M.; Tymoczko, J. L.; Stryer, L. *Biochemistry*; 5th Edition ed.; W.H. Freeman & Co Ltd, 2002.
- (4) Zhao, G.; Guan, Y. *Acta Biochim. Pol.* **2010**, *42*, 722.
- (5) Biles, B. D.; Connolly, B. A. *Nucleic Acids Res.* **2004**, *32*, e176.
- (6) Steitz, T. A. *J. Biol. Chem.* **1999**, *274*, 17395.
- (7) Berdis, A. J. *Chem. Rev.* **2009**, *109*, 2862.
- (8) Borsenberger, V.; Kukwikila, M.; Howorka, S. *Org. Biomol. Chem.* **2009**, *7*, 3826.
- (9) Russell, H. J.; Richardson, T. T.; Emptage, K.; Connolly, B. A. *Nucleic Acids Res.* **2009**, *37*, 7603.
- (10) Kennedy, E. M.; Hergott, C.; Dewhurst, S.; Kim, B. *Biochemistry* **2009**, *48*, 11161.
- (11) Jager, S.; Rasched, G.; Kornreich-Leshem, H.; Engeser, M.; Thum, O.; Famulok, M. *J. Am. Chem. Soc.* **2005**, *127*, 15071.
- (12) Jäger, S.; Famulok, M. *Angew. Chem., Int. Ed.* **2004**, *43*, 3337.
- (13) Obeid, S.; Baccaro, A.; Welte, W.; Diederichs, K.; Marx, A. *Proc. Natl. Acad. Sci. U. S. A.* **2010**, *107*, 21327.
- (14) Ji, J.; Clegg, N. J.; Peterson, K. R.; Jackson, A. L.; Laird, C. D.; Loeb, L. A. *Nucleic Acids Res.* **1996**, *24*, 2835.
- (15) Schachman, H. K.; Adler, J.; Radding, C. M.; Lehman, I. R.; Kornberg, A. *J. Biol. Chem.* **1960**, *235*, 3242.
- (16) Wells, R. D.; Larson, J. E.; Grant, R. C.; Shortle, B. E.; Cantor, C. R. *J. Mol. Biol.* **1970**, *54*, 465.
- (17) Karthikeyan, G.; Chary, K. V. R.; Rao, B. J. *Nucleic Acids Res.* **1999**, *27*, 3851.
- (18) Kühner, F.; Morfill, J.; Neher, R. A.; Blank, K.; Gaub, H. E. *Biophys. J.* **2007**, *92*, 2491.
- (19) Fresco, J. R.; Alberts, B. M. *Proc. Natl. Acad. Sci. U. S. A.* **1960**, *46*, 311.
- (20) Borovok, N.; Molotsky, T.; Ghabboun, J.; Cohen, H.; Porath, D.; Kotlyar, A. *FEBS Lett.* **2007**, *581*, 5843.
- (21) Schlotterer, C.; Tautz, D. *Nucleic Acids Res.* **1992**, *20*, 211.
- (22) Borovok, N.; Molotsky, T.; Ghabboun, J.; Porath, D.; Kotlyar, A. *Anal. Biochem.* **2008**, *374*, 71.

Chapter 6 – *Conclusions and further work*

Chapter 6 - *Conclusions and Future Work*

The polymers pyrrole (**py**), 2-(2-thienyl)pyrrole (**tp**) and 2,5-bis(2-thienyl)pyrrole (**tpf**) have been successfully synthesized and functionalized with a range of terminal alkyne linkers. The monomers and alkylated monomers were electrochemically characterized demonstrating that they all exhibit the redox properties essential for conducting polymers. 5-Thienyl-pyrrole demonstrated versatility in templating DNA through electrostatic interactions. Subsequent functionalization allowed the nucleation of silver nanoparticles on the alkyne moieties to produce a long, thin and uniform conductive wire. Furthermore, the alkyne moiety facilitated “click” chemistry with a fluorescent dansyl azide to produce a conductive and fluorescent nanowire with potential use as a biosensor.

The resulting alkylated monomers were united with deoxythymidine at the C5 position via Sonogashira-type chemistry. Cyclic voltammetry was performed to investigate the electrochemical properties of the modified nucleosides and whilst also taking into consideration the size and flexibility of the monomer linker, dT-5-**tp** (dT-5-**tp**) was chosen as the appropriate nucleoside for incorporation into DNA. Moreover, deoxycytidine was also modified with the 5-**tp** linker to formulate a direct comparison between the nucleosides after conversion into their corresponding triphosphates.

dT-**tp** was converted into its corresponding triphosphate via phosphorus (V) chemistry. Protection of the nucleoside was not required and the procedure according to Yoshikawa was followed. dC-**tp** was unreactive upon reaction with phosphorus (V) and so the more reactive phosphorus (III) method was used as an alternative. However, phosphorus (III) is also less regioselective than phosphorus (V) and hence protection of the 3'-OH was necessary, prior to the phosphorylation. The afforded triphosphates, dTTP* and dCTP* were then compatible for enzymatic extension via the appropriate polymerase.

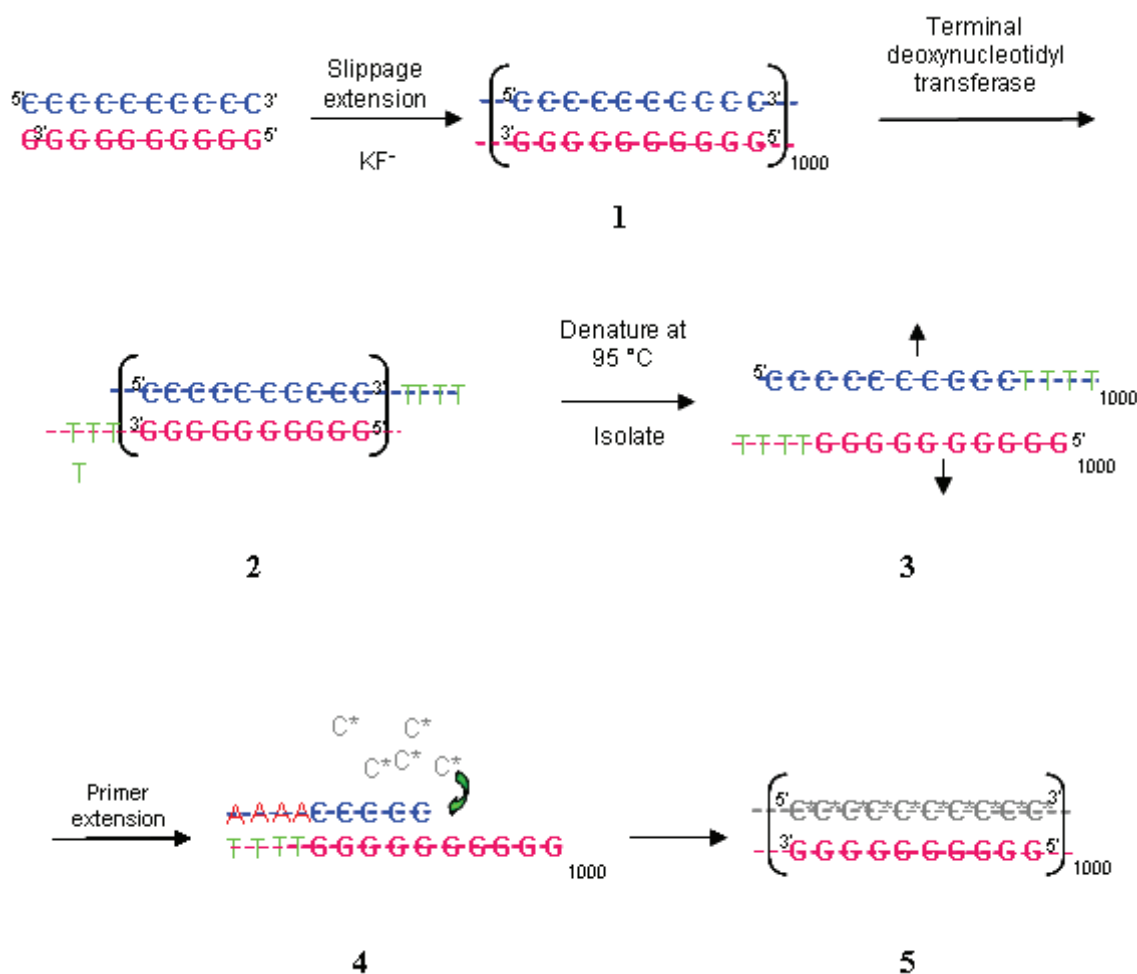
Initially dTTP* was examined for substrate suitability and the family B polymerase Pfu Pol B exo- was the enzyme that proceeded to completion most efficiently in primer extension reactions. Results were analyzed by denaturing polyacrylamide gel electrophoresis. qPCR was attempted but no amplification was observed.

Enzymatic extension via the slippage model was then attempted. Analysis by agarose gel electrophoresis revealed that unfortunately, the maximum extension of the modified duplex was to approximately 250 bp when employing dTTP* and Pfu Pol B exo-. Changes to the conditions of the reactions were performed to aid factors such as solubility, concentration of dNTP's, buffer systems, however, no improvements were observed. Concluded from this set of experiments was that Pfu Pol exo- cannot recognize dTTP* as a template to facilitate extension in such a mechanism.

Therefore, attention was turned to dCTP*. Once more, a range of polymerases were investigated to explore which polymerase accepted the modified nucleotide with the optimum fidelity. In this case, dCTP* was well tolerated by the family A polymerase KF⁻ and proceeded to full extension with the highest efficiency. qPCR could not be tested to recognize how the modified nucleotide acts as a template, due to the low temperatures at which KF⁻ functions at (37 °C). Unlike Pfu Pol B exo-, KF⁻ is not a thermostable polymerase and would denature and at the high temperatures (90 °C) involved in this technique.

The slippage extension was then undertaken with dCTP*. Agarose gel electrophoresis exhibited no extension when the modified nucleotide was incorporated. However, in contrast to Pfu Pol B exo-, extension with commercial dNTP's was observed. The extension spanned over 10,000 bp after 18 hr, when employing the poly(dC)₁₀-poly(dG)₁₀ homopolymer template.

Although no extension was observed when attempting to incorporate the modified nucleotide, the extension when employing commercial dNTP's is encouraging. Future experiments could potentially utilize the unmodified, slippage extended duplex and apply it to an exaggerated primer extension system. To elaborate, if the initial poly(dC)₁₀-poly(dG)₁₀ template was extended to its maximum length, i.e. approximately 10,000 bp (1), the required length could be obtained. After this step, an enzyme, namely terminal deoxynucleotidyl transferase (TdT), could be employed to add a short homo single strand to the 3' end of each strand of DNA (2). This is a special DNA polymerase that can add nucleotides to a 3' end of DNA without a template to incorporate against. Hence, a short strands of, for example, ten deoxythymidine residues could extend the length of each strand of the duplex. The resulting duplex could then be denatured and isolated in order to obtain each single strand (Scheme 1).



Scheme 1. Schematic to demonstrate the possible route to achieving the fully functional dsDNA.

The single stranded poly(dG)-(dT)₁₀ can now act as a copolymer template. A complementary copolymer primer consisting of poly(dA)₁₀-poly(dC)₁₀ could hybridize and set up the primer-template system that was observed earlier in Chapter 5 with the primer extension reactions. dCTP* could then fill in opposite every dG in order to extend the primer and produce a fully functional DNA duplex which is microns in length.

Attention should further be turned to the structure of the modified nucleosides/nucleotides. The manner by which the nucleoside was connected with the monomer could be re-examined. It has been proposed that elongation will commence as long as the incoming base can form stabilizing bonds, i.e. hydrogen-bonding or pi-stacking between bases, in addition to the polymerase holding the bases in the correct orientation. However, recent developments have suggested that the functionalized base must be able to form stabilizing bonds to the major or minor groove.¹ These stabilizing bonds have been presented in the form of polar linkers. In

Chapters 2 and 3, the approach was to modify the pyrrole derivatives with an alkyne linker in order to follow Sonogashira-type chemistry to unite the alkyne with the halonucleoside. The exceptionally non-polar system of an alkyne, hydrocarbon chain and heterocyclic monomers prevent the optimum solubility in enzymatic systems. Furthermore, this hydrophobic system lacks the supplementary hydrogen-bonding to the polymerase active site and the DNA grooves that aid stabilization. To circumvent this issue, an amide linker could replace the alkyne linker. The N-H and C=O functionalities in amides allow hydrogen bonding to the major and minor grooves of DNA. This enables further stabilization of the nucleotides to facilitate inclusion into the duplex by the DNA polymerase. Amides have been employed by many groups in recent work and have successfully incorporated modified nucleotides into dsDNA via methods such as primer extension and PCR.²

Although this project fell short of the ultimate goal, a strong platform has been crafted. The achievements thus far have created compelling potential for achieving the novel synthesis of an enzymatically synthesized, 1D conductive nanowire.

References

- (1) Loakes, D.; Holliger, P. *Chem. Commun.* **2009**, 4619.
- (2) Borsenberger, V.; Kukwikila, M.; Howorka, S. *Org. Biomol. Chem.* **2009**, 7, 3826.

Appendix

With special thanks to Dr. Ross Harrington for determining X-ray crystal structures.

Table 1. Crystal data and structure refinement for Compound 5.

Identification code	ah128	
Chemical formula (moiety)	C ₁₅ H ₁₀ NS ₂	
Chemical formula (total)	C ₁₅ H ₁₀ NS ₂	
Formula weight	268.36	
Temperature	150(2) K	
Radiation, wavelength	MoK α , 0.71073 Å	
Crystal system, space group	orthorhombic, Pna2 ₁	
Unit cell parameters	a = 16.7710(16) Å	$\alpha = 90^\circ$
	b = 7.1231(10) Å	$\beta = 90^\circ$
	c = 21.515(3) Å	$\gamma = 90^\circ$
Cell volume	2570.2(6) Å ³	
Z	8	
Calculated density	1.387 g/cm ³	
Absorption coefficient μ	0.393 mm ⁻¹	
F(000)	1112	
Crystal colour and size	colourless, 0.40 × 0.40 × 0.20 mm ³	
Reflections for cell refinement	152 (θ range 2.5 to 27.5°)	
Data collection method	Nonius KappaCCD diffractometer	
	ϕ and ω scans	
θ range for data collection	4.2 to 27.5°	
Index ranges	h -21 to 21, k -9 to 9, l -27 to 27	
Completeness to $\theta = 26.0^\circ$	99.5 %	
Reflections collected	26623	
Independent reflections	5755 ($R_{\text{int}} = 0.0594$)	
Reflections with $F^2 > 2\sigma$	4538	
Absorption correction	semi-empirical from equivalents	
Min. and max. transmission	0.8587 and 0.9256	
Structure solution	direct methods	
Refinement method	Full-matrix least-squares on F^2	
Weighting parameters a, b	0.0787, 2.3111	
Data / restraints / parameters	5755 / 1 / 326	
Final R indices [$F^2 > 2\sigma$]	R1 = 0.0567, wR2 = 0.1366	
R indices (all data)	R1 = 0.0839, wR2 = 0.1537	
Goodness-of-fit on F^2	1.115	
Absolute structure parameter	0.10(10)	
Extinction coefficient	0.0031(10)	
Largest and mean shift/su	0.000 and 0.000	
Largest diff. peak and hole	1.06 and -0.36 e Å ⁻³	

Table 2. Atomic coordinates and equivalent isotropic displacement parameters (\AA^2) for ah128. U_{eq} is defined as one third of the trace of the orthogonalized U^{ij} tensor.

	x	y	z	U_{eq}
S(1)	0.68674(6)	0.39962(16)	0.78305(5)	0.0283(3)
S(2)	1.04088(7)	-0.22482(18)	0.85576(5)	0.0339(3)
S(3)	1.27390(7)	-0.23773(17)	0.91172(6)	0.0311(3)
S(4)	0.92670(6)	0.39942(15)	0.98382(6)	0.0287(3)
N(1)	0.84916(18)	-0.0107(5)	0.76753(14)	0.0187(7)
N(2)	1.08722(18)	-0.0121(5)	1.00270(14)	0.0179(7)
C(1)	0.6286(2)	0.4322(6)	0.7181(2)	0.0279(9)
C(2)	0.6539(3)	0.3216(7)	0.6698(2)	0.0299(10)
C(3)	0.7221(2)	0.2127(7)	0.6849(2)	0.0251(10)
C(4)	0.7474(2)	0.2396(5)	0.74499(19)	0.0202(9)
C(5)	0.8197(2)	0.1692(6)	0.77618(19)	0.0214(8)
C(6)	0.8740(3)	0.2661(6)	0.8128(2)	0.0231(9)
C(7)	0.9386(3)	0.1457(6)	0.82487(18)	0.0241(9)
C(8)	0.9226(2)	-0.0263(6)	0.79730(18)	0.0202(8)
C(9)	0.9728(2)	-0.1920(6)	0.79524(19)	0.0222(9)
C(10)	0.9839(2)	-0.3271(6)	0.7499(2)	0.0238(9)
C(11)	1.0473(3)	-0.4546(6)	0.7646(2)	0.0293(10)
C(12)	1.0842(3)	-0.4145(7)	0.8199(2)	0.0339(11)
C(13)	0.8029(2)	-0.1689(6)	0.74270(18)	0.0208(8)
C(14)	0.8155(2)	-0.2087(6)	0.6760(2)	0.0226(9)
C(15)	0.8247(3)	-0.2408(7)	0.6220(2)	0.0312(11)
C(17)	1.3165(3)	-0.4284(7)	0.9474(2)	0.0307(10)
C(18)	1.2839(2)	-0.4626(7)	1.0037(2)	0.0303(10)
C(19)	1.2231(2)	-0.3313(6)	1.01990(19)	0.0217(8)
C(20)	1.2102(2)	-0.1981(6)	0.97428(18)	0.0199(8)
C(21)	1.1615(2)	-0.0270(6)	0.97404(16)	0.0184(8)
C(22)	1.1788(2)	0.1423(6)	0.94699(18)	0.0227(9)
C(23)	1.1149(3)	0.2638(6)	0.95985(19)	0.0222(9)
C(24)	1.0588(2)	0.1692(6)	0.99409(18)	0.0198(8)
C(25)	0.9867(2)	0.2398(6)	1.0232(2)	0.0217(9)
C(26)	0.9593(2)	0.2176(7)	1.0841(2)	0.0239(10)
C(27)	0.8911(3)	0.3279(7)	1.0973(2)	0.0289(10)
C(28)	0.8671(2)	0.4361(6)	1.0473(2)	0.0295(10)
C(29)	1.0400(2)	-0.1699(6)	1.02732(19)	0.0215(9)
C(30)	1.0526(2)	-0.2088(6)	1.0939(2)	0.0240(9)
C(31)	1.0624(3)	-0.2412(6)	1.1482(3)	0.0321(12)

Table 3. Bond lengths [\AA] and angles [$^\circ$] for ah128.

S(1)–C(1)	1.720(5)	S(1)–C(4)	1.734(4)
S(2)–C(9)	1.748(4)	S(2)–C(12)	1.717(5)
S(3)–C(17)	1.716(5)	S(3)–C(20)	1.742(4)
S(4)–C(25)	1.739(4)	S(4)–C(28)	1.713(5)
N(1)–C(5)	1.386(5)	N(1)–C(8)	1.392(5)
N(1)–C(13)	1.468(5)	N(2)–C(21)	1.393(5)
N(2)–C(24)	1.389(5)	N(2)–C(29)	1.473(5)
C(1)–H(1A)	0.9500	C(1)–C(2)	1.372(7)
C(2)–H(2A)	0.9500	C(2)–C(3)	1.420(6)

C(3)–H(3A)	0.9500	C(3)–C(4)	1.373(6)
C(4)–C(5)	1.473(6)	C(5)–C(6)	1.387(6)
C(6)–H(6A)	0.9500	C(6)–C(7)	1.407(6)
C(7)–H(7A)	0.9500	C(7)–C(8)	1.387(6)
C(8)–C(9)	1.451(6)	C(9)–C(10)	1.382(6)
C(10)–H(10A)	0.9500	C(10)–C(11)	1.434(6)
C(11)–H(11A)	0.9500	C(11)–C(12)	1.372(7)
C(12)–H(12A)	0.9500	C(13)–H(13A)	0.9900
C(13)–H(13B)	0.9900	C(13)–C(14)	1.477(6)
C(14)–C(15)	1.195(6)	C(17)–H(17A)	0.9500
C(17)–C(18)	1.351(7)	C(18)–H(18A)	0.9500
C(18)–C(19)	1.426(6)	C(19)–H(19A)	0.9500
C(19)–C(20)	1.382(6)	C(20)–C(21)	1.467(6)
C(21)–C(22)	1.370(6)	C(22)–H(22A)	0.9500
C(22)–C(23)	1.406(6)	C(23)–H(23A)	0.9500
C(23)–C(24)	1.372(6)	C(24)–C(25)	1.450(6)
C(25)–C(26)	1.398(6)	C(26)–H(26A)	0.9500
C(26)–C(27)	1.416(6)	C(27)–H(27A)	0.9500
C(27)–C(28)	1.383(7)	C(28)–H(28A)	0.9500
C(29)–H(29A)	0.9900	C(29)–H(29B)	0.9900
C(29)–C(30)	1.475(6)	C(30)–C(31)	1.201(7)
C(1)–S(1)–C(4)	92.2(2)	C(9)–S(2)–C(12)	92.7(2)
C(17)–S(3)–C(20)	92.2(2)	C(25)–S(4)–C(28)	92.8(2)
C(5)–N(1)–C(8)	109.1(3)	C(5)–N(1)–C(13)	124.7(3)
C(8)–N(1)–C(13)	125.0(3)	C(21)–N(2)–C(24)	108.6(3)
C(21)–N(2)–C(29)	125.5(3)	C(24)–N(2)–C(29)	124.9(3)
S(1)–C(1)–H(1A)	124.4	S(1)–C(1)–C(2)	111.2(3)
H(1A)–C(1)–C(2)	124.4	C(1)–C(2)–H(2A)	123.5
C(1)–C(2)–C(3)	112.9(4)	H(2A)–C(2)–C(3)	123.5
C(2)–C(3)–H(3A)	123.6	C(2)–C(3)–C(4)	112.9(4)
H(3A)–C(3)–C(4)	123.6	S(1)–C(4)–C(3)	110.8(3)
S(1)–C(4)–C(5)	119.5(3)	C(3)–C(4)–C(5)	129.4(4)
N(1)–C(5)–C(4)	123.2(3)	N(1)–C(5)–C(6)	107.6(3)
C(4)–C(5)–C(6)	128.9(4)	C(5)–C(6)–H(6A)	126.0
C(5)–C(6)–C(7)	107.9(4)	H(6A)–C(6)–C(7)	126.0
C(6)–C(7)–H(7A)	126.0	C(6)–C(7)–C(8)	108.0(4)
H(7A)–C(7)–C(8)	126.0	N(1)–C(8)–C(7)	107.4(3)
N(1)–C(8)–C(9)	124.3(4)	C(7)–C(8)–C(9)	128.2(4)
S(2)–C(9)–C(8)	117.7(3)	S(2)–C(9)–C(10)	110.1(3)
C(8)–C(9)–C(10)	131.8(4)	C(9)–C(10)–H(10A)	123.7
C(9)–C(10)–C(11)	112.7(4)	H(10A)–C(10)–C(11)	123.7
C(10)–C(11)–H(11A)	123.4	C(10)–C(11)–C(12)	113.2(4)
H(11A)–C(11)–C(12)	123.4	S(2)–C(12)–C(11)	111.3(4)
S(2)–C(12)–H(12A)	124.4	C(11)–C(12)–H(12A)	124.4
N(1)–C(13)–H(13A)	108.5	N(1)–C(13)–H(13B)	108.5
N(1)–C(13)–C(14)	115.2(3)	H(13A)–C(13)–H(13B)	107.5
H(13A)–C(13)–C(14)	108.5	H(13B)–C(13)–C(14)	108.5
C(13)–C(14)–C(15)	179.3(4)	S(3)–C(17)–H(17A)	124.0
S(3)–C(17)–C(18)	112.0(3)	H(17A)–C(17)–C(18)	124.0
C(17)–C(18)–H(18A)	123.5	C(17)–C(18)–C(19)	112.9(4)
H(18A)–C(18)–C(19)	123.5	C(18)–C(19)–H(19A)	123.6
C(18)–C(19)–C(20)	112.9(4)	H(19A)–C(19)–C(20)	123.6
S(3)–C(20)–C(19)	109.9(3)	S(3)–C(20)–C(21)	118.3(3)
C(19)–C(20)–C(21)	131.3(4)	N(2)–C(21)–C(20)	124.0(3)

N(2)–C(21)–C(22)	108.1(3)	C(20)–C(21)–C(22)	127.9(4)
C(21)–C(22)–H(22A)	126.4	C(21)–C(22)–C(23)	107.2(4)
H(22A)–C(22)–C(23)	126.4	C(22)–C(23)–H(23A)	125.5
C(22)–C(23)–C(24)	109.0(4)	H(23A)–C(23)–C(24)	125.5
N(2)–C(24)–C(23)	107.0(3)	N(2)–C(24)–C(25)	123.4(4)
C(23)–C(24)–C(25)	129.2(4)	S(4)–C(25)–C(24)	119.9(3)
S(4)–C(25)–C(26)	109.9(3)	C(24)–C(25)–C(26)	129.7(4)
C(25)–C(26)–H(26A)	123.5	C(25)–C(26)–C(27)	113.0(4)
H(26A)–C(26)–C(27)	123.5	C(26)–C(27)–H(27A)	123.6
C(26)–C(27)–C(28)	112.8(4)	H(27A)–C(27)–C(28)	123.6
S(4)–C(28)–C(27)	111.4(3)	S(4)–C(28)–H(28A)	124.3
C(27)–C(28)–H(28A)	124.3	N(2)–C(29)–H(29A)	108.6
N(2)–C(29)–H(29B)	108.6	N(2)–C(29)–C(30)	114.6(3)
H(29A)–C(29)–H(29B)	107.6	H(29A)–C(29)–C(30)	108.6
H(29B)–C(29)–C(30)	108.6	C(29)–C(30)–C(31)	179.5(5)

Table 4. Anisotropic displacement parameters (\AA^2) for ah128. The anisotropic displacement factor exponent takes the form: $-2\pi^2[h^2a^{*2}U^{11} + \dots + 2hka^*b^*U^{12}]$

	U^{11}	U^{22}	U^{33}	U^{23}	U^{13}	U^{12}
S(1)	0.0308(6)	0.0268(6)	0.0274(5)	-0.0044(5)	0.0037(5)	0.0041(4)
S(2)	0.0343(6)	0.0447(7)	0.0228(6)	0.0017(5)	-0.0050(5)	0.0086(5)
S(3)	0.0355(6)	0.0359(6)	0.0221(6)	0.0001(5)	0.0089(5)	0.0076(5)
S(4)	0.0292(5)	0.0245(6)	0.0323(6)	0.0009(5)	-0.0064(4)	0.0066(4)
N(1)	0.0175(15)	0.0198(17)	0.0189(17)	0.0017(13)	0.0001(12)	-0.0041(13)
N(2)	0.0194(16)	0.0187(17)	0.0154(15)	0.0012(13)	-0.0005(12)	-0.0004(13)
C(1)	0.023(2)	0.030(2)	0.031(2)	0.006(2)	0.0042(18)	0.0060(18)
C(2)	0.029(2)	0.033(3)	0.028(2)	0.000(2)	-0.0031(19)	0.0034(19)
C(3)	0.023(2)	0.026(2)	0.026(2)	-0.0003(19)	0.0011(16)	0.0036(17)
C(4)	0.024(2)	0.019(2)	0.018(2)	0.0000(15)	0.0037(16)	0.0001(16)
C(5)	0.0213(19)	0.023(2)	0.020(2)	-0.0023(17)	0.0037(16)	-0.0012(16)
C(6)	0.030(2)	0.019(2)	0.020(2)	-0.0045(16)	-0.0005(17)	-0.0003(17)
C(7)	0.024(2)	0.027(2)	0.021(2)	-0.0032(17)	-0.0013(16)	-0.0048(17)
C(8)	0.0197(18)	0.021(2)	0.020(2)	0.0020(15)	0.0000(15)	-0.0042(16)
C(9)	0.019(2)	0.026(2)	0.021(2)	0.0061(18)	0.0019(15)	-0.0053(16)
C(10)	0.0211(19)	0.020(2)	0.030(2)	-0.0016(18)	-0.0003(17)	-0.0017(16)
C(11)	0.027(2)	0.020(2)	0.041(3)	0.0002(19)	0.0034(19)	0.0000(17)
C(12)	0.030(2)	0.032(3)	0.040(3)	0.012(2)	0.0025(19)	0.007(2)
C(13)	0.0201(19)	0.023(2)	0.0192(19)	0.0010(16)	-0.0007(15)	-0.0077(16)
C(14)	0.0171(18)	0.024(2)	0.027(2)	-0.0060(19)	-0.0028(16)	-0.0006(16)
C(15)	0.029(2)	0.039(3)	0.025(3)	-0.006(2)	-0.0038(18)	-0.001(2)
C(17)	0.023(2)	0.033(3)	0.036(3)	-0.002(2)	0.0024(18)	0.0077(19)
C(18)	0.027(2)	0.025(2)	0.039(3)	0.002(2)	-0.0031(19)	0.0020(19)
C(19)	0.0193(19)	0.025(2)	0.021(2)	0.0003(17)	0.0014(15)	-0.0020(17)
C(20)	0.0200(18)	0.023(2)	0.017(2)	-0.0036(17)	0.0018(15)	-0.0013(15)
C(21)	0.0179(17)	0.024(2)	0.0134(18)	-0.0027(15)	0.0012(15)	-0.0010(16)
C(22)	0.024(2)	0.028(2)	0.0163(19)	0.0007(16)	0.0033(16)	-0.0053(18)
C(23)	0.032(2)	0.020(2)	0.015(2)	0.0037(15)	-0.0028(16)	0.0003(18)
C(24)	0.0230(19)	0.0173(19)	0.0192(19)	-0.0017(15)	-0.0052(15)	0.0022(16)
C(25)	0.0221(19)	0.018(2)	0.025(2)	-0.0018(15)	-0.0024(16)	0.0001(16)
C(26)	0.024(2)	0.029(2)	0.019(2)	-0.0004(19)	-0.0013(16)	0.0056(18)
C(27)	0.024(2)	0.034(3)	0.029(2)	-0.005(2)	0.0021(17)	0.0028(19)

C(28)	0.022(2)	0.024(2)	0.043(3)	-0.014(2)	-0.0043(18)	0.0092(17)
C(29)	0.0170(19)	0.020(2)	0.027(2)	0.0031(17)	0.0017(16)	-0.0003(16)
C(30)	0.022(2)	0.021(2)	0.029(2)	0.0020(19)	0.0043(18)	-0.0038(17)
C(31)	0.030(2)	0.029(3)	0.037(3)	0.006(2)	0.000(2)	-0.013(2)

Table 5. Hydrogen coordinates and isotropic displacement parameters (\AA^2) for ah128.

	x	y	z	U
H(1A)	0.5845	0.5159	0.7160	0.033
H(2A)	0.6285	0.3183	0.6303	0.036
H(3A)	0.7476	0.1299	0.6565	0.030
H(6A)	0.8684	0.3915	0.8271	0.028
H(7A)	0.9851	0.1767	0.8479	0.029
H(10A)	0.9529	-0.3346	0.7131	0.029
H(11A)	1.0623	-0.5566	0.7386	0.035
H(12A)	1.1281	-0.4829	0.8363	0.041
H(13A)	0.7456	-0.1431	0.7495	0.025
H(13B)	0.8166	-0.2829	0.7667	0.025
H(17A)	1.3580	-0.5015	0.9296	0.037
H(18A)	1.2998	-0.5634	1.0298	0.036
H(19A)	1.1945	-0.3350	1.0580	0.026
H(22A)	1.2254	0.1720	0.9238	0.027
H(23A)	1.1112	0.3911	0.9469	0.027
H(26A)	0.9839	0.1369	1.1135	0.029
H(27A)	0.8647	0.3275	1.1363	0.035
H(28A)	0.8231	0.5200	1.0481	0.035
H(29A)	1.0533	-0.2843	1.0033	0.026
H(29B)	0.9828	-0.1429	1.0205	0.026

Table 6. Torsion angles [$^\circ$] for ah128.

C(4)–S(1)–C(1)–C(2)	1.2(4)	S(1)–C(1)–C(2)–C(3)	-1.4(5)
C(1)–C(2)–C(3)–C(4)	0.8(6)	C(2)–C(3)–C(4)–S(1)	0.1(5)
C(2)–C(3)–C(4)–C(5)	-173.0(4)	C(1)–S(1)–C(4)–C(3)	-0.8(3)
C(1)–S(1)–C(4)–C(5)	173.1(3)	C(8)–N(1)–C(5)–C(4)	172.9(4)
C(8)–N(1)–C(5)–C(6)	-1.3(4)	C(13)–N(1)–C(5)–C(4)	-19.0(6)
C(13)–N(1)–C(5)–C(6)	166.8(4)	S(1)–C(4)–C(5)–N(1)	147.0(3)
S(1)–C(4)–C(5)–C(6)	-40.0(6)	C(3)–C(4)–C(5)–N(1)	-40.3(6)
C(3)–C(4)–C(5)–C(6)	132.6(5)	N(1)–C(5)–C(6)–C(7)	1.9(5)
C(4)–C(5)–C(6)–C(7)	-171.9(4)	C(5)–C(6)–C(7)–C(8)	-1.8(5)
C(6)–C(7)–C(8)–N(1)	1.0(4)	C(6)–C(7)–C(8)–C(9)	177.6(4)
C(5)–N(1)–C(8)–C(7)	0.2(4)	C(5)–N(1)–C(8)–C(9)	-176.5(4)
C(13)–N(1)–C(8)–C(7)	-167.9(3)	C(13)–N(1)–C(8)–C(9)	15.4(6)
N(1)–C(8)–C(9)–S(2)	-156.2(3)	N(1)–C(8)–C(9)–C(10)	31.4(7)
C(7)–C(8)–C(9)–S(2)	27.8(5)	C(7)–C(8)–C(9)–C(10)	-144.6(5)
C(12)–S(2)–C(9)–C(8)	-173.1(3)	C(12)–S(2)–C(9)–C(10)	0.8(3)
S(2)–C(9)–C(10)–C(11)	-0.2(5)	C(8)–C(9)–C(10)–C(11)	172.6(4)
C(9)–C(10)–C(11)–C(12)	-0.8(5)	C(10)–C(11)–C(12)–S(2)	1.4(5)
C(9)–S(2)–C(12)–C(11)	-1.3(4)	C(5)–N(1)–C(13)–C(14)	99.0(4)
C(8)–N(1)–C(13)–C(14)	-94.8(5)	N(1)–C(13)–C(14)–C(15)	-125(40)
C(20)–S(3)–C(17)–C(18)	0.5(4)	S(3)–C(17)–C(18)–C(19)	-0.7(5)

C(17)–C(18)–C(19)–C(20)	0.4(5)	C(18)–C(19)–C(20)–S(3)	0.0(5)
C(18)–C(19)–C(20)–C(21)	–171.8(4)	C(17)–S(3)–C(20)–C(19)	–0.3(3)
C(17)–S(3)–C(20)–C(21)	172.7(3)	C(24)–N(2)–C(21)–C(20)	179.1(3)
C(24)–N(2)–C(21)–C(22)	–0.9(4)	C(29)–N(2)–C(21)–C(20)	–11.7(6)
C(29)–N(2)–C(21)–C(22)	168.4(3)	S(3)–C(20)–C(21)–N(2)	150.8(3)
S(3)–C(20)–C(21)–C(22)	–29.2(5)	C(19)–C(20)–C(21)–N(2)	–38.0(6)
C(19)–C(20)–C(21)–C(22)	142.0(5)	N(2)–C(21)–C(22)–C(23)	0.8(4)
C(20)–C(21)–C(22)–C(23)	–179.2(4)	C(21)–C(22)–C(23)–C(24)	–0.4(5)
C(22)–C(23)–C(24)–N(2)	–0.1(4)	C(22)–C(23)–C(24)–C(25)	173.5(4)
C(21)–N(2)–C(24)–C(23)	0.6(4)	C(21)–N(2)–C(24)–C(25)	–173.5(4)
C(29)–N(2)–C(24)–C(23)	–168.7(3)	C(29)–N(2)–C(24)–C(25)	17.2(6)
N(2)–C(24)–C(25)–S(4)	–145.6(3)	N(2)–C(24)–C(25)–C(26)	43.0(7)
C(23)–C(24)–C(25)–S(4)	41.7(6)	C(23)–C(24)–C(25)–C(26)	–129.7(5)
C(28)–S(4)–C(25)–C(24)	–172.6(3)	C(28)–S(4)–C(25)–C(26)	0.3(3)
S(4)–C(25)–C(26)–C(27)	0.3(5)	C(24)–C(25)–C(26)–C(27)	172.3(4)
C(25)–C(26)–C(27)–C(28)	–1.0(6)	C(26)–C(27)–C(28)–S(4)	1.2(5)
C(25)–S(4)–C(28)–C(27)	–0.8(4)	C(21)–N(2)–C(29)–C(30)	93.6(4)
C(24)–N(2)–C(29)–C(30)	–98.9(4)	N(2)–C(29)–C(30)–C(31)	160(100)

Table 1. Crystal data and structure refinement for Compound **8b**.

Identification code	ah145	
Chemical formula (moiety)	C ₂₂ H ₂₃ N ₃ O ₅ S	
Chemical formula (total)	C ₂₂ H ₂₃ N ₃ O ₅ S	
Formula weight	441.49	
Temperature	150(2) K	
Radiation, wavelength	CuK α , 1.54178 Å	
Crystal system, space group	monoclinic, P2 ₁	
Unit cell parameters	a = 8.0959(4) Å	$\alpha = 90^\circ$
	b = 5.7246(3) Å	$\beta = 95.369(4)^\circ$
	c = 22.4170(9) Å	$\gamma = 90^\circ$
Cell volume	1034.38(9) Å ³	
Z	2	
Calculated density	1.418 g/cm ³	
Absorption coefficient μ	1.741 mm ⁻¹	
F(000)	464	
Crystal colour and size	yellow, 0.05 × 0.00 × 0.00 mm ³	
Reflections for cell refinement	2981 (θ range 2.0 to 66.6°)	
Data collection method	Oxford Diffraction Gemini A Ultra diffractometer thin-slice ω scans	
θ range for data collection	7.7 to 65.0°	
Index ranges	h -9 to 9, k -6 to 6, l -25 to 26	
Completeness to $\theta = 65.0^\circ$	99.1 %	
Reflections collected	10573	
Independent reflections	3425 ($R_{\text{int}} = 0.1142$)	
Reflections with $F^2 > 2\sigma$	2525	
Absorption correction	semi-empirical from equivalents	
Min. and max. transmission	0.9180 and 0.9983	
Structure solution	direct methods	
Refinement method	Full-matrix least-squares on F^2	
Weighting parameters a, b	0.0773, 0.0000	
Data / restraints / parameters	3425 / 154 / 303	
Final R indices [$F^2 > 2\sigma$]	R1 = 0.0576, wR2 = 0.1268	
R indices (all data)	R1 = 0.0879, wR2 = 0.1427	
Goodness-of-fit on F^2	0.979	
Absolute structure parameter	0.03(4)	
Extinction coefficient	0.0013(7)	
Largest and mean shift/su	0.010 and 0.000	
Largest diff. peak and hole	0.29 and -0.31 e Å ⁻³	

Table 2. Atomic coordinates and equivalent isotropic displacement parameters (\AA^2) for ah145. U_{eq} is defined as one third of the trace of the orthogonalized U^{ij} tensor.

	x	y	z	U_{eq}
S(1)	0.3844(5)	1.0076(5)	0.62819(10)	0.0320(6)
S(1A)	0.244(3)	1.304(4)	0.6955(9)	0.075(5)
O(1)	-0.2458(5)	0.4581(6)	0.97780(15)	0.0451(9)
O(2)	-0.3007(4)	0.6946(6)	0.85951(13)	0.0301(8)
O(3)	-0.5763(5)	0.9761(7)	0.88511(15)	0.0490(10)
O(4)	-0.0573(4)	1.5992(5)	0.75993(12)	0.0310(7)
O(5)	0.1026(4)	1.0788(6)	0.90997(13)	0.0373(8)
N(1)	0.1117(4)	1.5454(7)	0.56916(14)	0.0280(9)
N(2)	0.0374(5)	1.3532(7)	0.83778(16)	0.0320(9)
N(3)	-0.1491(4)	1.0435(7)	0.85630(14)	0.0266(8)
C(3)	0.240(3)	1.321(4)	0.7002(7)	0.029(2)
C(3A)	0.374(6)	0.987(9)	0.6409(18)	0.036(4)
C(1)	0.3848(6)	0.9491(10)	0.7024(2)	0.0393(11)
C(2)	0.3098(6)	1.1121(9)	0.7328(2)	0.0385(11)
C(4)	0.2830(6)	1.2641(9)	0.6344(2)	0.0303(10)
C(5)	0.2495(6)	1.4089(8)	0.58142(19)	0.0293(10)
C(6)	0.3455(6)	1.4312(9)	0.5335(2)	0.0362(11)
C(7)	0.2617(6)	1.5859(9)	0.4920(2)	0.0361(11)
C(8)	0.1201(6)	1.6561(9)	0.51553(19)	0.0356(11)
C(9)	-0.0341(5)	1.5596(8)	0.60304(18)	0.0293(10)
C(10)	-0.0399(6)	1.7846(8)	0.6391(2)	0.0303(10)
C(11)	-0.1959(6)	1.7913(9)	0.6729(2)	0.0329(10)
C(12)	-0.1997(6)	1.6024(8)	0.71819(18)	0.0290(9)
C(13)	-0.3023(6)	1.4308(8)	0.72741(19)	0.0296(9)
C(14)	-0.0776(5)	1.4086(8)	0.79551(19)	0.0288(10)
C(15)	-0.2280(6)	1.2974(8)	0.77815(18)	0.0265(9)
C(16)	-0.2629(5)	1.1093(8)	0.81198(18)	0.0283(9)
C(17)	0.0031(6)	1.1588(9)	0.8701(2)	0.0315(11)
C(18)	-0.1753(6)	0.8267(8)	0.89205(19)	0.0314(10)
C(19)	-0.2340(6)	0.8725(8)	0.95332(19)	0.0327(10)
C(20)	-0.3437(6)	0.6605(9)	0.9611(2)	0.0367(11)
C(21)	-0.4231(6)	0.6139(9)	0.89802(18)	0.0306(10)
C(22)	-0.5885(6)	0.7276(9)	0.8805(2)	0.0412(12)

Table 3. Bond lengths [Å] and angles [°] for ah145.

S(1)–C(1)	1.696(5)	S(1)–C(4)	1.694(6)
S(1A)–C(2)	1.45(2)	S(1A)–C(4)	1.45(2)
O(1)–H(1)	0.99(6)	O(1)–C(20)	1.434(6)
O(2)–C(18)	1.413(6)	O(2)–C(21)	1.450(5)
O(3)–C(22)	1.429(7)	O(4)–C(12)	1.415(5)
O(4)–C(14)	1.370(5)	O(5)–C(17)	1.234(6)
N(1)–C(5)	1.369(6)	N(1)–C(8)	1.366(6)
N(1)–C(9)	1.464(5)	N(2)–C(14)	1.304(6)
N(2)–C(17)	1.370(6)	N(3)–C(16)	1.344(6)
N(3)–C(17)	1.407(6)	N(3)–C(18)	1.503(6)
C(3)–H(3A)	0.950	C(3)–C(2)	1.49(2)
C(3)–C(4)	1.583(14)	C(3A)–H(3B)	0.950
C(3A)–C(1)	1.39(4)	C(3A)–C(4)	1.75(5)
C(1)–H(1B)	0.950	C(1)–C(2)	1.335(7)
C(2)–H(2)	0.950	C(4)–C(5)	1.453(6)
C(5)–C(6)	1.389(6)	C(6)–H(6A)	0.950
C(6)–C(7)	1.412(7)	C(7)–H(7A)	0.950
C(7)–C(8)	1.367(7)	C(8)–H(8A)	0.950
C(9)–H(9A)	0.990	C(9)–H(9B)	0.990
C(9)–C(10)	1.523(6)	C(10)–H(10A)	0.990
C(10)–H(10B)	0.990	C(10)–C(11)	1.533(6)
C(11)–H(11A)	0.990	C(11)–H(11B)	0.990
C(11)–C(12)	1.485(6)	C(12)–C(13)	1.316(7)
C(13)–H(13)	0.950	C(13)–C(15)	1.453(6)
C(14)–C(15)	1.397(6)	C(15)–C(16)	1.362(6)
C(16)–H(15A)	0.950	C(18)–H(17A)	1.000
C(18)–C(19)	1.517(6)	C(19)–H(18A)	0.990
C(19)–H(18B)	0.990	C(19)–C(20)	1.523(7)
C(20)–H(19A)	1.000	C(20)–C(21)	1.521(6)
C(21)–H(20A)	1.000	C(21)–C(22)	1.507(7)
C(22)–H(21A)	0.990	C(22)–H(21B)	0.990
C(1)–S(1)–C(4)	92.7(3)	C(2)–S(1A)–C(4)	108.8(13)
H(1)–O(1)–C(20)	105(4)	C(18)–O(2)–C(21)	111.2(3)
C(12)–O(4)–C(14)	105.1(3)	C(5)–N(1)–C(8)	109.5(3)
C(5)–N(1)–C(9)	127.5(4)	C(8)–N(1)–C(9)	122.7(4)
C(14)–N(2)–C(17)	114.6(4)	C(16)–N(3)–C(17)	123.9(4)
C(16)–N(3)–C(18)	120.3(4)	C(17)–N(3)–C(18)	115.8(4)
H(3A)–C(3)–C(2)	129.7	H(3A)–C(3)–C(4)	129.7
C(2)–C(3)–C(4)	100.6(11)	H(3B)–C(3A)–C(1)	128.9
H(3B)–C(3A)–C(4)	128.9	C(1)–C(3A)–C(4)	102(3)
S(1)–C(1)–C(3A)	4(2)	S(1)–C(1)–H(1B)	123.1
S(1)–C(1)–C(2)	113.8(4)	C(3A)–C(1)–H(1B)	122.6
C(3A)–C(1)–C(2)	114(2)	H(1B)–C(1)–C(2)	123.1
S(1A)–C(2)–C(3)	5.7(14)	S(1A)–C(2)–C(1)	113.3(9)
S(1A)–C(2)–H(2)	126.1	C(3)–C(2)–C(1)	118.9(7)
C(3)–C(2)–H(2)	120.5	C(1)–C(2)–H(2)	120.5
S(1)–C(4)–S(1A)	111.3(8)	S(1)–C(4)–C(3)	114.0(8)
S(1)–C(4)–C(3A)	10.7(14)	S(1)–C(4)–C(5)	118.8(3)
S(1A)–C(4)–C(3)	2.8(16)	S(1A)–C(4)–C(3A)	101.0(15)
S(1A)–C(4)–C(5)	129.8(8)	C(3)–C(4)–C(3A)	103.7(15)
C(3)–C(4)–C(5)	127.2(8)	C(3A)–C(4)–C(5)	129.1(14)
N(1)–C(5)–C(4)	125.2(4)	N(1)–C(5)–C(6)	107.3(4)

C(4)–C(5)–C(6)	127.5(4)	C(5)–C(6)–H(6A)	126.3
C(5)–C(6)–C(7)	107.4(4)	H(6A)–C(6)–C(7)	126.3
C(6)–C(7)–H(7A)	126.3	C(6)–C(7)–C(8)	107.3(4)
H(7A)–C(7)–C(8)	126.3	N(1)–C(8)–C(7)	108.4(4)
N(1)–C(8)–H(8A)	125.8	C(7)–C(8)–H(8A)	125.8
N(1)–C(9)–H(9A)	109.0	N(1)–C(9)–H(9B)	109.0
N(1)–C(9)–C(10)	112.9(4)	H(9A)–C(9)–H(9B)	107.8
H(9A)–C(9)–C(10)	109.0	H(9B)–C(9)–C(10)	109.0
C(9)–C(10)–H(10A)	109.5	C(9)–C(10)–H(10B)	109.5
C(9)–C(10)–C(11)	110.6(4)	H(10A)–C(10)–H(10B)	108.1
H(10A)–C(10)–C(11)	109.5	H(10B)–C(10)–C(11)	109.5
C(10)–C(11)–H(11A)	109.0	C(10)–C(11)–H(11B)	109.0
C(10)–C(11)–C(12)	113.0(4)	H(11A)–C(11)–H(11B)	107.8
H(11A)–C(11)–C(12)	109.0	H(11B)–C(11)–C(12)	109.0
O(4)–C(12)–C(11)	113.2(4)	O(4)–C(12)–C(13)	112.0(4)
C(11)–C(12)–C(13)	134.8(4)	C(12)–C(13)–H(13)	126.5
C(12)–C(13)–C(15)	107.1(4)	H(13)–C(13)–C(15)	126.5
O(4)–C(14)–N(2)	120.0(4)	O(4)–C(14)–C(15)	110.5(4)
N(2)–C(14)–C(15)	129.5(4)	C(13)–C(15)–C(14)	105.4(4)
C(13)–C(15)–C(16)	139.4(4)	C(14)–C(15)–C(16)	115.2(4)
N(3)–C(16)–C(15)	118.0(4)	N(3)–C(16)–H(15A)	121.0
C(15)–C(16)–H(15A)	121.0	O(5)–C(17)–N(2)	122.3(4)
O(5)–C(17)–N(3)	118.9(4)	N(2)–C(17)–N(3)	118.8(4)
O(2)–C(18)–N(3)	107.3(4)	O(2)–C(18)–H(17A)	109.4
O(2)–C(18)–C(19)	106.8(4)	N(3)–C(18)–H(17A)	109.4
N(3)–C(18)–C(19)	114.3(4)	H(17A)–C(18)–C(19)	109.4
C(18)–C(19)–H(18A)	111.4	C(18)–C(19)–H(18B)	111.4
C(18)–C(19)–C(20)	101.6(4)	H(18A)–C(19)–H(18B)	109.3
H(18A)–C(19)–C(20)	111.4	H(18B)–C(19)–C(20)	111.4
O(1)–C(20)–C(19)	111.1(4)	O(1)–C(20)–H(19A)	111.9
O(1)–C(20)–C(21)	106.0(4)	C(19)–C(20)–H(19A)	111.9
C(19)–C(20)–C(21)	103.5(4)	H(19A)–C(20)–C(21)	111.9
O(2)–C(21)–C(20)	104.1(4)	O(2)–C(21)–H(20A)	108.3
O(2)–C(21)–C(22)	110.3(4)	C(20)–C(21)–H(20A)	108.3
C(20)–C(21)–C(22)	117.1(4)	H(20A)–C(21)–C(22)	108.3
O(3)–C(22)–C(21)	111.0(4)	O(3)–C(22)–H(21A)	109.4
O(3)–C(22)–H(21B)	109.4	C(21)–C(22)–H(21A)	109.4
C(21)–C(22)–H(21B)	109.4	H(21A)–C(22)–H(21B)	108.0

Table 4. Anisotropic displacement parameters (\AA^2) for ah145. The anisotropic displacement factor exponent takes the form: $-2\pi^2[h^2a^{*2}U^{11} + \dots + 2hka^*b^*U^{12}]$

	U^{11}	U^{22}	U^{33}	U^{23}	U^{13}	U^{12}
S(1)	0.0311(11)	0.0297(11)	0.0357(13)	0.0008(10)	0.0053(10)	0.0037(9)
S(1A)	0.048(7)	0.052(7)	0.119(11)	0.030(8)	-0.025(8)	-0.002(6)
O(1)	0.061(2)	0.034(2)	0.0386(19)	-0.0007(15)	-0.0024(17)	-0.0010(18)
O(2)	0.0314(18)	0.0316(19)	0.0280(16)	-0.0036(13)	0.0070(14)	0.0002(15)
O(3)	0.046(2)	0.051(3)	0.051(2)	0.0084(18)	0.0089(17)	0.0025(19)
O(4)	0.0299(17)	0.0313(18)	0.0323(16)	-0.0016(14)	0.0057(13)	0.0009(15)
O(5)	0.0269(17)	0.049(2)	0.0342(17)	0.0065(15)	-0.0055(14)	0.0047(16)
N(1)	0.026(2)	0.033(2)	0.0257(18)	-0.0001(16)	0.0068(15)	0.0001(18)
N(2)	0.026(2)	0.040(3)	0.0296(19)	-0.0024(17)	0.0004(16)	-0.0023(19)
N(3)	0.0227(18)	0.031(2)	0.0257(18)	-0.0038(15)	0.0027(14)	0.0049(17)
C(3)	0.026(5)	0.039(5)	0.023(3)	-0.002(3)	0.006(4)	-0.003(4)
C(3A)	0.021(9)	0.039(7)	0.047(5)	0.000(6)	0.001(8)	0.011(7)
C(1)	0.027(2)	0.040(3)	0.051(3)	0.008(2)	-0.003(2)	0.000(2)
C(2)	0.032(3)	0.046(3)	0.036(2)	0.006(2)	-0.0014(19)	-0.003(2)
C(4)	0.025(2)	0.035(2)	0.031(2)	-0.0018(17)	0.0038(19)	0.002(2)
C(5)	0.029(2)	0.030(2)	0.030(2)	-0.0018(17)	0.0045(17)	0.003(2)
C(6)	0.032(2)	0.040(3)	0.038(2)	-0.0009(19)	0.0111(19)	-0.001(2)
C(7)	0.037(2)	0.036(3)	0.037(2)	0.0009(19)	0.0136(19)	-0.002(2)
C(8)	0.044(3)	0.033(3)	0.031(2)	0.0030(19)	0.011(2)	0.001(2)
C(9)	0.026(2)	0.035(3)	0.028(2)	-0.0024(18)	0.0060(17)	-0.001(2)
C(10)	0.033(2)	0.030(2)	0.030(2)	0.0014(17)	0.0106(18)	0.000(2)
C(11)	0.035(3)	0.033(2)	0.032(2)	-0.0040(17)	0.0107(19)	0.006(2)
C(12)	0.027(2)	0.033(2)	0.028(2)	-0.0037(17)	0.0059(17)	0.0056(19)
C(13)	0.029(2)	0.033(2)	0.027(2)	-0.0027(16)	0.0039(17)	0.0071(18)
C(14)	0.027(2)	0.031(3)	0.030(2)	-0.0028(19)	0.0102(17)	0.0034(19)
C(15)	0.026(2)	0.029(2)	0.025(2)	-0.0044(15)	0.0055(16)	0.0036(19)
C(16)	0.026(2)	0.032(2)	0.028(2)	-0.0048(17)	0.0068(18)	0.0034(19)
C(17)	0.030(3)	0.038(3)	0.027(2)	-0.009(2)	0.006(2)	0.003(2)
C(18)	0.034(3)	0.029(3)	0.031(2)	-0.0021(19)	0.0031(18)	-0.001(2)
C(19)	0.040(3)	0.028(2)	0.030(2)	-0.0041(18)	0.0048(19)	0.001(2)
C(20)	0.040(3)	0.039(3)	0.031(2)	-0.0004(19)	0.0028(18)	-0.002(2)
C(21)	0.039(2)	0.029(2)	0.024(2)	-0.0004(18)	0.0041(18)	-0.005(2)
C(22)	0.034(3)	0.041(3)	0.049(3)	-0.004(2)	0.005(2)	-0.004(2)

Table 5. Hydrogen coordinates and isotropic displacement parameters (\AA^2) for ah145.

	x	y	z	U
H(1)	-0.181(8)	0.502(12)	1.016(3)	0.068(18)
H(3A)	0.1846	1.4528	0.7149	0.035
H(3B)	0.4078	0.8876	0.6103	0.043
H(1B)	0.4339	0.8129	0.7206	0.047
H(2)	0.3012	1.0947	0.7745	0.046
H(6A)	0.4485	1.3561	0.5295	0.043
H(7A)	0.2973	1.6326	0.4546	0.043
H(8A)	0.0410	1.7637	0.4976	0.043
H(9A)	-0.0336	1.4247	0.6307	0.035
H(9B)	-0.1355	1.5489	0.5749	0.035
H(10A)	-0.0399	1.9204	0.6118	0.036
H(10B)	0.0600	1.7950	0.6680	0.036
H(11A)	-0.2016	1.9443	0.6932	0.039
H(11B)	-0.2950	1.7773	0.6437	0.039
H(13)	-0.4056	1.3999	0.7051	0.036
H(15A)	-0.3647	1.0270	0.8045	0.034
H(17A)	-0.0702	0.7340	0.8967	0.038
H(18A)	-0.2979	1.0198	0.9538	0.039
H(18B)	-0.1398	0.8786	0.9848	0.039
H(19A)	-0.4286	0.6919	0.9898	0.044
H(20A)	-0.4361	0.4412	0.8927	0.037
H(21A)	-0.6272	0.6840	0.8387	0.049
H(21B)	-0.6710	0.6701	0.9069	0.049

Table 6. Torsion angles [$^\circ$] for ah145.

C(4)–C(3A)–C(1)–S(1)	-79(30)	C(4)–C(3A)–C(1)–C(2)	7(3)
C(4)–S(1)–C(1)–C(3A)	97(30)	C(4)–S(1)–C(1)–C(2)	0.9(5)
S(1)–C(1)–C(2)–S(1A)	-0.1(12)	S(1)–C(1)–C(2)–C(3)	-1.2(12)
C(3A)–C(1)–C(2)–S(1A)	-5(3)	C(3A)–C(1)–C(2)–C(3)	-6(3)
C(4)–S(1A)–C(2)–C(3)	169(19)	C(4)–S(1A)–C(2)–C(1)	-0.9(18)
C(4)–C(3)–C(2)–S(1A)	-10(17)	C(4)–C(3)–C(2)–C(1)	0.9(15)
C(2)–S(1A)–C(4)–S(1)	1.5(17)	C(2)–S(1A)–C(4)–C(3)	-159(35)
C(2)–S(1A)–C(4)–C(3A)	5(2)	C(2)–S(1A)–C(4)–C(5)	-177.6(7)
C(2)–C(3)–C(4)–S(1)	-0.2(14)	C(2)–C(3)–C(4)–S(1A)	20(33)
C(2)–C(3)–C(4)–C(3A)	3(2)	C(2)–C(3)–C(4)–C(5)	-178.2(6)
C(1)–S(1)–C(4)–S(1A)	-1.4(11)	C(1)–S(1)–C(4)–C(3)	-0.3(10)
C(1)–S(1)–C(4)–C(3A)	-18(10)	C(1)–S(1)–C(4)–C(5)	177.9(4)
C(1)–C(3A)–C(4)–S(1)	157(13)	C(1)–C(3A)–C(4)–S(1A)	-7(3)
C(1)–C(3A)–C(4)–C(3)	-6(3)	C(1)–C(3A)–C(4)–C(5)	175.3(13)
C(8)–N(1)–C(5)–C(4)	-179.6(5)	C(8)–N(1)–C(5)–C(6)	-1.2(5)
C(9)–N(1)–C(5)–C(4)	-5.6(7)	C(9)–N(1)–C(5)–C(6)	172.8(4)
S(1)–C(4)–C(5)–N(1)	145.9(4)	S(1)–C(4)–C(5)–C(6)	-32.2(7)
S(1A)–C(4)–C(5)–N(1)	-35.1(14)	S(1A)–C(4)–C(5)–C(6)	146.9(13)
C(3)–C(4)–C(5)–N(1)	-36.2(12)	C(3)–C(4)–C(5)–C(6)	145.7(11)
C(3A)–C(4)–C(5)–N(1)	142(2)	C(3A)–C(4)–C(5)–C(6)	-36(2)
N(1)–C(5)–C(6)–C(7)	0.2(5)	C(4)–C(5)–C(6)–C(7)	178.5(5)

C(5)–C(6)–C(7)–C(8)	0.9(6)	C(5)–N(1)–C(8)–C(7)	1.7(5)
C(9)–N(1)–C(8)–C(7)	–172.6(4)	C(6)–C(7)–C(8)–N(1)	–1.6(6)
C(5)–N(1)–C(9)–C(10)	106.3(5)	C(8)–N(1)–C(9)–C(10)	–80.5(5)
N(1)–C(9)–C(10)–C(11)	179.3(4)	C(9)–C(10)–C(11)–C(12)	63.3(5)
C(14)–O(4)–C(12)–C(11)	–176.6(3)	C(14)–O(4)–C(12)–C(13)	1.1(4)
C(10)–C(11)–C(12)–O(4)	55.1(5)	C(10)–C(11)–C(12)–C(13)	–121.9(6)
O(4)–C(12)–C(13)–C(15)	–0.5(5)	C(11)–C(12)–C(13)–C(15)	176.5(5)
C(17)–N(2)–C(14)–O(4)	–179.7(4)	C(17)–N(2)–C(14)–C(15)	–1.0(6)
C(12)–O(4)–C(14)–N(2)	177.8(4)	C(12)–O(4)–C(14)–C(15)	–1.2(4)
O(4)–C(14)–C(15)–C(13)	0.9(5)	O(4)–C(14)–C(15)–C(16)	–178.0(3)
N(2)–C(14)–C(15)–C(13)	–177.9(4)	N(2)–C(14)–C(15)–C(16)	3.2(7)
C(12)–C(13)–C(15)–C(14)	–0.2(5)	C(12)–C(13)–C(15)–C(16)	178.3(5)
C(17)–N(3)–C(16)–C(15)	0.6(6)	C(18)–N(3)–C(16)–C(15)	–175.4(4)
C(13)–C(15)–C(16)–N(3)	178.9(5)	C(14)–C(15)–C(16)–N(3)	–2.7(6)
C(14)–N(2)–C(17)–O(5)	177.0(4)	C(14)–N(2)–C(17)–N(3)	–1.4(6)
C(16)–N(3)–C(17)–O(5)	–176.8(4)	C(16)–N(3)–C(17)–N(2)	1.6(6)
C(18)–N(3)–C(17)–O(5)	–0.6(5)	C(18)–N(3)–C(17)–N(2)	177.8(3)
C(21)–O(2)–C(18)–N(3)	–133.4(3)	C(21)–O(2)–C(18)–C(19)	–10.4(5)
C(16)–N(3)–C(18)–O(2)	16.4(5)	C(16)–N(3)–C(18)–C(19)	–101.9(5)
C(17)–N(3)–C(18)–O(2)	–160.0(3)	C(17)–N(3)–C(18)–C(19)	81.8(5)
O(2)–C(18)–C(19)–C(20)	28.5(5)	N(3)–C(18)–C(19)–C(20)	147.0(4)
C(18)–C(19)–C(20)–O(1)	78.2(5)	C(18)–C(19)–C(20)–C(21)	–35.2(5)
C(18)–O(2)–C(21)–C(20)	–12.4(5)	C(18)–O(2)–C(21)–C(22)	114.0(4)
O(1)–C(20)–C(21)–O(2)	–87.1(4)	O(1)–C(20)–C(21)–C(22)	150.8(4)
C(19)–C(20)–C(21)–O(2)	29.8(5)	C(19)–C(20)–C(21)–C(22)	–92.2(5)
O(2)–C(21)–C(22)–O(3)	–59.5(5)	C(20)–C(21)–C(22)–O(3)	59.2(5)